Curtin University

THE INSTITUTE FOR GEOSCIENCE RESEARCH (TIGeR)

TIGeR ANNUAL REPORT 2017

EXPLORING EARTH'S DYNAMIC EVOLUTION

Make tomorrow better.

scieng.curtin.edu.au

TIGeR: The Institute for Geoscience Research

About TIGeR – exploring Earth's dynamic evolution

The Institute for Geoscience Research (TIGeR) brings together active researchers across the spectrum of geosciences within Curtin University with the common goal of understanding the mechanisms and the timescales of the processes that control Earth's dynamic evolution.

TIGeR researchers study processes over a wide range of length scales, from the nanoscale to the macroscale – from reactions operating at grain boundaries in rocks to global tectonics and the origin of the Solar system.

Since the establishment of TIGeR, our researchers have been at the forefront of high-quality, world-leading research in the earth sciences. We produce geochronologic, geotectonic, geodetic and geochemical records, using the latest technology and field and laboratory data, to enhance our knowledge of the Earth's origin within the solar system, its evolution and its current configuration.

Our research forms the basis of understanding the element cycles operating on Earth and their application to the formation of natural resources such as mineral, oil, gas and coal deposits.

Widespread collaboration

TIGeR is a multidisciplinary group that brings together leading scientists in geology, inorganic and organic geochemistry, geodesy and geophysics with the common goal of advancing new and innovative geoscience research.

Our researchers are drawn from all the geoscience-related departments and centres across Curtin University, including the Department of Applied Geology, the John de Laeter Centre for Isotope Research, the Western Australian Centre for Geodesy, the Western Australian Organic and Isotope Geochemistry Group, the Department of Exploration Geophysics and the Department of Mining Engineering.

We work together with research teams across Australia and internationally and have an excellent track record of obtaining competitive national and international grants, publishing in leading international journals and producing highly-qualified postgraduates.

Cover photo: Andreas Beinlich

Contents

Mission statement

To obtain a fundamental understanding of the mechanisms behind complex processes in the Earth.

To establish and maintain a reputation as an international leader in this field.

To enhance our interdisciplinary research by establishing new collaborations and joint ventures.

To actively seek greater involvement with industrial applications of our research.

To find efficient ways of transmitting our basic research to industry, the education sector and the public.

Director's comments

The Institute of Geosciences Research (TIGeR) promotes excellence across the wide spectrum of Earth science related activities at Curtin University. The 2017 Annual Report is the third of a regular series that summarizes the peer-reviewed research publications for each year and serves as both a source of information as well as an archive. The Reports are available on the TIGeR website (tiger.curtin.edu.au).

The articles in this Report are a selection from over 300 peer-reviewed publications by TIGeR members in 2017, mostly chosen by the authors themselves as representative of their research topics. The very high level of productivity is also typical of previous years and is why Curtin University continues to be a leader in the "solid earth" disciplines of geology, geochemistry and geophysics. The Excellence in Research for Australia (ERA) results have acknowledged our international reputation with scores of 5 ("well above world standard") in geology and geochemistry and 4 ("above world standard") in geophysics.

I have chosen a few highlights from this Report to illustrate the range and depth of Geosciences Research at Curtin.

The beginning of 2017 saw the publication of one of the ground-breaking papers of the year. As a result of instrumental developments in laser ablation microanalysis led by the John De Laeter Centre in partnership with Canberra-based high technology instrument manufacturer ASI Pty Ltd it was possible to image the helium distribution in single crystals of zircon at high resolution. This was a "world-first" publication in *Science Advances* by Danišík *et al*., and opens the opportunity for a better understanding of the interpretation of (U-Th)/He dating.

Another highlight paper was a meticulous microstructural study by Timms *et al*. that unravelled the thermal history of a zircon grain that had suffered a meteorite impact, had dissociated to zirconia (ZrO_2) and silica (SiO_2) and then cooled. The complex phase transitions in zirconia during cooling left their evidence in the microstuctures which showed that the zirconia was initially formed as the cubic polymorph, requiring a temperature in excess of 2370ºC. Dubbed the "hottest rock in the Earth's crust" the paper, published in *Earth and Planetary Sciences*, attracted popular press attention and a follow-up article in the *New Scientist*.

Using a combination of compositional data and phase equilibria modelling Johnson *et al*. concluded that the Earth's first stable continents did not form as a result of subduction, at least not as we understand it at present. They suggest that multistage melting of basaltic precursors at high geothermal gradients is more likely. The paper, published in *Nature*, is already listed among the most Highly Cited papers in Web of Science.

The massive iron-ore deposit in the Hamersley has long been a source of research (and revenue) in Western Australia, yet the timing of the events that converted an Archaean banded iron formation (BIF) to a high grade ore have remained enigmatic. By U-Pb dating of tiny inclusions of xenotime within the hematite ore Sheppard *et al*., published in *Ore Geology Reviews*, have suggested that hydrothermal events spread over a billion years have had a cumulative effect resulting in the present-day deposits.

In quite a different field, two PhD students have attracted attention with their papers using microfossils and organic biomarkers to unravel aspects of the evolution of plants and animals. Plet *et al*., in *Scientific Reports* isolated red blood cell-like structures from the bones of ichthyosaurs and argued that their small size was due to an adaptation that resulted from the low oxygen levels in the Jurassic. Spaak *et al*., published in Global and Planetary Change, found the oldest land plant microfossils in Australia in our own backyard, the Canning Basin, using carbon isotopic compositions of biomarkers to identify specific cryptospores in the sediments.

Planetary Sciences and the Fireball Network continue to make news both academically and in public outreach. Particular mention goes to Katarina Miljkovic who managed both an ARC DECRA Award as well as an ARC Discovery Award in 2017 to work on the Mars crust and also to Gretchen Benedix for her ARC Future Fellowship. These projects coincide with the NASA InSight geophysical mission to Mars to be launched in May 2018 and hopefully landing in November. Together with the partnership between the Planetary Sciences group, (representing Australia's planetary research community) and NASA on the SSERVI (Solar System Exploration research Institute) this places Curtin in a very strong position on the international space exploration scene.

National and international collaboration is a characteristic of Geosciences research and TIGeR members continue to be active in multidisciplinary research projects as evidenced from the publications and projects reported here. TIGeR members are conspicuous at international conferences such as EGU, AGU and Goldschmidt and it is particularly pleasing to see young researchers and PhD students from Curtin presenting their work at such conferences through the financial help available from the TIGeR Small Grants Scheme.

The Annual TIGeR Conference is a highlight of the year and has already established itself as an international forum for in-depth discussion of specific research issues in Geosciences. In 2017 the Conference theme was "Timescales of Geological Processes" and attracted a very impressive list of international and national speakers. As a result of this, new collaborations have been initiated that give Curtin University, through TIGeR, an international visibility and an ever-increasing world-wide reputation of excellence in geosciences research. The Conference programme and abstracts are available for download from the TIGeR website.

So 2017 was another excellent year!

Andrew Putnis
Director, The Institute for
Geoscience Research (TIGeR)



2017 TIGeR Conference

The third TIGeR Conference was held in September with > 120 international and national participants from Universities and industry.

The details of the 2017 TIGeR Conference programme as well as downloadable abstracts can be found at: **tiger.curtin.edu.au/conferences**

Research reports

MINERAL SYSTEMS, FLUIDS AND ORE DEPOSITS

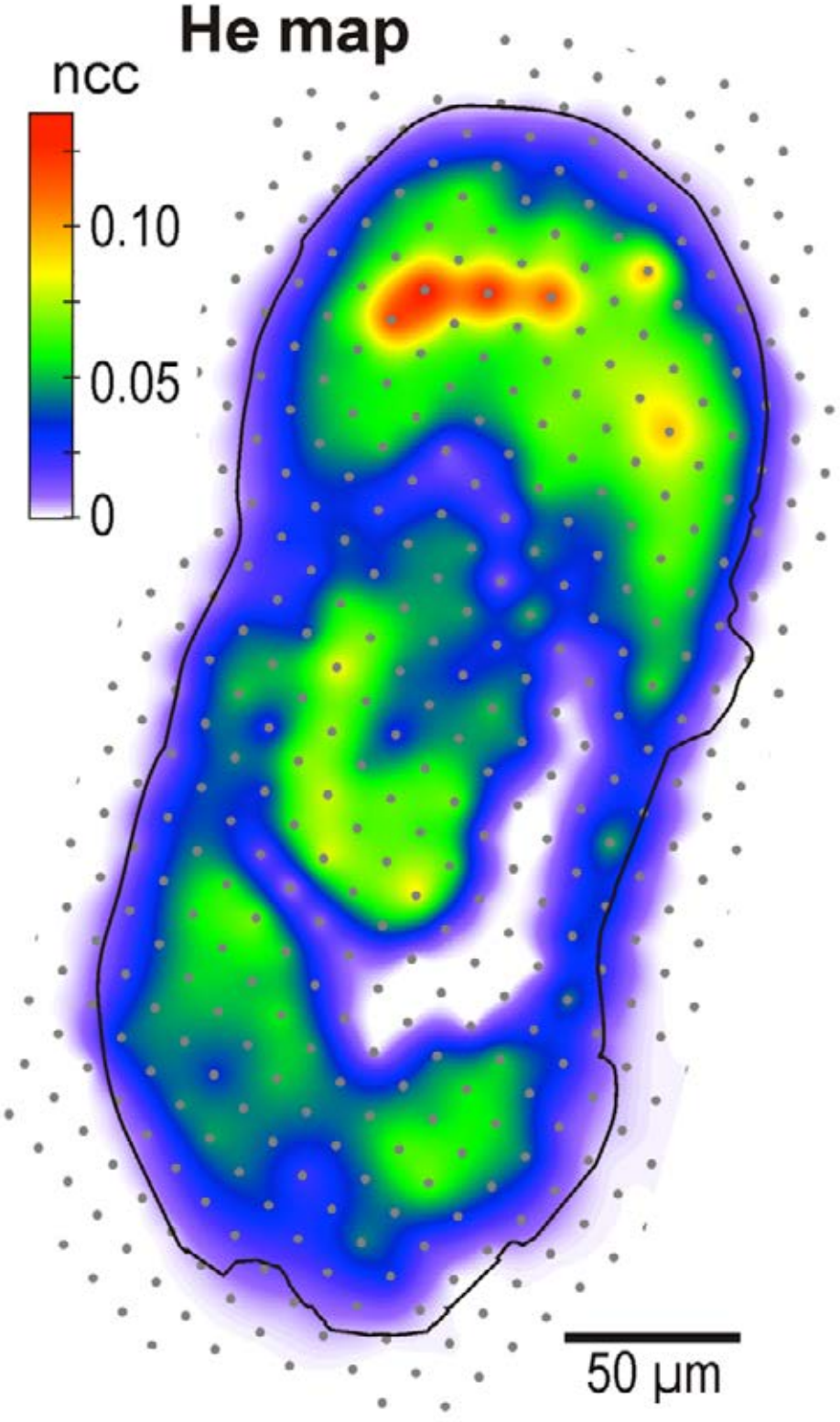

A world first: A map of the intracrystalline distribution of Helium in a zircon (Danišík *et al*. 2017).

Visualisation of Helium distribution in zircon and implications for (U-Th)/He dating

Zircon (U-Th)/He thermochronometry is an established radiometric dating technique used to place temporal constraints on a range of thermally sensitive geological events, such as crustal exhumation, volcanism, meteorite impact, and ore genesis. Isotopic, crystallographic, and/or mineralogical heterogeneities within analysed grains can result in dispersed or anomalous (U-Th)/He ages. Understanding the effect of these grain-scale phenomena on the distribution of He in analysed minerals should lead to improvements in data interpretation.

Danišík *et al.,* (2017) in a study published in Science Advances combined laser ablation microsampling and noble gas and trace element mass spectrometry to provide the first two-dimensional, grain-scale zircon He "maps" and quantify intragrain He distribution. These maps illustrate the complexity of intracrystalline He distribution in natural zircon and, combined with a correlated quantification of parent nuclide (U and Th) distribution, provide an opportunity to assess a number of crystal chemistry processes that can generate anomalous zircon (U-Th)/He ages. The technique provides new insights into fluid inclusions as potential traps of radiogenic He and confirms the effect of heterogeneity in parent-daughter isotope abundances and metamictization on (U-Th)/He systematics. Finally, they presented a new inversion method where the He, U, and Th mapping data can be used to constrain the high- and low-temperature history of a single zircon crystal.

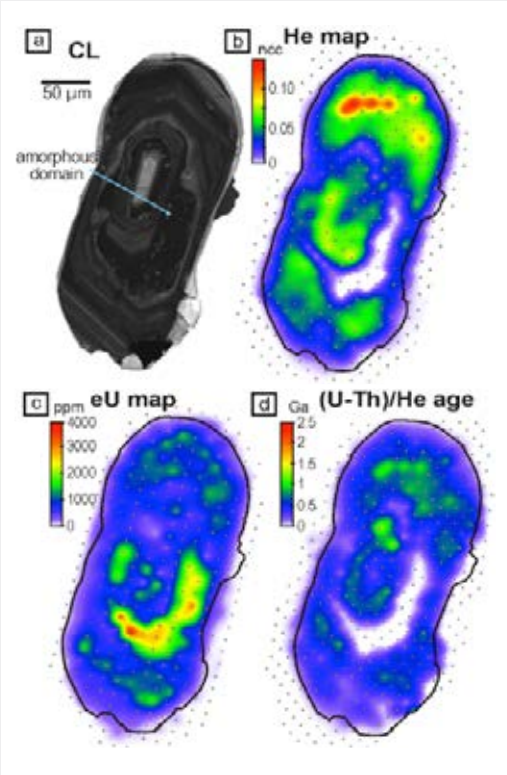

CL image of a zircon crystal (a) with corresponding He concentration (b), effective Uranium (c) and spot (U-Th)/He age map (d) measured on the RESOchron. It shows a complicated relationship of He, zircon chemistry and structure. This is the world's first visualisation of intra-crystal He distribution, which is invaluable for interpreting of (U-Th)/He data.

Danišík, M., McInnes, B. I., Kirkland, C. L., McDonald, B. J., Evans, N. J., Becker, T. (2017). Seeing is believing: Visualization of He distribution in zircon and implications for thermal history reconstruction on single crystals. *Science Advances*, 3(2), e1601121.

Cumulative hydrothermal events result in the high grade iron ore deposits in the Pilbara: first U-Pb dating of xenotime in hematite

The origin of bedded iron-ore deposits developed in greenstone belt-hosted (Algoma-type) banded iron formations of the Archean Pilbara Craton has largely been overlooked during the last three decades. Two of the key problems in studying these deposits are a lack of information about the structural and stratigraphic setting of the ore bodies and an absence of geochronological data from the ores. Sheppard *et al.,* (2017) present geological maps for nearly a dozen former mines in the Shay Gap and Goldsworthy belts on the northeastern margin of the craton, and the first U-Pb geochronology for xenotime intergrown with hematite ore using the sensitive high-resolution ion microprobe (SHRIMP). Their results suggest that iron mineralisation was the cumulative result of several Proterozoic hydrothermal events: the first at c. 2250 Ma, followed by others at c. 2180 Ma, c. 1670 Ma and c. 1000 Ma. The cause of the first growth event is not clear but the other age peaks coincide with well-documented episodes of orogenic activity at 2210–2145 Ma, 1680–1620 Ma and 1030–950 Ma along the southern margin of the Pilbara Craton and the Capricorn Orogen farther south. These results suggest that high-grade hematite deposits are a product of protracted episodic reactivation of a structural architecture that developed during the Mesoarchean. The development of hematite mineralisation along major structures in Mesoarchean BIFs after 2250 Ma implies that fluid infiltration and oxidative alteration commenced within 100 myr of the start of the Great Oxidation Event at c. 2350 Ma.

Sheppard S., Krapež B., Zi J-W, Rasmussen B. and Fletcher I.R. (2017) Young ores in old rocks: Proterozoic iron mineralisation in Mesoarchean banded iron formation, northern Pilbara Craton, Australia. *Ore Geology Reviews* 89, 40-69.

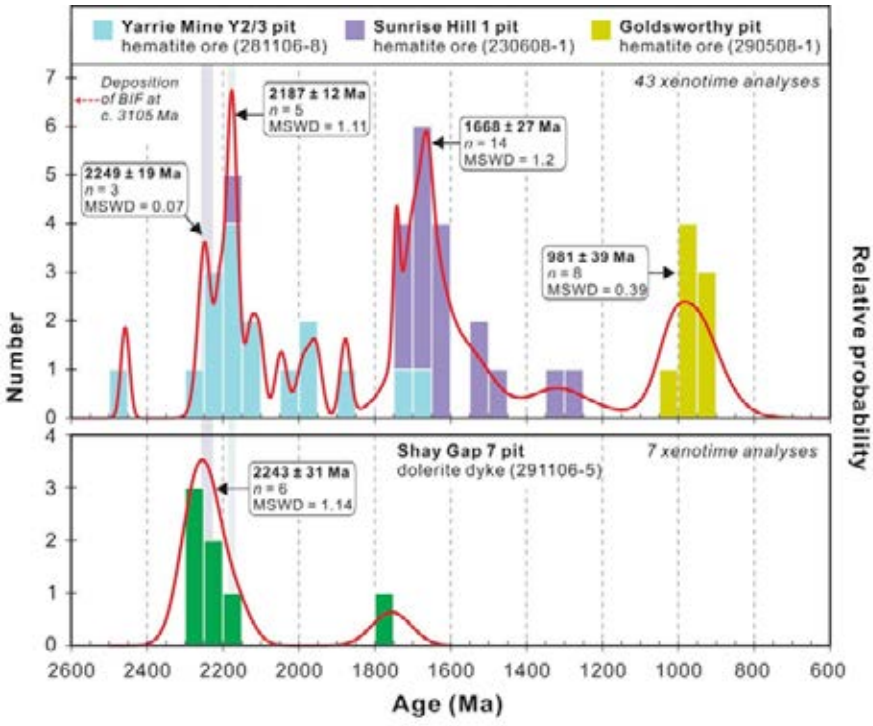

U-Pb Monazite and Xenotime Geochronology determines the Age of Orogenic Gold Mineralization: the Paulsens Mine, Southern Pilbara Craton

Paulsens is a mesothermal orogenic gold deposit located in the Wyloo Inlier on the southern margin of the Pilbara craton of Western Australia. Gold occurs in quartz-sulphide veins hosted within a folded and faulted gabbro dike, from which baddeleyite yields a U-Pb crystallization age of 2701 ± 11 Ma. Monazite and xenotime in the veins and from hydrothermally altered country rocks yield three distinct U-Pb dates of ca. 2400, 1730, and 1680 Ma. Textural relationships between euhedral xenotime and pyrite with rounded native gold inclusions from within the quartz-sulphide veins show that the primary gold mineralization was synchronous with xenotime crystallization at 2403 ± 5 Ma, and coeval with pervasive alteration of the host rocks, which yield monazite ages of 2398 ± 37 and 2403 ± 38 Ma. Regional-scale hydrothermal events at ca. 1730 and 1680 Ma are linked to the growth of monazite within phyllitic rocks at 1730 ± 28 and 1721 ± 32 Ma, carbonate veining at 1655 ± 37 Ma, and gold remobilization or introduction of new gold at 1680 ± 9 Ma. The ca. 2400 Ma age for mineralization and hydrothermal alteration does not correspond with any known deformation event in the region, indicating a signifcantly different and more complicated low-temperature tectonothermal evolution for the southern Pilbara region than previously recognized.

Fielding I.O.H., Johnson S.P., Zi J-W., Rasmussen B., Muhling J.R. Dunkley D.J., Sheppard S., Wingate M.T.D. and Rogers J.R. (2017) Using In Situ SHRIMP U-Pb Monazite and Xenotime Geochronology to Determine the Age of Orogenic Gold Mineralization: An Example from the Paulsens Mine, Southern Pilbara Craton. *Economic Geology* 112, 1205-1230.

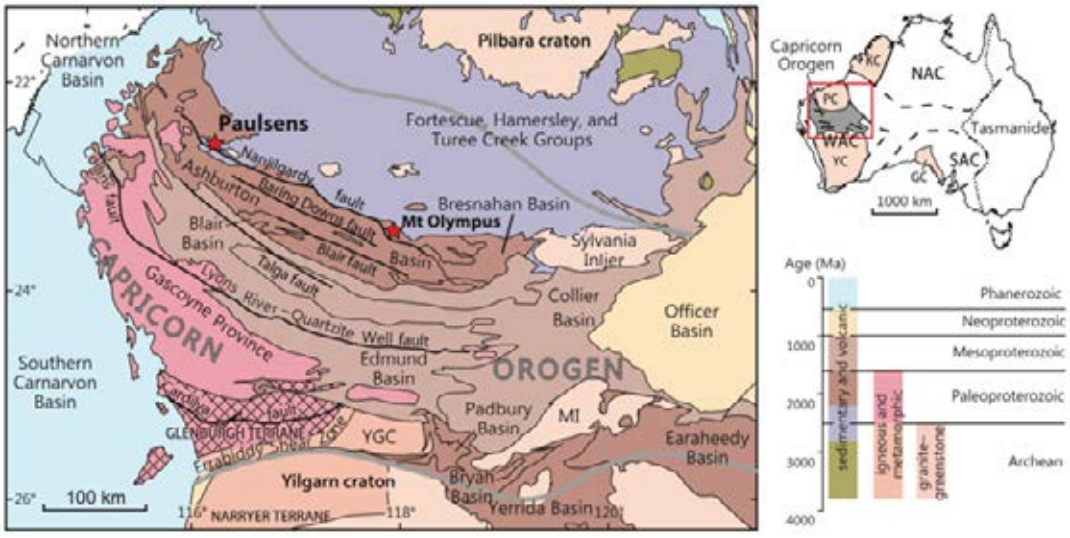

Regional geologic setting of the northern Capricorn Orogen, showing the location of the Paulsens gold mine.

The advantages of monazite over zircon for SHRIMP U–Pb geochronology to determine emplacement ages of leucocratic granites.

Piechocka *et al.,* (2017) have demonstrated that U–Th–Pb monazite geochronology is preferable for determining the crystallisation ages of Precambrian low-temperature, peraluminous leucocratic granites for the following reasons: (1) new monazite growth occurs readily at a range of P–T conditions remaining robust over time with a closure temperature of 720–750ºC; (2) monazite contains high U and Th and incorporates minor common Pb; (3) monazite, unlike zircon, generally does not contain inherited cores and is immune from radiogenic Pb loss at low temperatures; (4) occurrences of inherited monazite, although common in Tertiary S-type granites are uncommon in Precambrian rocks; and (5) magmatic monazite is one of the most common accessory mineral in granites and is abundant in peraluminous compositions. Their study has also resolved the duration of two generations of magmatism: in one instance emplacement occurred over a much shorter time interval (~30 million years) implying a higher rate of magma production than previously thought, and second, whereas purely leucocratic granites and pegmatites of the Thirty-Three Supersuite span a remarkably long duration of c. 130 million years implying a very low rate of magma generation. Finally, the use of monazite geochronology was able to narrow the possible window of magmatism to a discrete reworking event significantly reducing the time span previously thought.

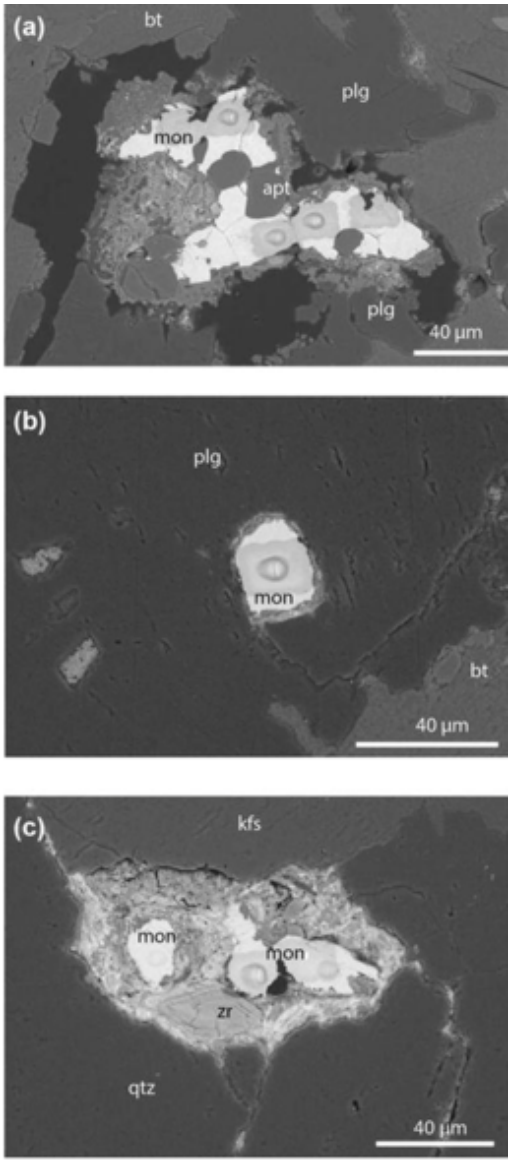

Back-scattered electron (BSE) images of representative in situ monazite.

Piechocka A.M., Courtney J.G., Zi J-W., Sheppard S., Wingate M.T.D. and Rasmussen B. Monazite trumps zircon: applying SHRIMP U–Pb geochronology to systematically evaluate emplacement ages of leucocratic, low-temperature granites in a complex Precambrian orogen. *Contibutions to Mineralogy and Petrology* 172:63 https://doi.org/10.1007/s00410-017-1386-5.

Using monazite geochronology to test the plume model for carbonatites

Carbonatites and associated REE resources are of great scientific and economic significance. The fact that many carbonatites world-wide lack reliable age constraints has hampered a full understanding of the genesis of carbonatites and their tectonic settings. The difficulty in dating carbonatites largely stems from the protracted and complicated magmatic and metasomatic histories which are typically episodic and may last for hundreds of millions of years. Monazite, a versatile U-Th-Pb geochronometer, commonly occurs as a main REE-carrier in most REE-bearing carbonatites.

Zi *et al*., (2017) working on the Gifford Creek complex demonstrate that monazite geochronology can play a crucial role in determining the age of carbonatite intrusion and associated metasomatism. The approach used in this study, i.e. in situ SHRIMP U-Th-Pb dating of monazite from a wide spectrum of rocks in a carbonatite complex, is potentially applicable to other localities. However, an important implication from their work is that dating one or two samples from a complex is unlikely to give the correct intrusive age; rather, systematic sampling of carbonatites and their host rocks is required to understand the complete intrusive and hydrothermal history.

Zi J-W., Courtney J.G., Rasmussen B., Sheppard S. and Muhling J.R. Using monazite geochronology to test the plume model for carbonatites: The example of Gifford Creek Carbonatite Complex, Australia. *Chemical Geology* 463, 50-60 (2017).

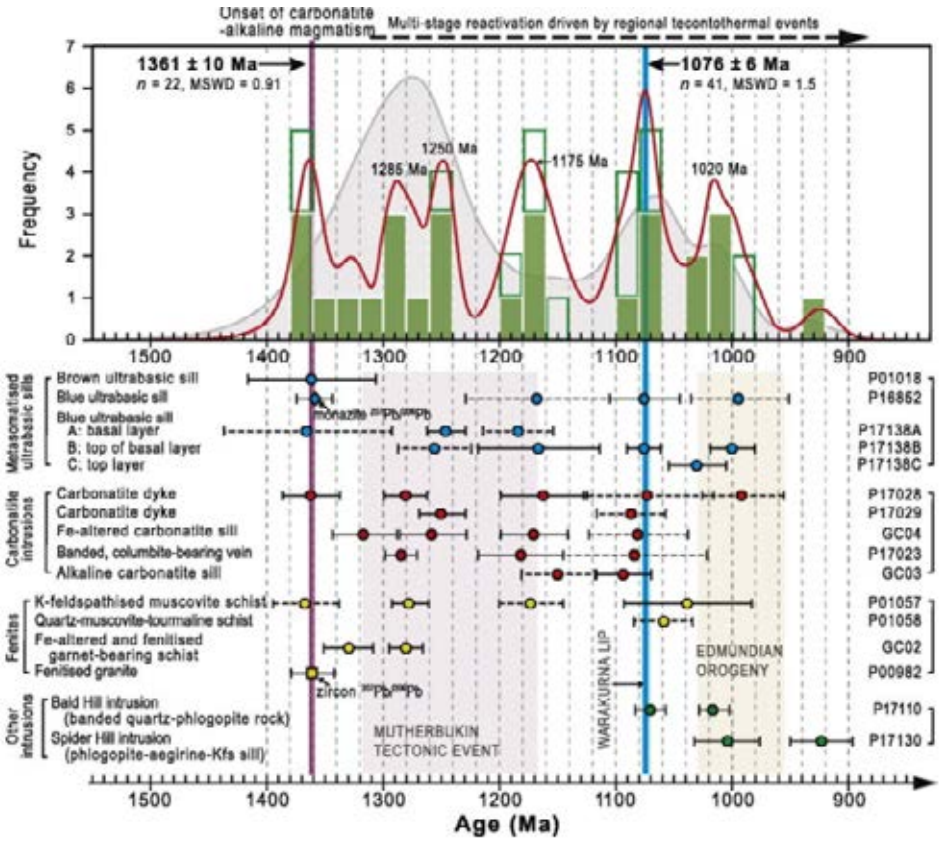

Diagram summarizing in situ U-Th-Pb monazite dating results from the Gifford Creek Carbonatite Complex.

Field trip, NE Scotland.

Two Stages of Mineralization in West Africa's Largest Gold Deposit

The timing of gold mineralisation in the Obuasi giant gold deposit (62 Moz Au; Ashanti belt, Ghana) has been debated between authors. In this study, Fougerouse *et al.,* (2017) used field and microstructural observations to reinvestigated the controls on gold mineralisation and its timing.

Microstructural evidence, such as strain shadows surrounding gold-bearing arsenopyrite parallel with the dominant S2 cleavage but folded by the overprinting S3 cleavage, indicates that the gold-bearing sulphide mineralisation formed during the D2 deformation event (Fig. 1). However, cross-cutting relationships indicate that the high-gold grades are controlled by S3 structures and support a gold mineralisation event during the D3 mineralisation event.

The gold event occurring during D2 was not previously documented in the literature and these observations constitute the first evidence for multiple stages of gold deposition at the Obuasi deposit, reconsolidating previous debates.

Fougerouse, D., Micklethwaite, S., Ulrich, S., Miller, J., Godel, B., Adams, D.T., and McCuaig, T.C. (2017) Evidence for Two Stages of Mineralization in West Africa's Largest Gold Deposit: Obuasi, Ghana. *Economic Geology*, 112(1), 3-22.

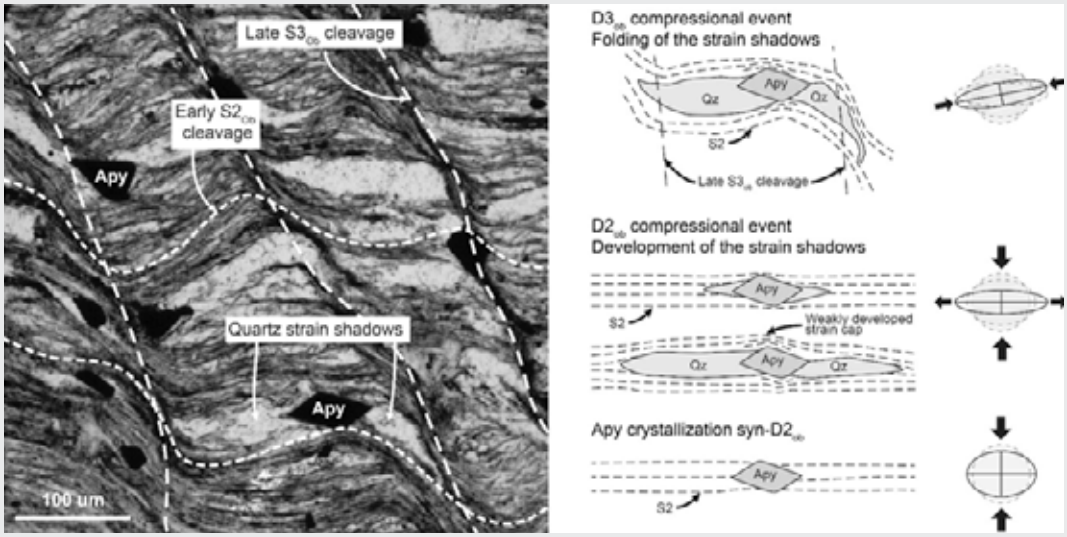

Optical micrograph of gold-bearing arsenopyrites in sedimentary rocks (phyllites). Most of the arsenopyrites have strain shadows aligned with the main pervasive cleavage (S2) and refolded by the later spaced cleavage (S3). Their strain caps, developed by the accumulation of cleavage planes against a hard object, are only weakly developed; Interpretative diagram of the evolution of the strain shadows surrounding gold-bearing arsenopyrite and the associated strain ellipsoid; the arsenopyrite grains crystallize during D2 and develop strain shadows during this period. They are later folded during D3, defining an early gold event at Obuasi.

The role of carbonaceous material in gold precipitation in metasediment-hosted orogenic gold deposits

Carbonaceous material (CM) is commonly associated with gold and sulfides in metasediment-hosted orogenic gold deposits. The role of CM in Au deposition is controversial; CM has been proposed to contribute to gold deposition by reducing Au bisulfide complexes, or by facilitating sulfidation, which destabilizes Au in bisulfide complexes with resultant Au deposition. Hu *et al.,* (2017) have integrated petrographic observations, thermodynamic models, and geochemical data from metasediment-hosted orogenic gold deposits in New Zealand, Australia, Canada, and West Africa to reveal genetic links between sulfides, CM, and mineralization.

The results are consistent with the coexistence of CM and pyrite as a consequence of their codeposition from ore fluids, with a minor proportion of CM originally in situ in the host rocks. Au is deposited when pyrite and CM deposition decreases H_2S concentration in ore fluids, destabilizing $Au(HS)_2^-$ complexes. Most CM in gold deposits is deposited from CO_2 and CH_4 in ore fluids. These findings are applicable to similar deposits worldwide.

Hu, S.Y., Evans, K., Craw, D., Rempel, K., Grice, K. (2017). Resolving the role of carbonaceous material in gold precipitation in metasediment-hosted orogenic gold deposits. *Geology*, 45(2), 167-170.

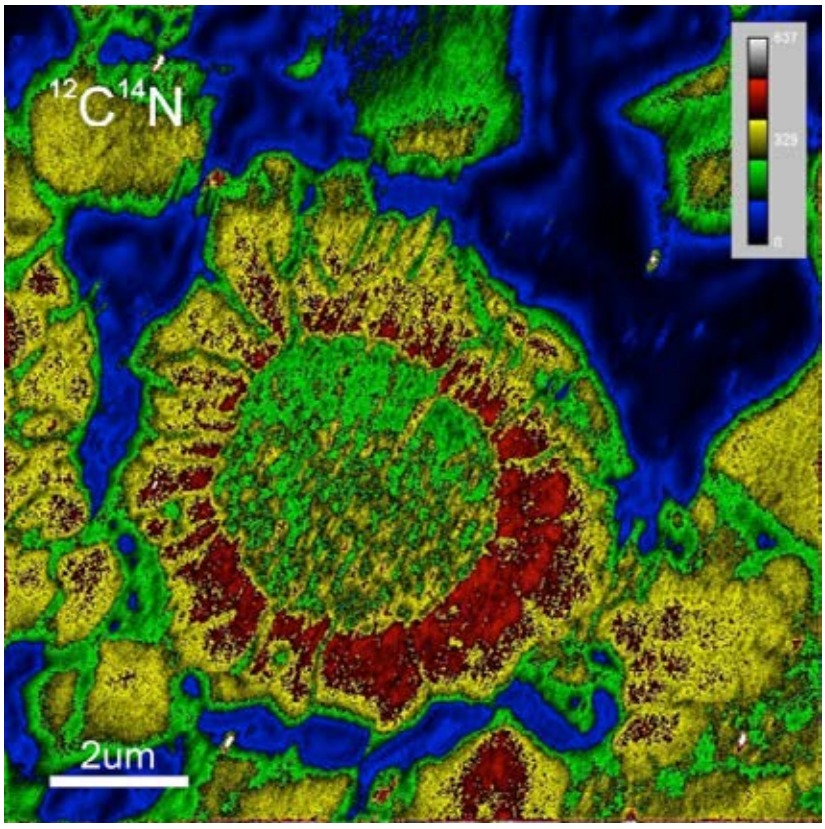

CN content (organic matter) zoning in pyrite from a gold deposit in the West Quinling Orogen. Image taken using the nano-SIMS at UWA by Yafei Wu.

Provenance of detrital pyrite in Archean sedimentary rocks: examples from the Witwatersrand Basin

Detrital pyrite is a redox-sensitive mineral that occurs as an accessory phase in clastic sedimentary rocks deposited prior to the initial rise of atmospheric oxygen in the early Paleoproterozoic. Its preservation in sedimentary rocks older than c. 2.4 Ga and its disappearance after that time indicates a rapid rise in atmospheric oxygen to levels >0.01 atm. Da Costa *et al*., (2017) discuss the provenance of detrital pyrite that is abundant in some conglomerates enriched in gold, constituting the famous placer gold quartz pebble conglomerates of the Witwatersrand-type. Potential sources for detrital pyrite include (1) sediments and sedimentary rock successions, (2) volcanogenic massive sulfide (VMS) deposits, (3) sedimentary exhalative (SEDEX) deposits, (4) magmatic, magmatic-hydrothermal, or metamorphism-related hydrothermal sulfide deposits, and (5) igneous rocks.

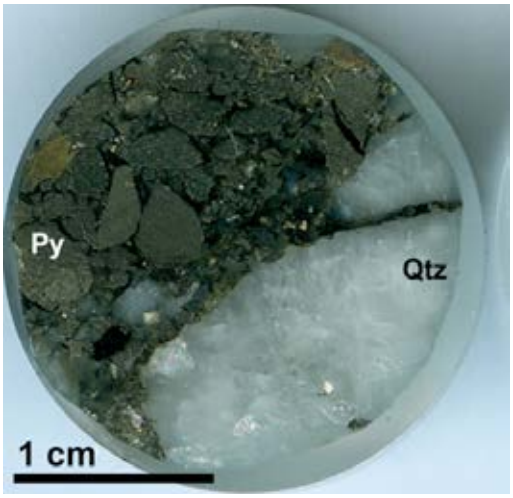

Polished quartz-pyrite pebble conglomerate from the Ventersdorp Contact Reef of the Witwatersrand Supergroup, South Africa

---

Da Costa, G., Hofmann, A., Agangi A. (2017) Provenance of detrital pyrite in Archean sedimentary rocks: examples from the Witwatersrand Basin. In *"Sediment provenance"*, Ed. Mazumder, Elsevier, 509-531 pp. dx.doi.org/10.1016/B978-0-12-803386-9.00018-6

The role of hydrothermal activity in element cycling between lithosphere and hydrosphere

The onset of hydrothermal interaction between the hydrosphere and the lithosphere on Early Earth marked a fundamental shift in the operation of our planet because it increased the chemical complexity in the oceans and lubricated the onset of plate tectonics. The discovery of chemotrophic hyper-thermophilic microbes in seafloor hydrothermal vents has led to the idea that life on Earth could be originated in hydrothermal environments (e.g., Aupova *et al*., 2017). In submarine volcanic environments, hydrothermal fluids leach soluble elements from oceanic crust and lithosphere during water-rock interaction and transport these elements into the hydrosphere. Many of these soluble elements precipitate at, or near, the seafloor during the mixing of high-temperature fluids and seawater, sometime in form of hydrothermal chimneys (Maslennikov *et al*., 2017).

Certain isotopes of the metallic elements concentrated in these precipitates are the daughter products of radioactive decay. For example, ^{187}Os is a product of the β-decay of ^{187}Re, making the Re-Os isotopic system a relatively new geochemical tool that can be applied to identify the source of metals and role of hydrothermal activity in elements cycling between lithosphere and hydrosphere (e.g., Tessalina *et al*., 2017). Studies of the Re-Os isotope system have several important applications in metallogenesis. Firstly, the precise measurement of Re and Os isotopes and high Re/Os ratios in most ore samples allow the establishment of the age of ore formation, providing the Re-Os system remains closed since the ore deposition event (Tessalina *et al*., 2017). In addition, Os belongs to the suite of Platinum Group Elements (PGE), and the studies of its distribution in mineral deposits relative to the abundance of the PGEs can be useful for the understanding of PGE behaviour within mineral systems (Tessalina and Belousova, 2017). Studies of these hydrothermal precipitates in Archean and Paleoproterozoic volcanic rocks provide important information linking the co-evolution of the lithosphere and the hydrosphere on the Yilgarn Craton and Capricorn Orogen (Hollis *et al*., 2017; Sergeev *et al*., 2017; Pirajno *et al*., 2017).

Tessalina S.G., Jourdan F., Belogub E.V. (2017). Significance of Late Devonian - Lower Carboniferous ages of hydrothermal sulphides and sericites from the Urals Volcanic-Hosted Massive Sulphide deposits. *Ore Geology Reviews*, 85, 131-139.

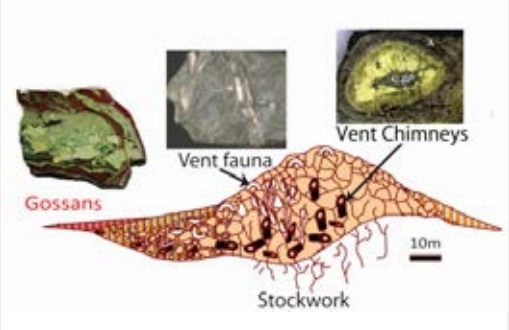

Schematic cross-section across the Volcanic-Hosted Hydrothermal Massive Sulphide deposit Yaman-Kasy, Urals (Tessalina *et al*., 2017). The fragment of hydrothermal chimney, vent fauna and clastic ore breccia with surrounding gossany rocks are shown. Chimney consists of: A – outer pyrite-marcasite wall; B – inner chalcopyrite wall; C – pyrite-marcasite-sphalerite core.

U–Pb dating of metamorphic monazite establishes a Pan-African age for tectonism in the Nallamalai Fold Belt, India

The Nallamalai Fold Belt comprises deformed sedimentary rocks from the eastern side of Peninsular India. Sheppard *et al.,* (2017) have dated metamorphic monazite in low-grade metasedimentary rocks by SHRIMP at 531+/-7 Ma and provided the first direct evidence that nappe-stacking, folding and low-grade metamorphism in the Fold Belt is related to Pan-African incorporation of India into the Gondwana supercontinent.

Sheppard S. Rasmussen B., Zi J-W., Soma Sekhar V., Sarma D.S., Mohan M.R., Krapez B., Wilde S.A., McNaughton N.J. (2017). U–Pb dating of metamorphic monazite establishes a Pan-African age for tectonism in the Nallamalai Fold Belt, India. *Journal of the Geological Society*, 174, 1062-1069.

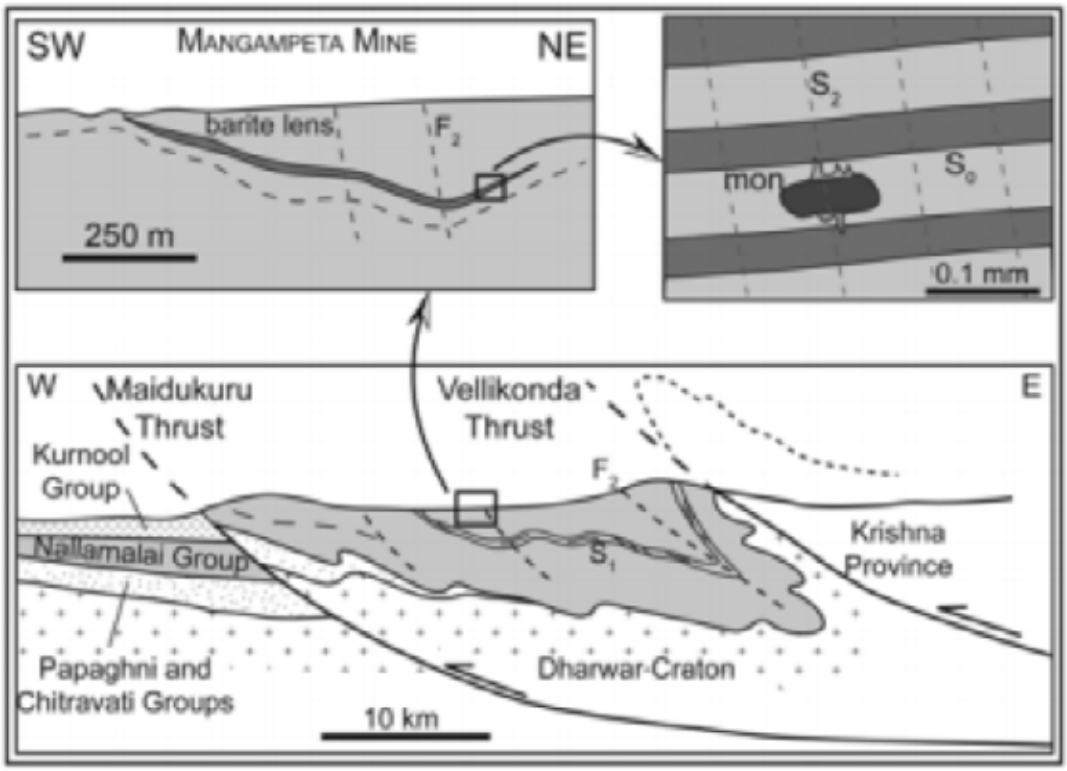

Schematic cross-section through the southern Nallamalai Fold Belt showing how large-scale structures at the fold belt scale can be related to metamorphic monazite growth in the foliation direction at the microscopic scale.

Unravelling the geochronology of Shetland Island Group, Scottish Caledonides.

The Shetland Island group occupies a central position in the North Atlantic Ocean. The older geological components acquired their present disposition during the Ordovician-Silurian Caledonian Orogeny. Among these older components are units that have been correlated on structural and lithological grounds with the Lewisian Gneiss Complex (LGC) of mainland Scotland and the Outer Hebrides, and with the Scottish Moine Supergroup. In order to test these correlations, TIGeR researchers and BSc Honours students have undertaken zircon age dating of rocks from Shetland as part of an ongoing collaboration with Professor Rob Strachan and colleagues from the University of Portsmouth, U.K.

Jahn *et al.,* (2017) report on results from a basement inlier at Cullivoe on the northeastern coast of the island of Yell. Meta-gabbro and orthogneiss of tonalite–trondhjemite–granodiorite (TTG) affiliation yielded protolith U–Pb crystallization ages of c. 2850 – 2700 Ma, making correlation with the LGC plausible. Ages of detrital zircons in Moine-like metasedimentary rocks from the adjacent Yell Sound Group show that deposition occurred after c. 1019 Ma and that high-grade metamorphism occurred during the Tonian-aged Renlandian orogeny. Overall, the effects of the Renlandian orogeny are more apparent on Shetland than they are on mainland Scotland.

Strongly lineated gneiss from the Cullivoe Inlier, Yell, Shetland.

Honours students Inalee Jahn and Shaun Davis working with Chris Clark on Yell.

Jahn I., Strachan R.A., Fowler M., Bruand E., Kinny P.D., Clark C., Taylor R.J.M. (2017). Evidence from U-Pb zircon geochronology for early Neoproterozoic (Tonian) reworking of an Archaean inlier in northeastern Shetland, Scottish Caledonides. *Journal of the Geological Society*, London, 174, 217–232.

Maidmonts Isle, Labrador.

Fluvial transport of shocked zircons across Africa

Documenting impact events on the early Earth is critical for understanding the tug-of-war between habitable and hostile surface conditions that ultimately gave rise to life. However, recreating the terrestrial cratering record is hampered by the observation that no impact crater formed prior to 2 billion years ago has survived. The study of detrital shocked minerals, which are shock-damaged minerals eroded from impact craters and deposited as sand grains in sedimentary rocks, offers a way to investigate the sedimentary record to search for evidence of ancient impact events where the source crater is entirely eroded. However, the longevity of detrital shocked minerals is an open question.

Montalvo *et al.,* (2017) demonstrate that detrital shocked zircon, eroded from the giant 300 km diameter Vredefort impact structure in the interior of the Kaapvaal Craton, can survive ~2000 km of fluvial transport in rivers to where they were sampled on the beach along the Atlantic coast of South Africa. Each detrital shocked zircon recovered contains unique microstructural damage diagnostic of impact processes, as well as the U-Pb age of the source terrane the impact formed in. One major implication of these results is that shocked zircon is resilient enough to survive in sediments and be transported far beyond the basin where the impact formed. This bodes well for searching for evidence of early Earth impacts in populations of detrital zircon in Archean siliciclastic sediments, as far-traveled detrital shocked zircon eroded from Archean-Hadean impact structures are likely to be preserved in younger sedimentary rocks.

Montalvo, S.D., Cavosie, A.J., Erickson, T.M., and Talavera, C. (2017. Fluvial transport of impact evidence from cratonic interior to passive margin: Vredefort-derived shocked zircon on the Atlantic coast of South Africa. *American Mineralogist*, v. 102, 813-823.

Colourful heavy mineral sands along the beach at the mouth of the Orange River, on the Atlantic coast of southern Africa, where it defines the border between South Africa and Namibia. The beach sand is coarse and rich in garnet (red), magnetite (black), and other dense minerals, including zircon, as a consequence of the southerly Benguela current that winnows away fines. Detrital shocked zircons from the Vredefort Dome impact structure, located ~2000 km upstream from the coast, were found in beach sand at this locality.

CO_2 fluid inclusions in Jack Hills zircons

The discovery of Hadean to Paleoarchean zircons from Jack Hills has catalyzed intensive study of their mineral inclusions as they potentially represent a unique geochemical archive that can be used to unravel the geological evolution of the early Earth.

Menneken *et al*., (2017) report the occurrence and physical properties of previously undetected CO_2 inclusions in 3.36-3.47 Ga and 3.80-4.13 Ga zircon grains by confocal micro-Raman spectroscopy. The minimum P-T conditions were determined from the highest density of the inclusions using the density dependence of the Fermi diad splitting in the Raman spectrum and Ti-in-zircon geothermometry. For both groups of zircons the CO_2 densities and geothermometry correspond to high-grade metamorphic conditions (>5 to >7 kbar at ~670 to 770ºC) that are typical of mid-crustal regional metamorphism. In addition, disordered graphite inclusions were identified in two zircons from the older population that also contained CO_2 inclusions. Transmission electron microscopy showed that the graphite forms a thin amorphous film on the inclusion wall while the rest of the inclusion was likely to have been occupied by CO_2. This would indicate a close relationship between the CO_2 and the carbon and suggest that the carbon precipitated from a CO_2-rich fluid. This is inconsistent with a previously proposed biogenic origin for the carbon inclusions in Jack Hills zircons.

Menneken, M., Geisler, T., Nemchin, A.A., Whitehouse, M.J., Wilde, S.A., Gasharova, B., Pidgeon, R.T. (2017), CO_2 fluid inclusions in Jack Hills zircons. *Contributions to Mineralogy and Petrology*, 172, 66. DOI 10.1007/s00410-017-1382-9.

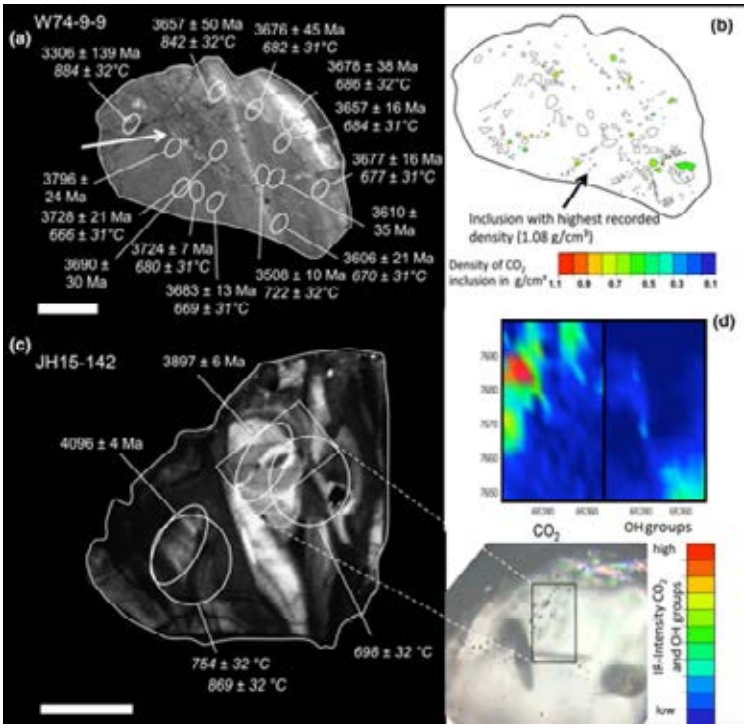

Cathodoluminescence images with ages and determined temperatures of zircons from Jack Hills together with the density distribution of inclusions and hyperspectral IR images showing the intensities of the CO_2 and OH/H_2O bands.

Quantifying fault zone processes: Making carbon from limestone, graphite behaviour in megafaults, and automated fracture pattern quantification

Identification of the nano-scale to micro-scale mechanochemical processes occurring during fault slip is of fundamental importance to understand earthquake nucleation and propagation. Delle Piane *et al.,* (2017) experimentally sheared carbonate rocks at subseismic rates (~3 × 10^{-6} m s^{-1}) simulated upper crustal conditions and produced a nano-grained fault gouge. Strain in the gouge is accommodated by cataclastic comminution of calcite grains and concurrent crystal-plastic deformation through twinning and dislocation glide, producing a crystallographic preferred orientation (CPO). Continued wear of fine-grained gouge particles results in the mechanical decomposition of calcite and production of significant amounts of amorphous carbon. They show that CPO and the production of amorphous carbon, previously attributed to frictional heating and weakening during seismic slip, can be produced at low temperature during stable slip at subseismic rates without slip weakening.

Delle Piane C., Piazolo, S., Timms N.E., Luzin V., Saunders M., Bourdet J., Giwelli A., Clennell M.B., Kong C., Rickard W.D., Verrall M. (2017). Generation of amorphous carbon and crystallographic texture during low-temperature subseismic slip in calcite fault gouge. *Geology*. 46 (2), 163-166.

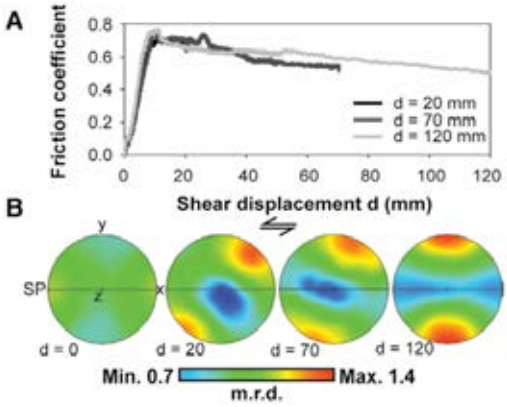

Evolution of friction coefficient as a function of shear displacement (d) in the travertine samples used in this study. B: Calcite (006) pole figures measured via neutron diffraction on cohesive wafers of gouge extracted from blocks sheared to different amount of shear displacement (d, in mm). SP—shear plane. Color bar is in multiple of random distribution (m.r.d.).

The behavior of carbon (graphite) in the Alpine Fault – an active, crustal-scale fault in New Zealand was investigated by Kirilova *et al.,* (2017). They found a microtextural record of graphite mobilization as a function of temperature and ductile then brittle shear strain with fault evolution. Changes in the abundance, spatial distribution, habit, and degree crystallinity of graphite reflects changing thermal, mechanical, and fluid-related processes during mylonitzation and cataclasis. Graphitization in fault zones is important because it is associated both with fault weakening and orogenic gold mineralization..

Kirilova M., Toy V.G., Timms N., Halfpenny A., Menzies C., Craw D., Beyssac O., Sutherland R., Townend J., Boulton C., Carpenter B.M. (2017). Textural changes of graphitic carbon by tectonic and hydrothermal processes in an active plate boundary fault zone, Alpine Fault, New Zealand. *Geological Society, London, Special Publications*, 453, SP453-13.

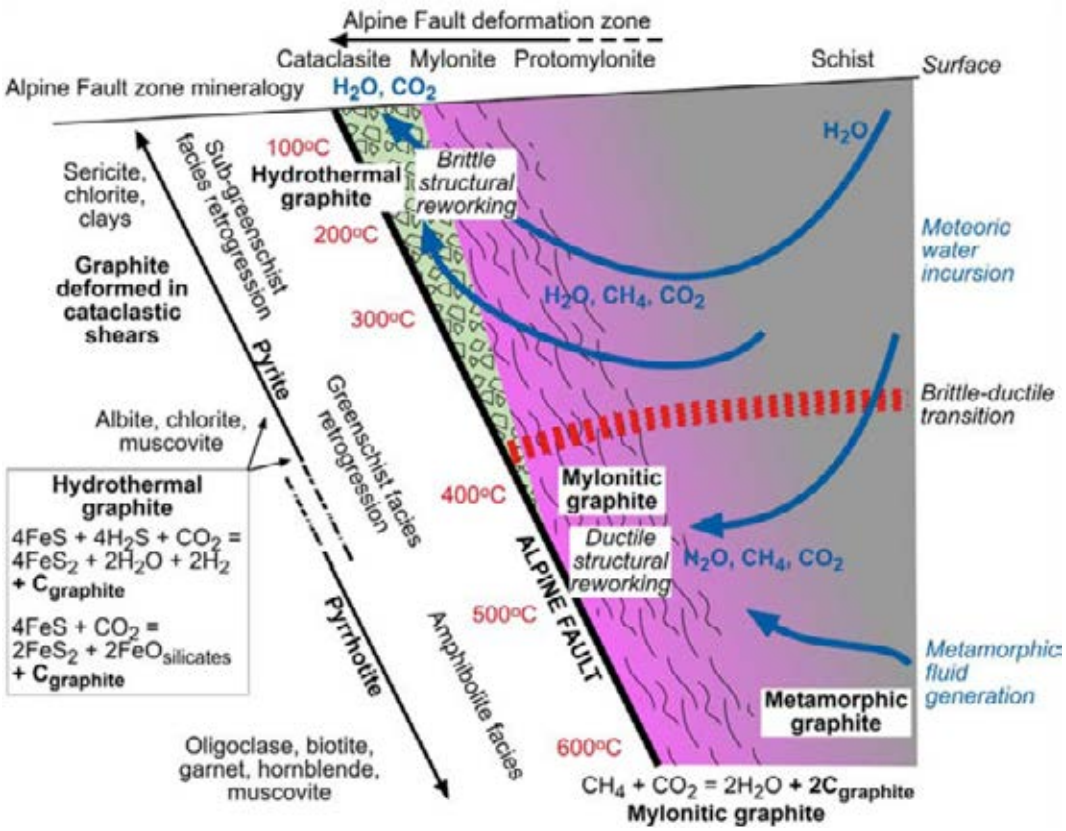

Fractures rarely occur in isolation, and their patterns are often highly complex. New MATLAB-based software for automated quantification of fracture patterns - FracPaQ – recently developed by Healy et al. (2017, JSG) permits rapid assessment their geometrical attributes. Understanding fracture patterns is important in many sub-disciplines of earth and planetary sciences: structural geology and tectonics, impact geology, rock physics and geophysics, hydrogeology, mineral exploration, mining and extraction, energy and storage of hazardous products.

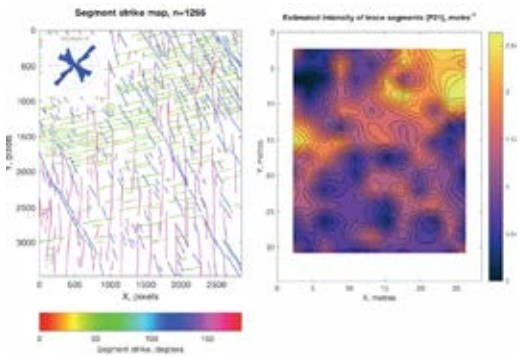

Healy D., Rizzo R.E., Cornwell D.G., Farrell N.J., Watkins H., Timms N.E., Gomez-Rivas E., Smith M. (2017). FracPaQ: a MATLABTM toolbox for the quantification of fracture patterns. *Journal of Structural Geology*, 95, 1-16.

K-feldspar phenocrysts, Maidmonts Isle, Labrador.

Reconstructing phase transformation history from deformation microstructures in shocked zircon

Accessory minerals, such as zircon, monazite, and xenotime, can provide valuable insights into meteorite impact events throughout geological time. They record these events by deforming in different and distinctive ways. Timms *et al.,* (2017a) summarised the variety of deformation responses of zircon during impacts, providing a comprehensive guide on how the microstructures can be interpreted, and developed a new phase diagram for this important mineral to extreme pressures and temperatures. They developed the concept of phase heritage, whereby information encoded in the crystallographic relationships in shocked grains can be used to reconstruct phase transformation history and, in combination with the new phase diagram, permit pressure-temperature history to be deduced. Some of this was made possible due to a new understanding of the transformation mechanisms of zircon to the high-pressure polymorph reidite (Erickson *et al.,* 2017a).

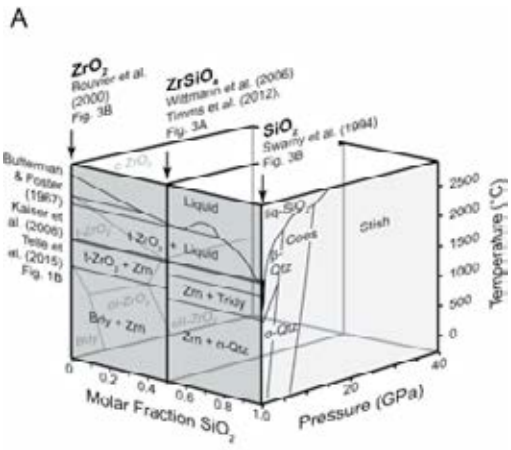

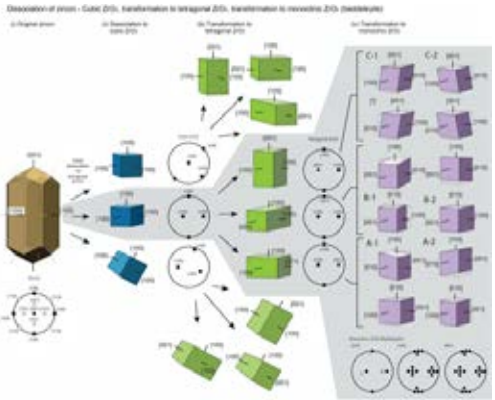

Timms N.E., Erickson T.M., Pearce M.A., Cavosie A.J., Schmieder M., Tohver E., Reddy S.M., Zanetti M., Nemchin A.A., Wittmann A. (2017). A pressure-temperature phase diagram for zircon at extreme conditions. *Earth Science Reviews*, 165, 185-202.

Erickson T.M., Pearce M.A., Reddy S.M., Timms N.E., Cavosie A.J., Bourdet J., Rickard W.D.A., Nemchin A.A. (2017). Microstructural constraints on the mechanisms of the transformation to reidite in naturally shocked zircon. *Contributions to Mineralogy and Petrology*, 172 (1), 6.

The hottest crust on Earth

Timms *et al*., (2017b) have shown from microstructural analysis of zircon grains that have partially dissociated to ZrO_2 and SiO_2 when they were immersed in an impact melt from the ~38 Ma, 28 km Mistastin Lake Crater in Canada that the ZrO_2 transformed from its cubic polymorph. The existence of cubic ZrO_2 requires superheating in excess of 2370ºC without complete vaporization.

This is the hottest temperature recorded by any rock in the Earth's crust. Their 'zirconia phase heritage' approach represents a new geothermometer that provides much needed geological constraints on impact melt temperatures that bridges the gap between nature and theory. The transience of the heat generated during this single impact event only had a local effect. However, changes to the geochemistry of target rocks during high temperature melting could be more globally significant and enduring early in Earth's history when it was supposed to undergo significantly higher levels of bombardment. In their paper, Timms *et al*., flag possibilities for volatile loss of some elements but not others during extremely high temperatures, potentially changing the physical and chemical properties of solidified melt rocks. Volatile loss of things such as H_2O and CO_2 from rocks would clearly have implications for the evolution of the atmosphere, hydrosphere, and even life itself.

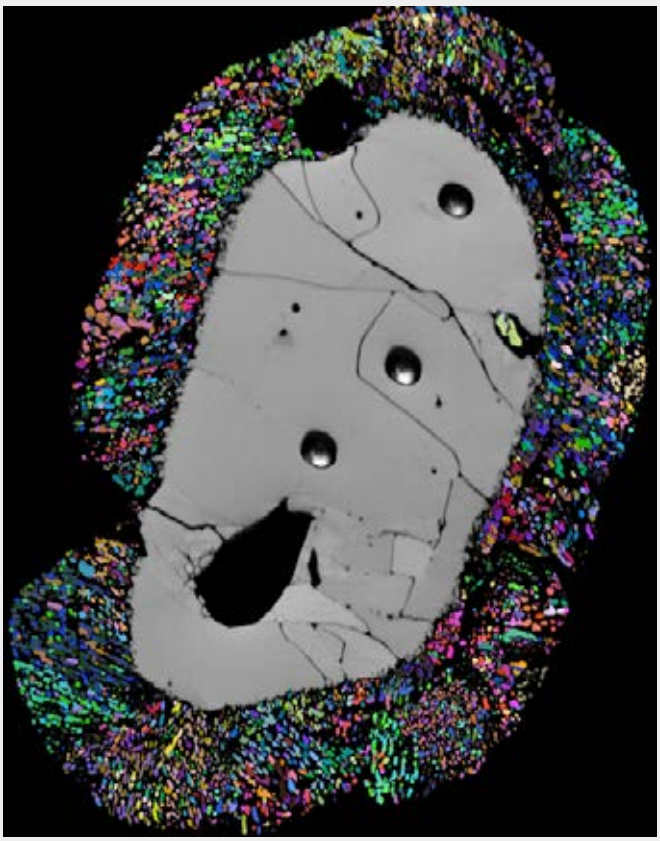

Timms N.E., Erickson T.M., Zanetti M.R., Pearce M.A., Cayron C., Cavosie A.J., Reddy S.M., Wittmann A., Carpenter P.K. (2017). Cubic zirconia in >2370ºC impact melt records Earth's hottest crust. *Earth and Planetary Science Letters*, 477, 52-58. Also reported in New Scientist https://www.newscientist.com/article/mg23531433-600-found-the-hottest-place-ever-found-on-earths-surface/).

Dating impact events from shocked monazite

Dating of shocked monazite represents a significant development in dating meteorite impacts events. New research by Erickson *et al.,* (2017b) has demonstrated that targeted in situ U-Th-Pb analysis of particular microstructures in shocked monazite can yield robust and precise impact ages. This approach has been benchmarked using monazite grains from the central uplift of the Vredefort impact structure, South Africa, and impact melt from the Araguainha impact structure, Brazil. Shocked monazite is especially promising for dating impact structures where subsequent metamorphism and alteration can reset other isotope systems in other minerals.

Erickson T.M., Timms N.E., Kirkland C.L., Tohver E., Cavosie A.J., Pearce M.A., Reddy S.M. (2017b). Shocked monazite chronometry: integrating microstructural and in situ isotopic age data for determining precise impact ages. *Contributions to Mineralogy and Petrology*, 172 (2-3), 11.

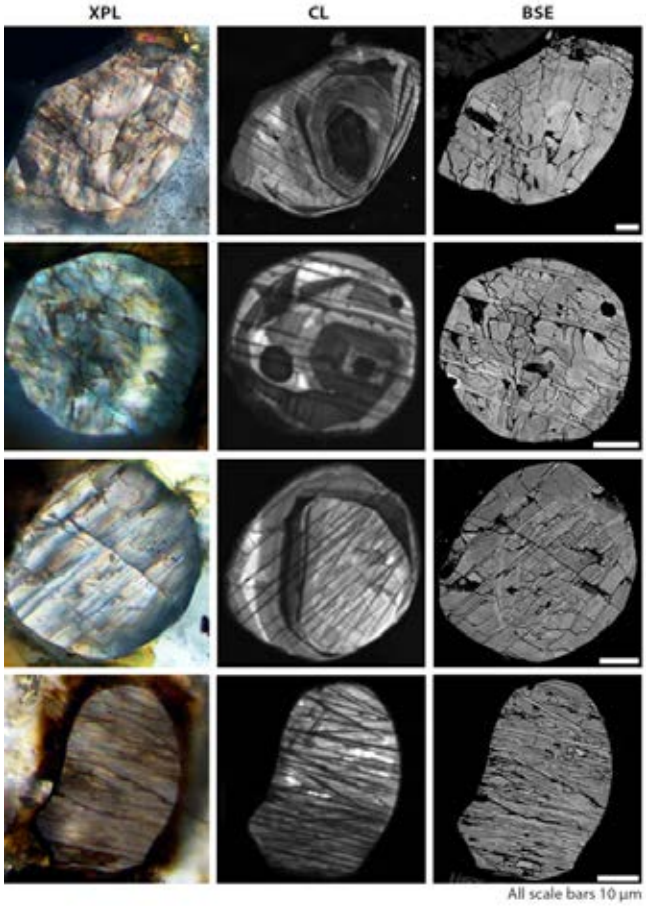

Microstructures in shocked monazite.

Using Lu-Hf isotope ratios to model Archaen crustal evolution

The lutetium–hafnium (Lu–Hf) isotope record, typically measured in zircon crystals, provides a major tool for the study of crustal growth and differentiation. Interpretations of Hf isotope datasets use an evolution array defined by source $^{176}Lu/^{177}Hf$. However, the very process that drives crustal differentiation to produce such arrays – partial melting – is precisely that which may modify the trajectory of the array due to variable degrees of anatexis allied with the differing compatibilities of Lu and Hf in residual minerals. Further, Lu/Hf estimates derived from the composition of present-day continental crust may be inappropriate for modelling Archaean crustal evolution, where different geodynamic styles and magmatic sources prevailed.

Gardiner *et al.*, (2017) use an approach combining phase equilibria, trace element and isotopic modelling, to quantify the effects of partial melting of an Archaean mafic source on melt Lu/Hf. They show a partial melting event imposes a greater control on the resulting crustal reservoir Lu/Hf than the degree of melting. Archaean continental crust has a lower Lu/Hf than that of the average mid to upper continental crust, and there has been a secular change in average crustal Lu/Hf, with the median Lu/Hf of Proterozoic and Phanerozoic magmatic rocks being higher than that of Archaean TTG+G.

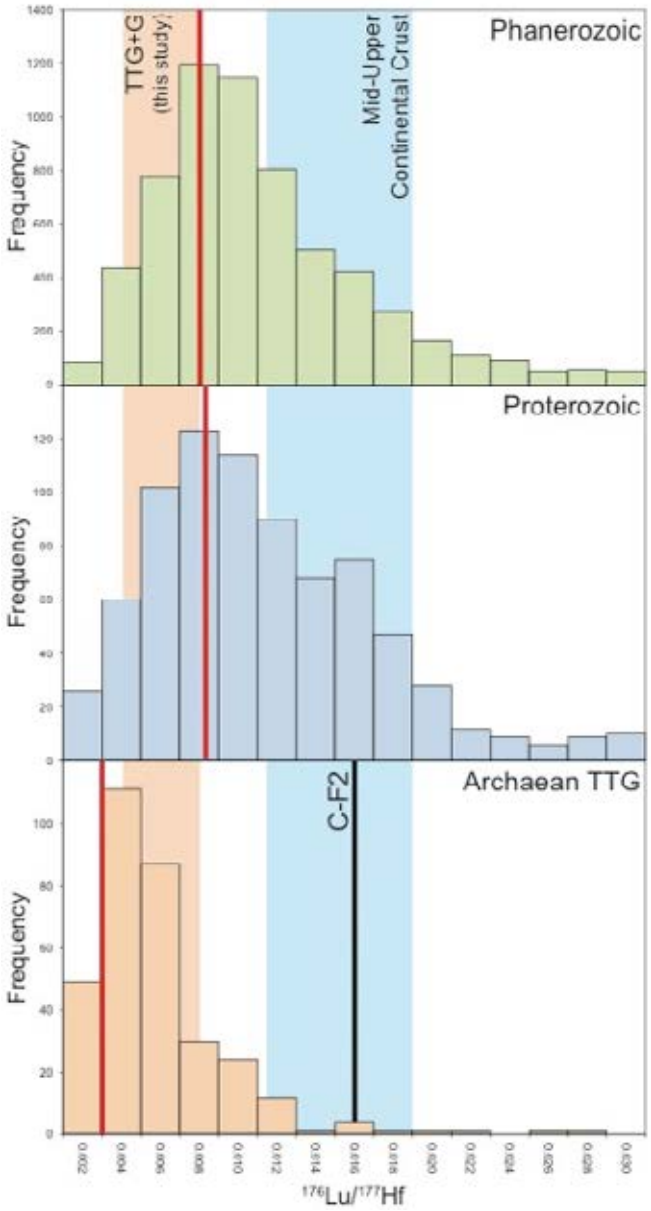

Gardiner, N.J., Johnson, T.E., Kirkland, C.L., Smithies, R.H. (2017). Melting Controls on the Lutetium–Hafnium Evolution of Archaean Crust. *Precambrian Research, 305*, 479-488.

The Savannah Mine, WA.

Multi-scale magnetic monitoring of peridotite carbonation processes

Peridotite and serpentinite carbonation represents a critical step within the long-term carbon cycle by sequestering volatile CO_2 in solid secondary Mg- and Mc-Ca-carbonate phases. This has also been proposed as one potential pathway to mitigate the effects of greenhouse gas release. Most of our current understanding of reaction mechanisms, rates and efficiencies is based on hand specimen and laboratory-scale analyses. However, linking observations made in the laboratory to the field remains challenging due to complex scaling relationships and the typically large number of unconstrained parameters.

Tominaga *et al.*, (2017) present the first geophysical characterization of serpentinite carbonation across scales ranging from km to sub-mm by combining aeromagnetic observations, outcrop- and thin section-scale SQUID magnetic mapping. At all scales, magnetic anomalies coherently change across reaction fronts separating assemblages indicative of incipient, intermittent, and final reaction progress. The change in magnetic anomalies is related to the formation and breakdown of magnetite, the main magnetic carrier phase, during the transition from serpentinite to soapstone (magnesite + talc) and from soapstone to listvenite (magnesite + quartz), respectively. Soapstone formation is accompanied by an increase in magnetic field strength, while the breakdown of magnetite during listvenite formation effectively erased the magnetic signal. This correlation represents a foundation for characterizing the extent and degree of in situ ultramafic rock carbonation in space and time by remote geophysical measurements and furthermore shows that the magnetic character of rocks is susceptible to alteration by hydrothermal fluids.

Tominaga M., Beinlich A., Hampton B., Tivey M., Hart L., Lima E.A., Weiss B., Harigane Y. (2017). Multi-scale magnetic monitoring of peridotite carbonation processes. *Nature Communications*, 8, 1870.

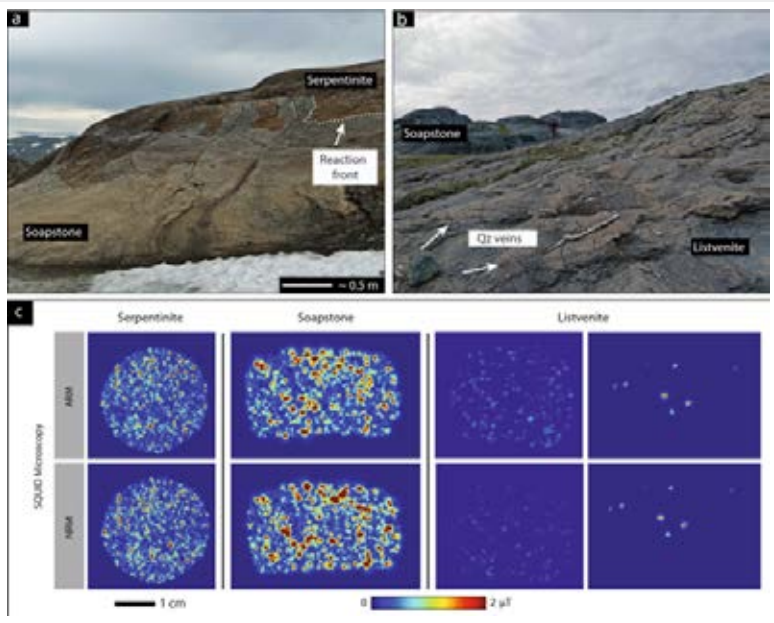

How did the first stable continents form?

The geodynamic environment in which Earth's first stable continents formed remains controversial. Most exposed Archaean crust comprises tonalite–trondhjemite–granodiorite rocks (TTGs) that were formed from partial melting of a low magnesium mafic source and which have trace element signatures resembling crust produced in modern subduction settings. In the East Pilbara Terrane, Western Australia, low magnesium basalts of the Coucal Formation at the base of the Pilbara Supergroup have trace element compositions consistent with the source rocks for TTGs and may be remnants of a ≥35 km-thick pre-3.5 Ga basaltic crust that is predicted if mantle temperatures were much hotter than today.

Using phase equilibria modelling of the Coucal basalts, Johnson *et al*., (2017) confirm their suitability as TTG parents, and suggest the TTGs were produced by ~20–30% melting along high geothermal gradients (≥700ºC/GPa). Moreover, the trace element composition of the Coucal basalts indicates they were derived from an earlier generation of mafic rocks, suggesting the arc-like signature in Archaean TTGs was inherited from an ancestral source lineage. The protracted multistage process required for production and stabilisation of the first continents, coupled with the high geothermal gradients, are incompatible with modern-style subduction and favour a stagnant lid regime in the early Archaean.

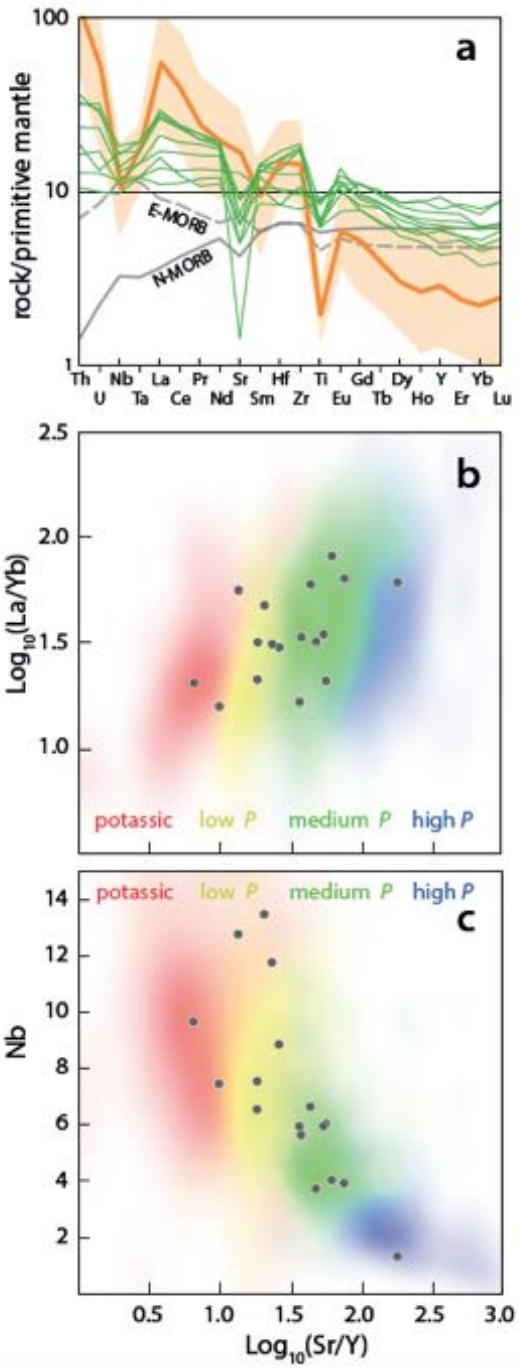

Johnson, T.E., Brown, M., Gardiner, N.J., Kirkland, C.L. & Smithies, R.H. (2017). Earth's first stable continents did not form by subduction. *Nature*, 543, 239–242.

Interpreting granulite facies events from Rare earth element partitioning

Rare earth element (REE) partitioning is a widely used tool in metamorphic studies, linking the growth or modification of geochronometers to the silicate mineral assemblage. The most commonly used mineral pair for the study of high-grade metamorphic rocks is zircon and garnet. The link between U–Pb ages provided by zircon to the pressure and temperature information recorded by garnet can be interpreted in relation to experimental data. The simplistic approach of taking the average REE values for zircon and garnet and comparing them directly to experimentally derived partition coefficients is flawed, in that it cannot represent the complexity in a natural rock system. By using all the zircon REE data from a sample, and comparing it to garnet using the most important REE values, it is possible to define zircon–garnet equilibrium using an array rather than an average. The parameter plot describes partitioning between zircon and garnet using D_{Yb} and D_{Yb}/D_{Gd} as the defining features of the relationship. This approach provides far more sensitivity to mineral reactions and diffusional processes, enabling a more detailed interpretation of metamorphic history of the sample.

Taylor, R.J.M., **Clark, C.**, Harley, S.L., Kylander-Clark, A.R.C., Hacker, B., Kinny, P.D. (2017) Interpreting granulite facies events through rare earth element partitioning arrays. *Journal of Metamorphic Geology*. 35, 759-775.

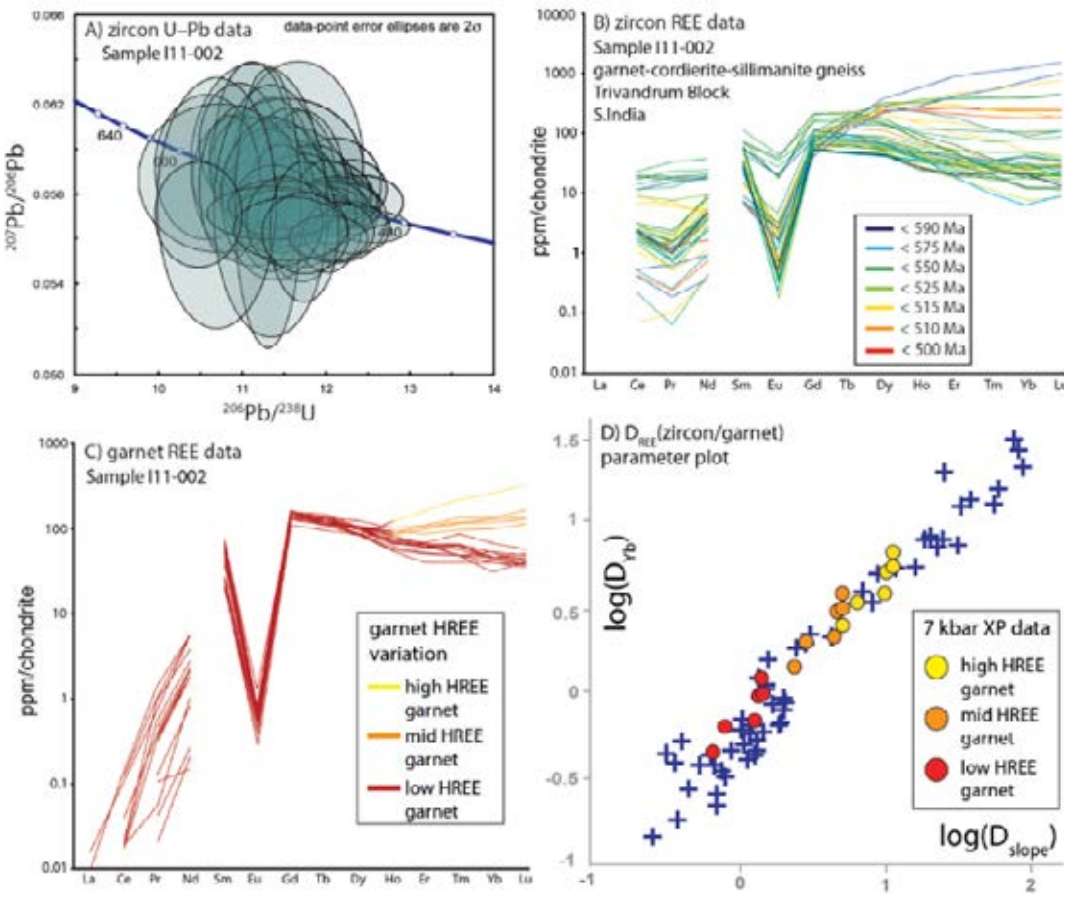

Rare earth element partitioning arrays for a granulite facies metapelite from southern India.

The redox state of fluids released by subducted mantle lithosphere

Evans *et al.,* (2017) used the opaque and accessory mineral phase assemblage and bulk rock ferric iron content to constrain the redox budget of fluids that would be released during subduction by rocks from (a) a sub-arc mantle setting and (b) oceanic slow/ultra slow ridge or ocean-continent transition setting.

The results suggest that rocks serpentinised in the latter settings undergo higher fluid:rock ratio settings, are more likely to produce oxidizing fluids, than rocks serpentinised in other settings. Rocks serpentinised in ultra slow/OCT settings are over-represented in obducted ophiolites that we have available to study so caution must be applied when we use results from ophiolites such as the Zermatt-Saas zone to infer global budgets of elements released by recycling of serpentinites in subduction zones.

Evans, K.A., Reddy, S.M., Tomkins, A.G., Crossley, R.J., Frost, B.R. (2017). Effects of geodynamic setting on the redox state of fluids released by subducted mantle lithosphere. *Lithos*, 278-281, 26-42.

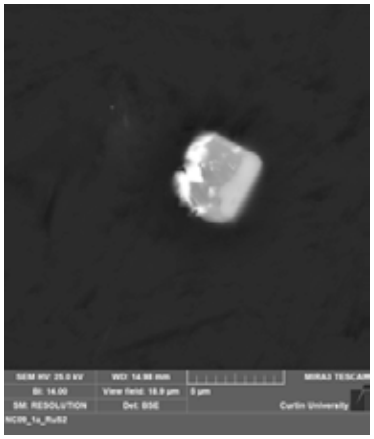

Ruthenium alloy (bright) with laurite (RuS2, second brightest) from sub-arc mantle serpentinite, New Caledonia.

Evolution of the Eucla basement and implications to the destruction of oceanic crust during continent formation

The crystalline basement beneath the Cretaceous to Cenozoic Bight and Eucla Basins, in Western Australia has received comparatively little attention even though it lies on the eastern margin of one of the most mineral resource endowed regions on the planet. This basement is characterized by a complex geological evolution spanning c. 2 billion years, but paucity of outcrop and younger basin cover present a daunting challenge to understand the basement geology. Recent work by CET-Curtin in collaboration with GSWA (Kirkland *et al*., 2017) has revealed the Hf isotopic composition of the unexposed Proterozoic crystalline basement to the Bight and Eucla Basins. This region includes two geophysically defined basement entities: the Madura Province and the Coompana Province. New isotopic and geochemical data shows that the Madura and Coompana regions together represent a huge tract of predominantly juvenile material. Magma sources recognized, include; 1) depleted mantle; 2) recycled c. 1950 Ma crust reworked in primitive arcs and in intra-plate settings and; 3) minor evolved material representing fragments of hyperextended continent. The observed isotopic evolution pattern is comparable to that of other central Australian Proterozoic provinces, including the Musgrave Province, the northern margin of the Gawler Craton, and components within the Rudall Province. Linking these isotopic signatures defines the Mirning Ocean, and its subducted and underplated equivalents. In a global context we suggest c. 1950 Ma crust production reflects the onset of ordered oceanic spreading centres, which swept juvenile crustal fragments into Nuna.

Kirkland, C. L., R. H. Smithies, C. V. Spaggiari, M. T. D. Wingate, R. Quentin de Gromard, C. Clark, N. J. Gardiner, and E. A. Belousova. (2017). Proterozoic crustal evolution of the Eucla basement, Australia: Implications for destruction of oceanic crust during emergence of Nuna. *Lithos* 278-281: 427-444.

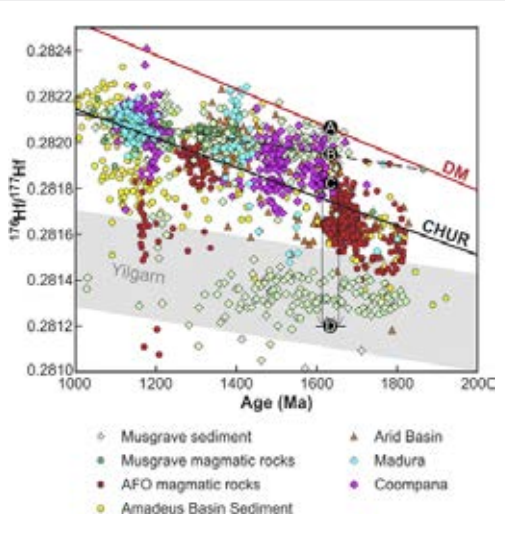

Hf evolution of the Madura Province and western Coompana Province compared to the Albany–Fraser Orogen, Musgrave Province, and adjacent sedimentary basins.

Metamorphic processes and seismicity: the Bergen Arcs as a natural laboratory

The Bergen Arcs expose rocks that formed the root zone of the Caledonian Mountain chain formed by the collision of Laurentia and Baltica at ~400 Ma. They display a well-exposed, high-grade metamorphic terrane where Sveconorwegian granulites, and Caledonian eclogite and amphibolite parageneses co-exist spatially and provide challenging problems related to their inter-relationships and their geodynamic settings. Putnis *et al*., (2017) review some of the ideas that have been proposed for the formation of the granulites and the mechanism of their retrograde hydration during the Caledonian orogeny. They highlight existing problems that need more research. In particular they make some preliminary microstructural observations on the earliest stages of retrogression and suggest that much progress in understanding metamorphism in terranes such as the Bergen Arcs could be made by greater attention to the relationship between seismicity and metamorphism.

The Bergen Arcs have all the attributes of a natural laboratory where questions could be answered on the extent to which seismicity and cataclasis are a necessary precursor to fluid infiltration and metamorphism, the volume of rock processed by cataclasis during an orogenic event and the role of deviatoric stress on the metamorphic reactions.

Putnis A., Austrheim H. and Jamtveit B (2017) Metamorphic processes and seismicity: the Bergen Arcs as a natural laboratory. *Journal of Petrology* 58, 1871-1898.

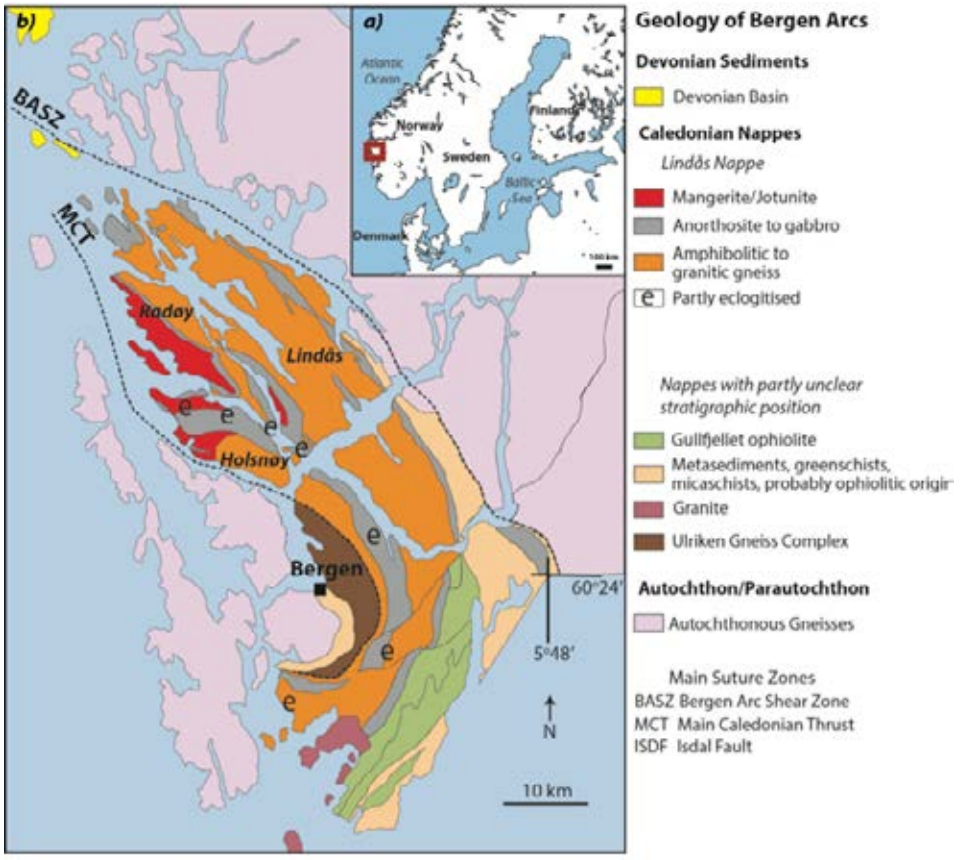

Figure 1

Wilyabrup Sea Cliffs, Margaret River region, WA.

Hydrothermal experiments on symplectite formation

Spruzeniece *et al.,* (2017) describe the microstructural and chemical development of symplectites, obtained in fluid-mediated mineral replacement experiments. During the experiments polymineralic feldspar-rich samples were exposed to aqueous Na–SiO_2 solution at 600ºC and 2 kbar confining pressures for durations of 12 h to 20 days. The resulting reaction rims display high mineralogical and structural complexity and contain two varieties of symplectites, represented by nanometre-scale intergrowths of gehlenite–zeolite and grossular–zeolite grains. The experimental fluid was enriched in ^{18}O isotope in order to trace oxygen redistribution during the reaction. The elevated ^{18}O concentration in the reaction products and the heterogeneity in its distribution suggest that symplectite formation was controlled by dissolution–precipitation mechanisms rather than volume-diffusion processes. Microstructural and chemical observations suggest that symplectite formation occurred in multiple stages in response to spatially heterogeneous and temporarily evolving fluid composition at the reaction interfaces. Their results shed light on the fundamental processes involved in symplectite formation and interpretation of symplectite microstructures.

Spruzeniece L., Piazolo S., Daczko N.R., Kilburn M.R. and Putnis A. (2017) Symplectite formation in the presence of a reactive fluid: insights from hydrothermal experiments. *Journal of Metamorphic Geology* 35, 281-299.

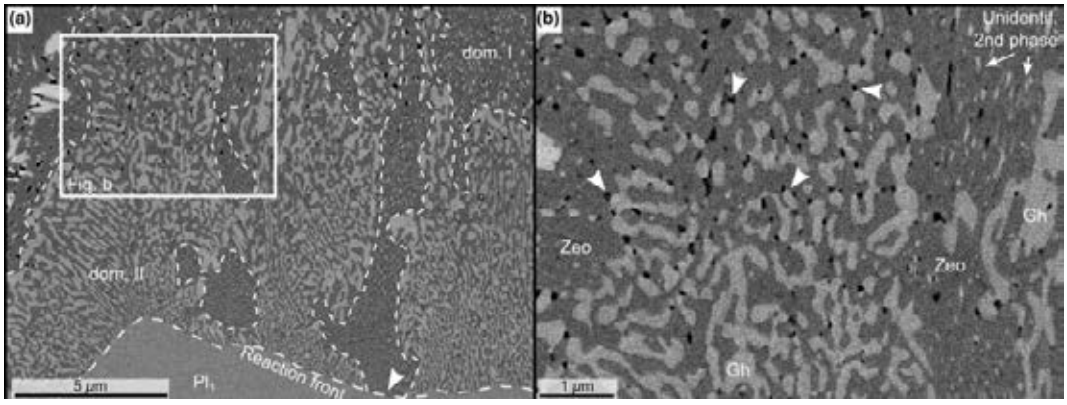

BSE micrographs of typical reaction microstructures showing interface of the reaction rim and parent plagioclase grain Pl_1). Domain I is nano-porous zeolite with small amounts of sub-micrometre sized non-identified second mineral grains, domain II is gehlenite–zeolite symplectite. The white arrowhead marks a discontinuity in domain II where domain I has a direct interface with the parent plagioclase.

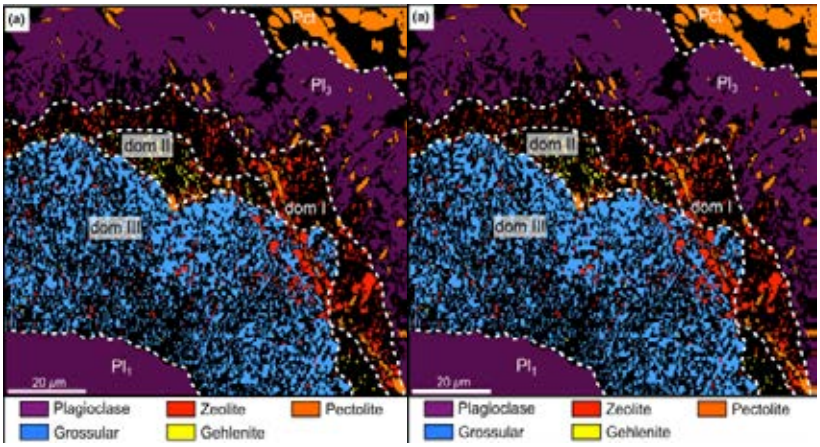

Replacing calcite by fluorite in hydrothermal experiments

Understanding the mechanism and kinetics of the replacement of carbonates by fluorite has applications in Earth sciences and engineering. Pedrosa *et al.*, (2017) reacted samples of Carrara marble with an ammonium fluoride (NH_4F) solution for different reaction times and temperatures. The microstructure of the product phase (fluorite) was analyzed using SEM. The kinetics of replacement was monitored using Rietveld refinements of X ray powder diffraction patterns of the products. After reaction, all samples preserved their size and external morphology (a pseudomorphic replacement). The grain boundaries of the original marble were preserved although each calcite grain was replaced by multiple fine crystals of fluorite creating inter-crystal porosity. The empirical activation energy *Ea* (kJ/mol) of the replacement reaction was determined by both model-fitting and model-free methods. The isoconversional method yielded an empirical activation energy of 41 kJ/mol, and a statistical approach applied to the model-fitting method revealed that the replacement of Carrara marble by fluorite is better fitted to a diffusion-controlled process. These results suggest that the replacement reaction depends on the ion diffusion rate in the fluid phase through the newly formed porosity.

Pedrosa E.T., Boeck L., Putnis C.V. and Putnis A. (2017) The replacement of a carbonate rock by fluorite: Kinetics and Microstructure. *American Mineralogist* 102, 126-134.

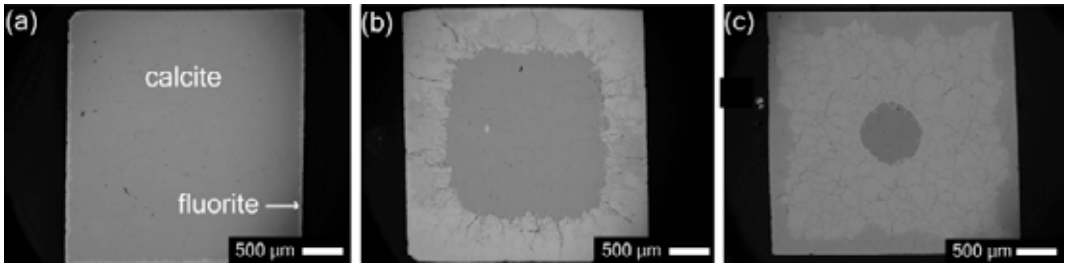

Images of cross sections of cubes of Carrara marble reacted with ammonium fluoride solution (a) for 1 hour at 600ºC (b) for 48 hours at 600ºC and (c) for 4 hours at 1400ºC. The core is the original calcite; the rim is fluorite.

The dynamic olivine surface at high temperatures: implications for extraterrestrial reactivity

Mineral surfaces play a critical role in the solar nebula as a catalytic surface for chemical reactions and potentially acted as a source of water during Earth's accretion by the adsorption of water molecules to the surface of interplanetary dust particles. However, nothing is known about how mineral surfaces respond to short-lived thermal fluctuations that are below the melting temperature of the mineral.

King *et al*., (2017) show that mineral surfaces react and rearrange within minutes to changes in their local environment despite being far below their melting temperature. Polished surfaces of the rock and planetary dust-forming silicate mineral olivine ($(Mg,Fe)_2SiO_4$) show significant surface reorganization textures upon rapid heating resulting in surface features up to 40 nm in height observed after annealing at 1200ºC. Thus, high-temperature fluctuations should provide new and highly reactive sites for chemical reactions on nebula mineral particles. Our results also may help to explain discrepancies between short and long diffusion profiles in experiments where diffusion length scales are of the order of 100 nm or less.

King H.E., Plümper O., Putnis C.V., O'Neill H.St.C., Klemme S. and Putnis A. (2017) Mineral Surface Rearrangement at High Temperatures: Implications for Extraterrestrial Mineral Grain Reactivity. *ACS Earth and Space Chemistry* 1, 113-121.

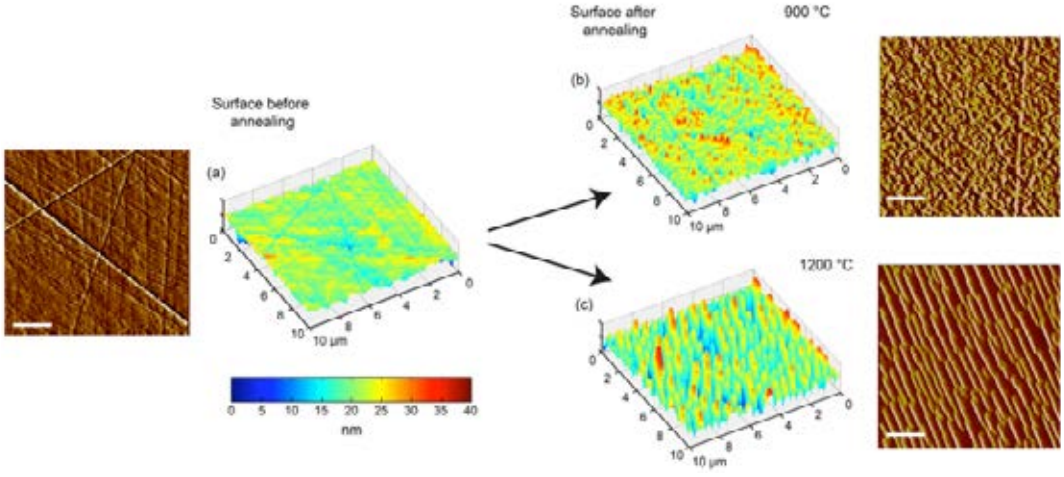

Three-dimensional plots of San Carlos olivine ($Mg_{1.8}Fe_{0.2}SiO_4$) surface topography. Scratches are present on the surfaces before annealing (a) along with some areas of slightly higher topography. (a) A typical example of an original surface from the 1200ºC experiment; different crystals were used for the experiments at the two different temperatures. These areas of higher topography are aligned with the polishing scratches. (b) After annealing at 900ºC for 1750 min, the surface has a clear increase in roughness with the formation of small islands. Some scratches are still present on the surface, however the roughness islands now have an orientation unrelated to the scratch orientations. (c) When San Carlos is annealed at 1200ºC for 1300 min, orientated undulations are visible on the surface reaching up to 40 nm in height. Evidence of original scratches is minimal. Scale bar in AFM deflection images is 2 µm.

The Western Australian $^{40}Ar/^{39}Ar$ Isotope Facility (WAAIF)

The $^{40}Ar/^{39}Ar$ dating method is used to measure the age and timing of a large variety of geological processes, from meteorite samples as old as the Earth (4.5 billion years) to the age of historical events such as the Vesuvius eruption (79 AD). The Ar technique can be applied to any rocks and minerals that contain K (e.g. hornblende, sanidine, plagioclase and basalts) is also used to date a myriad of other geological events such as volcanism, tectonic plate movements, mountain building rates, sediment formation, weathering and erosion, hydrothermal fluid movements, and alteration and diagenesis of minerals. The Western Australian Argon Isotope Facility includes two noble gas mass spectrometer (MAP 215-50 and the ultra-precise ARGUS VI) and is equipped with two laser systems and a furnace and is operated by A/ Prof. Fred Jourdan.

The ARGUS VI noble gas mass spectrometer.

Serpentinite.

Research reports

ADVANCED RESOURCE CHARACTERI-SATION FACILITY

Advanced Resource Characterisation Facility

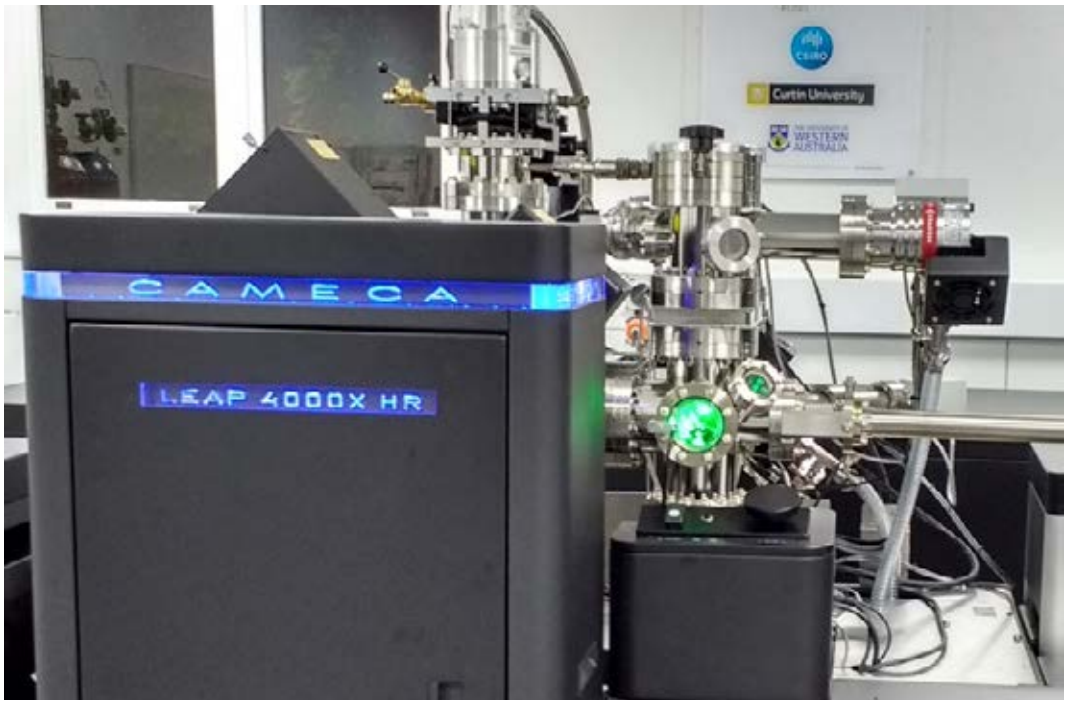

Geoscience Atom Probe Facility

The Advanced Resource Characterisation Facility (ARCF) is a multi-institutional facility comprising high-end analytical equipment located at Curtin, UWA and CSIRO. At Curtin University, the Facility includes the Cameca LEAP 4000X HR atom probe microscope and a Tescan LYRA FIB-SEM, both housed within the John de Laeter Centre (JdLC). These laboratories have been particularly focused on the development of nanoscale analysis of geological materials, since their establishment in 2015. The installation of the FEI Talos TEM in the JdLC in 2017 has provided a powerful complementary tool for the analysis of minerals at nanometer scales. In addition to imaging and microanalysis of FIB-prepared TEM foils, the TEM has also been used for correlative imaging of atom probe needle specimens.

In 2017 the geoscience atom probe has enabled research across a wide range of minerals, addressing many geoscience questions in fields from geochronology to fossilisation processes.

Particular highlights from 2017 include studies of refractory metal nuggets from ancient meteorites. This work has revealed the incorporation of sulfur into some of the first solid material to have condensed during the early stages of solar system formation. The discovery of sulfur in these sub-m refractory metal nuggets places constraints on the dynamics of the photo-planetary disc and reveals some of the first geochemical evidence for large solar-system-wide transport processes.

The atom probe was also used to investigate the nanoscale mobility of Pb in monazite from the Sandmata Metamorphic Complex (Rajasthan, India) – the first published atom probe study of monazite. Clusters 10 nm in size, and with a composition consistent with apatite, were observed throughout the

sample volume (Figure 1), and found to be enriched in ^{208}Pb, unsupported by the parent ^{232}Th. This nanoscale inhomogeneity in Pb has implications for using monazite as a geochronometer, depending on the analysis volume used in dating the sample.

In 2017, the atom probe facility contributed to 25 conference presentations, including several keynote and invited talks, and a 2-day workshop on correlative microscopy in the geosciences. Several articles were also published in leading journals.

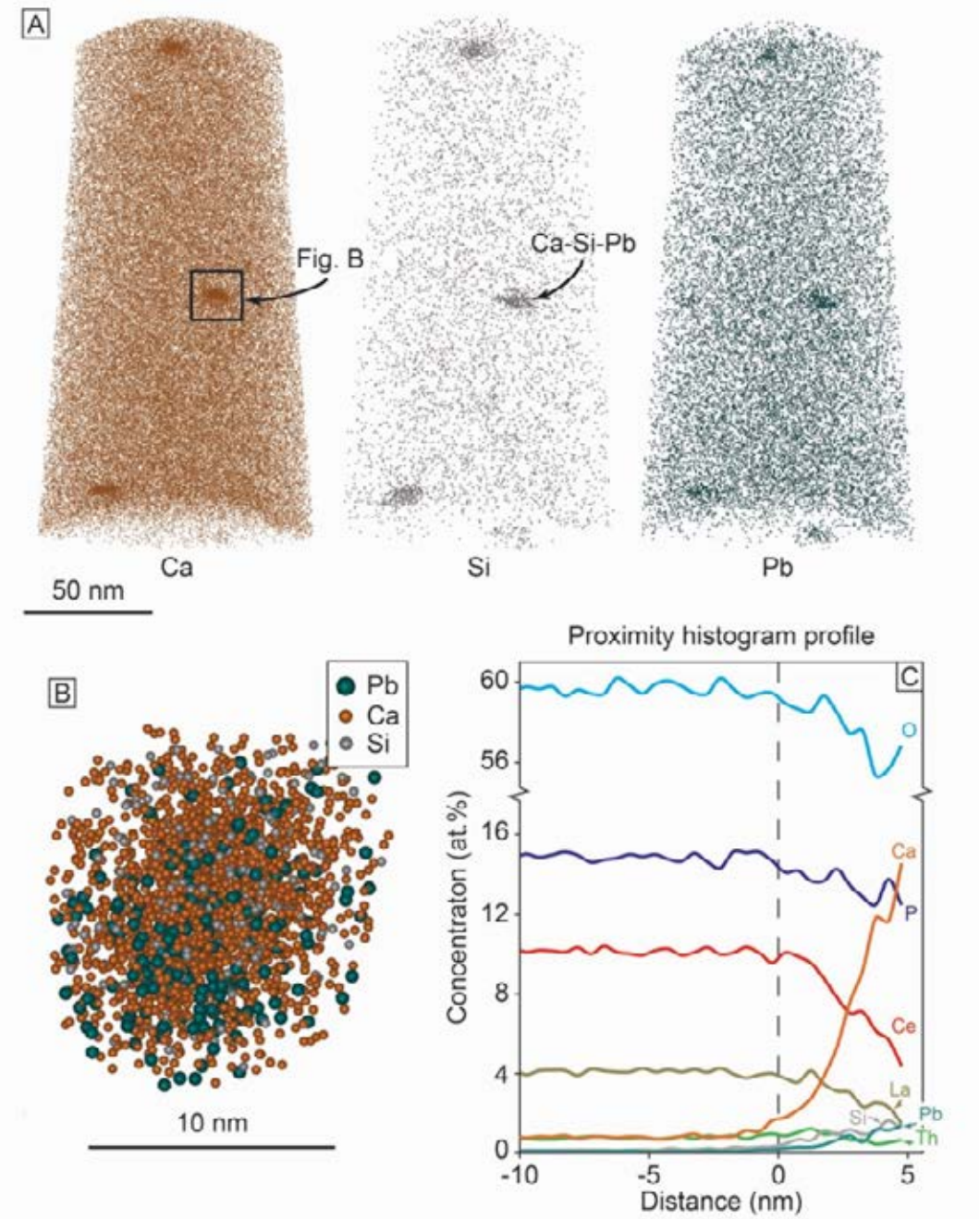

Figure 1. A) Reconstructed three-dimensional atom probe image of Ca, Si and Pb (^{206}Pb + ^{208}Pb) distribution within monazite. Each sphere represents one atom. The maps show the presence of three Ca-Si-Pb clusters. B) Close up of the largest cluster. C) Proximity histogram profile, referenced to a 1.3 at.% Ca isoconcentration surface. The histogram shows the decrease of O, P and REEs but the increase of Ca, Si and Pb.

Kimberley WA.

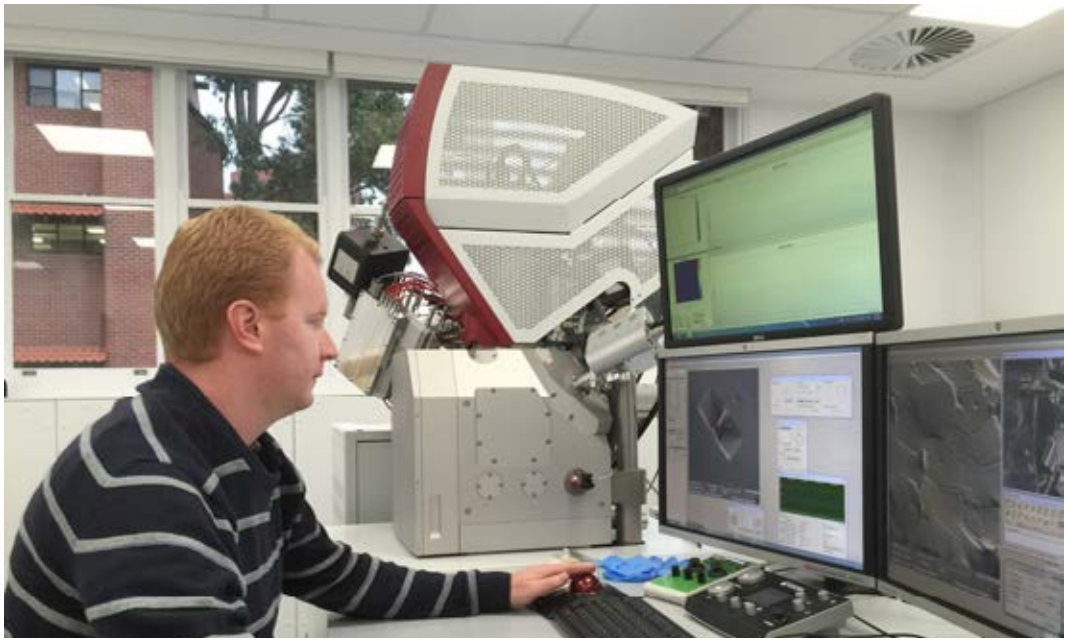

Tescan Lyra FIB-SEM with ToF-SIMS

The Tescan Lyra focused ion beam scanning electron microscope (FIB-SEM) facility is used to support research involving the Geoscience Atom Probe as well as for high spatial resolution time of flight secondary ion mass spectrometry (ToF-SIMS). The Lyra is central to a number of analysis workflows and thus was involved in broad range of projects in 2017. Data from the instrument was used in 8 journal articles and a number of conference presentations/papers that were published in 2017. Research highlights included high spatial resolution mapping of the lithium distribution in various micaceous ores; the discovery of low temperature decomposition of calcite to amorphous carbon under stable sub-seismic slip conditions; the discovery of red and white blood cell-like structures in collagen and cholesterol in a 180 Ma ichthyosaur bone (figure 2); and, part of the refractory metal nugget project summarised above.

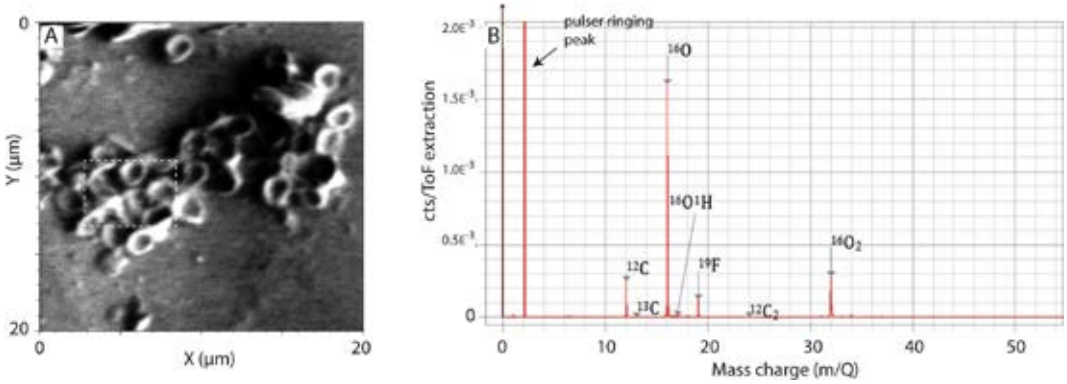

Figure 2. ToF -SIMS analysis of RBC-like structures in the ichthyosaur vertebra. (A) Secondary image of the RBC-like structures by ToF-SIMS. The white rectangle corresponds to the area where the mass spectra was acquired. (B) Negative ions mass spectra showing the presence of C, O and Fluorine (F) specifically associated with the RBC-like structures. Plet *et al.* 2017.

Research reports

ORGANIC AND ISOTOPE GEOCHEMISTRY

Organic and Isotope Geochemistry

(Paleo)climate, Oceans, Continents, Life & Our Resources

The molecular, genetic and stable isotopic composition of organic matter is determined by its source. The elements – hydrogen, carbon, sulfur and nitrogen are basic constituents of organic matter and play key roles in biochemistry, ecology, climate change, hydrologic and atmospheric processes. Therefore stable isotopic compositions preserved in organic matter can provide powerful insights into these processes.

Compound specific isotope analysis – CSIA is important for determining the stable isotopic compositions of individual organic components in complex mixtures (e.g., petroleum, natural gases, sediments, soils, groundwater, potable waters and extracts from plants and other media). The WA Organic & Isotope Geochemistry (WA-OIG) led by Professor Kliti Grice are applying the CSIA technique (carbon, hydrogen & nitrogen) and molecular geochemical and (paleo) genomic techniques to infer relationships between components so that their origins and formation pathways can be established.

Research Themes

The research themes investigated within WA-OIG using compound specific isotopes, lipid biomarker geochemistry and (paleo) genomics are:

1. Natural Resources (Petroleum & Minerals)
2. Microbial Communities
3. Biochemical Pathways
4. Integrated Ocean Drilling Projects (IODP) & Petroleum
5. Mass Extinctions
6. Climate & Paleoclimate
7. Environment
8. Medical Geochemistry

Image: Alex Session.

Viruses in microbial mats from Shark Bay, WA: unravelling their role during petroleum biodegradative processes

Viruses represent only 5% of total biomass of microbial mats but are significantly more abundant than bacterial and archaeal communities. A number of previous studies have demonstrated that bacteria in microbial mats are involved in degradation of petroleum compounds but the role that viruses play in regulating these and other bacteria in microbial mats remains unknown.

This study will explore the role of viral communities in microbial mats from a hypersaline environment in Shark Bay (Western Australia), and their potential role in biodegradation of petroleum. Smooth and Pustular microbial mats samples are being exposed to petroleum during a time series incubation experiments to monitor viral, microbial, chemical and isotopic changes in this ecosystem.

Jiménez Y., Coolen M., Grice K. (2017). Revealing the role of viruses during a petroleum biodegradative experiment, using microbial mats of Shark Bay, WA. *2017 TIGeR Conference*, WA: Perth

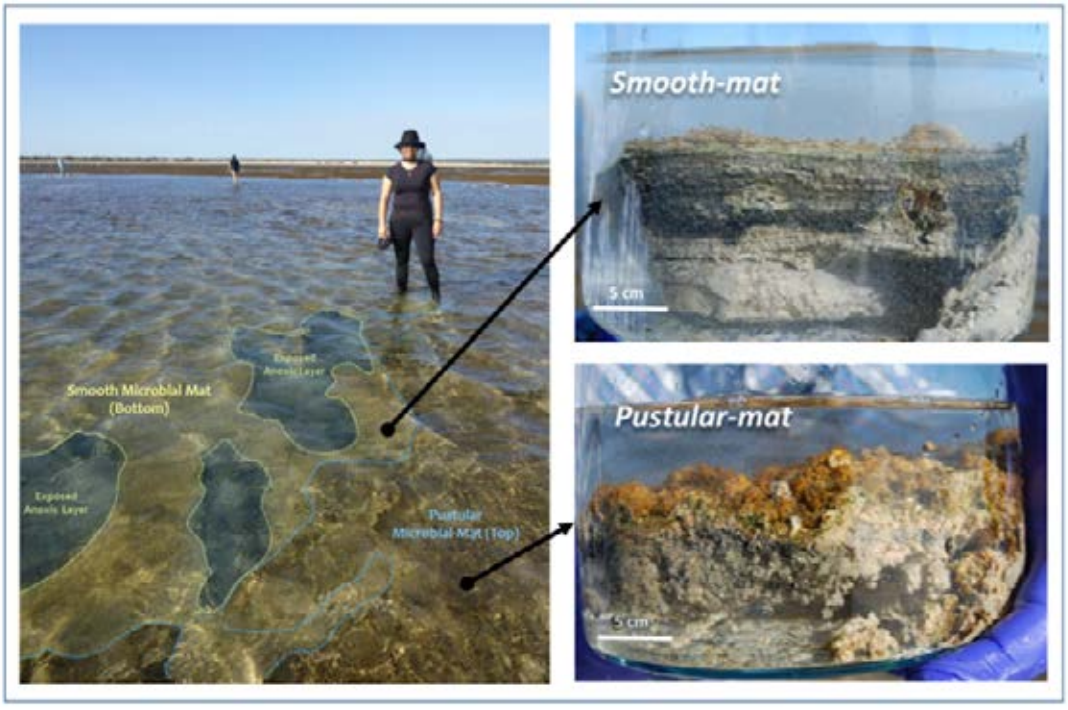

Nilemah Embayment, Hamelin Pool, Shark Bay, Western Australia: Intertidal/subtidal zone (left). Samples collected for experimentation: Smooth and Pustular mats (right).

Fieldwork, Shark Bay WA.

Utilizing microbial genomics and lipid biomarkers to study maturity, provenance, and biodegradation of subsurface petroleum

Studying the genomic diversity and metabolic function of microbial communities in petroleum reservoirs of the North West Shelf (NWS), Western Australia. Petroleum reserves in the NWS, especially the North Carnarvon Basin, is subject to extensive biodegradation. While there is abundant geochemical data pertaining to biodegradation in the NWS, there is a lack of microbial ecology data from the NWS that relates to petroleum degradation.

Cheah *et al*., (2017) are using a combination of methods involving organic and isotope geochemistry, metagenomics and metatranscriptomics, and anaerobic incubations, to analyze microbial community structure and function, as well as parameters relating to microbial degradation of petroleum. The information that will be gleaned from microbial ecology studies will be applied to secondary extraction of heavy oil trapped in reservoirs and conversion of residual oil to economically viable methane. Cheah has recently presented his research for candidacy and is currently in the process of obtaining samples and preparing them for analyses.

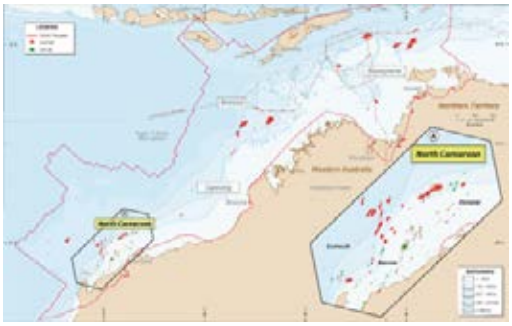

Figures modified from Longley *et al.,* (2001)

Cheah D., Wuchter C., Grice K., & Coolen M.J.L. (2017). Utilizing microbial genomics and lipid biomarkers to study maturity, provenance, and biodegradation of subsurface petroleum in the North West Shelf, Western Australia. Poster presented at TIGeR 2017 meeting, Bentley, WA.

Oldest land-plant microfossils in Australia found in WA's Canning Basin

The Great Ordovician Biodiversification Event (GOBE) is regarded as one of the most significant evolutionary events in the history of Phanerozoic life. Spaak *et al*., (2017) integrated palynological, petrographic, molecular and stable isotopic (δ13C of biomarkers) analyses of cores from four boreholes that intersected the Goldwyer Formation, Canning Basin, Western Australia, to determine depositional environments and microbial diversity within a Middle Ordovician epicontinental, tropical sea.

Research into early land plants relies mostly on the preservation and recovery of acid resistant cryptospores found in sedimentary rock. Cryptospores were identified in drillcores and are most likely derived from bryophyte-like plants, making this is the oldest record of land plants in Australian Middle Ordovician strata. Biomarkers in several samples from this unit that also support derivation from terrestrial organic matter include benzonaphthofurans and δ13C-depleted mid-chain n-alkanes.

This research contributes to a greater understanding of Ordovician marine environments from a molecular perspective since few biomarker studies have been undertaken on age-equivalent sections. Furthermore, the identification of the oldest cryptospores in Australia and their corresponding terrestrial biomarkers provides further insight into the geographical distribution and evolution of early land plants.

Spaak G., Edwards D.S., Foster C.B., Pagès A., Summons R.E., Sherwood N., Grice K. (2017). Environmental conditions and microbial community structure during the Great Ordovician Biodiversification Event; a multi-disciplinary study from the Canning Basin, Western Australia. *Global and Planetary Change*, 159, 93-112.

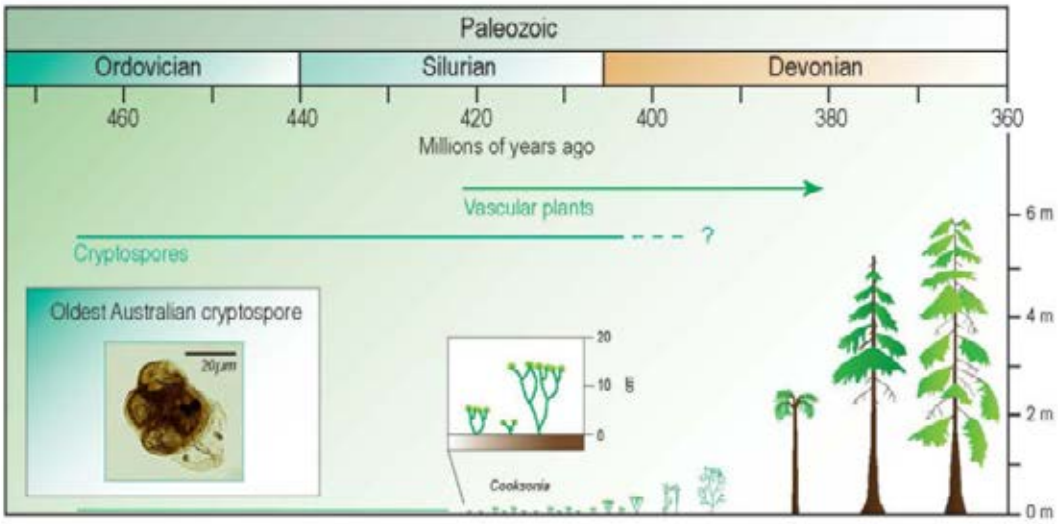

How Jurassic ichthyosaurs adapted to low oxygen levels

Carbonate concretions are known to contain well-preserved fossils and soft tissues. Recently, biomolecules (*e.g.* cholesterol) and molecular fossils (biomarkers) were also discovered in a 380 million-year-old concretion, revealing their importance in exceptional preservation of biosignatures.

Plet *et al.,* (2017) used a range of microanalytical techniques, biomarkers and compound specific isotope analyses to report the presence of red and white blood cell-like structures as well as platelet-like structures, collagen and cholesterol in an ichthyosaur bone encapsulated in a carbonate concretion from the Early Jurassic (~182.7 Ma). The red blood cell-like structures are four to five times smaller than those identified in modern organisms. Transmission electron microscopy (TEM) analysis revealed that the red blood cell-like structures are organic in composition.

They propose that the small size of the blood cell-like structures results from an evolutionary adaptation to the prolonged low oxygen atmospheric levels prevailing during the 70 Ma when ichthyosaurs thrived. The $\delta 13C$ of the ichthyosaur bone cholesterol indicates that it largely derives from a higher level in the food chain and is consistent with a fish and cephalopod diet. The combined findings above demonstrate that carbonate concretions create isolated environments that promote exceptional preservation of fragile tissues and biomolecules.

Plet, C., Grice, K., Pagès, A., Verrall, M., Coolen, M.J.L., Ruebsam, W., Rickard, W.D.A., Schwark, L., 2017. Palaeobiology of red and white blood cell-like structures, collagen and cholesterol in an ichthyosaur bone. *Scientific Reports* 7, 13776.

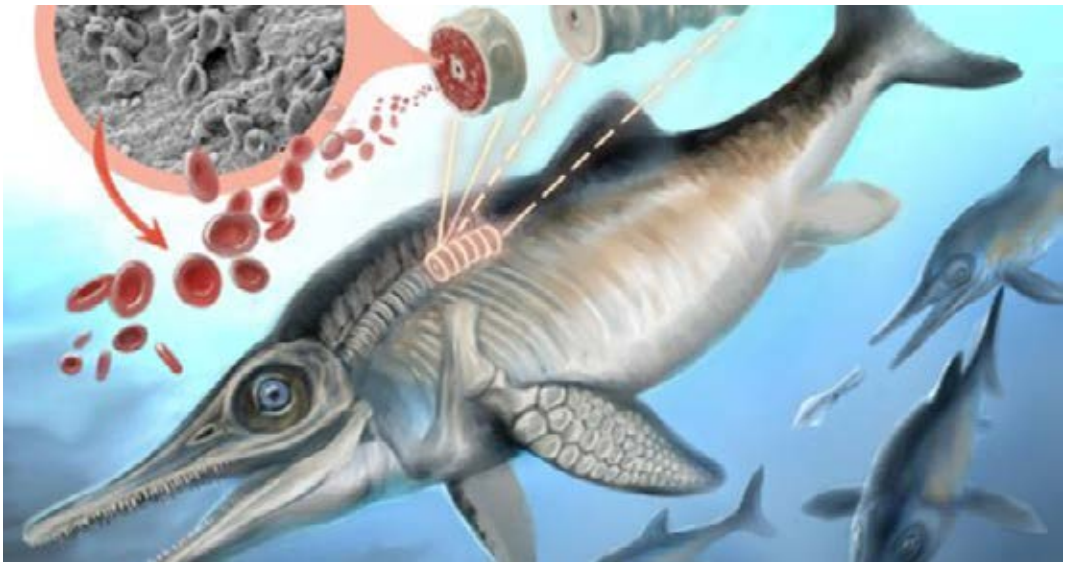

Occurrence and significance of phytanyl arenes across the Permian-Triassic boundary interval

Phytanyl benzene and phytanyl toluene were identified in Permian-Triassic (P/T) boundary sections from mid-palaeolatitude locations (Spitbergen, Eastern Greenland and Western Australia). These compounds appear almost exclusively in post-extinction intervals, and show similar distribution patterns to the previously-identified P/T marker *n*-C_{33} alkylcyclohexane, suggesting their parent organisms flourished after the extinction and shared a similar ecological niche. Their absence in the equatorial P/T section in Meishan, South China may indicate that their source is climate-controlled.

Grotheer H., Le Métayer P., Piggott M.J., Lindeboom E. J., Holman A. I., Twitchett R. J., Grice K. (2017). Occurrence and significance of phytanyl arenes across the Permian-Triassic boundary interval. *Organic Geochemistry*, 104, 42-52.

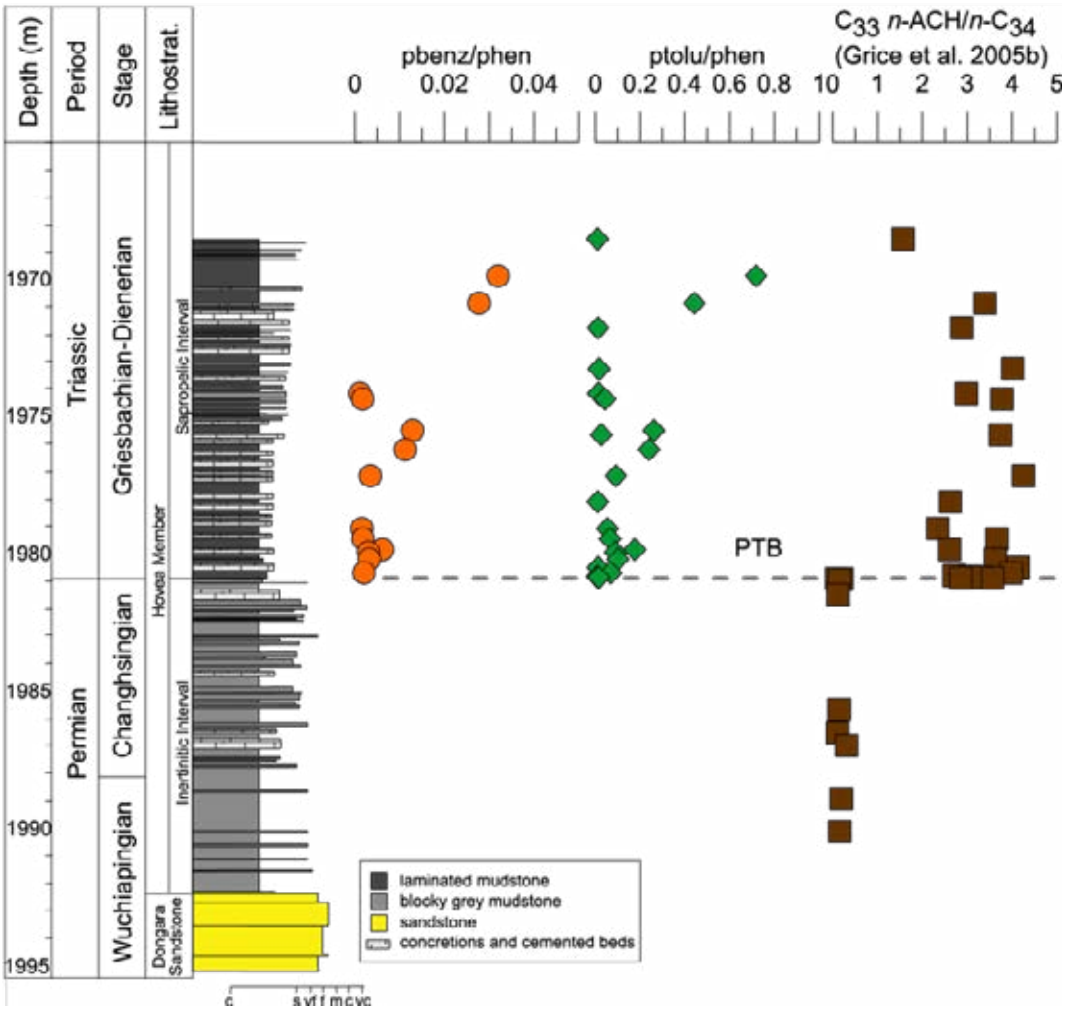

Relative abundances of phytanyl benzene, phytanyl toluene, and *n*-C_{33} alkylcyclohexane in the P/T Hovea-3 core, Perth Basin, Western Australia. Phytanyl benzene, phytanyl toluene are observed only after the P/T boundary, coincident with an increase in abundance of *n*-C_{33} alkylcyclohexane.

Stromatolites, Shark Bay WA.

1-Chloro-*n*-alkanes: Potential mangrove and saltmarsh vegetation biomarkers

Distinct distributions of long-chain 1-chloro-*n*-alkanes were identified in solvent extracts from a variety of Australian mangrove species and salt marsh vegetation. The distribution of various chain lengths, and their $\delta^{13}C$ values, suggest that the biosynthesis of these compounds is related to that of other plant wax compounds, i.e. via decarboxylation of long-chain *n*-alkanols. Their biological function however remains unknown. The higher abundance of 1-chloro-*n*-alkanes in mangrove and saltmarsh species indicates a possible use as halophyte biomarkers.

Tulipani S., Schwark L., Holman A.I., Bush R.T., Grice K. (2017). 1-Chloro-n-alkanes: Potential mangrove and saltmarsh vegetation biomarkers. *Organic Geochemistry*, 107, 54-58.

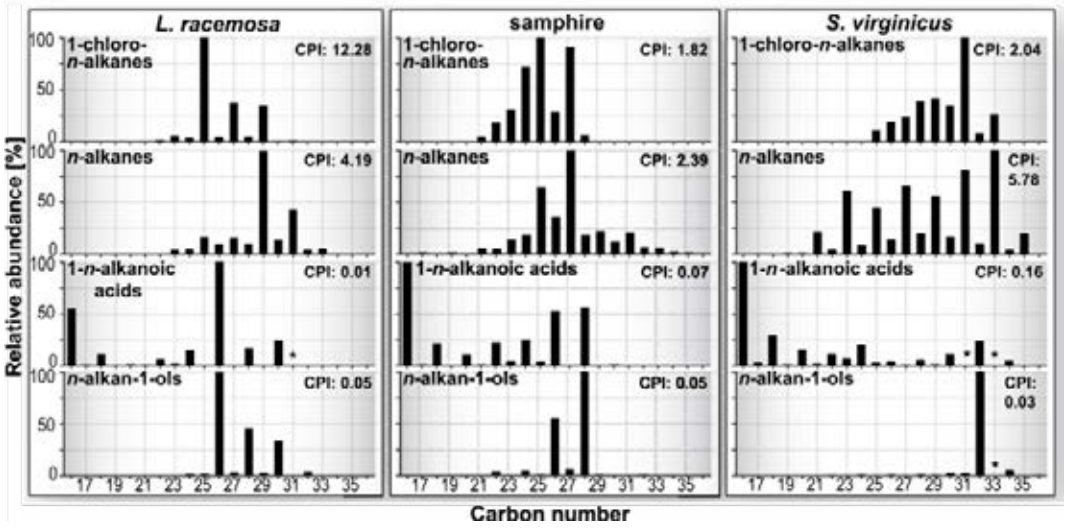

Chain length distribution of 1-chloro-*n*-alkanes compared to other plant wax compounds in three species of Australia halophytes.

δ34S character of organosulfur compounds in kerogen and bitumen fractions of sedimentary rocks

Although it is becoming common to analyse organic extracts of rocks for their carbon isotopic signatures, sulfur isotopes are much more rarely studied. Grotheer et al (2017) reported the use of hydropyrolysis (HyPy) of sulfur-containing oil mature rock samples from two geologic settings. Each were found to produce much higher concentrations of organosulfur compounds (OSCs) compared to their free occurrence in the bitumen. The isotopic sulfur signature δ34S values of the most abundant OSCs from the kerogen and in the bitumen, were measured by gas chromatography inductively coupled plasma mass spectrometry (GC-ICP-MS). The tricyclic sulfur-containing dibenzothiophene and its methylsubstituted homologues from the HyPy processed kerogen fractions showed a distinct 34S depletion, with δ34S values up to 12‰ lighter than their bitumen occurrence. The different δ34S values of OSCs from the kerogen and bitumen fractions is likely reflective of differences in timing of production, reduced sulfur sources or organic sulfurisation mechanism.

Grotheer H., Greenwood P.F., McCulloch M.T., Böttcher M.E., Grice K. (2017). δ34S character of organosulfur compounds in kerogen and bitumen fractions of sedimentary rocks. *Organic Geochemistry*, 110, 60-64.

Palaeoclimatology

Using isotopic signatures in micromammal teeth for palaeoclimatic reconstructions

Barham *et al.,* (2017) and Roelofs et al (2017) have made significant advances in the use of biogenic apatite O-isotopes for palaeoenvironmental/palaeoecological/ palaeoclimatic reconstructions across marine and terrestrial settings.

Palaeoenvironmental O-isotope studies in marine environments are typically restricted to the Cenozoic for carbonates, while phosphatic conodont microfossils have been analysed for the Palaeozoic. Our work has investigated several problems associated with histological variation and ecology to demonstrate the potential for the robust biogenic apatite tissues of fish to be utilised as a environmental proxy across most of the Phanerozoic.

On land, interest has grown in the application of O-isotope studies to micro-mammal teeth since they are a common predator-concentrated fossil within cave sequences that are commonly investigated for their archaeological and geological records. However, previously no-one considered the potential modification of the geochemical signature of fossils caused by partial digestion during predation. Our work presents data to demonstrate the potential for a common predator (barn-owls) to modify O-isotope values of ingested teeth and also discusses the broader chemical and physical modification differences reflected in ingested teeth across various predator species. This will have a significant bearing on future utilisation of micro-mammal teeth to produce high-resolution terrestrial palaeoclimatic/environmental records.

Barham, M., Blyth, A., Wallwork, M., Joachimski, M., Martin, L., Evans, N., Mawson, P., McDonald, B. (2017). Digesting the data? Effects of predator ingestion on the oxygen isotopic signature of micromammal teeth. *Quaternary Science Reviews*, 176, 71-84.

Roelofs, B., Barham, M., Cliff, J., Joachimski, M., Martin, L., Trinajstic, K. (2017). Assessing the fidelity of fossil marine microvertebrate $\delta^{18}O$ signatures and their potential for palaeo-ecological and –climatic reconstructions. *Palaeogeography, Palaeoclimatology, Palaeoecology*, 465 (A), 79-92.

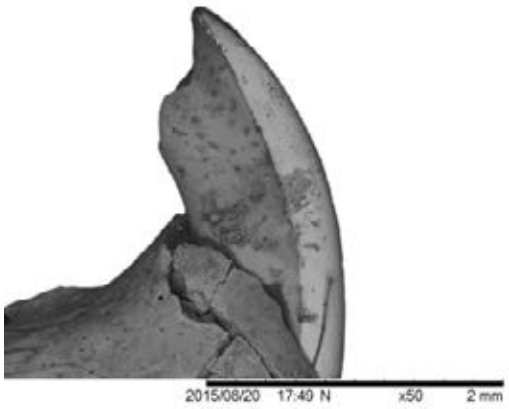

Degraded extension of an untreated mandibular mouse incisor recovered from a male ghost bat scat. Tooth shows significant reduction of exposed tip and progressive degradation of enamel-dentine junction and exaggeration of enamel crystallite texture as a result of partial digestion.

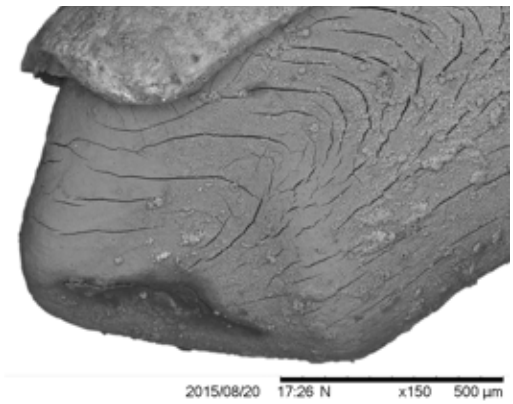

Tip of an untreated mouse incisor recovered from the scat of a female Tasmanian devil exhibiting significant tissue degradation, dentinal cracking, enamel corrosion, tissue separation and reduction of protrusions as a result of partial digestion.

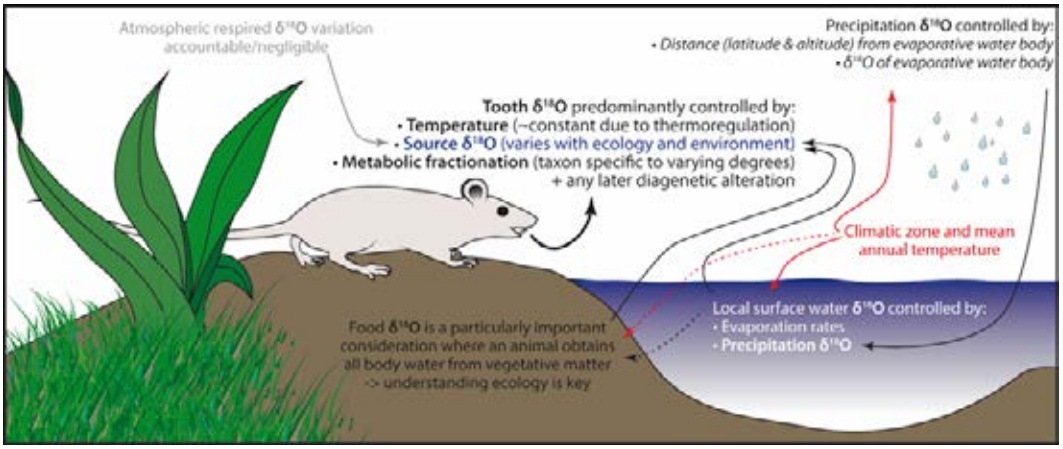

Summary of the known significant controls on the $\delta^{18}O$ signature of micro-mammal teeth prior to this work.

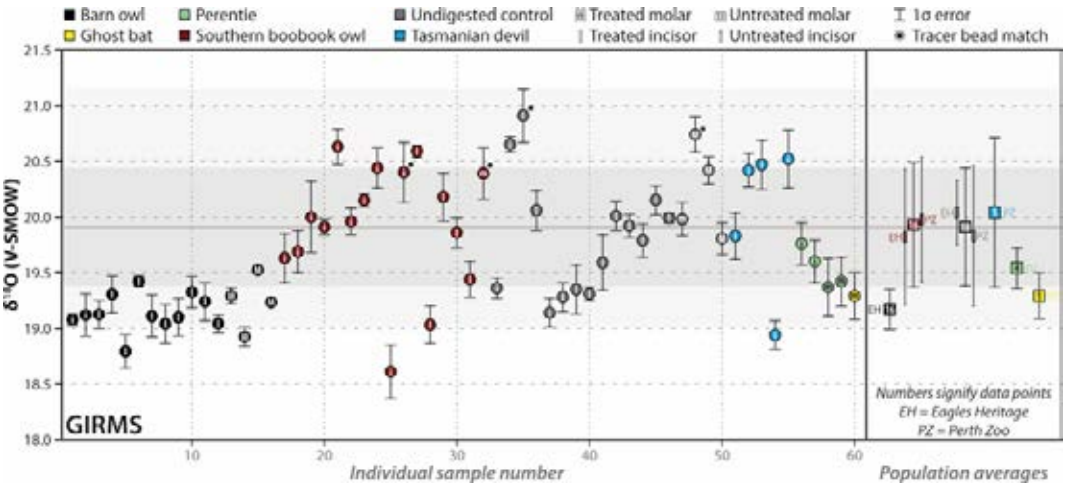

Gas isotope ratio mass spectrometry O-isotope data of micromammal teeth ingested by various predator species. Data are shaded and arranged according to predator species with letters indicating the tooth type and whether the sample was treated or untreated to remove organics. Overall population averages are given on the right along with the source of samples. Grey horizontal shading corresponds to the average, population 1σ and maximum range of the 18 non-ingested control teeth analysed. Asterisks indicate samples matched to an individual mouse cadaver using tracer beads. Note the clear depletion in teeth ingested by Barn owls, suggesting this species is capable of modifying the oxygen isotopic composition of ingested prey biominerals.

Fieldworkers, Shark Bay WA.

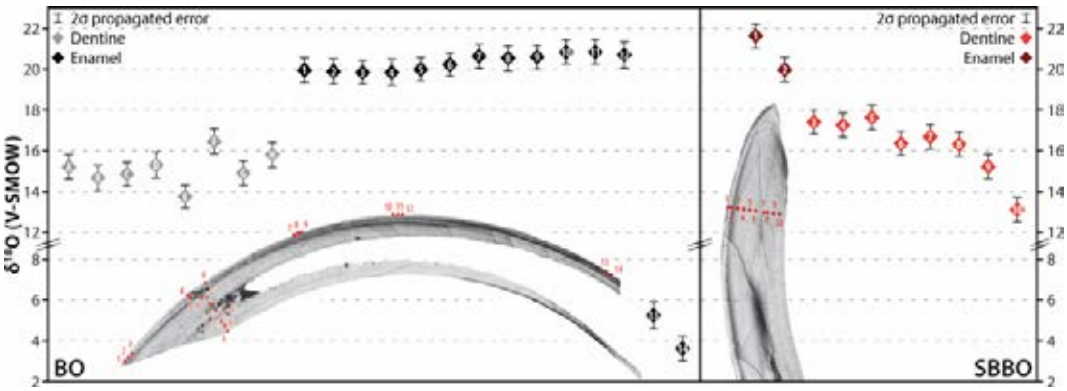

Secondary ion mass spectrometry O-isotopic histological and spatial spot transects of mouse incisors partially digested during predator ingestion. Greyscale images of cut and polished teeth taken after SIMS analysis and show cracks developed subsequent to mounting due to pressure differences and desiccation. Note the break in the y-axis between 8 and 12‰. BO - barn owl; SBBO - southern boobook owl. Note the significant depletion in dentine O-isotope values due to the more labile nature of the less mineralised tissue.

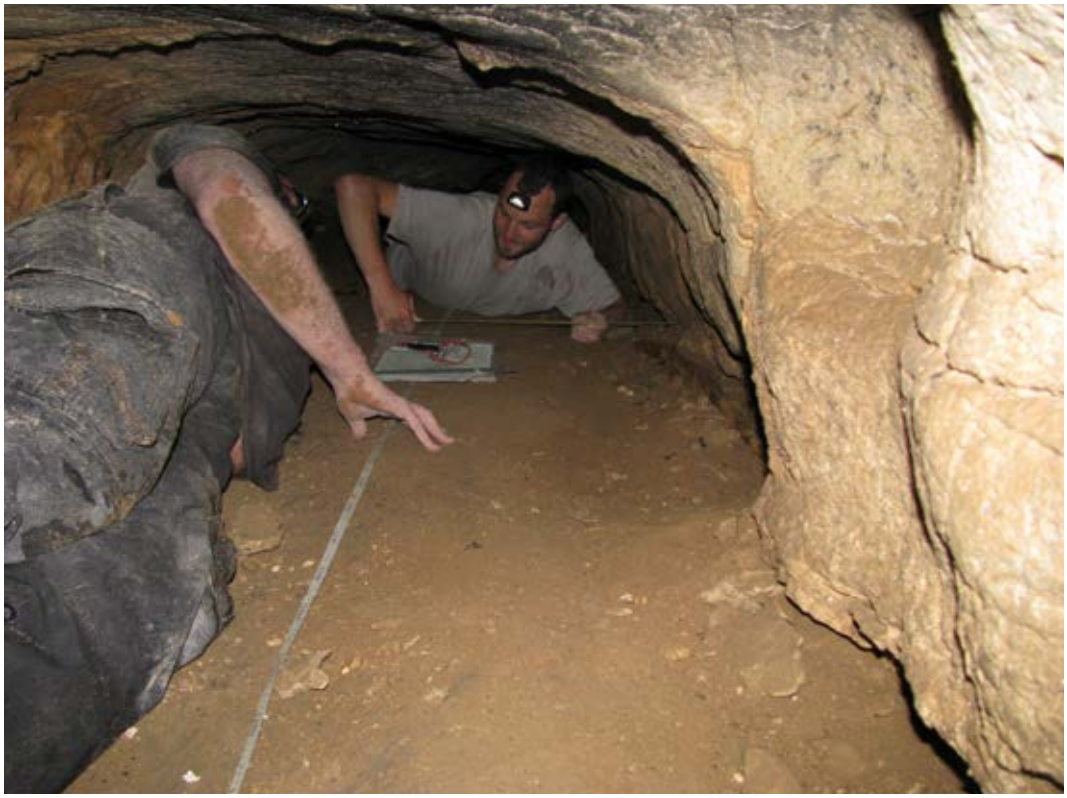

Research reports

TECTONICS AND GEODYNAMICS

Tectonics and geodynamics

Tectonics and geodynamics involve the understanding of processes related to the motion of tectonic plates through time such as mountain building, basin formation and cyclic evolution of supercontinents, and the interaction of tectonic plates with the Earth's deep interior. Such knowledge is essential for understanding life evolution, environmental changes, and the exploration of mineral and energy resources.

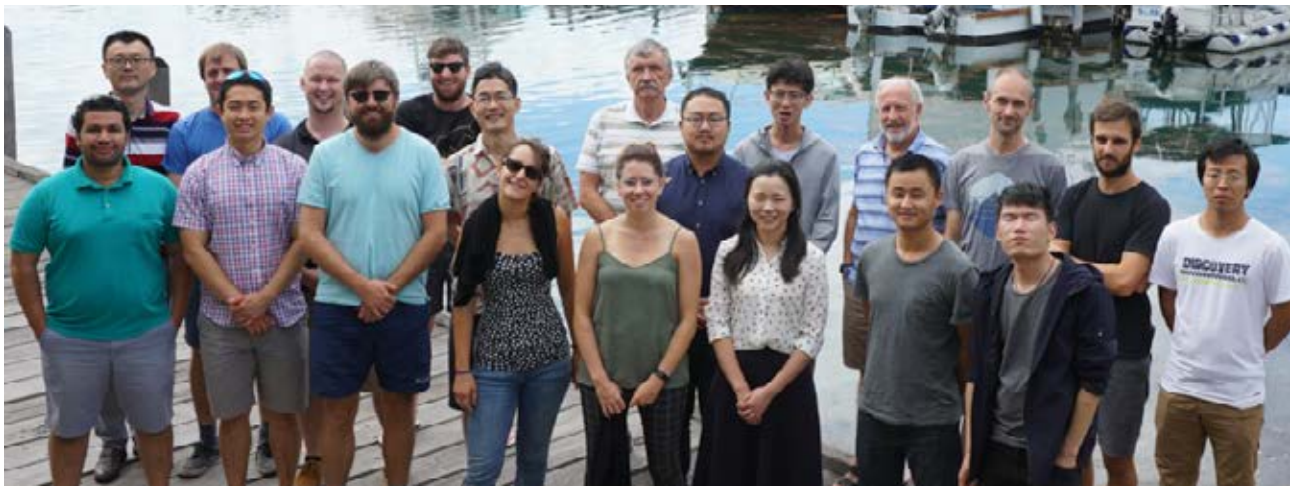

The Earth Dynamics Research Group.

The Earth Dynamics Research Group

Supercontinent Cycles and Global Geodynamics — How the Earth Engine Works, is mainly funded by an ARC Laureate Fellowship grant to Zheng-Xiang Li, a flagship research project funded by the ARC Center of Excellence for Core to Crust Fluid Systems and Curtin University matching funds.

We study the dynamic distribution and evolution of tectonic plates on Earth through time, geodynamic driving mechanisms and tectonic processes, and their relevance to Earth resources and environments. We have a particular focus on supercontinent cycles, global plume records, and 4D geodynamic modelling.

Our research involves palaeomagnetism, all aspects of field-based studies, geochemical, petrological, and geochronological analyses, data-mining, numerical modelling, and regional to global syntheses.

The North Queensland team.

Our field regions cover all major cratons of Australia, and many other parts of the world. In 2017 our research programs started to produce groundbreaking results, including field-based program to investigate northeastern Australia's record of the assembly and breakup of the supercontinent Nuna, geochronological and palaeomagnetic investigations of Precambrian mafic igneous rocks, 4D geodynamic modeling, and global syntheses. Some of the results were published during the year, but most will be published in 2018.

LIP barcoding the Yilgarn Craton: the discovery of the 1.9 Ga Boonadgin dyke swarm points to a possible link with India

Mafic dyke swarms are important markers for supercontinent reconstructions and mantle plumes and also act as indicators of local tectonic setting, including paleostress fields and pre-existing crustal weaknesses. Stark *et al*., (2017) identified a new NW-trending mafic dyke swarm in southwestern Yilgarn Craton, dated at 1888 ± 9 Ma with ID-TIMS U-Pb method on baddeleyite from a single dyke and at 1858 ± 54 Ma, 1881 ± 37 and 1911 ± 42 Ma with *in situ* SHRIMP U-Pb on baddeleyite from three dykes. The newly named Boonadgin dyke swarm is synchronous with post-orogenic extension and deposition of granular iron formations in the Earaheedy basin in the Capricorn Orogen and its emplacement may be associated with far field stresses. Emplacement of the dykes may also be related to initial stages of rifting and formation of the intracratonic Barren Basin in the Albany-Fraser Orogen, where the regional extensional setting prevailed for the following 300 million years. Recent studies and new paleomagnetic evidence raise the possibility that the dykes could be part of the coeval 1890 Ma Bastar-Cuddapah LIP in India. Globally, the Boonadgin dyke swarm is synchronous with a major orogenic episode and records of intracratonic mafic magmatism on many other Precambrian cratons, having been "missing" in the Yilgarn Craton until now.

Stark, J.C., Wang, X.-C., Denyszyn, S.W., Li, Z.-X., Rasmussen, B., Zi, J.-W., Sheppard, S., Liu, Y., 2017. Newly identified 1.89 Ga mafic dyke swarm in the Archean Yilgarn Craton, Western Australia suggests a connection with India. Precambrian Res. *In Press*. https://doi.org/10.1016/j.precamres.2017.12.036

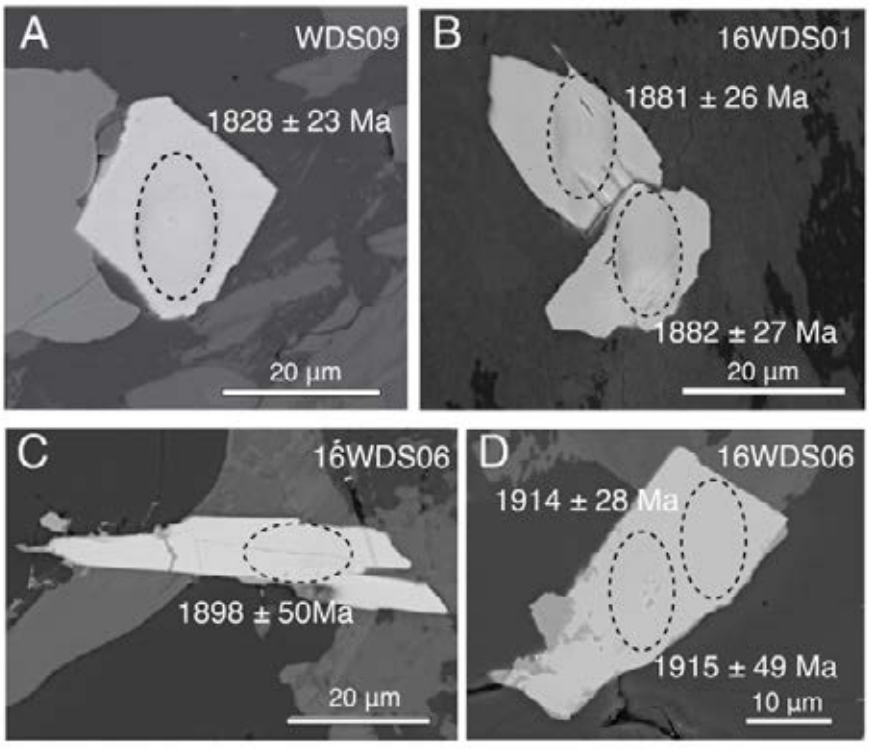

SEM backscatter images showing SHRIMP baddeleyite spots and dates for the Boonadgin dykes. (A) WDS09-2B (B) 16WDS01-372B (C) 16WDS06-405B (D) 16WDS06-406B.

Lake Bassong, Tibetan Plateau.

Finding melted mud in the mantle

As direct observation of sediment melt generation at mantle depths is not possible, melting of subducted sediment remains controversial. Geochemical fingerprints provide indirect evidence for subduction delivery of sediment to the mantle; however, sediment abundance in mantle-derived melt is generally low (0%–2%), and difficult to detect.

Spencer *et al*., (2017) provide evidence for melting of subducted sediment in granite sampled from an exhumed mantle section found in the Oman-UAE ophiolite. Peraluminous granite dikes that intrude peridotite in the Oman–United Arab Emirates ophiolite have U-Pb ages that predate obduction. The dikes have unusually high oxygen isotope ($\delta^{18}O$) whole rock and quartz values and yield the highest $\delta^{18}O$ zircon values known (14–28‰ VSMOW). The extremely high oxygen isotope ratios uniquely identify the melt source as high-$\delta^{18}O$ pelitic and/or siliciceous mud, as no other source could produce granite with such anomalously high $\delta^{18}O$. Formation of high-$\delta^{18}O$ sediment-derived granite within peridotite requires subduction of sediment to the mantle, where it melted and intruded the overlying mantle wedge.

The granite suite contains the highest oxygen isotope ratios reported for igneous rocks, yet it intruded mantle peridotite below the petrologic Moho, the most primitive oxygen isotope reservoir in the silicate Earth. Identifying the presence and quantifying the extent of sediment melting within the mantle has important implications for understanding subduction recycling of supracrustal material and effects on mantle heterogeneity over time.

Spencer C.J., Cavosie A.J., Raub T.D., Rollinson H., Searle M.P., Miller J.A., and Jeon H. (2017). Evidence for melting mud in Earth's mantle from extreme oxygen isotope signatures in zircon. *Geology*, v. 45(11), 975-978.

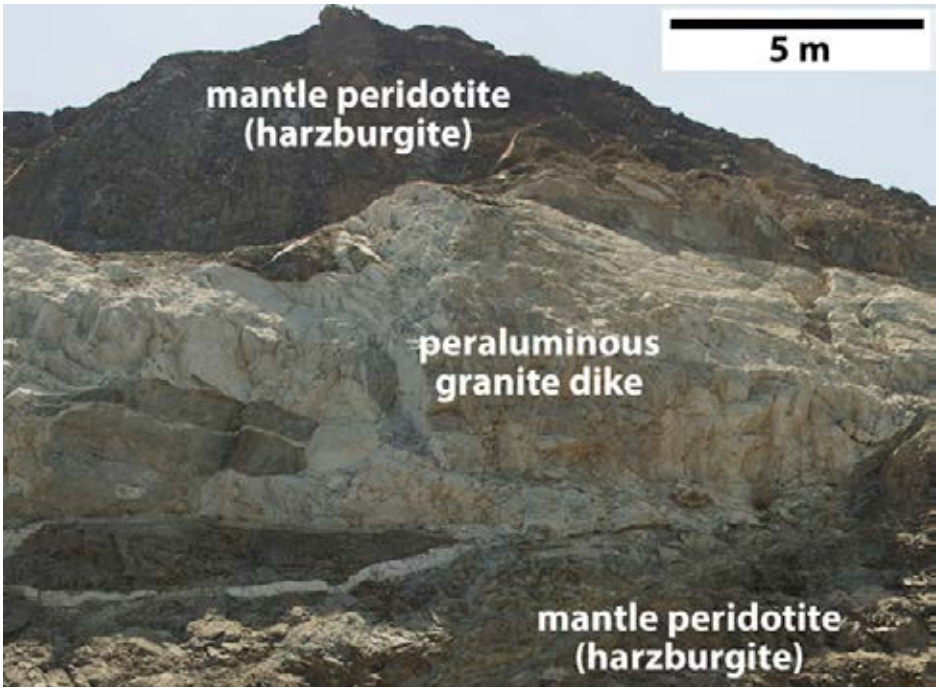

Sub-Moho S-type granite intruding peridotite in the UAE-Oman ophiolite.

An Australian source for Pacific-Gondwana zircon

A study of sediment provenance across Australia using U-Pb-Hf systematics in zircon revealed the Paterson-Petermann Orogen of Central Australia to be the major source for the so-called "characteristic Pacific-Gondwana zircons" found in eastern Australia. These data also re-affirmed links between Western Australia and the Lhasa Terrane in the Ediacaran-Paleozoic time, and led us to re-evaluate the tectonic drivers of the Paterson-Petermann Orogen. We conclude that the Orogen was likely subduction driven, and may represent a Neoproterozoic suture in the middle of Australia.

Martin E. L., Collins W. J., and Kirkland C. L. (2017) An Australian source for Pacific-Gondwanan zircons: *Implications for the assembly of northeastern Gondwana: Geology*, v. 45, no. 8, p. 699-702.

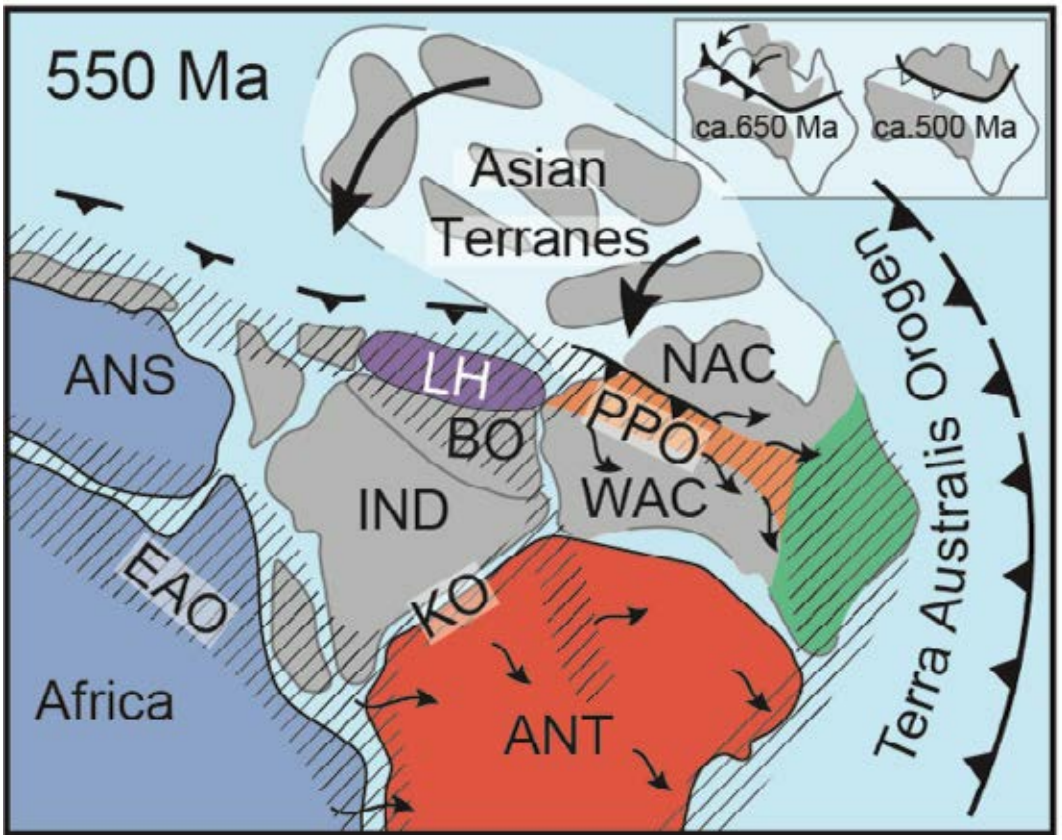

Northeastern Gondwana at 550 Ma showing collision of North Australian craton–Asian terranes into West Australian craton–Lhasa terrane. Large arrows show movement of outboard terranes during Paterson-Petermann orogen. Small arrows show sediment transport across Pacific-Gondwana region.

The formation of mantle "lone plumes"

It has been widely accepted that the vast majority of the Mesozoic-Cenozoic mantle plumes formed above the two large low shear velocity provinces (LLSVPs) in the lower mantle. However, there are obvious exceptions. One possible case is the Yellowstone plume which is at present outside the Pacific LLSVP. Another is the Hainan plume in the South China Sea region that is located within the broad global mantle downwelling zone. Li *et al*., (2014) therefore classified such plumes as "lone plumes". Here, Zhang *et al*. (2017) use the Hainan plume example to investigate the feasibility of such lone plumes being generated by subducting slabs in the mantle downwelling zone using 3D geodynamic modelling. Our geodynamic model has a high-resolution regional domain embedded in a relatively low resolution global domain, which is set up in an adaptive-mesh-refined, 3D mantle convection code ASPECT. They use a recently published plate motion model to define the top mechanical boundary condition. Their modelling results show that the Western Pacific subduction systems started to promote the formation of a lower-mantle thermal-chemical pile in the vicinity of the future South China Sea region since 70 Ma ago. As the top of this lower-mantle thermal-chemical pile rises, it first moved to the west, and finally rested beneath the South China Sea. The presence of a thermal-chemical layer (possible the D″ layer) in the model helps stabilizing the plume root.

Zhang, N., Li, Z.X., 2018. Formation of mantle "lone plumes" in the global downwelling zone — A multiscale modelling of subduction-controlled plume generation beneath the South China Sea. *Tectonophysics* 723, 1-13.

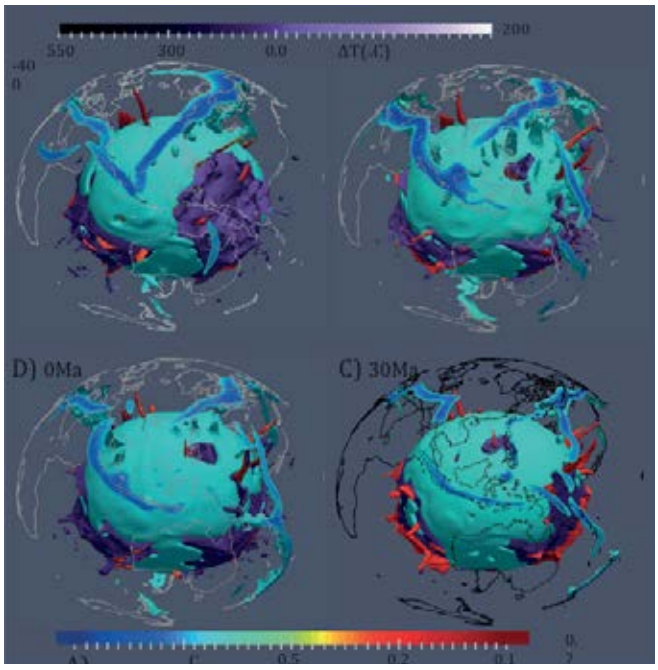

3D Hainan-hemispherical views of thermochemicalstructures for case PL1 at (A) 70 Ma, (B) 50 Ma, (C) 30 Ma,and (D) the present day. The thermal structures are plotted as iso-volumes (ParaView) of residual temperature with contour levels of −100ºC (blue) and 350ºC (red), and thechemical structures are plotted as iso-volumes of compositional field (purple). The core mantle boundary is plotted as a dark red spherical surface. The present-day coastlines are plotted for reference.

Palaeozoic evolution of the North Tianshan based on palaeomagnetic data – transition from Gondwana towards Pangaea

The palaeogeographic evolution of one of world's largest accretionary orogens, the Central Asian Orogenic Belt (CAOB), still attracts huge attention in the geoscience community. Since the famous proposal of the 'single arc' concept of AMC Şengör in 1993 ("Evolution of the Altaid tectonic collage and Palaeozoic crustal growth in Eurasia") in *Nature*, many authors presented evidence against the evolution of the CAOB originating from only one single arc. The fact that this paper, which was published around 25 years ago, had its most citations last year shows that the discussion is, however, still ongoing. Addressing this debate, Kirscher *et al*., (2017) carried out an extended palaeomagnetic study of Palaeozoic rocks from the Russian Tianshan to get additional constraints for the palaeogeography during the formation of the CAOB. To obtain the samples they carried out fieldwork in high altitudes within the Tianshan Mountains.

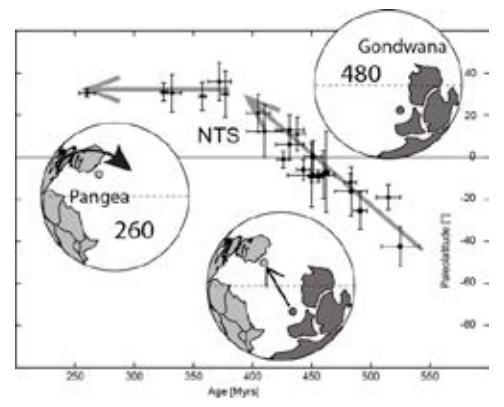

Plot of palaeolatitude of all available high quality palaeomagnetic data from the Russian North Tianshan (NTS) versus age. Also shown are the positions of the NTS related to the respective supercontinents Gondwana and Pangaea.

Combining their newly acquired Cambrian and Ordovician palaeomagnetic data with published high quality results revealed a continuous and steady northward motion of the North Tianshan terranes between the Cambrian and Devonian, when the movement ceased suddenly. They interpreted this data as being evidence for the rifting of the Tianshan terranes from Gondwana towards a zone of global downwelling, where further accretion led to the subsequent amalgamation of Eurasia with the CAOB terranes in its centre. Furthermore, the confinement of all palaeolatitudes obtained from this area argues against a giant single arc, which should create a range of palaeolatitudes at least during the Cambrian-Ordovician time. More high quality data is, however, needed to strengthen this palaeomagnetic argument.

Kirscher, U., Bachtadse, V., Mikolaichuk, A., Kröner, A., Alexeiev, D.V. (2017). Palaeozoic evolution of the North Tianshan based on palaeomagnetic data – transition from Gondwana towards Pangaea. *International Geology Review*, 59(16), 2003-2020.

Stone Forrest, Kumming S.China.

A full plate global reconstruction of the Neoproterozoic

Neoproterozoic tectonic geography was dominated by the formation of the supercontinent Rodinia, its break-up and the subsequent amalgamation of Gondwana. The Neoproterozoic was a tumultuous time of Earth history, with large climatic variations, the emergence of complex life and a series of continent-building orogenies of a scale not repeated until the Cenozoic.

Merdith *et al*., (2017) synthesised available geological and palaeomagnetic data and have built the first Neoproterozoic topological model of the evolution of the tectonic plate configurations. Topological models trace evolving plate boundaries and facilitate the evaluation of "plate tectonic rules" such as subduction zone migration through time when building plate models. There is a rich history of subduction zone proxies preserved in the Neoproterozoic geological record, providing good evidence for the existence of continent-margin and intra-oceanic subduction zones through time. These are preserved either as volcanic arc protoliths accreted in continent-continent, or continent-arc collisions, or as the detritus of these volcanic arcs preserved in successor basins. Their model predicts less subduction (ca. 90%) than on the modern earth, suggesting that the model is conservative and is likely underestimating the amount of subduction, either due to a simplification of tectonically complex areas, or because of the absence of preservation in the geological record. The reconstruction of plate boundary geometries provides constraints for global-scale earth system parameters, such as the role of volcanism or ridge production on the Cryogenian icehouse climatic excursion. We expect that our model can provide constraints for both geodynamic and palaeoclimate models.

Meredith A.S., Collins A.S., Williams S.E., Pisarevsky S., Foden J.D., Archibald D.B., Blades M.L., Alessio B.L., Armistead S., Plavsa D., Clark C., Müller R.D. (2017). A full-plate global reconstruction of the Neoproterozoic. *Gondwana Research*. 50, 84-134.

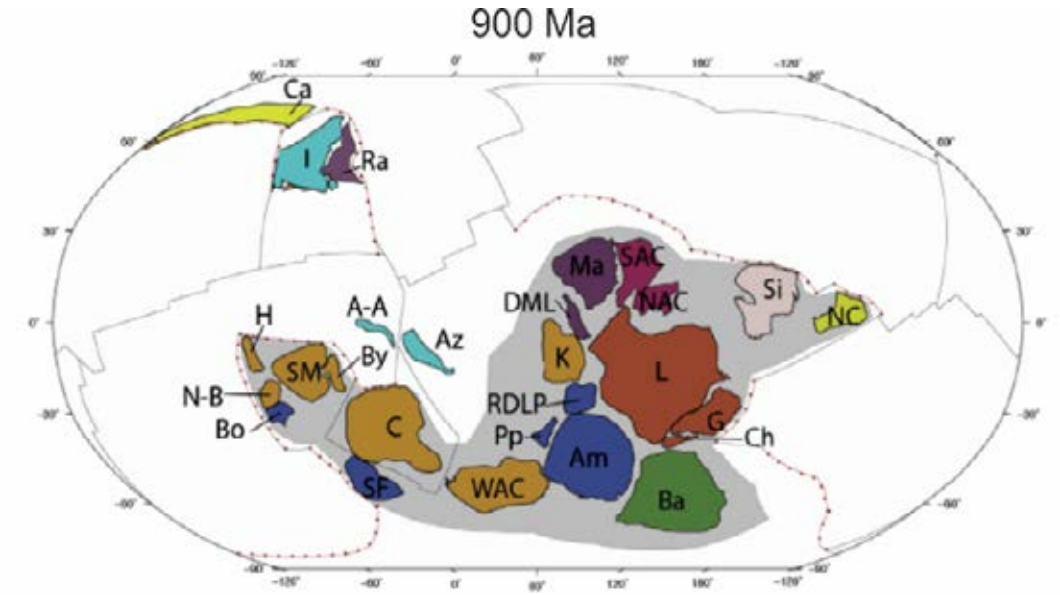

The full plate global paleogeography at 900 Ma. **A-A**, Afif-Abas Terrane; **Am**, Amazonia; **Az**, Azania; **Ba**, Baltica; **Bo**, Borborema; **By**, Bayuda; **Ca**, Cathaysia (South China); **C**, Congo; **Ch**, Chortis; **G**, Greenland; **H**, Hoggar; **I**, India; **K**, Kalahari; **L**, Laurentia; **Ma**, Mawson; **NAC**, North Australian Craton; **N-B**, Nigeria-Benin; **NC**, North China; **Pp**, Paranapanema; **Ra**, Rayner (Antarctica); **RDLP**, Rio de la Plata; **SAC**, South Australian Craton; **SF**, São Francisco; **Si**, Siberia; **SM**, Sahara Metacraton; **WAC**, West African Craton.

Fennoscandia before Nuna/ Columbia

Numerous mafic dykes, sills and intrusions with ages between 1985 Ma and 1960 Ma are exposed near the Onega Lake in southern Karelia, Russia. The paleomagnetic analysis of these rocks has revealed a stable remanence with directions belonging to two groups. The directions of the first group characterize ten intrusions including the dated 1970 ± 3 Ma Unoi sill and 1976 ± 9 Ma Suna River Canyon dolerite, the corresponding paleomagnetic pole is 44.4°N, 101.5°E, A_{95} = 6.3°. The second group comprises two intrusions including the 1984 ± 8 Ma Pudozhgora intrusion and Krestoviy Navolok dyke with the corresponding paleopole calculated from 5 site mean poles is 60.9°N, 144.8°E, A_{95} = 6.8°. Both remanence directions are supported by robust baked contact tests.

Lubnina *et al.*, (2017) propose the first group's pole as the key 1975 Ma Fennoscandian pole. The second one is well dated, but based only on two intrusions without proper averaging of the paleosecular variations. They have also carried out a complimentary paleomagnetic study of the previously investigated 2504 Ma Shalskiy gabbronorite dyke. The remanence of this dyke is now supported by the inverse contact test and statistics can be improved. Using their 1975 Ma pole together with coeval poles from Superior, Slave and Amazonia cratons they propose a provisional 1975 Ma paleogeographic reconstruction.

Lubnina N.V., Pisarevsky S.A., Stepanova A.V., Bogdanova S.V., Sokolov S.J. (2017). Fennoscandia before Nuna/Columbia: Paleomagnetism of 1.98–1.96 Ga mafic rocks of the Karelian craton and paleogeographic implications. *Precambrian Research*, 292, 1-12.

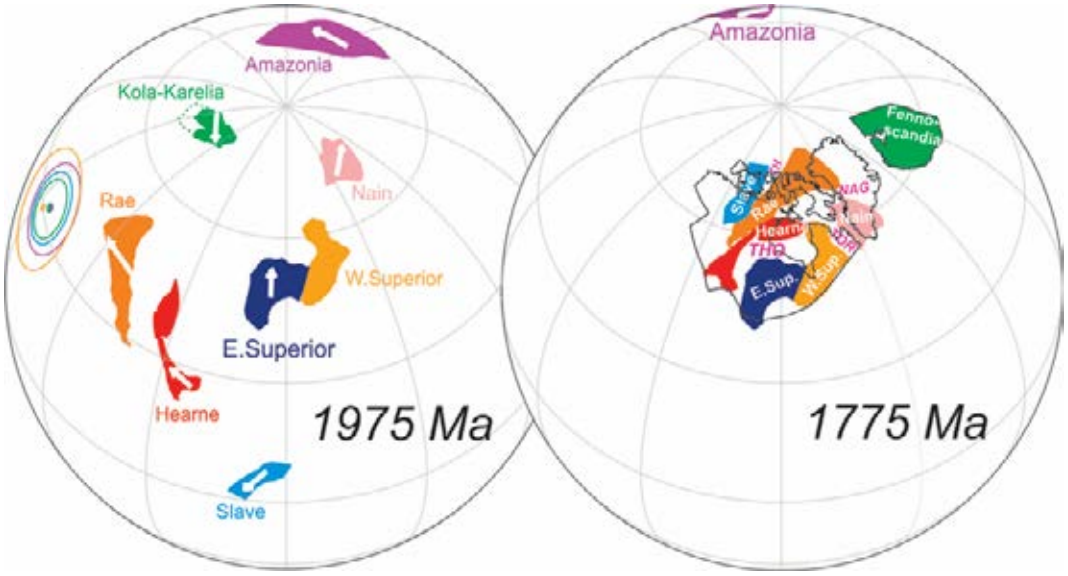

Paleogeographic reconstructions at 1975 Ma and 1775 Ma in Laurentian (North American)coordinates and paleomagnetic poles. 1.9–1.8 Ga orogens: THO – Trans-Hudson; TOR – Torngat; NAG – Nagssugtoqidian; TH – Thelon. Arrows show direction to the North.

Australia-China Joint Research Centre for Tectonics and Earth Resources (ACTER)

ACTER (http://tectonics.curtin.edu.au) is a joint research centre led by two top geoscience research organisations in Australia and China – the Institute for Geoscience Research at Curtin University, and the Institute of Geology and Geophysics of the Chinese Academy of Sciences, and participated by key collaborating institutions from the two countries. It aims to facilitate collaborative research and research training in geotectonics and mineral and hydrocarbon resources.

A highlight of ACTER in 2017 was the annual ACTER Field Symposium on the Tectonic Evolution and Granite Petrogenesis of the Lachlan Fold Belt, Eastern Australia, led by Professor Bill Collins. The event was well attended, with 42 staff and graduate students from Curtin University, the University of Newcastle, The University of Adelaide, Geoscience Australia, the Geological Survey of New South Wales, the Institute of Geology and Geophysics – Chinese Academy of Sciences, Guangzhou Institute of Geochemistry – Chinese Academy of Sciences, the Chinese Academy of Geological Sciences, Sun Yat-Sen University, Peking University, Chang'an University and Zhejiang University. Several members of the Geological Survey of New South Wales contributed significant knowledge of the local geology which added to the success of the trip.

Complementary to the incredible geology, were the fantastic evenings, filled with many laughs, discussions and great company. The 2017 ACTER Field Symposium was a raging success, giving locals and those not so familiar with eastern Australia the opportunity to see some of its most iconic sites and spectacular rocks, with a great group of people crossing different institutions, career stages, gender, disciplines, and culture backgrounds. Old friendships were renewed, and many new ones were established. Along the way numerous collaborative research and exchange initiatives were made. It certainly was a sign of good things to come for ACTER.

Professor Bill Collins talking about Lachlan geology.


ACTER

Rodinia 2017 a great success

The Rodinia 2017 Conference, organised by the IGCP648 team and co-sponsored by TIGeR, was successfully held at the tranquil tropical grove of the Seagulls Resort along the foreshore of Townsville City in North Queensland, Australia. About 70 participants, including many students, from Australia, Canada, Africa, Asia and Europe, enjoyed four days of intense scientific debate on all aspects related to supercontinent cycles, global geodynamics, and the formation and preservation of mineral resources. IGCP648 grants helped to bring member speakers from Ethiopia, China, Canada, and six student members to attend the event. The meeting was preceded by a 2-day workshop to introduce a group of about 30 geologists to the database systems that have been developed for IGCP 509 and 648. A post-conference field trip, led by George Gibson (Australian National University) and Ian Withnall (Geological Survey of Queensland) to the Mount Isa area, was attended by 20 of the delegates. Below are brief descriptions of the highlights from the tripartite Rodinia 2017 Conference.

All aspects of supercontinents Pangea, Rodinia and Nuna, the supercontinent cycle in general, and related geodynamic processes, were interrogated at the Rodinia 2017 Conference in Townsville: geophysics (seismology, paleomagnetism, numerical modeling), geochemistry (geochronology, tectonics), and geobiology (sedimentology, ocean-atmosphere and biosphere). Both the scope and relevance of the scientific contributions were nothing short of astounding. Also, a young generation of male and female early career scientists and students appear to be emerging in order to test the ideas put forth by the generations before them (e.g., Ian Dalziel and three Australian Laureate Fellows). Discussions were as intense as they were enjoyable and educating, occurring both during the meeting sessions and continuing into the evenings. The inspiring, scientific atmosphere broke down all disciplinary, cultural and generation boundaries. The following are some members' reflections of the event:

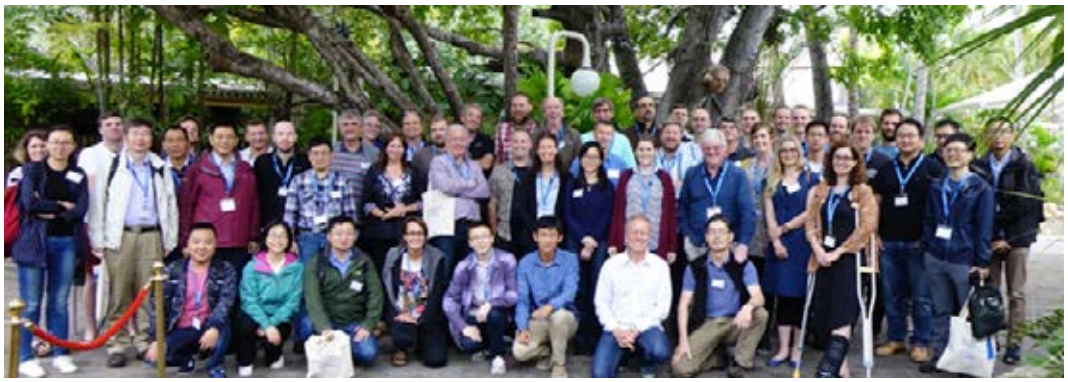

A six-day field excursion to the Mt Isa region was led by George Gibson and Ian Withnall, examining Paleo- to early Mesoproterozoic tectonostratigraphic record of the Mt Isa Inlier which have been correlated to that of north-western Laurentia in the reconstruction of the supercontinent Nuna. The spirit of intense discussion and debate during the Rodinia meeting continued into the field trip, to the enlightenment of seasoned academics and students alike. Ongoing research in both northeastern Australian and its possible Canadian counterpart in Nuna are being conducted by Australian and Canadian IGCP 648 members.

Unconformity, Solund Basin, western Norway.

Western Australia Palaeomagnetic and Rock-Magnetic facility

The Western Australia Palaeomagnetic and Rock-magnetic Facility, recently upgraded and relocated to Curtin University's Bentley campus, is a national research infrastructure with the latest upgrade co-funded by the Australian Research Council and collaborating institutions including Curtin University, the University of Western Australia (UWA), the Australian National University, Macquarie University and University of Queensland.

The latest upgrade includes the construction of a magnetically shielded room in mid-2015 by Dr Gary Scott's team, which provides a laboratory space with ambient magnetic fields less than 0.5% of the local geomagnetic field. Within this shielded room we now have a new 2G 755 superconducting rock magnetometer with a vertical Model 855 automated sample handler (the RAPID system) and other accessories attached to it (automated AF demagnetiser, susceptibility meter, etc.). The RAPID system, the first and only one in Australia, was installed and commissioned in February 2017. Other systems now operating inside the shielded room include an AGICO JR-6A spinner magnetometer and ASC TD-48SC and MAGNETIC MEASUREMENTS thermal demagnetisers. A number of key pieces of apparatus are currently being relocated from UWA to the new Curtin precinct.

The new purchases represent a major enhancement to the productivity and capabilities of the facility. Apparatus which is now available in the facility include:

- a 2G 755 superconducting rock magnetometer with a vertical Model 855 automated sample handler (the RAPID system) and other accessories (including; AF coils, susceptibility meter, and ARM system),
- a second 2G 755 cryogenic magnetometer upgraded (LE0668377) to a 4K DC SQUID system (currently returned to 2G enterprises for a minor upgrade and for repair of the lightning-damaged cold head),
- An AGICO JR-6A spinner magnetometer,
- 1x MMTD80, 2x MMTD18 and a TD-48-SC thermal demagnetiser,
- a Petersen Instruments Variable Field Translation Balance (VFTB),
- an AGICO MFK-1FA kappabridge,
- a Bartington MS2 susceptibility meter with MS2W furnace, and
- a MAGNETIC MEASUREMENTS MMPM5 pulse magnetiser.

The facility supports a wide range of research topics, including reconstruction of global palaeogeography (the configuration and drifting history of continents) through Earth's history, studying the evolving geomagnetic field (e.g., palaeointensity) through time, analyses of regional and local structures and tectonic histories, dating sedimentary rocks and thermal/chemical (e.g. mineralisation) events, studying past climate changes, and orienting rock cores from drill-holes.

The Palaeomag Lab.

Tectonics of East Asia and the onset of subduction of the Palaeo-Pacific plate

Liu *et al.,* (2017a, b) have studied two regions in East Asia as part of a project on the Early Cretaceous evolution of the Pacific Margin. In the Southern Sikhote-Alin orogenic belt in the Russian Far East, sandstone samples were collected along a 200 km long traverse for U-Pb dating and Lu-Hf isotope analysis to constrain the provenance and evaluate the evolution of the northwest pacific margin at that time.

In the eastern part of the Central Asian Orogenic Belt, the Khanka granitoids record the Paleo-Pacific subduction during the Mesozoic. Using whole rock geochemistry combined with U-Pb dating and Lu-Hf isotopic signatures of zircons Liu *et al.*, conclude that the granitoids record the early stage of subduction which commenced at least 250 Ma ago.

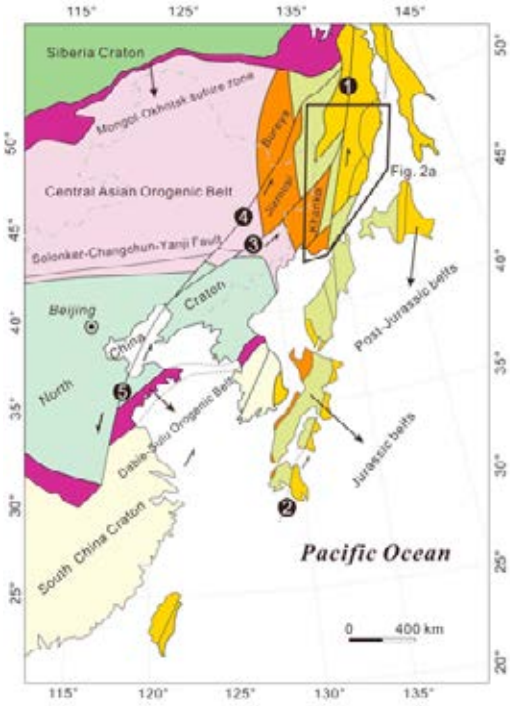

The East Asian continent consists of three major cratons which are, from north to south, the Siberia Craton, North China Craton, and South China Craton. Several orogenic belts/suture zones welded the cratons to form the tectonic framework of northeastern Asian continent.

Liu, K., Zhang, J., Wilde, S.A., Liu, S., Guo, F., Kasatkin, S.A., Golozoubov, V.V., Ge, M., Wang, M., Wang, J. (2017). U-Pb dating and Lu-Hf isotopes of detrital zircons from the southern Sikhote-Alin Orogenic Belt, Russian Far East: Tectonic implications for the Early Cretaceous evolution of the Northwest Pacific Margin. *Tectonics*, 36, 2555-2598.

Liu, K., Zhang, J., Wilde, S,A,, Zhou, J., Wang, M., Ge, M., Wang, J., Ling, Y. (2017) Initial subduction of the Paleo-Pacific Oceanic plate in NE China: Constraints from whole-rock geochemistry and zircon U–Pb and Lu–Hf isotopes of the Khanka Lake granitoids. *Lithos*, 274-275, 254-270.

Sedimentation and magmatism in the Palaeoproterozoic of India and consequences for lithospheric extension

Sheppard *et al*., (2017) have dated felsic tuffs and intruded mafic sills in the Cuddapah Basin as part of a study to test previously published suggestions that the sills were part of a large igneous province (LIP). Collectively, the new data indicate that mafic sill emplacement spanned more than 30 myr so that it is likely to have been a protracted event or series of events, and therefore unlikely to represent a LIP. The time span for the mafic magmatism is more compatible with episodic, lithospheric extension (passive rifting) during basin evolution than it is with a mantle plume (active rifting).

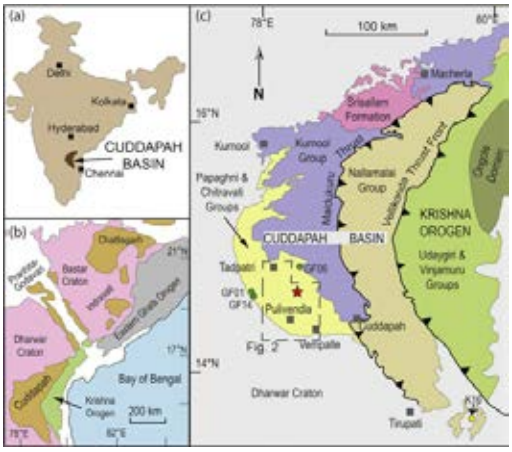

Sheppard, S., Rasmussen, B., Zi, J.W., Somasekhar, V., Srinivasa Sarma, D., Ram Mohan, M., Krapež, B., Wilde, S.A., McNaughton, N.J. (2017). Sedimentation and magmatism in the Paleoproterozoic Cuddapah Basin, India: Consequences of lithospheric extension. *Gondwana Research*, 48. 153-163.

Research reports

PLANETARY SCIENCE

Planetary science

Curtin Planetary Group 2107.

Planetary science is a historical area of strength at Curtin: John de Laeter was a world-renowned cosmochemist and planetary scientist. That strength continues through to the present day. With 26 members, TIGeR is home to the largest planetary science group in Australia, with 14 members of staff publishing in the field as their principal area of interest and 8 PhD students full-time on planetary projects.

Desert Fireball Network

The Planetary Science group direct the Australia node for the NASA Solar System Exploration Research Virtual Institute (SSERVI), representing Australia's planetary research community to NASA. Curtin researchers in mission concept development have enhanced opportunities for collaboration directly with NASA teams.

The partnership will result in great scientific discoveries in planetary science as well as advancing lunar and planetary science research, and human exploration of the solar system.

Chasing Fireballs

The Desert Fireball Network (DFN) uncovers mysteries surrounding the origins of the Solar System by studying meteorites, fireballs and their pre-Earth orbits.

Digital skyward facing cameras capture pictures of meteors as they fall, while purpose-built computer programs calculate the speed, direction, and potential landing zone so the meteorite can be recovered and analysed.

Tracking OSIRIS-REx

Curtin's Desert Fireball Network team tracked NASA's OSIRIS-REx spacecraft flight over Australia and New Zealand on its way to Bennu, a carbonaceous asteroid whose regolith may record the earliest history of our solar system. They imaged the 2.5 m spacecraft from a distance of 60,000 km.

Satellite tracking with Lockheed Martin

Partnering with Lockheed Martin Space Systems, the DFN team have modified the automated fireball observatories and adapted them for satellite tracking. The resulting system combines wide angle coverage with precision orbit determination for multiple objects.

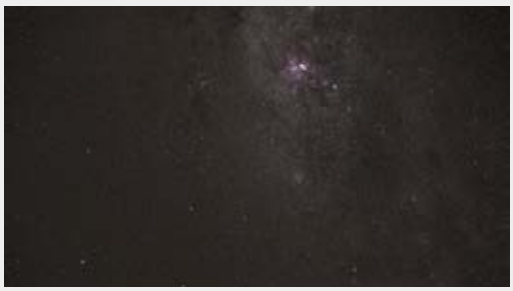

Observing Mars

Through successful Australian Research Council (ARC) grants and NASA InSight mission involvement, Curtin Planetary Science researchers Alexander Nemchin, Gretchen Benedix, Katarina Miljkovic and Eleanor Sansom are building capacity at TIGeR to explore the geoscience of Mars. The group aims to develop an absolute timescale for and detailed geologic map of Mars, and to decipher the inner workings of the planet's crust and interior.

Mission Involvement

Members of the planetary science group have a history of collaboration on space missions. Currently we involved in 5 active missions with international partners: NASA OSIRIS-Rex [Phil Bland,]; NASA InSight [Katarina Miljkovic, Eleanor Sansom]; JAXA BepiColombo (Phil Bland), ESA ExoMars (Martin Towner).

Public Engagement

Fireballs in the Sky continues to be the flagship ongoing outreach initiative for Curtin Planetary Science, with its citizen science app upgraded with 34,769 downloads in 90 countries and 3,416 reports. The program was presented at the 2017 Citizen Science Conference in Minnesota, and the American Geophysical Union with our NASA partners from SSERVI Central. Through the collaborative endeavors of SSERVI, the program will expand in Spanish thanks to the Mexican Space Agency translation. Engagement Lead Renae Sayers visited international partners at NASA Goddard Space Flight Centre, NASA Ames, and hosted a webinar for NASA JPL to expand collaborations, grow our media profile, and meet common goals in science outreach.

Alongside the NASA DFN OSIRIS-REx Observation campaign, the team engaged astronomy communities and the media across Australia to track the spacecraft.

Workshops

Shock metamorphism in terrestrial and extra-terrestrial rocks: this multidisciplinary four-day workshop brought together 32 Australian and international researchers from state-of-the-art laboratory methodologies in terrestrial and extra-terrestrial rocks, mineral and meteorite sample analyses. Researchers conducted numerical modelling and laboratory experiments on shock-wave progression in geologic and planetary analogue materials. The meeting was followed by a three-day field trip to the Wolfe Creek crater, located near Halls Creek in Western Australia.

Multi-messenger Observations of a Binary Neutron Star Merger

On 2017 August 17 a binary neutron star coalescence candidate (later designated GW170817) with merger time 12:41:04 UTC was observed through gravitational waves by the Advanced LIGO and Advanced Virgo detectors.

DFN systems observed this event from 2 min before the GW170817 trigger and was the only optical facility that imaged the source region during the event. Although no transient sources were detected within the host galaxy NGC4993, the calibrated limiting magnitude of DFN systems of magv=6 gave an upper bound on the optical brightness of the neutron star merger.

Localization of the gravitational-wave, gamma-ray, and optical signals. The left panel shows an orthographic projection of the 90% credible regions from LIGO (190 deg2; light green), the initial LIGO-Virgo localization (31 deg2; dark green), IPN triangulation from the time delay between *Fermi* and *INTEGRAL* (light blue), and *Fermi*-GBM (dark blue). The inset shows the location of the apparent host galaxy NGC 4993 in the Swope optical discovery image at 10.9 hr after the merger (top right) and the DLT40 pre-discovery image from 20.5 days prior to merger (bottom right). The reticle marks the position of the transient in both images.

Abbott B.P. *et al.* with Bland,P.A. (2017) Multi-messenger observations of a binary neutron star merger. *The Astrophysical Journal* **848**: L12.

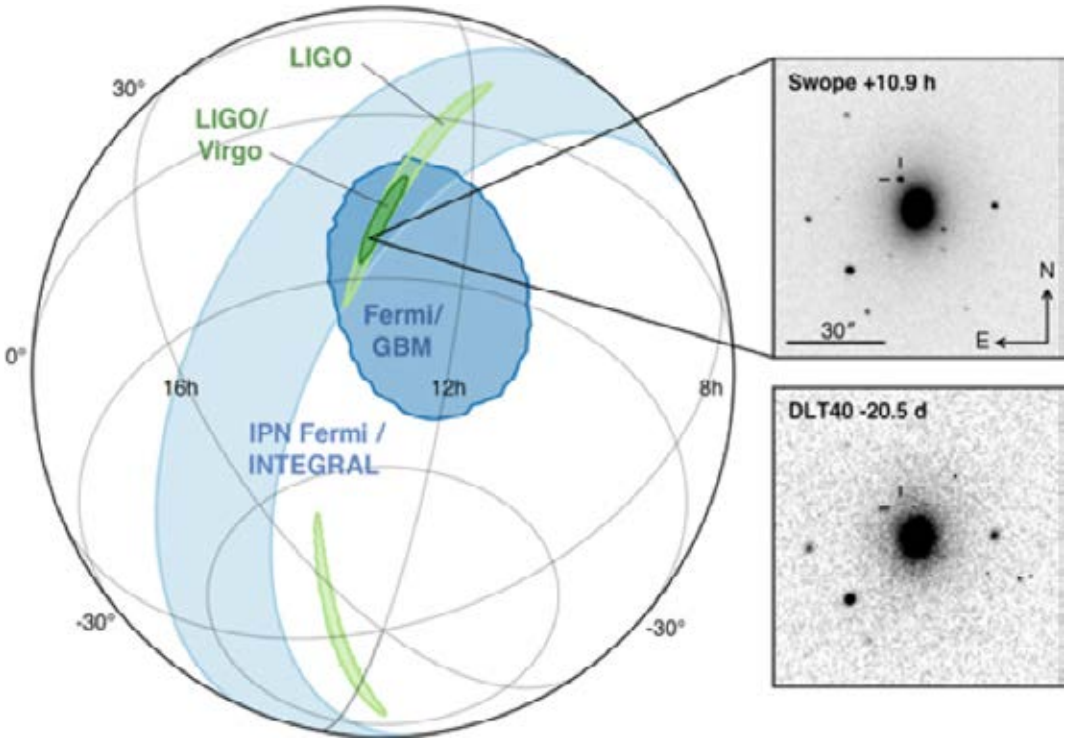

Depiction of the Mars Lander

Bunburra Rockhole: Exploring the geology of a new differentiated asteroid

Bunburra Rockhole is the first recovered meteorite of the Desert Fireball Network. Eucrites are part of the group of HED meteorites that are typically thought to originate from 4 Vesta. After an expanded bulk chemical study of the Bunburra Rockhole meteorite, minor and trace element analyses are exactly on the basaltic eucrite trend. New oxygen isotope analyses however show large variations that are well outside the HED parent body fractionation line. Cr isotope results of this rock are also distinct from HEDs.

Benedix *et al.,* (2017) conclude that Bunburra Rockhole represents a sample of a new differentiated asteroid, one that may have more variable oxygen isotopic compositions than 4 Vesta. The fact that Bunburra Rockhole chemistry falls on the eucrite trend perhaps suggests that multiple objects with basaltic crusts accreted in a similar region of the Solar System.

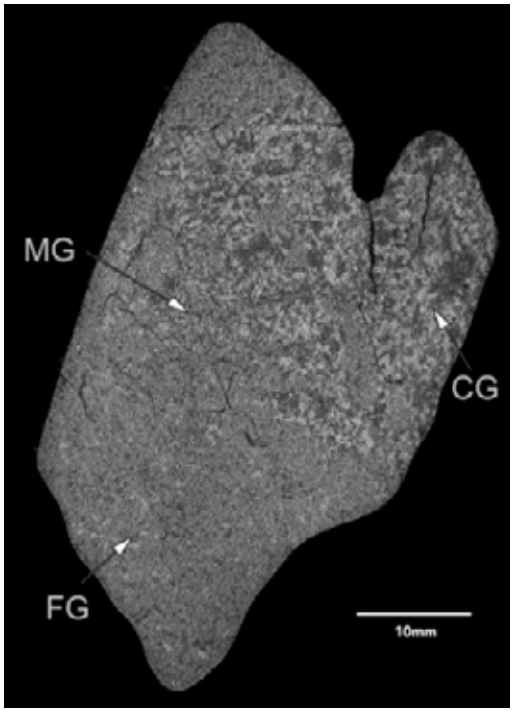

X-ray computed tomographic (CT) slice through the Bunburra Rockhole meteorite. Image is optimized for contrast and brightness to illustrate different lithology types. Scale bar is 10 mm.

Benedix G.K., Bland P.A., Friedrich J.M., Mittlefehldt D.W., Sanborn E., Yin Q.-Z., Greenwood R.C., Franchi I.A., Bevan A.W.R., Towner M.C., Perrotta G.C. and Mertzman S.A. (2017) Bunburra Rockhole: Exploring the geology of a new differentiated asteroid. *Geochimica et Cosmochimica* Acta 208, 145-159.

Nebula sulphidation and evidence for migration of 'free floating' refractory metal nuggets revealed by atom probe microscopy

Disk models have been proposed that imply particles migrate rapidly in a protoplanetary disk. However, the only physical constraints on these processes from meteorites are observations of refractory inclusions in cometary material from the NASA Stardust mission. Atom probe microscopy of sub-micrometer refractory metal nuggets (RMNs) within the carbonaceous meteorite ALH 77307 suggest they were exposed to a S-condensing gas and likely "free floating" during this exposure. This requires early, rapid migration of RMNs to cooler regions of the disk and has implications for mobility of particles during disk formation.

Daly L., Bland P.A., Saxey D.W., Reddy, S.M., Fougerouse D., Rickard W.D.A. and Forman L.V. (2017) Nebular sulfidation and evidence for 'free floating' refractory metal nuggets revealed by atom probe microscopy. *Geology* **45**, 847-850.

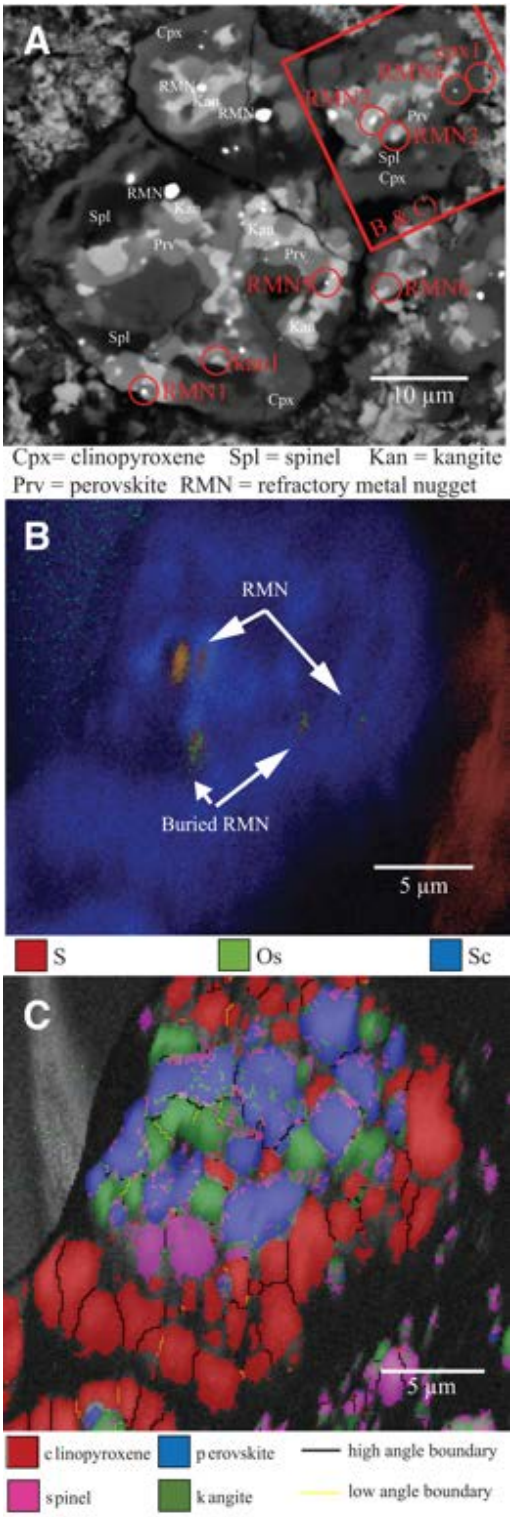

Electron backscatter diffraction (EBSD) and energy dispersive X-ray spectroscopy (EDS) analyses of region of interest from ALH 77307 CO3.0 meteorite (from Allan Hills, Antarctica).

Giant convecting mud balls of the early solar system

Carbonaceous asteroids may have been the precursors to the terrestrial planets, yet despite their importance, numerous attempts to model their early Solar System geological history have not converged on a solution. The assumption has been that hydrothermal alteration was occurring in rocky asteroids with material properties similar to meteorites. However, these bodies would have accreted as a high-porosity aggregate of igneous clasts (chondrules) and fine-grained primordial dust, with ice filling much of the pore space. Short-lived radionuclides melted the ice, and aqueous alteration of anhydrous minerals followed. However, at the moment when the ice melted, no geological process had acted to lithify this material. It would have been a mud, rather than a rock.

Bland and Travis (2017) tested the effect of removing the assumption of lithification. Mud convection both moderates internal temperature and reduces variation in temperature throughout the object. As the system is thoroughly mixed, soluble elements are not fractionated, preserving primitive chemistry. These results are consistent with observations from aqueously altered meteorites (CI and CM chondrites) and spectra of primitive asteroids. The "mudball" model therefore appears to be the general solution long sought after.

Bland P.A. and Travis B.J. (2017) Giant convecting mudballs of the early solar system. *Science Advances* **3**: e1602514.

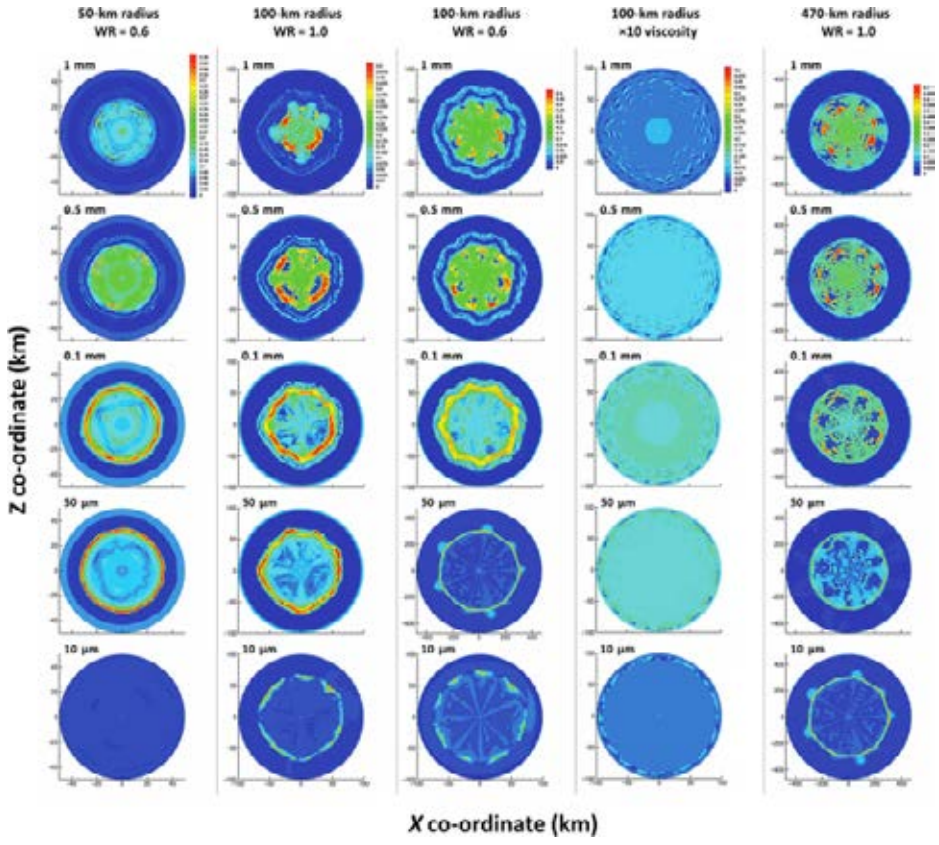

Particle size distribution in sample model asteroids that accrete a range of chondrule sizes, showing the variety of chondrule sorting.

Defining the mechanism for compaction of the CV chondrite parent body

Forman *et al*., (2017) present some of the first significant evidence for shock compaction of the CV parent body. The Allende meteorite is a relatively unaltered member of the CV carbonaceous chondrite group and contains primitive crystallographic textures that can inform our understanding of early Solar System planetary compaction. Olivine grains were analyzed by electron backscatter diffraction (EBSD) techniques, with the large area map presented being one of the most extensive EBSD maps to have been collected in application to extraterrestrial materials. Lithostatic pressure within plausible chondritic model asteroids is not sufficient to drive compaction or create the microstructures observed for a cold aggregate. Rather the microstructures are indicative of crystal-plastic deformation from small, brief heating events. The crystallographic textures reflect impact compaction and are able to indicate shock-wave directionality.

Forman L.V., Bland P.A., Timms N.E., Daly L., Benedix G.K., Trimby P.W., Collins G.S. and Davison T.M. (2017). "Defining the mechanism for compaction of the CV chondrite parent body. *Geology* 45(6), 599-562

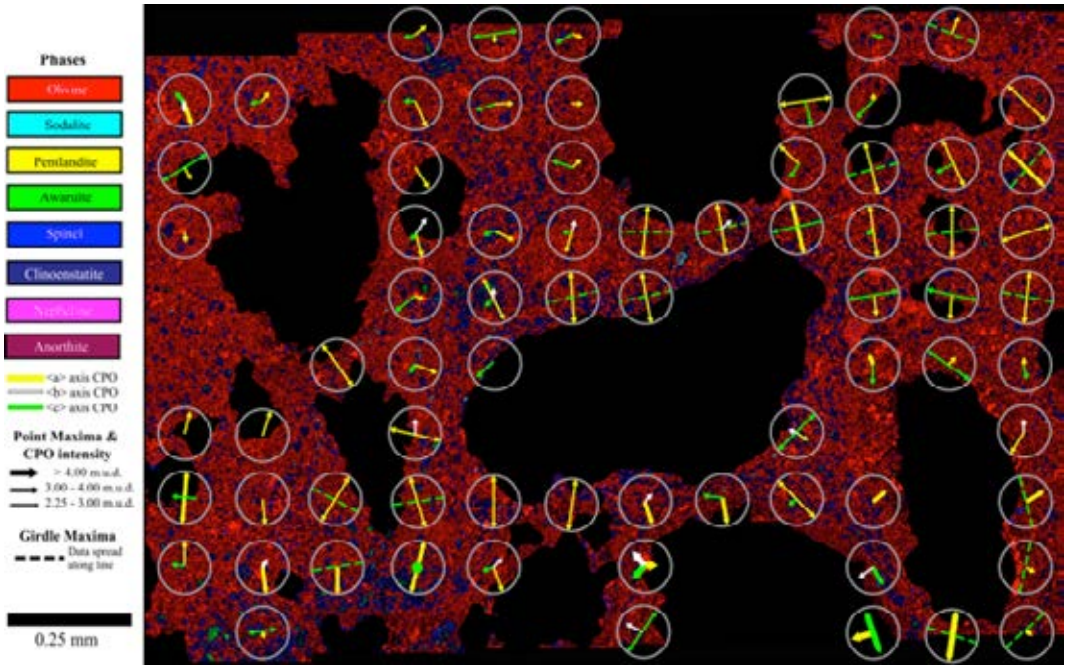

Full crystallographic preferred orientation (CPO) analysis overlaid onto the phase map. Black regions are chondrules.

Depth of Origin of the Peak (Inner) Ring in Lunar Impact Basins

Numerical modeling of peak-ring impact basin formation shows that a peak-ring forms from the central uplift material being outwardly thrust over the inwardly collapsing transient crater rim. Simulations of lunar basin formation shows that this material is composed of the overturned crust and deep-seated material, possibly from the upper mantle.

Miljkovic *et al*., (2017) estimate the scaling trends between basin size and the depth of origin of material exposed within the ring report the likely crust, mantle, and projectile abundances exposed within the ring. Quantifying the excavation depths during the formation of the peak or inner ring provides a step toward understanding the lunar crust and mantle stratigraphy.

Miljkovic, K., Lemelin, M., Lucey, P.G. (2017) Depth of Origin of the Peak (Inner) Ring in Lunar Impact Basins. *Geophys. Res. Lett.*, 44, 10,140–10,146

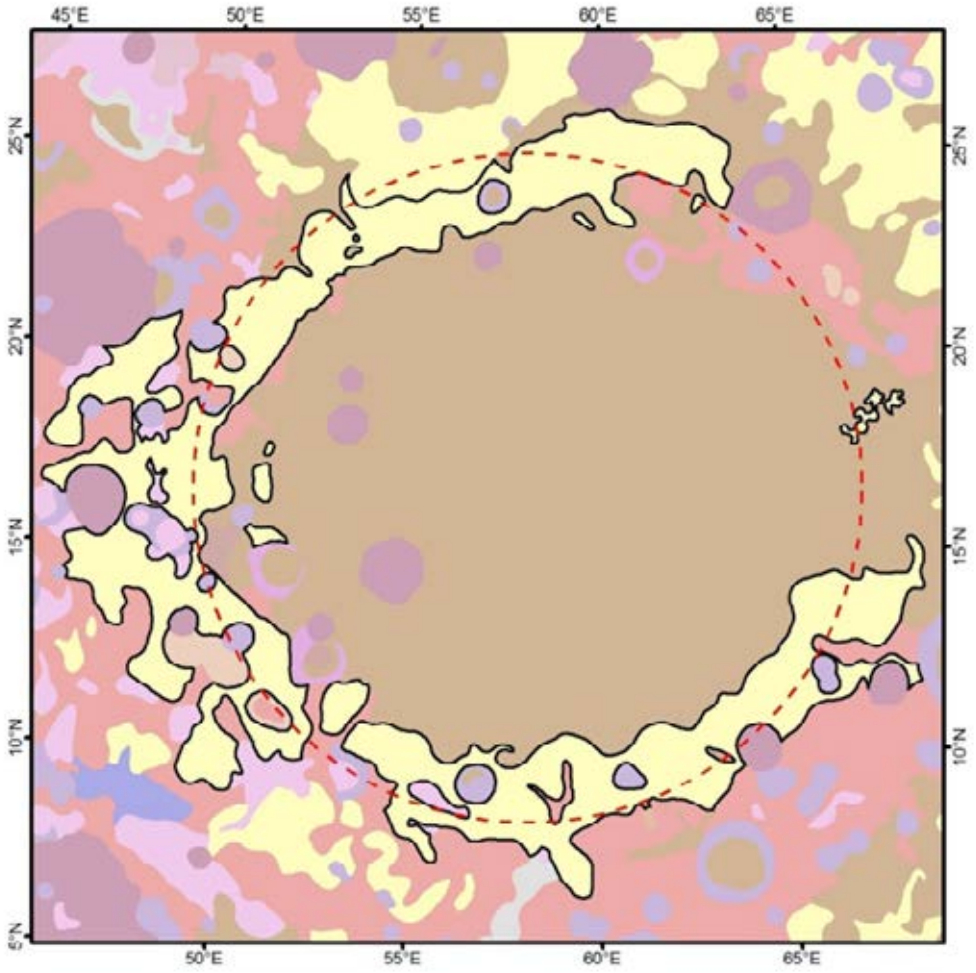

USGS map of geologic units of the Crisium basin on the Moon, emphasizing the "circumbasin material" in yellow, associated with the peak-ring material that was exposed from various depths during basin formation.

Collisional history of asteroid Itokawa

In situ extraterrestrial samples returned for study (e.g., from the Moon) are crucial in understanding the origin and evolution of the Solar System as, contrary to meteorites, they provide a known geological context for the samples and their analyses. Asteroid 25143 Itokawa is a rubble-pile asteroid consisting of reaccumulated fragments from a catastrophically disrupted monolithic parent asteroid, and from which regolith dust particles have been recovered by the Hayabusa space probe (Japan Aerospace Exploration Agency).

Jourdan *et al.*, (2017) analyzed two dust particles using electron backscatter diffraction and $^{40}Ar/^{39}Ar$ dating techniques. A new temperature-pressure-porosity model, coupled with diffusion models was used to show that the relatively low pressure and high temperature involved in the impact process can be reconciled only if the asteroid was already made of porous material at ~2.3 Ga. One of the Itokawa grains analysed shows signs of 15–25 GPa impact shock pressure, with an age of 2.3 ± 0.1 Ga. If asteroid Itokawa was already formed, this provides a minimum age for catastrophic asteroid breakup. A second particle shows no sign of deformation, indicating shock pressure of <10 GPa and a calculated maximum temperature of ~200ºC. This low temperature estimate is compatible with a lack of isotopic resetting for this particle. This suggests that the breakup of Itokawa's parent was a relatively low-temperature process at the scale of the asteroid, and occurred on a pre-shattered parent body.

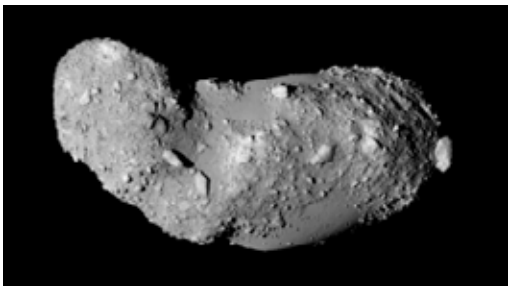

Asteroid Itokawa: credit JAXA.

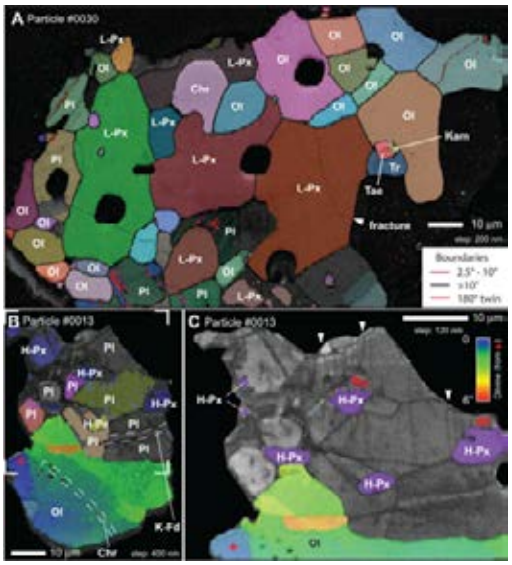

Crystallographic orientation maps of particles from asteroid Itokawa, measured by electron back scatter diffraction (EBSD).

Jourdan F., Timms N.E., Eroglu E., Mayers C., Frew A., Bland P.A., Collins G.S., Davison T.M., Abe M., Yada T. (2017). Collisional history of asteroid Itokawa. *Geology*, 45 (9), 819-822.

Collecting a shatter cone sample, Wolf Creek Crater WA.

Research reports

SEDIMENTARY ENVIRONMENTS, BASINS AND ENERGY RESOURCES

Sedimentary environments, basins and energy resources

Our publications and conference presentations reflect our continued focus on understanding the evolution of Australian sedimentary basins, and their relationship to the geodynamic processes that have formed Australia's current continental margins. Our overall approach is conduct regional scale mapping that addresses questions of:

- Palaeozoic basin evolution and its implications for younger rift events
- The nature of Triassic tectonic events and their significance for the accumulation of thick sedimentary sequences in the Northern Carnarvon Basin
- Variations in timing and style of Mesozoic extension, associated rift-related uplift and sediment dispersal
- Salt tectonics on the North West Shelf
- Post breakup deformation, neotectonic structures and submarine mass transport complexes

Extensional fault evolution within the Exmouth Sub-basin, North West Shelf, Australia

Black *et al.,* (2017) have analysed structures from the Indian Merge 3D seismic survey. They identified three populations of normal faults within the Exmouth Sub-basin of the North West Shelf volcanic margin of Australia: (1) latest-Triassic to Middle Jurassic N-NNE-trending normal faults (Fault Population I); (2) Late Jurassic to Early Cretaceous NE-trending normal faults (Fault Population II); and (3) latest-Triassic to Early Cretaceous N-NNE faults (Fault Population III).

Quantitative evaluation of >100 faults demonstrated that fault displacement occurred during two time periods (210–163 and 145–138 Ma) separated by ~20 Myr of tectonic quiescence. Latest Jurassic to Early Cretaceous (145–138 Ma) evolution

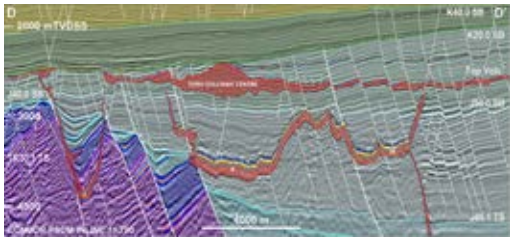

Depth structure map with preserved volcanic topography.

comprises magmatic addition and contemporaneous domal uplift ~70 km wide characterised by ≥ 900 m of denudation. This polyphase and bimodal structural evolution impacts current hydrocarbon exploration rationale by defining the nature of latest Jurassic to Early Cretaceous fault nucleation and reactivation within the southern Exmouth Sub-basin.

Black, M., McCormack, K.D., Elders, C. & Robertson, D. (2017). Extensional fault evolution within the Exmouth Sub-basin, North West Shelf, Australia. *Marine and Petroleum Geology*, 85, 301-315.

Estimating the amount of eroded sediment

To accurately reconstruct the burial and thermal history of sedimentary basins, key uncertainties that should be addressed are the accurate delineation of the maximum burial depths and estimation of the thickness of eroded sections in the basin. Several methods have been routinely utilized to account for this, but each with its limitations.

Johnson *et al.,* (2017) have utilized the sonic transit time data to account for the amounts of removed sections in the Broome Platform of the partly exhumed Canning Basin, Western Australia. The observed exhumed values are further compared with the values from AFTA (Apatite Fission Track Analysis) data as well as results of exhumation observed from the projection of vitrinite reflectance data. Furthermore, a mathematical relationship is established between the amounts of exhumation and the sonic transit time (DT) and depth.

The results from the calculated exhumed sections show a good correlation with the estimated removed sections reported from AFTA but poor correlations with the projected vitrinite reflectance profiles. While AFTA and vitrinite reflectance methods are widely used in the industry, the exhumation estimates derived from sonic-porosity logs are usually independent of the thermal history of the basin and thereby would provide more accurate inputs or further constraints into the burial history model. Also, in this study, the results from the AFTA usually allows for a wide range of uncertainty, while the calculation of exhumation values from the new approach gives an absolute exhumation value for the well locations. Furthermore, the sonic log approach has been able to identify and estimate the magnitude of an older erosional event that was not previously reported in the Geotrack report based on thermal history methods.

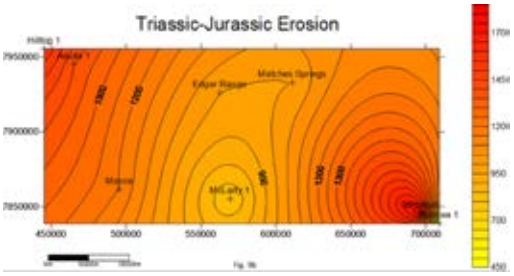

Contour map showing the magnitude of erosion of the Broome Platform.

Johnson, L.M., Rezaee, R., Kadkhodaiea, A., Smith, G., Yu, H. (2017). A new approach for estimating the amount of eroded sediments, a case study from the Canning Basin, Western Australia. *Journal of Petroleum Science and Engineering*, 156, 19-28.

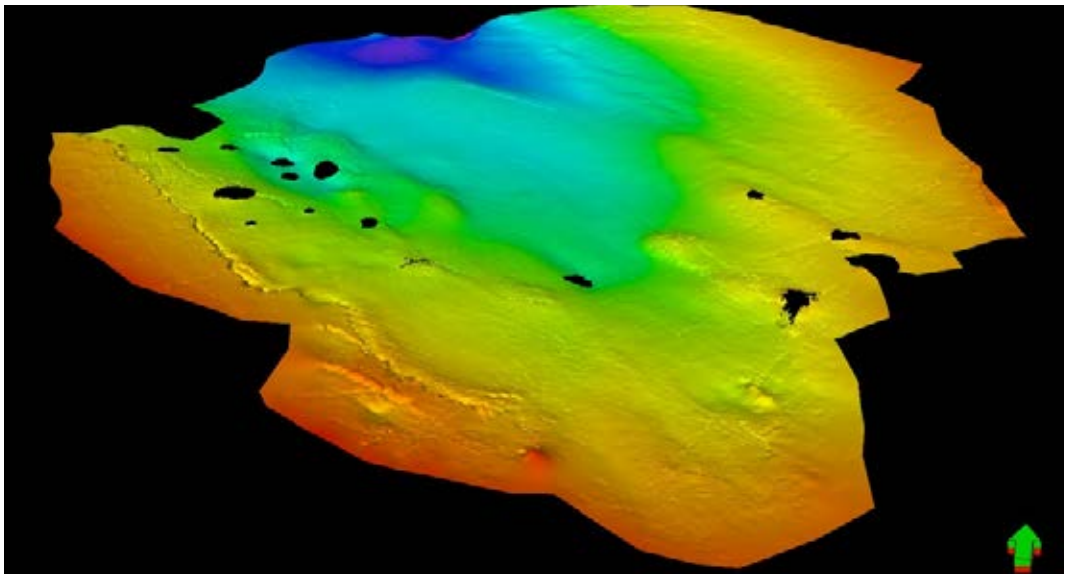

A three dimensional representation of the Top Permian horizon in the Petrel Basin showing the distribution of salt cored anticline and salt diapirs relative to the main basin-bounding fault structures.

A three dimensional representation of the Top Permian horizon in the Petrel Basin showing the distribution of salt cored anticline and salt diapirs relative to the main basin-bounding fault structures.

The Barrel Award

A highlight of the year was the success of our team of honours and masters students who took part in the "Barrel Award" competition organised by the American Association of Petroleum Geologists. This required them to carry out a geological evaluation of seismic and well log data from the Taranaki basin in New Zealand, and then to make recommendations for further hydrocarbon exploration activity in the area. Having come first in the Asia-Pacific regional heat, they were placed third in the international finals held at the AAPG Annual meeting on Houston in April.

We continue to be actively engaged with the wider Petroleum Geoscience community in Perth, through leadership positions in PESA (Petroleum Exploration Society of Australia) and taking a leading role in convening the 2017 Basins Workshop - a 2 day meeting that brought together representatives of industry, government and academia in an informal environment designed to encourage the exchange and sharing of ideas.

Conference Presentations

Chen, P. (2017). Fault segmentation, linkages and reactivation in multi-phase extension, Rowley sub-basin, Roebuck Basin, Australia. Specialist Group in Tectonics and Structural Geology, Denmark, WA

Chen, P. (2017). An Enigmatic Transverse Structural Domain of the Northwest Passive Margin of Australia. AAPG Annual Conference & Exhibition, Houston, USA

Cunneen, J. (2017). Basement controls on the evolution of the Outer Basin High, Ceduna Shelf: Integration of seismic and gravity data. Specialist Group in Tectonics and Structural Geology, Denmark, WA

Cunneen, J. (2017). Evolution of the outer basin high, Ceduna Sub-basin, southern Australia. APPEA Conference & Exhibition, Perth, WA

Elders, C. (2017). Salt tectonics in the Petrel Basin, Australia. Specialist Group in Tectonics and Structural Geology, Denmark, WA

Elders, C. (2017). Salt tectonics in the Petrel Basin, Australia. AAPG International Conference & Exhibition, London, UK

Elders, C. (2017). Regional scale mapping of the Carnarvon and Roebuck Basins. Specialist Group in Tectonics and Structural Geology, Denmark, WA

McHarg, S. (2017). A possible structural control of the Lewis Trough. Specialist Group in Tectonics and Structural Geology, Denmark, WA

Rohead-O'Brien, H. (2017). Controls on Mesozoic rift-related uplift syn-extensional sedimentation in the central Exmouth Plateau. Specialist Group in Tectonics and Structural Geology, Denmark, WA

Smith, G. (2017). Portfolio analysis of petroleum fields and prospects—a robust statistical method.

Terraced cliffs of an Oligo-Miocene carbonate succession. Ras ir Raheb, Malta.

Research reports

SPATIAL SCIENCES

Geodesy and Spatial Sciences

Geodesy

Geodesy involves the study of the Earth's shape and gravity field. It forms the scientific basis for precise positioning over large areas, navigation, mapping and charting, and studies of the physics and dynamics of the Earth. It therefore contributes to the Earth-present theme in TIGeR.

Earth and planetary gravity field modelling

The Geodesy Group's continuing work on gravity field modelling in 2017 has focussed on new gravimetric quasigeoid models for Australia and New Zealand, gravimetric terrain corrections on a 30 m grid over the whole of the Australian continent, an astronomical profile of vertical deflections across the Perth Basin, and high-resolution (2 km) gravity field models of the Moon. Quasigeoid models are commonly used to transform GPS heights to heights based on mean sea level and thus be compatible with topographic maps.

The Australian gravimetric quasigeoid model supersedes AUSGeoid09 (also computed at Curtin) and now includes location-specific error estimates (Figure 1), allowing GPS users to gain some insight into the precision of their height conversions. The New Zealand gravimetric quasigeoid model uses a new nation-wide airborne gravity survey (McCubbine *et al.*, 2017a), thus accounting for previously problematic mountainous and coastal regions (Figure 2). The Australian gravimetric terrain corrections and their estimated errors (Fig. 3) comprise 18.3 billion values, which posed some computational challenges that were overcome by the "Fastest Fourier Transform in the West" (McCubbine *et al.*, 2017b). The vertical deflection (the direction of the gravity vector) profile in the Perth Basin shows good agreement with Australian data, but also highlights deficiencies in the coastal zone. Finally, our lunar gravity models use a more rigorous computational procedure than used before in planetary gravity field modelling and incorporate 3D density information.

McCubbine J.C., Stagpoole V., Caratori Tontini F., Amos M.J., Smith E., Winefield R. (2017a). Gravity Anomaly Grids for the New Zealand region. *New Zealand Journal of Geology and Geophysics*, 60(4), 381-391.

McCubbine J.C., Featherstone W.E., Kirby J.F. (2017b). Fast Fourier-based Error Propagation for the Gravimetric Terrain Correction. *Geophysics*, 82(4), G71-G76.

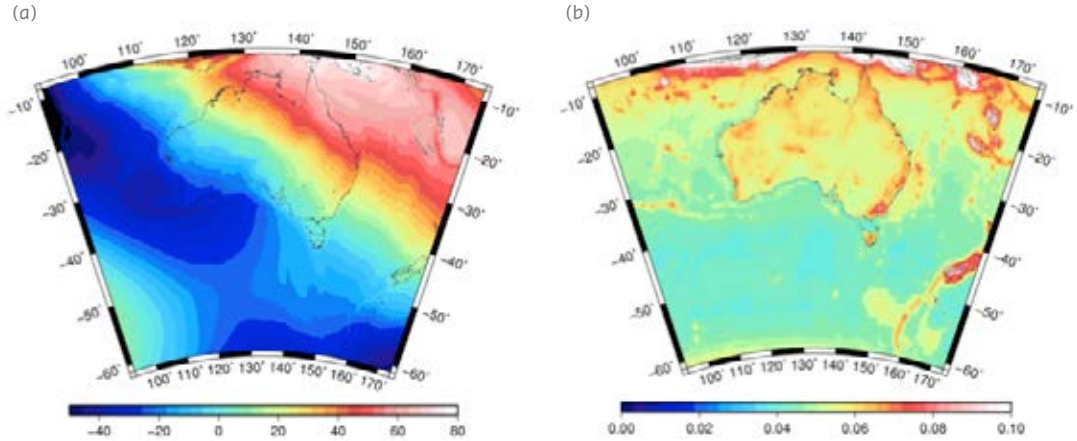

Figure X1: (a) The Australian gravimetric quasigeoid model 2017 (AGQG2017), and (b) its associated location-specific error map/chart. Units in metres.

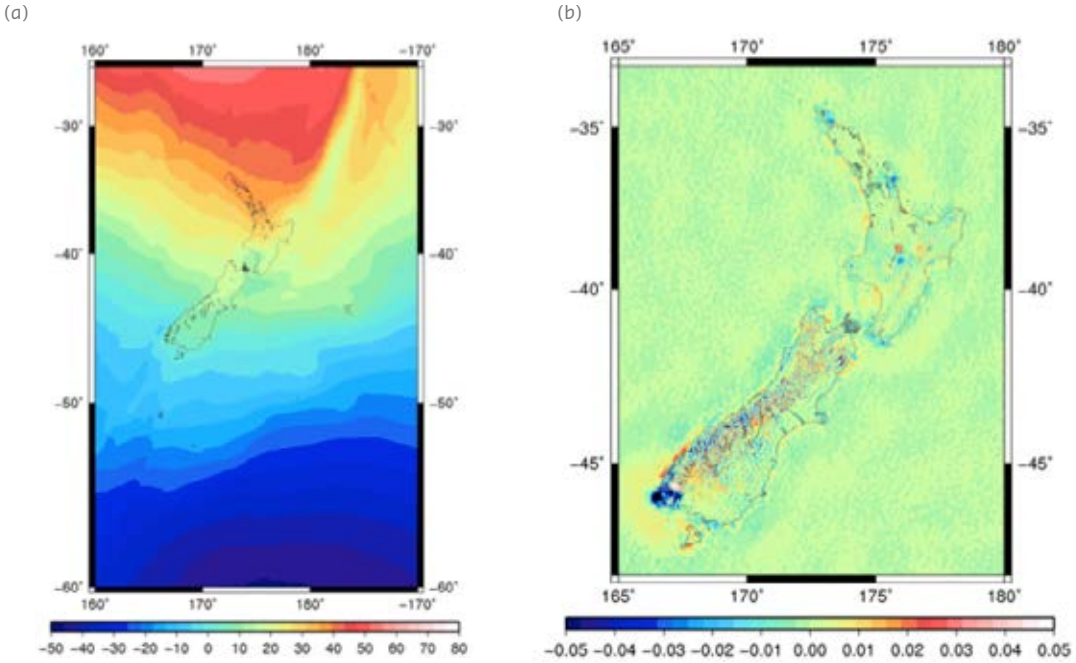

Figure 2: (a) The New Zealand gravimetric quasigeoid model 2017 (NZGEOID2017), and (b) the changes in quasigeoid heights achieved by including airborne gravity data. Units in metres.

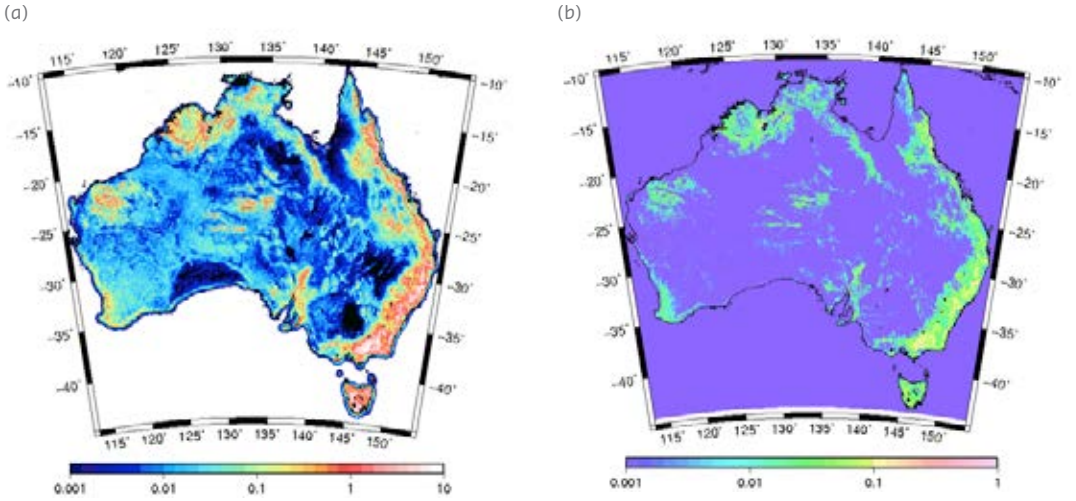

Figure 3: (a) Planar gravimetric terrain corrections (mGal) over Australia, and (b) error in the planar terrain correction for correlated height errors. Units in mGal.

The Perth Basin imaged from Sentinel-1A InSAR

This research uses satellite radar imagery to measure ground displacements in the Perth Basin linked to groundwater extraction. It includes publication of the very first results from the new Sentinel-1 satellite over Australia, revealing subsidence at rates > 20 mm/yr coincident with wetlands, and over broader (>5 km wide) regions at rates up to 15 mm/yr. Longer time-series are required to now determine whether these displacements are representative of long-term behaviour or seasonal variations. The results serve as a useful reconnaissance tool, and show promise for a roll out of additional applications in other Australian locations. Satellite radar is just one component of the geodetic monitoring system we have developed in Perth.

Our recent research has also involved establishing guidelines for installing ground-infrastructure to integrate these measurements with other ground instrumentation such as GNSS. This work has been featured in the press in "position" and "spatial source" magazines.

Parker A.L., Filmer M.F., Featherstone W.E. (2017) First results from Sentinel-1A InSAR over Australia: Application to the Perth Basin. *Remote Sensing*, 9(3), 299, doi:10.3390/rs9030299.

Parker A.L., Featherstone W.E., Penna N.T., Filmer M.F., Garthwaite M.C. (2017) Practical considerations before installing ground-based geodetic infrastructure for integrated InSAR and cGNSS monitoring of vertical land motion. *Sensors*, 17(8), 1753, doi:10.3390/s17081753.

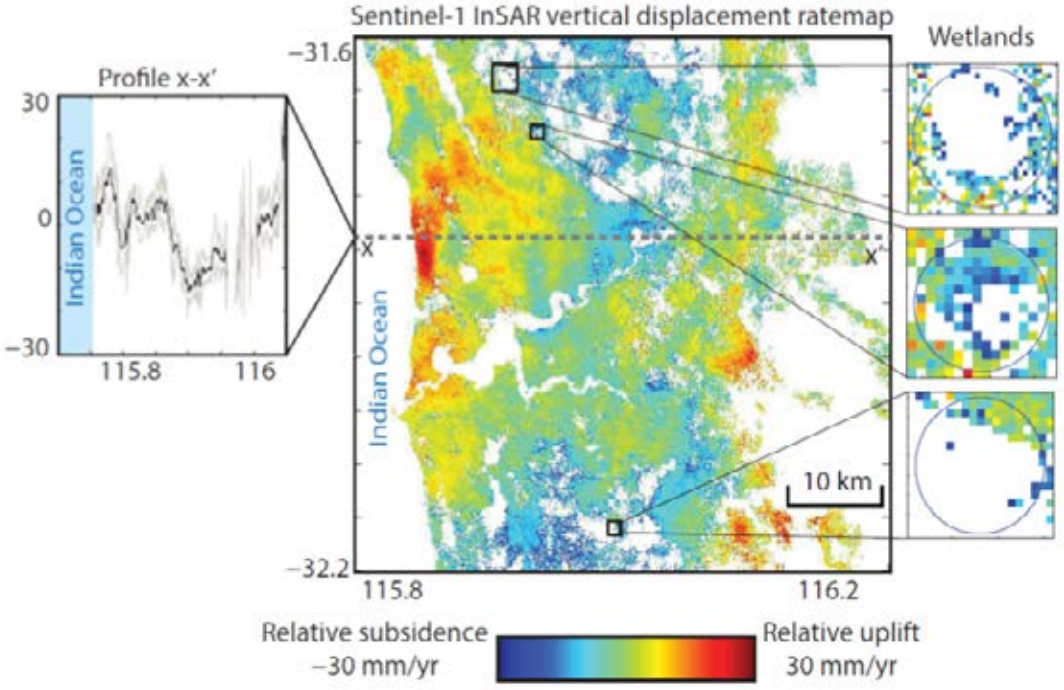

Spatial variations in the effective elastic thickness of the lithosphere in Southeast Asia

As a proxy for long-term lithospheric strength, detailed information on lateral effective elastic thickness (T_e) variations can aid in understanding the distribution pattern of surface deformation and its response to long-term forces. Shi *et al*., (2017) present high-resolution maps of spatial variations of T_e for the complex SE Asian region by analyzing the coherence of topography and Bouguer gravity anomaly data. They find that after considering the gravity deficit of less dense sediment, the recovered T_e maps are more representative of the geology, particularly in elongated rift basins. The results show that the Te variation pattern in SE Asia, in general, agrees well with its tectonic provinces and major tectonic boundaries. The oceanic basins, the Indosinian suture zones between the Indochina and Sibumasu blocks, and the Makassar Strait are characterized by low T_e, while moderate and high T_e values are recovered in the Khorat plateau, West Burma, the Singapore Ridge, the Con Song Swell, Borneo, the northern Australian margin and the Molucca Sea.

The results suggest that East Borneo might share a similar crustal basement, and represent a broad tectonic zone of the destroyed Meso-Tethys Ocean extending from West-Middle Java, through East Borneo to northern Borneo of the Sarawak and Sabah. The Indosinian zones between the Indochina and Sibumasu blocks might extend further southeastward across Billiton Island to offshore of southern Borneo, and the Singapore platform and SWBorneo might belong to the same block.

Shi X., Kirby J., Yu C., Jiménez-Díaz A., Zhao J. (2017). Spatial variations in the effective elastic thickness of the lithosphere in Southeast Asia. *Gondwana Research*, 42, 49-62.

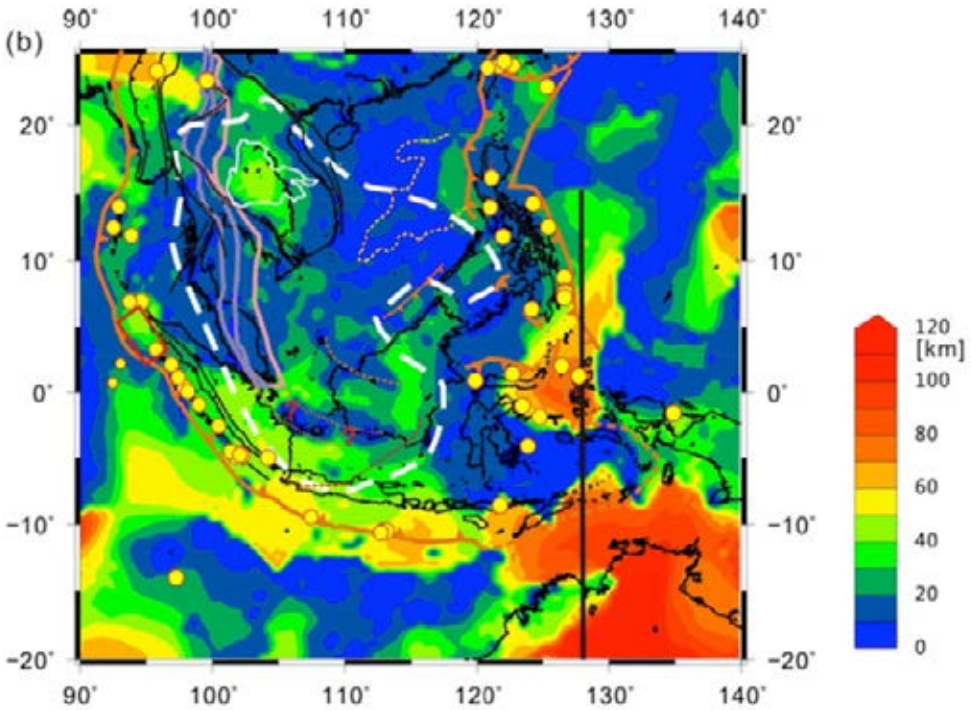

Sediment-corrected elastic thickness of the lithosphere in SE Asia.

Wilyabrup Sea Cliffs, Margaret River region, Western Australia.

Convergence and divergence in spherical harmonic series of the gravitational field generated by high-resolution planetary topography

Hirt and Kuhn (2017) have studied the convergence/divergence behaviour of spectral domain gravity forward modelling on the Moon based on 'external' spherical harmonic series expansions commonly used to model the external gravitational field of Earth, Moon and other planetary bodies. While this study numerically confirmed the well-known theory that convergence is guaranteed when evaluating on or outside a sphere enclosing all field generating masses (known as the Brillouin sphere) it also provided valuable new insight into the behaviour when evaluating inside the Brillouin sphere where the series may be convergent or may be divergent. A set of synthetic experiments have been conducted comparing results for the gravitational attraction of the Moon's topography using spherical harmonic series and numerical integration (e.g. Newtonian integration) where the latter is free from any divergence issues. Evaluations have been done at various height levels and different levels of resolutions, increasing from degree 90 to 2160 (~60 to 2.5 km spatial scales).

Results show that the 'external' spherical harmonic series expansions are numerically convergent outside the field generating masses considering low spectral resolutions up to about degree 180 (~30 km spatial scales). However, for higher spatial resolutions serious divergence issues start to be present at locations deep inside the Brillouin sphere prohibiting accurate gravity modelling. For the highest resolution considered (degree 2016; ~2.5 km spatial scales) divergence is present over most of the Moon's surface (cf. Figure 1). In this case alternate modelling techniques have to be used such as the Newtonian integration (as done in this study) or a combination of 'external' and 'internal' potential spherical harmonic series expansions being numerically more intensive. As a key result a new hypothesis has been formulated based on the behaviour of potential degree variances (e.g. spectral power) to predict divergence inside the Brillouin sphere. Results suggest, if the potential degree variances show a minimum, then the 'external' spherical harmonic series expansions diverge somewhere inside the Brillouin sphere.

Hirt C., Reußner E., Rexer M., Kuhn M. (2016). Topographic gravity modeling for global Bouguer maps to degree 2160: Validation of spectral and spatial domain forward modelling techniques at the 10 μGal level. *Journal of Geophysical Research* 121, 6846–6862.

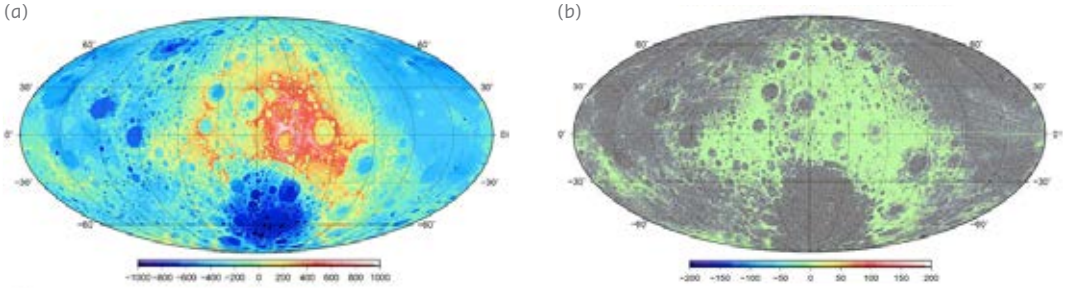

Forward modelling results using a degree-2160 model of the Moon's topography (obtained from the Lunar Orbiter Laser Altimeter, LOLA). Panel a: Gravitational attraction from Newtonian Integration (NI), panel b: Gravitational attraction from 'external' spherical harmonic series expansions minus NI at the topographic surface, unit in mGal (1 mGal = 1×10^{-5} ms^{-2}). Grey colour in panel b indicates severe divergence issues with several 1000 mGal amplitudes.

Spectral models of Earth's gravitational and topographic potential

A number of contemporary studies compare high-resolution models of the Earth's topographic and gravitational potential. However, depending on the modelling techniques and underlying levels of approximation, the correlation at high degrees vary significantly, as do the conclusions drawn.

Hirt *et al*., (2017) compare a number of models of topographic potential constituents (e.g., potential implied by land topography, ocean water masses, etc.), and provide a guide on global correlation measures with particular emphasis on approximation effects in topographic potential modelling. The importance of compatibility of approximation levels in topographic/gravitational potential comparisons has been demonstrated. Very significant short-scale correlation between Earth's gravitational potential and the potential generated by Earth's land topography (correlation +0.92, and 60% reduction rates) has been identified. However, the potential generated by the Earth's oceans water masses is largely unrelated to the gravitational potential at short scales, suggesting that altimetry-derived gravity and/or bathymetric data sets are significantly underpowered at 5 arc-min scales. It has also been shown that the Bouguer shell and terrain correction are responsible for ~20% and ~25% of short-scale gravitational signals, respectively.

Gravity disturbances synthesised in band 2 to 2000 at 4000 m height above reference. Left: sphEGM2008 model, reference surface = sphere, Right: EGM2008, reference = GRS80 ellipsoid. Units in mGal, grids equally spaced in terms of geocentric latitude, area shown is Northern Polar region (80º-90º geocentric latitude). The figure illustrates that band-limited operations such as truncation below the maximum model degree are permitted for sphEGM2008, while high-latitude striations prohibit the band-limited use of EGM2008 (in spherical harmonic representation).

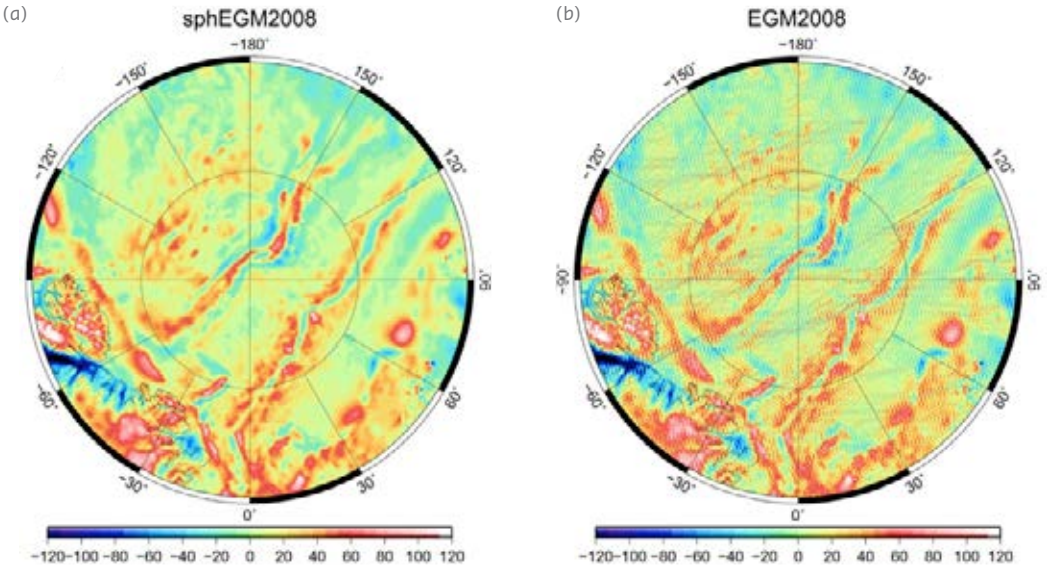

Forward modelling results using a degree-2160 model of the Moon's topography (obtained from the Lunar Orbiter Laser Altimeter, LOLA). Panel a: Gravitational attraction from Newtonian Integration (NI), panel b: Gravitational attraction from 'external' spherical harmonic series expansions minus NI at the topographic surface, unit in mGal (1 mGal = 1×10^{-5} ms^{-2}). Grey colour in panel b indicates severe divergence issues with several 1000 mGal amplitudes.

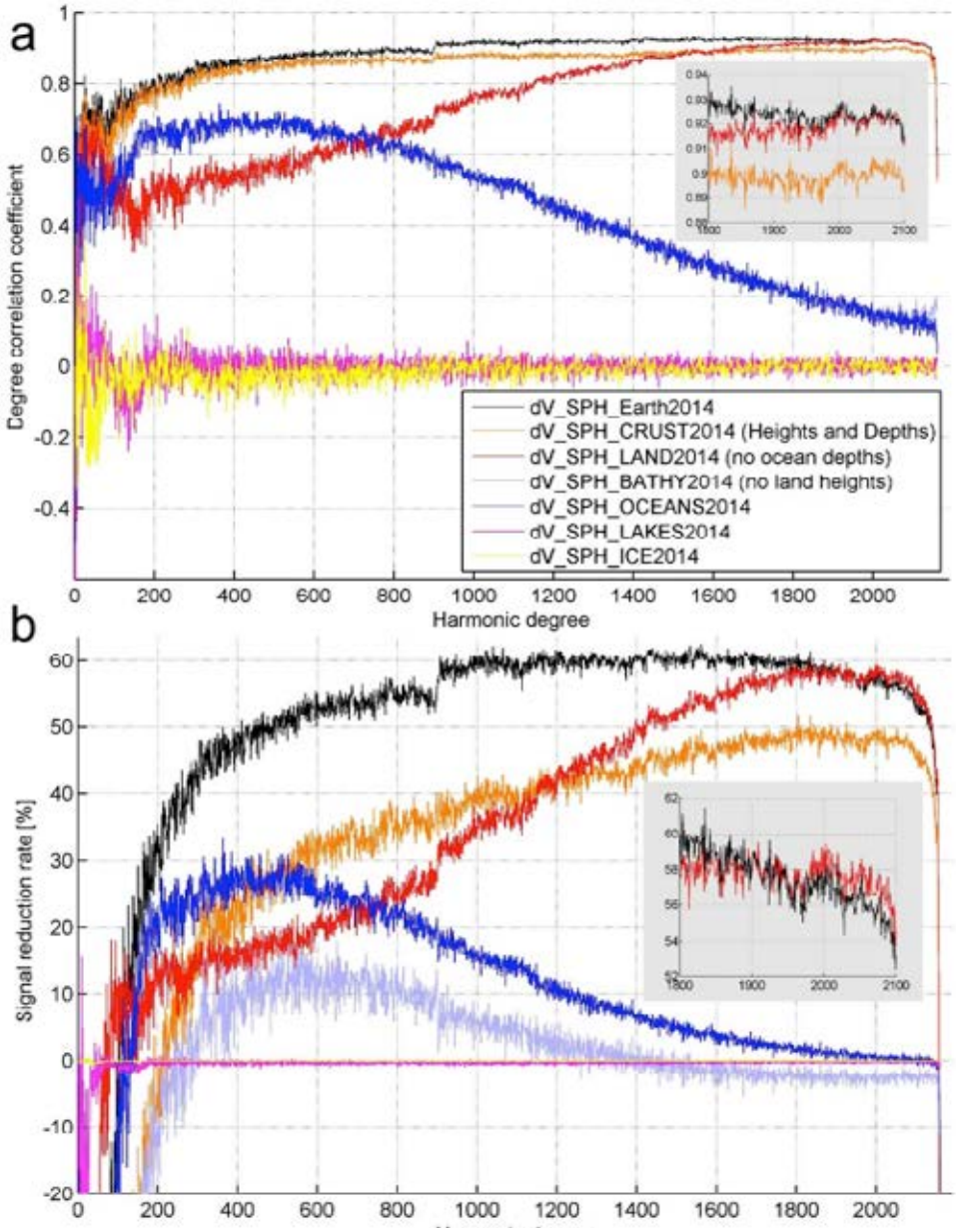

Top: Correlation between the gravitational potential model sphEGM2008 and the topographic potential model dV_SPH_Earth2014 (black) and its constituents (various colours); Bottom: the same in terms of reduction rates. The top figure shows the correlation between the constituents of the topographic potential with the gravitational potential and the bottom figure shows the amount (percentage) of gravitational signal explained by the topographic potential and its constituents.

Hirt C., Rexer M., Claessens S.J., Rummel R. (2017). The relation between degree-2160 spectral models of Earth's gravitational and topographic potential: a guide on global correlation measures and their dependency on approximation effects. *Journal of Geodesy*, 91, 1179-1205.

Hydrogeological characterisation of groundwater over Brazil using remotely sensed and model products

For Brazil, a country frequented by droughts and whose rural inhabitants largely depend on groundwater, reliance on isotope for its monitoring, though accurate, is expensive and limited in spatial coverage. Hu *et al*., (2017) exploit total water storage (TWS) derived from Gravity Recovery and Climate Experiment (GRACE) satellites to analyse spatial-temporal groundwater changes in relation to geological characteristics. Large-scale groundwater changes are estimated using GRACE-derived TWS and altimetry observations in addition to GLDAS and WGHM model outputs. Additionally, TRMM precipitation data are used to infer impacts of climate variability on groundwater fluctuations.

The results indicate that climate variability mainly controls groundwater change trends while geological properties control change rates, spatial distribution, and storage capacity. Granular rocks in the Amazon and Guarani aquifers are found to influence larger storage capability, higher permeability (> 10^{-4} m/s) and faster response to rainfall (1 to 3 months' lag) compared to fractured rocks (permeability < 10^{-7} m/s and lags > 3 months) found only in Bambui aquifer. Groundwater in the Amazon region is found to rely not only on precipitation but also on inflow from other regions. Areas beyond the northern and southern Amazon basin depict a 'dam-like' pattern, with high inflow and slow outflow rates (recharge slope > 0.75, discharge slope < 0.45). This is due to two impermeable rock layer-like 'walls' (permeability < 10^{-8} m/s) along the northern and southern Alter do Chão aquifer that help retain groundwater. The largest groundwater storage capacity in Brazil is the Amazon aquifer (with annual amplitudes of > 30 cm). Amazon's groundwater declined between 2002 and 2008 due to below normal precipitation (wet seasons lasted for about 36 to 47% of the time). The Guarani aquifer and adjacent coastline areas rank second in terms of storage capacity, while the northeast and southeast coastal regions indicate the smallest storage capacity due to lack of rainfall (annual average is rainfall <10cm).

Hu, Awange *et al*., (2017). Science of the Total Environment, doi:10.1016/j.scitotenv.2017.04.188.

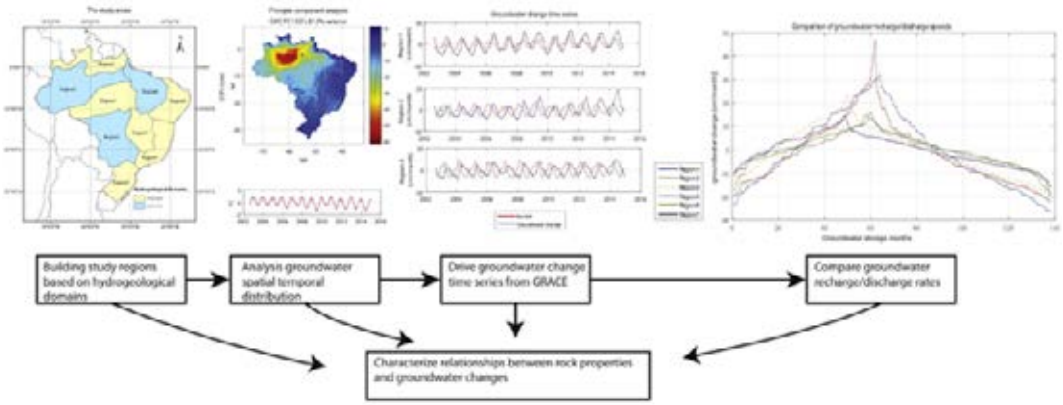

Precise Point Positioning

El-Mowafy *et al*., (2017a-d) provide a solution to a serious problem when using the Precise Point Positioning (PPP) method in real-time natural hazard early warning systems, i.e. when communication breaks take place resulting in a discontinuity in receiving the needed observation correction data. A method is presented to maintain real-time PPP with 3D accuracy less than a decimetre when such a break takes place. For a short corrections outage of a few minutes we predict the IGS-RTS orbits using a fourth order polynomial, and for longer outages up to 3 hours, the most recent IGS ultra-rapid orbits are used. The IGS-RTS clock corrections are predicted using a second order polynomial and sinusoidal terms. The models parameters are estimated sequentially using a sliding time window such that they are available when needed. Evaluation of the proposed method shows that positioning precision of less than 10cm can be maintained for up to two hours after the break.

In another research we address the need for continuous and trustworthy positioning as a critical capability for advanced driver assistance systems (ADAS). To achieve continuous positioning, Global Navigation Satellite Systems Real-Time Kinematic (GNSS-RTK), Doppler-based positioning, and positioning using low-cost inertial measurement unit (IMU) with car odometer data are combined in this study. A novel integrity monitoring approach is presented to guarantee reliable positioning for the proposed integrated system. A new protection level is presented to bound the maximum directional position error. The proposed approach was validated through a kinematic test in an urban area in Japan achieving 100% positioning availability and the target integrity level that is more than 99%.

———

El-Mowafy, A., Deo, M. Kubo, N. (2017), Maintaining real-time precise point positioning during outages of orbit and clock corrections. *GPS Solutions*, 21(3), 937-947. ARC-DP170103341.

———

El-Mowafy, A., Kubo N. (2017). Integrity Monitoring of Vehicle Positioning in Urban Environment Using RTK-GNSS, IMU and Speedometer. *Measurement, Science and Technology*, 28(5), 055102, 1-12.

———

El-Mowafy, A. (2017). Advanced Receiver Autonomous Integrity Monitoring Using Triple Frequency Data with a Focus on Treatment of Biases. *Advances in Space Research*, 59(8), 2148-2157.

———

El-Mowafy, A. (2017). Impact of Predicting Real-Time Clock Corrections during their Outages on Precise Point Positioning. *Survey Review*, DOI 10.1080/00396265.2017.1405155.

Test Vehicle and test trajectory (Tokyo).

Research reports

COMPUTATIONAL GEOSCIENCES

Computational Geochemistry

The incorporation of the Computational Geochemistry group led by Professor Julian Gale is a major addition to the strengths of TIGeR.

The computational geochemistry group, in the Department of Chemistry provides an important new perspective on the problem of crystal growth mechanisms. They work at the atomic level, looking at the fundamental processes by which materials and minerals form. The computations involve up to a million atoms or more, and can test how their behaviour changes in response to different experimental conditions. Such research is made possible by through accessing the petascale computer at the Pawsey Centre.

The research in computational geochemistry involves studying the nucleation and growth of minerals from aqueous solutions using computer simulations based on both force fields and *ab initio* quantum mechanics. In particular, they are focusing on minerals relevant to biomineralisation including those composed of calcium in combination with carbonate, oxalate, sulphate or phosphate. This spans processes from ion pairing and formation of pre-nucleation clusters through to mineralogy and polymorphism.

During the past year, they have reported several significant findings. Firstly, they have mapped for the first time the free energy landscape for both calcium and carbonate ions binding to the acute and obtuse step edges of calcite. This provides important insights for how this mineral will grow from solution. The key finding is that initially only carbonate binds, while Ca^{2+} subsequently attaches to form an adsorbed ion pair. However, the first addition of $CaCO_3$ results in an ion pair that has one ion on top of the step and one at the bottom, in contrast to the conventional view of kink nucleation which has both ions at the bottom in order to grow the step. Secondly, they have shown that the lack of a specific orientation for particular organic molecules when adsorbed on calcite is the result of binding on top of the water layer, rather than direct coordination to the surface.

The thermodynamics of calcium-sulfate ion pair formation

Byrne *et al.*, (2017) have studied he thermodynamics of ion pair formation between Ca^{2+} and SO_4^{2-} using a rigid ion force field, the polarizable AMOEBA force field, and *ab initio* molecular dynamics simulation. The results obtained from the three methods are remarkably similar and consistent with the available experimental data and show that the ion association is driven by an increase in entropy, which can be related to the release of water molecules as previously found for Ca^{2+} and CO_3^{2-}.

Two new rigid ion force fields targeting different solvation free energies for sulfate have been developed. The comparison between static and dynamic properties of the solvated anion, as well as the pairing free energy with Ca^{2+}, suggest that the model with the strongest solvation is more realistic, which may help to resolve the inconsistency in the current literature.

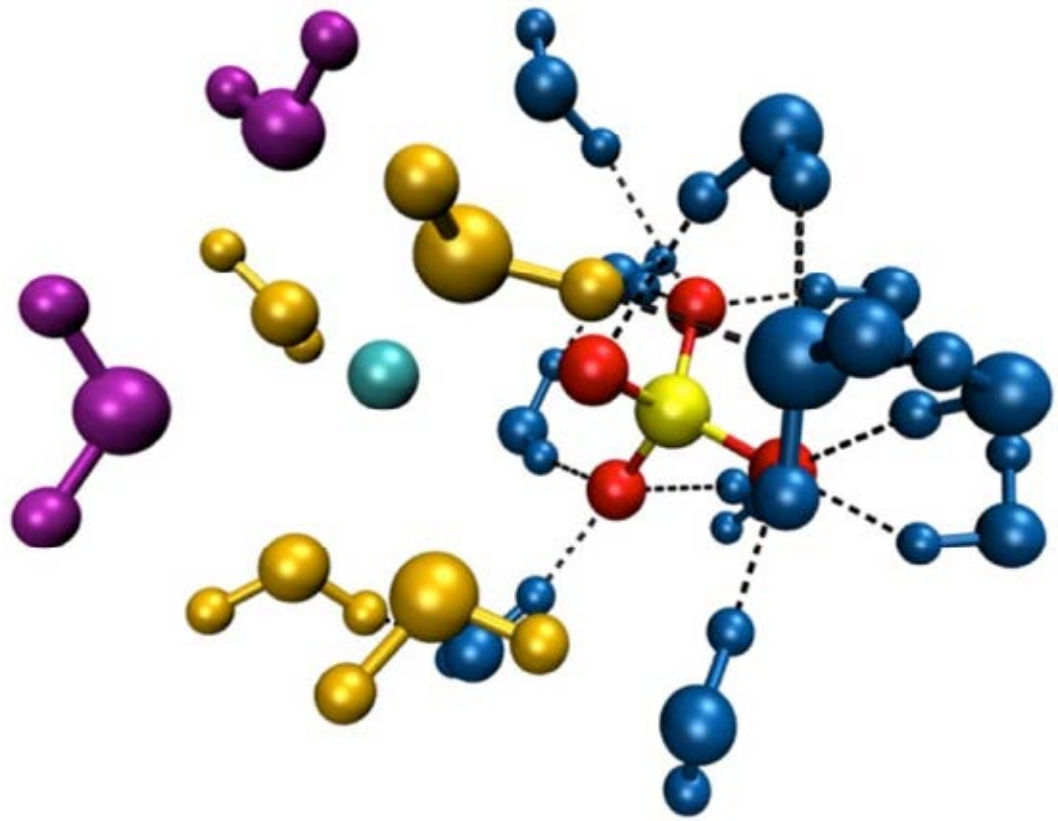

Contact ion pair between the Ca^{2+} (cyan) and SO_4^{2-} (yellow and red) with their first hydration shells. The purple and blue water molecules belong to the solvation shell of Ca^{2+} and SO_4^{2-}, respectively, while the gold water molecules bridge the two solvation shells. The dashed lines show the hydrogen bonding between the water molecules and the SO_4^{2-} ion.

Byrne E., Raiteri P., Gale J.D. (2017). Computational insight into calcium-sulfate ion pair formation. *J. Phys. Chem. C*, 121, 25956-25966.

The atomistic mechanism for how calcite steps grow

Computer simulations have been used to map the initial thermodynamics for the growth of steps on a calcite surface from aqueous solution, leading to the identification of the competing atomic pathways. This revealed that growth is limited by the rearrangement of adsorbed ion pairs from the exposed corner of the step edge to kink nucleation sites.

Free energy iso-surfaces for a calcium ion adsorbing at the obtuse (a,c) and acute (b,d) calcite steps when carbonate is present at either the growth site (a,b) or step edge (c,d). The colored energy scale represents where Ca^{2+} is more stable than in an ion pair in water.

De La Pierre M., Raiteri P., Stack A.G., Gale J.D. (2017). Uncovering the atomistic mechanism for calcite step growth. *Angewandte Chem. Int*. Ed., 56, 8464-8474.

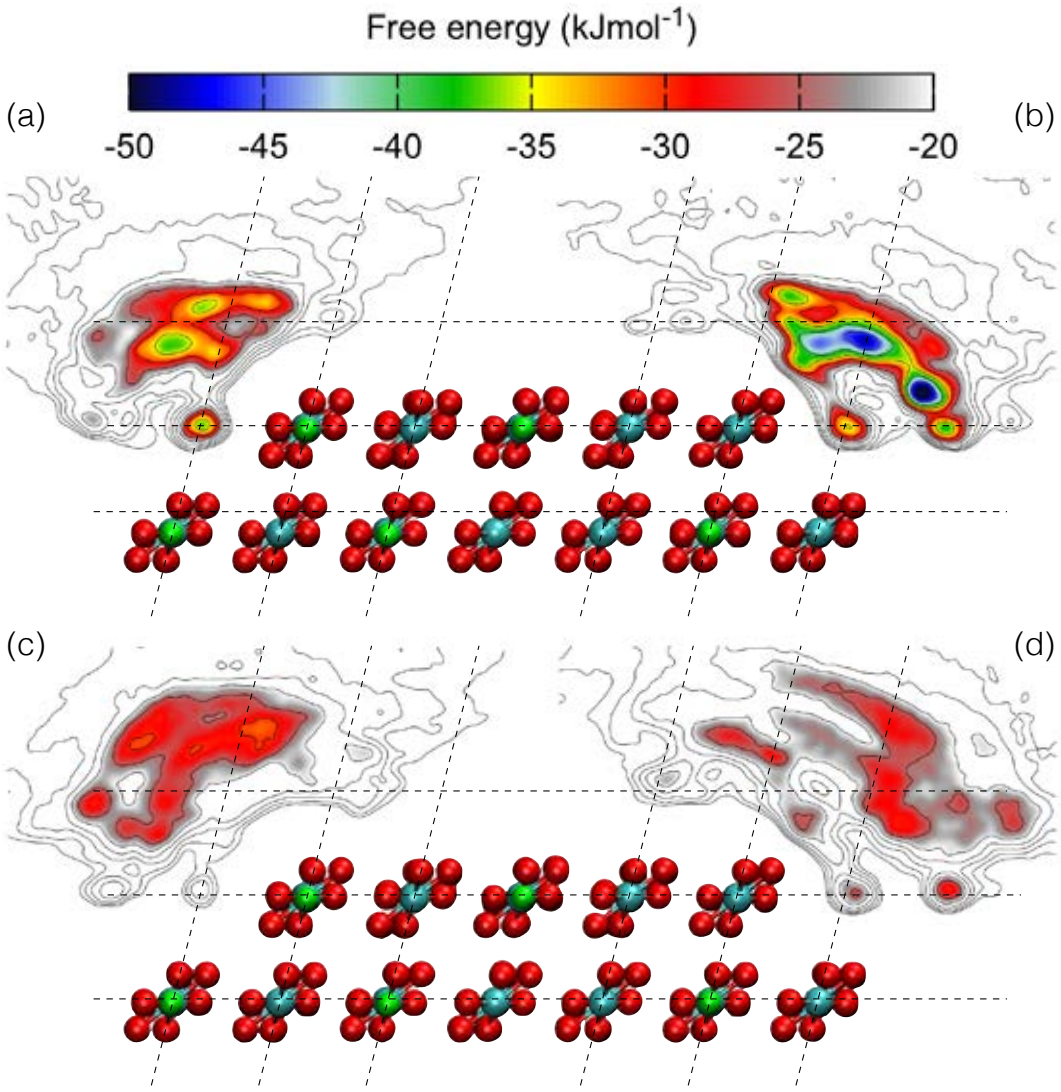

Experimental crystal growth at the nanoscale

Computations and experiments are complementary and Atomic Force Microscopy (AFM) enables crystal growth to be observed in situ in a fluid cell at the nanoscale. The results of such experiments identify research questions that can be resolved with modelling techniques as well as provide constraints on the molecular modelling. In turn, molecular modelling provides the theoretical basis to explain the experimental observations. Some examples of published work during 2017 are given below.

Nanoscale imaging of the sequestration of phosphates on the brucite surface

Phosphorus is a major growth-limiting nutrient of plants and other organisms. Elevated P input into soil solutions and aquatic environments leads to eutrophication and thereby increasing the risk of environmental pollution. In order to evaluate the organic P cycle and the ultimate fate in the environment, it is critical to understand the effects of mineral interfaces on the reactivity, adsorption and precipitation of organic P phases. Wang *et al*., (2017) used Atomic force microscopy (AFM) to directly observe *in situ* the kinetics of coupled dissolution and precipitation on cleaved surfaces of brucite ($Mg(OH)_2$).

Such direct nanoscale observations of the transformation of adsorption/complexation-surface precipitation, combined with spectroscopic characterization and species simulations may improve the mechanistic understanding of P sequestration by mineral replacement reactions through a mechanism of coupled dissolution-precipitation occurring at mineral-solution interfaces in the environment.

Wang, L.J., Putnis, C.V., King, H.E. Hoevelmann J., Ruiz-Agudo E., Putnis A. (2017). Imaging organophosphate and pyrophosphate sequestration on brucite by in situ atomic force microscopy. *Environmental Science & Technology*, 51, 328-336.

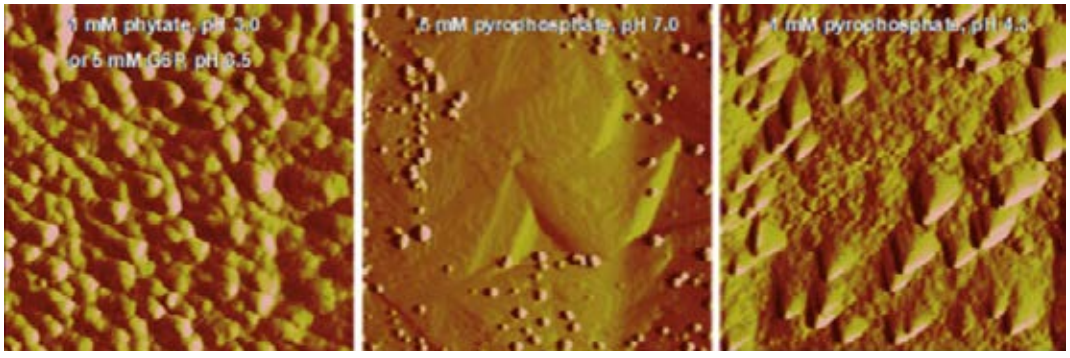

The AFM mages are all 3x3 µm and show Mg-P nanoparticles forming on a brucite surface by an interface-coupled dissolution-precipitation mechanism

Using less soluble oxalate to form a protective layer on marble cultural heritage

A relatively new idea for preserving marble artifacts is to use an oxalate solution that will react with the calcite by a coupled dissolution-precipitation mechanism to form a thin layer of calcium oxalate, which is more durable than marble, on the surface. The efficacy of this procedure however depends on a detailed understanding of the crystal morphology, porosity and coherence with the underlying marble substrate.

The influence of pH and citrate concentration on the replacement of calcite by calcium oxalate has been investigated by *in-situ* nanoscale observations in flow-through experiments performed using atomic force microscopy (AFM). Significant changes in the morphology of the precipitated whewellite ($CaC_2O_4 \cdot H_2O$) crystals were observed, as well as in the degree of interface coupling of the dissolution-precipitation reactions, depending on the pH of the solution. Citrate also influences whewellite morphology. The results of this study may help in the understanding of kidney stone formation and prevention as well as in the design of effective treatments for the protection of calcareous stone, based on the natural process of patina formation that occurs in monuments. Ultimately understanding the reactions at the nanoscale will help to elucidate the process of unwanted oxalate precipitate formation and its control by small organic molecules such as citrate.

Burgos-Cara, A., Putnis, C. V., Ortega-Huertas, M., Ruiz-Agudo E. (2017). Influence of pH and citrate on the formation of oxalate layers on calcite revealed by in situ nanoscale imaging. *CrystEngComm*., 19, 3420-3429.

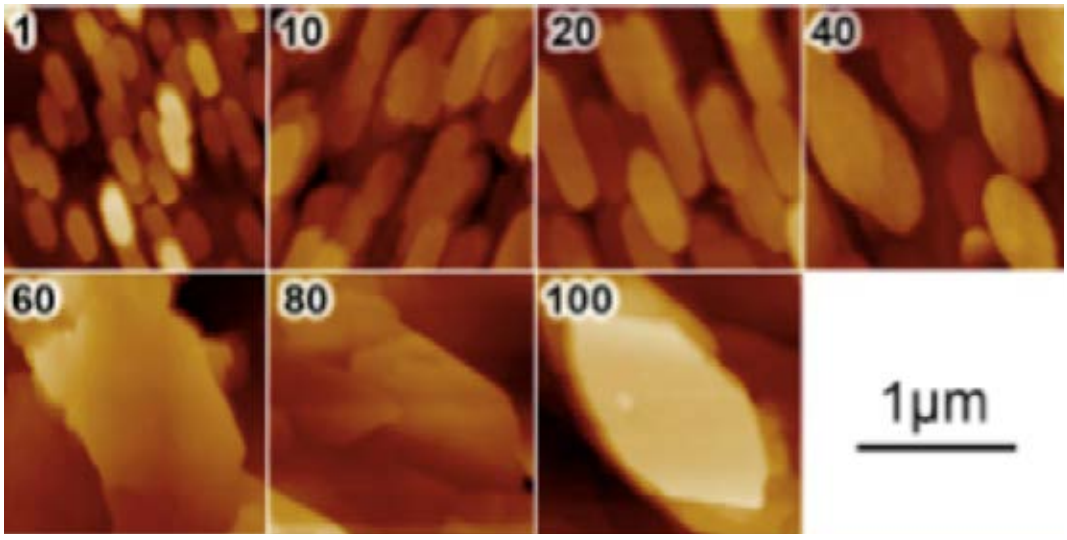

AFM height images of calcite surfaces covered with Ca-oxalate nano-crystals precipitated in the presence of citrate of increasing concentration (in mM) shown in upper left hand corner of each image after reaction with Na-oxalate solutions (25mM at pH 2.5).

Computational Geoscience

Multiscale Modelling

In 2017, the group led by Prof Victor Calo published nineteen papers on the multiscale and multiphysics modelling of materials. The research group works on a wide range of topics. For example, in 2017 they spent a significant amount of effort in understanding the quality of the discrete approximations to several differential operators' spectra. They mainly develop and analyse the dispersion properties of the finite element and isogeometric analysis (IGA) methods for wave propagation. This understanding helps us design better ways to simulate seismic wave propagation using less computational resources.

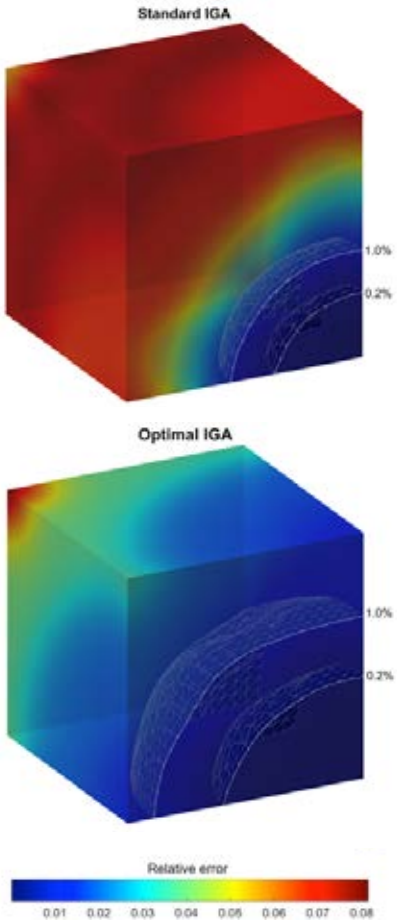

3D eigenproblem: relative error for C1 quadratic IGA.

Refereed Archival Journals

Sarmiento, A., Espath, L., Vignal, P., Dalcin, L., Parsani, M., Calo, V. (2017). An energy-stable generalized-α method for the Swift-Hohenberg equation. *Journal of Computational and Applied Mathematics*, DOI: 10.1016/j.cam.2017.11.004.

Muñoz Matute, J., Alberdi Celaya, E., Pardo, D., Calo, V. (2017). Time-domain goal-oriented adaptivity using pseudo-dual error representations, *Computer Methods in Applied Mechanics and Engineering*, 325, 395-415.

Puzyrev, V., Deng, Q., Calo, V. (2017). Dispersion-optimized quadrature rules for isogeometric analysis: modified inner products, their dispersion properties, and optimally blended schemes. *Computer Methods in Applied Mechanics and Engineering*, 320, 421-443.

Calo, V., Deng, Q., Puzyrev, V. (2017). Quadrature blending for isogeometric analysis. *Procedia Computer Science*, 108, 798-807.

Puzyrev, V., Vilamajo, E., Queralt, P., Ledo, J., Marcuello, A. (2017). Three-dimensional modeling of the casing effect in onshore controlled-source electromagnetic surveys. *Surveys in Geophysics*, 38(2), 527-545.

Egorov, A., Pevzner, R., Bona, A., Glubokovskikh, S., Puzyrev, V., Tertyshnikov, K., Gurevich, B. (2017). Time-lapse full waveform inversion of vertical seismic profile data: workflow and application to the CO2CRC Otway project. *Geophysical Research Letters*, 44, 7211-7218.

Deng, Q., Ginting, V. (2017). Locally Conservative Continuous Galerkin FEM for Pressure Equation in Two-Phase Flow Model in Subsurfaces. *Journal of Scientific Computing*, 1-22.

Deng, Q., Ginting, V., McCaskill, B., Torsu, P. (2017). A locally conservative stabilized continuous Galerkin finite element method for two-phase flow in poroelastic subsurfaces. *Journal of Computational Physics*, 347, 78-98.

Zou, Q., Guo, L., Deng, Q. (2017). High Order Continuous Local-Conserving Fluxes and Finite-Volume-Like Finite Element Solutions for Elliptic Equations. *SIAM Journal on Numerical Analysis*, 55(6), 2666-2686.

Espath, L., Sarmiento, A., Dalcin, L., Calo, V. (2017). On the thermodynamics of the Swift-Hohenberg theory. *Continuum Mechanics and Thermodynamics*, 29(6), 1335-1345.

Vignal, P., Collier, N., Dalcin, L., Brown, D., Calo, V. (2017). An energy-stable time-integrator for phase-field models. *Computer Methods in Applied Mechanics and Engineering*, 316, 1179-1214.

Bartoň, M., Ait-Haddou, R., Calo, V. (2017). Gaussian quadrature rules for C1 quintic splines with uniform knot vectors. *Journal of Computational and Applied Mathematics*, 322, 57-70.

Poveda, L., Galvis, J., Calo, V. (2017). Localized harmonic characteristic basis functions for multiscale finite element methods. *Computational and Applied Mathematics*, 1-15.

Mora, J., Mantilla, J., Calo, V. (2017). A multiscale formulation for FEM and IGA. *Boletin de Matematicas*, 24(1), 101-115.

Sarmiento, A., Cortes, A., Garcia, D., Dalcin, L., Collier, N., Calo, V. (2017). PetIGA-MF: a multi-field high-performance toolbox for structure-preserving B-splines spaces. *Journal of Computational Science*, 18, 117-131.

Aboueisha, H., Calo, V., Jopek, K., Moshkov, M., Paszyńka, A., Paszyński, M., Skotniczny, M. (2017). Element Partition Trees For H-Refined Meshes to Optimize Direct Solver Performance. Part I: Dynamic Programming. *International Journal of Applied Mathematics and Computer Science*, 27(2), 351-365.

Cortes, A., Dalcin, L., Sarmiento, A., Collier, N., Calo, V. (2017). A scalable block-preconditioning strategy for divergence-conforming B-spline discretizations of the Stokes problem. *Computer Methods in Applied Mechanics and Engineering*, 316, 839-858.

Bartoň, M., Calo, V. (2017). Gauss-Galerkin quadrature rules for quadratic and cubic spline spaces and their application to isogeometric analysis. *Computer-Aided Design*, 82, 57-67.

Garcia, D., Pardo, D., Dalcin, L., Paszyński, M., Collier, N., Calo, V. (2017). The value of continuity: Refined isogeometric analysis and fast direct solvers. *Computer Methods in Applied Mechanics and Engineering*, 316, 586-605.

Book chapters

Barton, M., Calo, V., Deng, Q., Puzyrev, V. (2017). Generalization of the Pythagorean eigenvalue error theorem and its application to isogeometric analysis. To appear in *Numerical methods for PDEs. Lectures from the fall 2016 thematic quarter at Institut Henri Poincaré, Eds: Di Pietro, D., Ern, A., Formaggia*, L., SEMA-SIMAI Series, Springer.

Kheriji, W., Efendiev, Y., Calo, V., Gildin, E. (2017). Model reduction for near-well & reservoir models using multiple space-time discretizations. *Model Red of Param Systems*, 17, 471-490.

Modelling the evolution of metamorphic rocks

In an ongoing project the aim is to describe the chemo-mechanical interactions of rocks which lead to phase transformation and cracking. In particular, we seek to model reaction-diffusion processes that generate physical and chemical changes in metamorphic rocks.

Such processes control the evolution of the metamorphic system by determining the inhomogeneous pressure distribution of e.g. quartz inclusions in garnet. A related process is the growth of new minerals along the boundaries between reactant minerals, which yields the rim growth associated with reactive minerals. From metamorphic petrology, we know that the chemical processes in rocks trigger substantial volume changes that induce stresses that lead to cracking. Following this line of thought, we divide this research project into three stages. The first line models chemical interactions in rocks as reaction-diffusion phase-transformation processes. The second line relates and models the interleaving between the chemo-mechanical interactions. Finally, in the third line studies the fracture formation as a consequence of such chemo-mechanical interactions. Herein, we summarize the main ingredients for the modelling and description of the stages mentioned above as well as the percentage of progress.

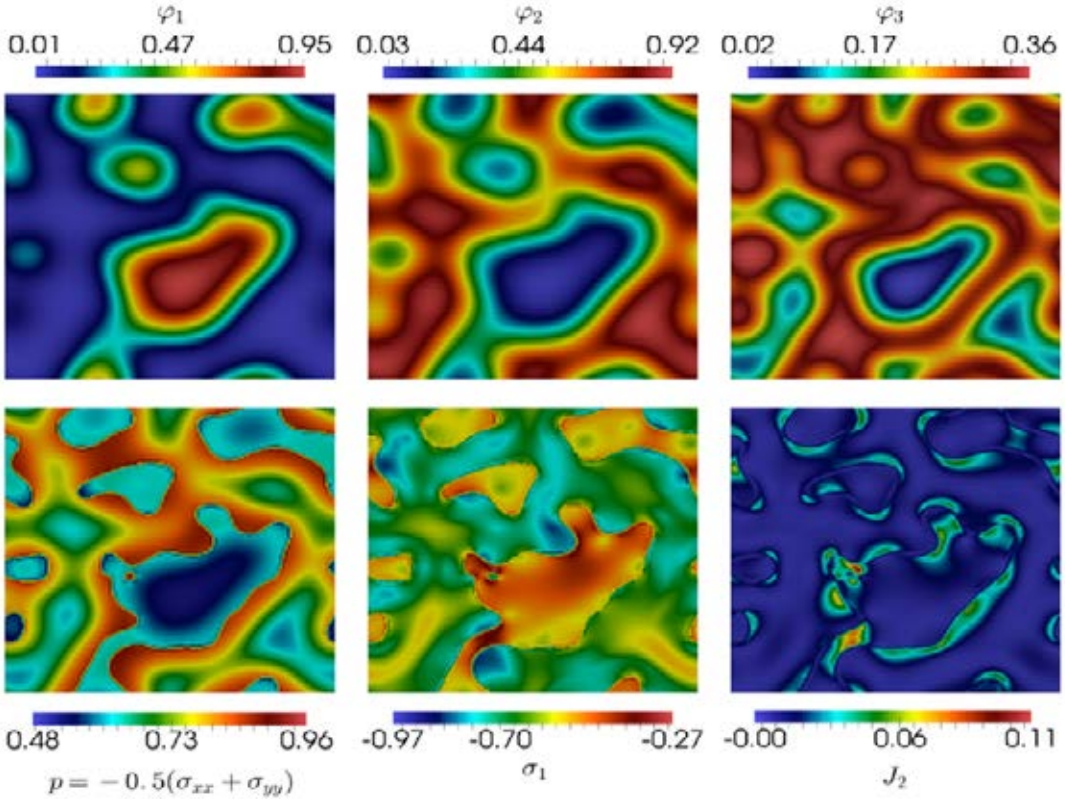

Inhomogeneous pressure distribution and rim growth.

The Savannah Mine, WA.

Research reports

EXPLORATION GEOPHYSICS

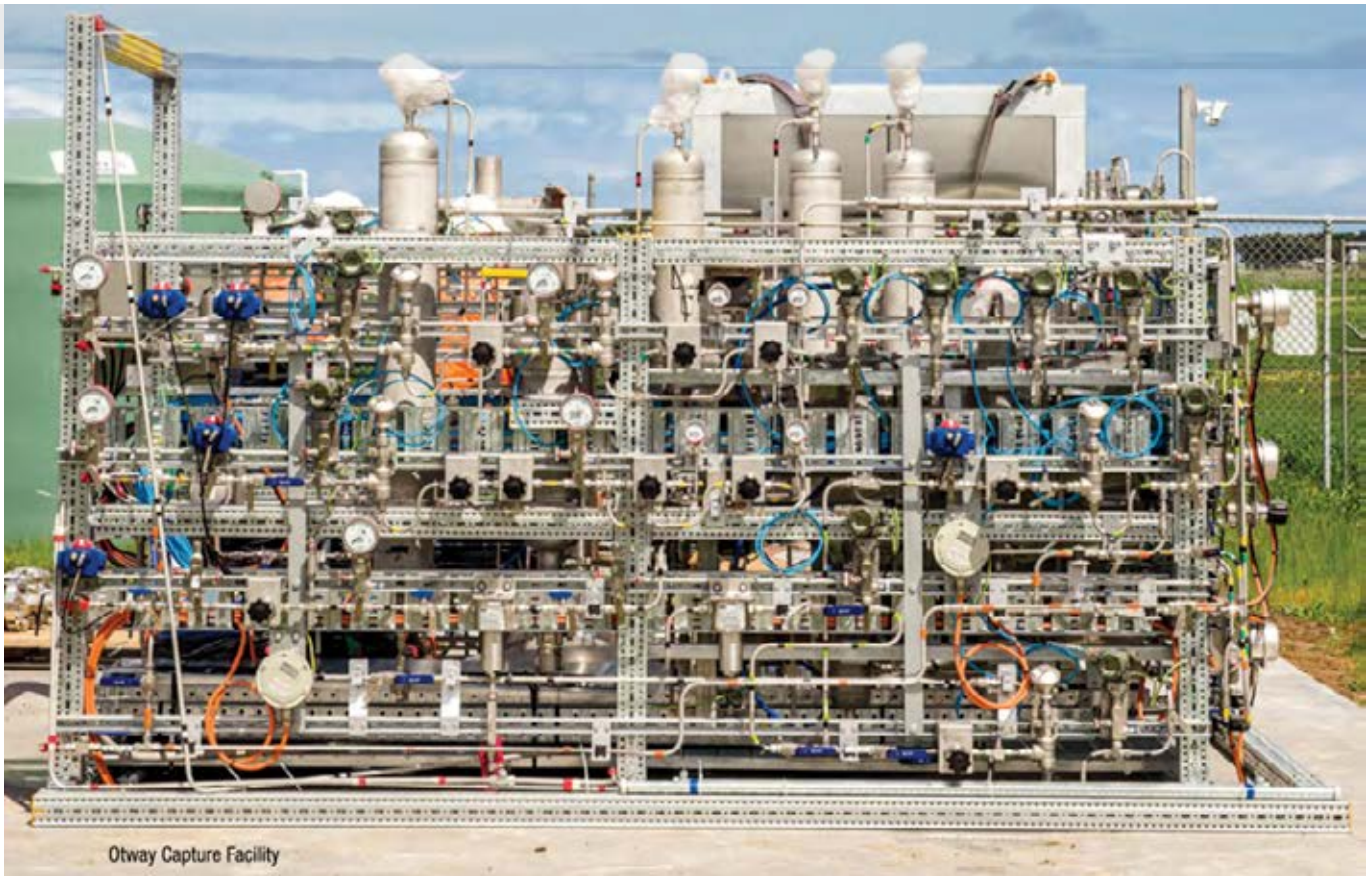

From the CO2CRC 2016/17 Annual Report: http://www.co2crc.com.au/wp-content/uploads/2017/11/AR16-17_web.pdf

Carbon sequestration in porous rocks

CO2CRC's Otway research facility is Australia's first demonstration of the deep geological storage of carbon dioxide. Researchers in the Department of Exploration Geophysics are involved in various aspects of the methods used for monitoring CO_2 sequestration and its effects, developing the theoretical basis for interpreting data from the injection wells as well as simulating the effects of rock properties on the CO_2 plume behaviour and its trapping capacity.

Impact of salinity and rock wettability on CO_2 storage efficiency

In a series of papers related to underground geological carbon storage (Al-Khdheeawi *et al.*, 2017a-e) have investigated the impact of rock wettability and its spatial distribution on the CO_2 plume behaviour and its trapping capacity.

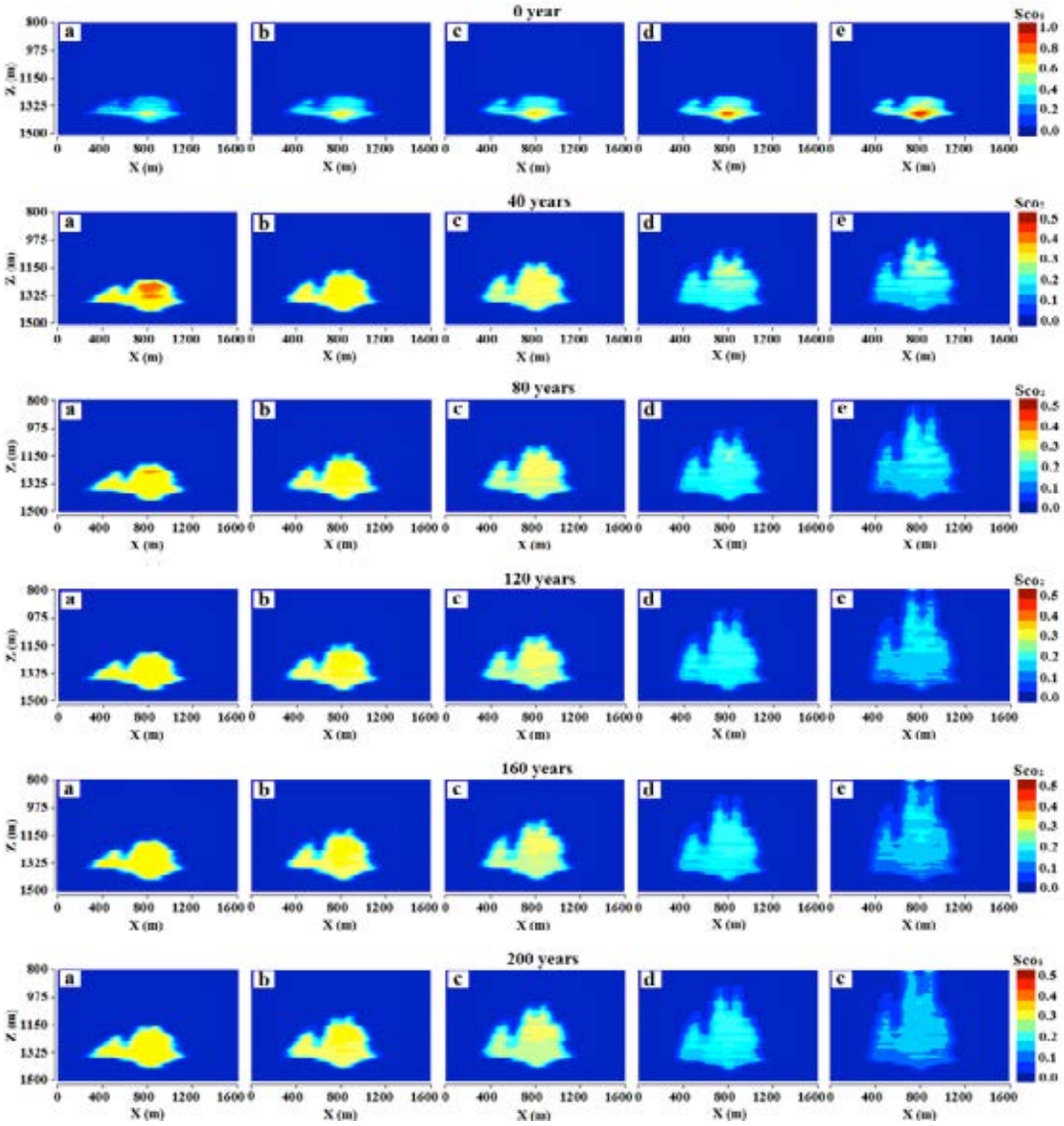

2D vertical cross-sections through the centre of the storage reservoir. CO_2 is injected at a depth of (1373m) through a one vertical well. The CO_2 plume shape and height in the reservoir are shown for 5 different rock wettability types: a) strongly water-wet; b) weakly water-wet; c) intermediate-wet; d) weakly CO_2-wet; e) strongly CO_2-wet. 2 Mt of CO_2 was injected in total.

This study was performed through multiphase flow simulations using TOUGH2 software package; an intensive laboratory data set acquired in house was used to constrain and model capillary pressure and relative permeability curves that include hysteresis behaviour. Wettability, within and between reservoirs, can vary drastically, from strongly water-wet to strongly CO_2-wet, but usually, most simulations use default parameters and do not include wettability heterogeneity or hysteresis. They found that wettability has a significant effect on CO_2 migration and trapping capacities: strongly water-wet formations are preferable sinks for CO_2, with the least vertical plume migration and the highest storage capacity (less residual CO_2 but more dissolved CO_2). This is an important result for the choice of an optimal storage reservoir or for designing geo-engineering solutions that enhance storage capacity.

Refereed Archival Journals

Al-Khdheeawi, E., **Vialle, S.**, Barifcani, A., Sarmadivaleh, M., and Iglauer S. (2017a), Impact of salinity on CO_2 storage efficiency in highly heterogeneous reservoirs, *Greenhouse Gases: Science and Technology*, 8(1), 95-105, doi: 10.1002/ghg.1723.

Al-Khdheeawi, E., **Vialle, S.**, Barifcani, A., Sarmadivaleh, M., and Iglauer S. (2017b), Influence of Rock Wettability on CO_2 Migration and Storage Capacity in Deep Saline Aquifers, *Energia Procedia*, 114, 4357-4365, doi: 10.1016/j.egypro.2017.03.1587.

Al-Khdheeawi, E., **Vialle, S.**, Barifcani, A., Sarmadivaleh, M., and Iglauer S. (2017c) Effect of brine salinity on CO_2 plume migration and trapping capacity in deep saline aquifers, *The APPEA Journal*, 57, 100–109, doi: 10.1071/AJ16248.

Al-Khdheeawi, E., **Vialle, S.**, Barifcani, A., Sarmadivaleh, M., and Iglauer S. (2017d), Influence of injection well configuration and rock wettability on CO_2 plume behaviour and CO_2 trapping capacity in heterogeneous reservoirs, *Journal of Natural Gas Science and Engineering*, 43, doi:10.1016/j.jngse.2017.03.016.

Al-Khdheeawi, E., **Vialle, S.**, Barifcani, A., Sarmadivaleh, M., and Iglauer S. (2017e), Impact of reservoir wettability and heterogeneity on CO_2 plume migration and trapping capacity, *International Journal of Greenhouse Gas Control*, 58, doi: 10.1016/j.ijggc.2017.01.012.

Time lapse full waveform inversion of vertical seismic profile data: application to the CO2CRC Otway project

Vertical seismic profile (VSP) is one of the technologies for monitoring CO_2 geosequestration. However, quantitative interpretation of time-lapse VSP is challenging due to its irregular distribution of source-receiver offsets. One way to overcome this challenge is to use full waveform inversion (FWI), which does not require regular offsets. Egorov *et al*., (2017) present a workflow of elastic FWI applied to offset vertical seismic profile data for the purpose of identification and estimation of time-lapse changes introduced by injection of 15,000 t of CO_2-rich gas mixture at 1.5 km depth. Application of this workflow to both synthetic and field data shows that elastic FWI is able to detect and quantify the time-lapse anomaly in P wave velocity with the magnitude of 100–150 m/s.

Comparison of baseline and monitor VP inverted models and their difference. (a) Baseline inverted VP; (b) monitor inverted VP, all traces included in monitor inversion; (c) difference between monitor and baseline inverted VP models, all traces included in monitor inversion; (d) monitor inverted VP, traces with high time-lapse noise level removed from the monitor inversion; and (e) difference between monitor and baseline inverted VP models, traces with high time-lapse noise level removed from the monitor inversion.

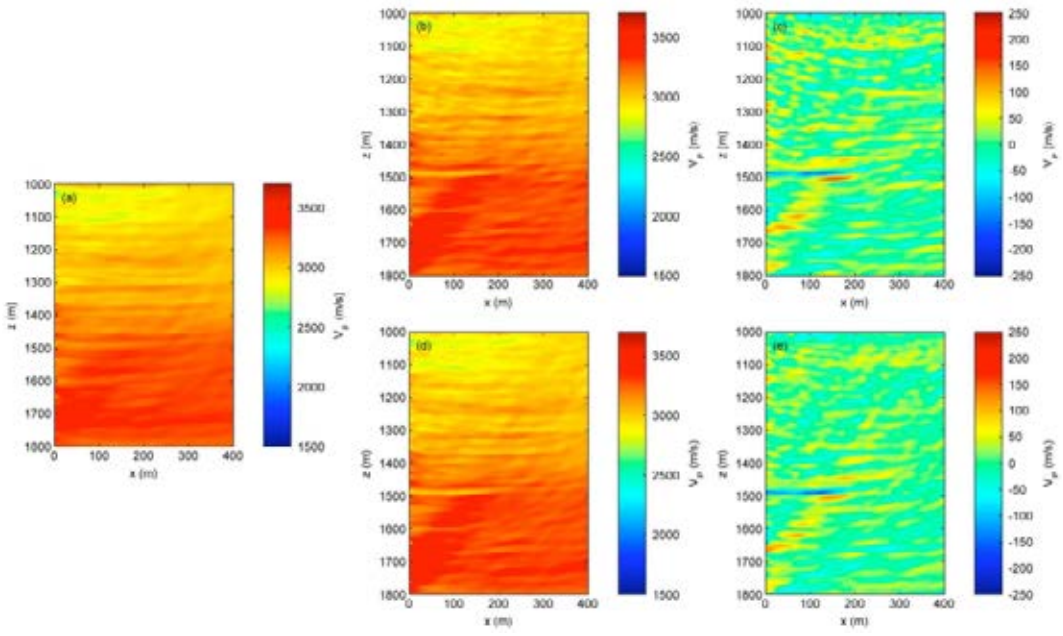

Egorov, A., R. Pevzner, A. Bóna, S. Glubokovskikh, V. Puzyrev, K. Tertyshnikov, and B. Gurevich. 2017. "Time-lapse full waveform inversion of vertical seismic profile data: Workflow and application to the CO2CRC Otway project." *Geophysical Research Letters* 44 (14): 7211-7218.

Skippy Rock, Cape Leeuwin, WA.

Using 4D surface seismic monitoring to track supercritical CO_2 injection into the subsurface: application to the CO2CRC Otway Project

Time-lapse (4D) seismic monitoring of injected CO_2 in geological formations is being increasingly employed as the principal method for ensuring containment of the CO_2 and testing conformance of predicted plume behaviour. However, to bring further confidence in this method, the CO_2 volume detection limit in the seismic monitoring and key factors controlling it need to be quantitatively understood. The CO2CRC Otway Project attempts to improve this understanding by exploring the capability of seismic reflection method to detect and monitor a 15,000 t injection of supercritical CO_2/CH_4 mixture in a saline aquifer at a depth of 1500 m.

To increase the signal to noise ratio and to reduce the disruption to land users, seismic acquisition is performed using a buried geophone array. Seismic acquisition occurred at injection intervals of 5000, 10,000 and 15,000 t over a 5-month period. The seismic images clearly show the distribution and evolution of the stored CO_2/CH_4 plume. The analysis confirms that signal from pure CO_2 would be of similar magnitude to the signal from CO_2/CH_4 mixture. The results demonstrate the potential of time-lapse reflection seismic to provide key information to both operators and regulators for confirming the security and behaviour of stored CO_2 at very small volumes.

Pevzner, R., M. Urosevic, D. Popik, V. Shulakova, K. Tertyshnikov, E. Caspari, J. Correa, T. Dance, A. Kepic, S. Glubokovskikh, S. Ziramov, B. Gurevich, R. Singh, M. Raab, M. Watson, T. Daley, M. Robertson, and B. Freifeld. 2017. "4D surface seismic tracks small supercritical CO<inf>2</inf>injection into the subsurface: CO2CRC Otway Project." *International Journal Of Greenhouse Gas Control* 63: 150-157.

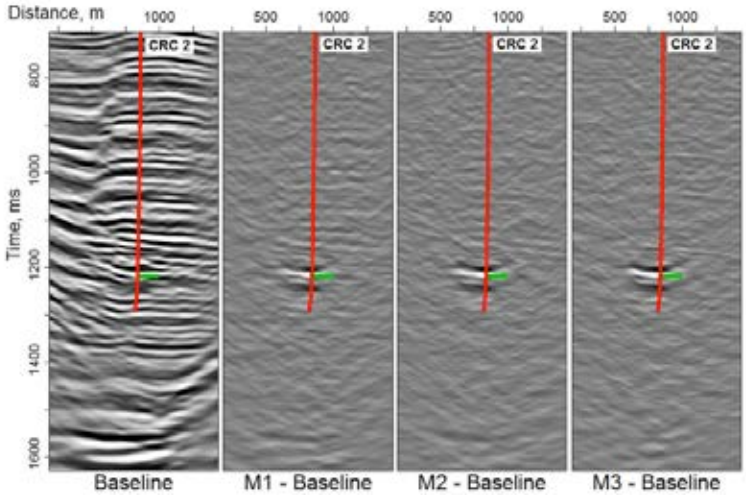

Fast-tracked time-lapse processing results, a line passing through the CRC-2 (Xline 124 in Fig. 1), left to right: baseline data and three difference volumes after injection of 5000, 10,000 and 15,000 t, respectively. The injector well track is shown in red. Well perforation interval is shown in green.

Research reports

EXTRACTIVE METALLURGY

Extractive Metallurgy

Gold Technology Group at Curtin University.

Process Metallurgy (pyro-, hydro-, and electrometallurgy), Minerals Engineering, Waste Processing and Geometallurgy constitute the related fields in the broad church of Extractive Metallurgy which features in the broader field of Resources Engineering and involves the study, evaluation, development and design of processes used in the extraction and beneficiation of economically important metals and minerals from their concentrates and ores.

As such it utilises the knowledge areas of geology and mineralogy, chemistry, microbiology, chemical (process) engineering, electronic engineering and mechanical engineering. As it relates to the chemical environments in which minerals and rocks interact and react with aqueous solutions (in the case of hydrometallurgy and mineral processing) or high temperature melts such as molten slags, mattes and alloys (in the case of pyrometallurgy), it strongly intersects the earth sciences and are often similar, albeit at accelerated reaction rates, to the ore genesis, metamorphosis and weathering processes occurring during the formation of mineral deposits. Conversely, these ore genesis, metamorphosis and weathering processes often inspire and serve as reference cases for the development of industrial metal and mineral extraction processes.

Extractive metallurgy research is chaired by Prof Eksteen, who manages the Gold Technology Group (GTG) and who is the project manager of the AMIRA P420F project. The research activities of the group are predominantly sponsored by industry and research is geared towards innovations that have commercialisation potential. The staff members of the GTG is shown on the following pages.

Figure 2. Australia Technologies Competition Award (Mining Technologies Division).

The research work has been sponsored either directly, or indirectly (through AMIRA, ARC Linkage or MRIWA) by Anglogold Ashanti, Barrick Gold, Evolution Mining, Newmont Mining, Newcrest Mining, Northern Star Resources, Mining and Process Solutions, St Barbara, Orica, Kemix, Gekko Systems, Vega Industries, CSBP-AGR, Pionera, FLSmidth, Lhoist Recherche et Développement, Mineral Research Institute of Western Australia, Panoramic Resources, the Changchung Gold Research Institute, CPL Carbon Link, and Lynas Corporation.The AMIRA P420F project commenced in June 2016 and will continue until June 2019. The project is sponsored by 15 industry sponsors. In addition it obtained financial support from the Cooperative Research Centre for the Optimisation of Resource Extraction (CRC ORE). The current project (cash, excluding in-kind) budget for the 3-year project is circa $5.246 million. During 2017, further amino acid based processing patents were either submitted of progressed to the PCT level (Eksteen and Oraby, 2017), and the various amino-acid based technologies are being commercialised through Mining and Process Solutions Pty Ltd (MPS). MPS was awarded the METS Ignited Award for winning the Mining Technologies division in the Australia Technologies Competition (http://www.austechcomp.com/winners) for commercialising the alkaline amino acid processing approach invented by Curtin Researchers Eksteen and Oraby. The award is shown in Figure 2.

In addition, Curtin University assigned the marketing rights of the "Carbon Scout" carbon meter developed by the GTG team members to Gekko Systems in 2016. In 2017 two "Carbon Scout" units were sold to Anglogold Ashanti and commissioned at their WA operations.

The GTG is also performed the further research sponsored by the Mineral Institute of Western Australia (MRIWA) through research grant M458. Prof Eksteen and Dr Oraby continued research ARC Linkage Grant (LP160101121 based upon funding support by Newcrest Mining and Mining and Processing), titled: "A benign alkaline process for scarce metal extraction and reagent recycle".

Precious Metals Research

Precious metals (gold, silver and platinum group metals) are often associated ore deposits with large spatial geometallurgical variation which significantly impacts downstream metallurgical processing. As such, the metallurgist have to be able to characterise the ores with regards to the anticipated process impacts, and design and operate the processes in such a way as to be robust with regards to the geometallurgical variations. In addition, for leach processes, it becomes important that dissolution is selective to prevent excessive reagent consumption.

In the area of the processing of the ores, concentrates, process intermediated and solutions associated with Platinum Group Metals (PGMs), Cabri *et al*., (2017) investigated the mineralogical and processing potential of two mineralization types in the platinum group element and Ni-bearing Kapalagulu Intrusion, Western Tanzania. Research also continued on the processing of chromitite rich ores such as the Panton Sill deposit in Western Australia, where Mpinga *et al*., (2017) investigated various direct leach approaches to remove and recover base metals from such ores prior to PGM extraction. Research by Schoeman *et al*., (2017a, b) have shown the potential of strong base ion exchange resins to adsorb PGMs and that they can be successfully be eluted. Bezuidenhout *et al*., (2017) investigated a flame optical emission spectroscopy system for converter iron end-point control associated with Ni-Cu-S-PGM converter mattes. Such a system has been successfully implemented at the smelter of a major South African PGM producer. Thyse *et al*., (2017) subsequently have shown how iron endpoint and Ni-Cu-PGM converter matte mineralogy influence breakage and grinding behaviour of these mattes after water granulation.

In the area of gold (and associated base metals) processing, the research fell into three major categories:

- The galvanic interaction of gold bearing minerals such as pyrrhotite, pyrite and arsenopyrite with grinding media and different water types. The work was reported by Rabieh *et al*., (2017a, 2017b, 2017c). It was shown that while the nature of the grinding media galvanic interaction had very little impact on flotation behaviour (in the case of pyrite), it had a remarkable impact on leach behaviour with the order of the reduction in subsequent gold leaching being the most for pyrrhotite, followed by arsenopyrite and pyrite.
- Arsenic in gold ores is a problematic deleterious element (particularly when mobilised in its arsenite form). Various approaches have been identified to remove it from alkaline solutions and immobilise it. Feng *et al*., (2017a,b) investigated the preparation and exploitation of various coated magnetic nano-particles to remove both arsenite and arsenate anions from alkaline effluents using either zirconia coatings on maghemite (γ-Fe_2O_3-ZrO_2) or titania coated on silica coated magnetite (Fe_3O_4-SiO_2-TiO_2). The research has shown that both the arsenite and arsenate anions can be effectively adsorbed and stripped using these coated nanoparticles, opening up new approaches for arsenic on readily recoverable magnetic particles. Figure 3 show how these arsenic-loaded particles are effective removed by the application of a magnetic field.

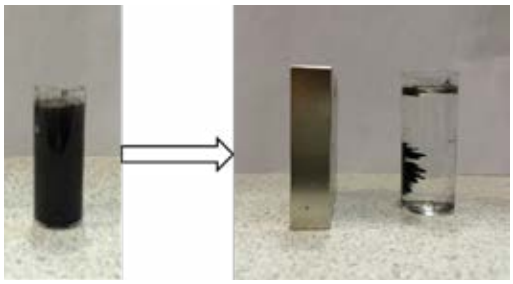

Figure 3. Removal of arsenic coated magnetic nanoparticles using a magnetic field.

- The recovery of gold and copper from copper-gold ores and concentrates remains challenging to perform economically and in an environmentally responsible way. This is due to very large reagent consumption, in particular of sodium cyanide, and the consequent generation of environmentally problematic weak-acid dissociable (WAD) cyanides. It was shown by Oraby and Eksteen (2017) that a synergistic mixture containing only catalytic amounts of cyanide (at starvation levels) and the amino acid glycine can be used effectively to treat these copper-gold ores and concentrates, leading to high extraction rates of these metals while minimising the use of cyanide and the concomitant generation of WAD cyanides. In addition, Tanda *et al*., (2017) made an important contribution to the research by researching the leach behaviour of various copper oxides minerals such as malachite, azurite, cuprite and chrysocolla. This is particularly important for the oxide domain of many copper-gold ores.

Critical Metals Research

Critical metals, in the field of mineral economics normally refers to high technology metals of which their supply chains are at risk due to either natural scarcity, high processing costs and high geopolitical or other risks associated with the primary sources of the materials. Typically, Rare Earth Elements (REEs), niobium, tantalum, lithium and cobalt fall within this category. These metals have gained particular prominence due to their use in renewable energy technologies such as wind turbines, rechargeable batteries and energy storage solutions.

Prof Eksteen has been working with Prof Elizabeth Watkin, Dr Melissa Corbett and Mr Homayoun Fathollahzadeh in the development of a process whereby REE bearing phosphate minerals, such as monazite and xenotime, and their ores are leached using phosphate solubilising micro-organisms. Recent research has identified micro-organisms with significant potential to release REE's and further research is being performed to obtain a better understanding of the mechanisms of REE leaching, focussing on monazite minerals. Corbett *et al*., (2017a) have studied how the incorporation of indigenous microorganisms increases leaching rates of rare earth elements from Western Australian monazite. Moreover, Corbett *et al*., (2017b) also investigated the interactions of phosphate solubilising microorganisms with natural rare-earth phosphate minerals.

Publications in 2017

1. Rabieh, A., Eksteen, J.J. and Albijanic, B., 2017*a*. Galvanic interaction of grinding media with arsenopyrite and pyrite and its effect on gold cyanide leaching. *Minerals Engineering*, 116, pp. 46-55.

2. Rabieh, A., Eksteen, J.J. and Albijanic, B., 2017*b*. The effect of grinding chemistry on cyanide leaching of gold in the presence of pyrrhotite. *Hydrometallurgy*, 173, pp. 115-124.

3. Corbett, M.K., Eksteen, J.J., Niu, X.-Z., Watkin, E.L.J., 2017. Incorporation of indigenous microorganisms increases leaching rates of rare earth elements from Western Australian monazite. *Solid State Phenomena*, 262 SSP, pp. 294-298.

4. Mpinga, C.N., Eksteen, J.J., Aldrich, C., Dyer, L., 2017. Identification of the significant factors determining extractability of Ni and Cu after sulfation roasting of a PGM-bearing chromitite ore. *Minerals Engineering*, 110, pp. 153-165.

5. Tanda, B.C., Oraby, E.A., & Eksteen, J.J. (2017b). Recovery of copper from alkaline glycine leach solution using solvent extraction. *Separation and Purification Technology*, 187, pp. 389–396.

6. Feng, C., Aldrich, C., Eksteen, J.J. and Arrigan, D.W.M., 2017*a*. Removal of Arsenic from Alkaline Process Waters of Gold Cyanidation by Use of γ-Fe_2O_3@ ZrO_2 Nanosorbents. *Hydrometallurgy*, 174, pp. 71-77.

7. Feng, C., Aldrich, C., Eksteen, J.J. and Arrigan, D.W.M., 2017*b*. Removal of Arsenic from Alkaline Process Waters of Gold Cyanidation by Use of Fe_3O_4@ SiO_2@TiO_2 Nanosorbents. *Minerals Engineering*, 110, pp. 40-46.

8. Melissa K. Corbett, Jacques J. Eksteen, Xi Zhi Niu, Jean Philippe Croue, Elizabeth L. J. Watkin, 2017. Interactions of phosphate solubilising microorganisms with natural rare-earth phosphate minerals: a study utilizing Western Australian monazite. *Bioprocess and Biosystems Engineering*, 40, pp. 929–942.

9. Thyse, E.L., Akdogan, G., Mainza, A., Eksteen, J., 2017. PGM converter matte mineral characteristics and effects on downstream processing. *International Journal of Mineral Processing*, 166(10), pp. 89-101

10. Cabri, L.J., Wilhelmij, H.R., Eksteen, J.J., 2017. Contrasting mineralogical and processing potential of two mineralization types in the platinum group element and Ni-bearing Kapalagulu Intrusion, western Tanzania. *Ore Geology Reviews*, 90, pp. 772-789.

11. Eksteen, J.J. Oraby, E.A. and Tanda, B.C., 2017. A conceptual process for copper extraction from chalcopyrite in alkaline glycinate solutions. *Minerals Engineering*, 108, pp. 53-66

12. Schoeman, E., Bradshaw, S.M., Akdogan, G., Snyders, C.A., Eksteen, J.J., 2017. The elution of platinum and palladium cyanide from strong base anion exchange resins. *International Journal of Mineral Processing*, 162, pp. 19-26

13. Schoeman, E., Bradshaw, S.M., Akdogan, G., Snyders, C.A., Eksteen, J.J., 2017. The extraction of platinum and palladium from a synthetic cyanide heap leach solution with strong base anion exchange resins. *International Journal of Mineral Processing*, 162, pp. 27-35

14. Oraby, E.A., Eksteen, J.J., and Tanda, B.C., 2017. Gold and copper leaching from gold-copper ores and concentrates using a synergistic lixiviant mixture of glycine and cyanide. *Hydrometallurgy*, 169, 2017, pp. 339-345

15. Tanda, B.C., Eksteen, J.J. and Oraby, E.A., 2017. An investigation into the leaching behaviour of copper oxide minerals in aqueous alkaline glycine solutions. *Hydrometallurgy*, 167, pp. 153-162

16. Rabieh, A., Eksteen, J.J. and Albijanic, B., 2017c. Influence of grinding media and water quality on flotation performance of gold bearing pyrite. *Minerals Engineering*, 11, pp. 68-76.

17. Bezuidenhout, G.A., Eksteen, J.J., Akdogan, G. Van Beek, B., Wendt, W. Persson, W., 2017. Implementation of flame optical emission spectroscopy system for converter Fe end-point control associated with Ni-Cu-S-PGM converter mattes. *Minerals Engineering*, 100, pp. 132-143.

Bioleaching

the bioleaching group at the School of Biomedical Sciences is led by Prof Elizabeth Watkin. Elizabeth Watkin is an environmental microbiologist and the overarching theme of her research is the microbial ecology of environmental systems and covers the fields of mining biotechnology and mineral resource recovery, microbial induced corrosion, microbial fouling of water (particularly within mining systems).

Her research team investigates biotechnological processes for environmental and industrial applications and approaches to mitigate microbially caused problems such as biocorrosion, biofouling and bioclogging.

Multiple osmotic stress responses in *Acidihalobacter prosperus* result in tolerance to chloride ions

Extremely acidophilic microorganisms (pH optima for growth of ≤3) are utilized for the extraction of metals from sulfide minerals in the industrial biotechnology of "biomining." A long term goal for biomining has been development of microbial consortia able to withstand increased chloride concentrations for use in regions where freshwater is scarce. However, when challenged by elevated salt, acidophiles experience both osmotic stress and an acidification of the cytoplasm due to a collapse of the inside positive membrane potential, leading to an influx of protons.

In collaboration with Mark Dopson (Sweden) and David Holmes (Chile) the ability of the halotolerant acidophile *Acidihalobacter prosperus* to grow and catalyze sulfide mineral dissolution was tested in elevated concentrations of salt. They identified chloride tolerance mechanisms in Ac. *prosperus* as well as the chloride susceptible species, *Acidithiobacillus ferrooxidans*. *Ac. prosperus* had optimum iron oxidation at 20 g L−1 NaCl while *At. ferrooxidans* iron oxidation was inhibited in the presence of 6 g L−1 NaCl. The tolerance to chloride in *Ac. prosperus* was consistent with electron microscopy, determination of cell viability, and bioleaching capability. The *Ac. prosperus* proteomic response to elevated chloride concentrations included the production of osmotic stress regulators that potentially induced production of the compatible solute, ectoine uptake protein, and increased iron oxidation resulting in heightened electron flow to drive proton export by the F0F1 ATPase. In contrast, *At. ferrooxidans* responded to low levels of Cl− with a generalized stress response, decreased iron oxidation, and an increase in central carbon metabolism. One potential adaptation to high chloride in the *Ac. prosperus* Rus protein involved in ferrous iron oxidation was an increase in the negativity of the surface potential of Rus Form I (and Form II) that could help explain how it can be active under elevated chloride concentrations. These data have been used to create a model of chloride tolerance in the salt tolerant and susceptible species *Ac. prosperus* and *At. ferrooxidans*, respectively.

Dopson M., Holmes D.S., Lazcano M., McCredden T.J., Bryan C.G., Mulroney K.T., Steuart R., Jackaman C., Watkin E.L.J. (2017). Multiple osmotic stress responses in *Acidihalobacter prosperus* result in tolerance to chloride ions. *Frontiers in Microbiology*. 05 January 2017 | https://doi.org/10.3389/fmicb.2016.02132

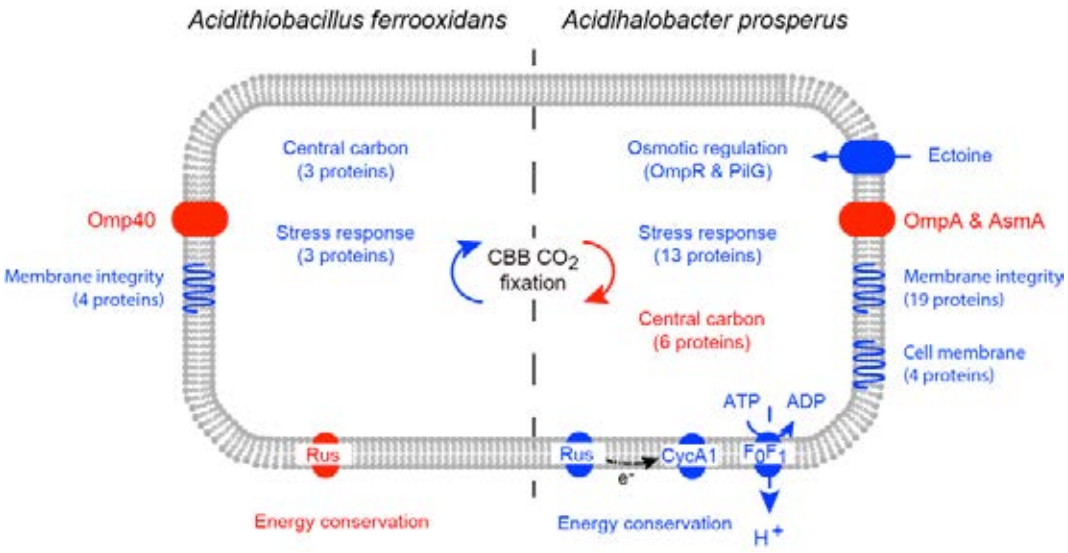

A model of the cellular response of At. *ferrooxidans*^{T} (left) and *Ac. prosperus*^{T} (right) to increased NaCl levels. Increases in protein abundance in high NaCl conditions are represented by blue and decreases in protein abundance in high NaCl conditions are represented by red. Differential protein expression was determined by 2D-PAGE for *At. ferrooxidans*^{T} and iTraq for *Ac. prosperus*^{T}.

Permian Hopeman Sandstone, Cabrach How, Moray coast, NE Scotland.

Research reports

TIGeR PUBLICATION LIST

TIGeR publication list 2017

Books and book chapters

Barton, M., Calo, V., Deng, Q., Puzyrev, V. (2017). Generalization of the Pythagorean eigenvalue error theorem and its application to isogeometric analysis. To appear in Numerical methods for PDEs. Lectures from the fall 2016 thematic quarter at Institut Henri Poincaré, Eds: Di Pietro, D., Ern, A., Formaggia, L., SEMA-SIMAI Series, Springer.

Blum T.B., Darling, J. R., Kelly, T. F., Larson, D. J., Moser, D. E., Perez-Huerta, A., Prosa, T. J., Reddy, S. M., Reinhard, D. A., Saxey, D. W., Ulfig, R. M., Valley, J. W. 2017. Best Practices for Reporting Atom Probe Analysis of Geological Materials. In: Moser, D., Corfu, F. Reddy, S.M., Darling, J. & Tait. K. (eds.) "Microstructural Geochronology: Planetary Records Down to Atom Scale". American Geophysical Union. Geophysical Monograph 232. John Wiley & Sons, Inc. pp. 369-373.

Da Costa, G., Hofmann, A., Agangi A. (2017) Provenance of detrital pyrite in Archean sedimentary rocks: examples from the Witwatersrand Basin. In "Sediment provenance," Ed. Mazumder, Elsevier, 509-531 pp.. dx.doi.org/10.1016/B978-0-12-803386-9.00018-6

Demichelis R., Raiteri P., and Gale J.D. (2017) Ab Initio Modelling of the Structure and Properties of Crystalline Calcium Carbonate; Chapter 6 in: New perspectives on mineral nucleation and growth: From solution precursors to solid materials, pp 113-135, Springer.

Evans, K.A., Bartlett, A., Jaceglav, M. (2017). 'Keeping watch': environmental custodianship and citizen science. In: Gaynor, A., Newman, P., Jennings, P. (Eds.), Never Again: Reflections on Environmental Responsibility After Roe 8. UWA Publishing, Perth, 230-244.

Kusiak, M.A., Wilde, S.A., Wirth, R, Whitehouse, M.J., Dunkley, D.J., Lyon, I. & Reddy, S.M., Berry, A. & De Jonge, M. 2017. Detecting micro- and nano-scale variations in element mobility in high-grade metamorphic rocks: implication for precise U-Pb dating of zircon. In: Moser, D., Corfu, F. Reddy, S.M., Darling, J. & Tait. K. (eds.) "Microstructural Geochronology: Planetary Records Down to Atom Scale". American Geophysical Union. Geophysical Monograph 232. John Wiley & Sons, Inc. pp. 279-291.

Moser, D., Corfu, F. Darling, J., Reddy, S.M., & Tait. K. (eds.) 2018. Microstructural Geochronology: Planetary Records Down to Atom Scale, Geophysical Monograph 232, American Geophysical Union. John Wiley & Sons. pp. 373.

Oliveira E.P., Windley B.F., McNaughton N.J., Bueno J.F., Nascimento R.S. Carvalho M.J., Araujo M.N.C. (2017). The Sergipano Belt. In Sao Francisco Craton, Eastern Brazil, M. Heilbron et al. (eds), Regional Geology Reviews, 241-254.

Pirajno F., Sergeev N., Burlow R. and Tessalina S. (2017). Paroo Station (Magellan–Cano) supergene lead deposits, Capricorn Orogen. In: Australian Ore Deposits, Monographs 32. Ed Neil Philips, 401-403.

Playton T.E., Hocking R.M., Tohver E., Hillbun K., Haines P.W., Trinajstic K., Roelofs B., Katz D.A., Kirschvink J.L., Grice K., Montgomery P., Hansma J., Yan M., Pisarevsky S., Tulipani S., Ratcliffe K., Caulfield-Kerney S., Wray D. (2017). Integrated stratigraphic correlation of Upper Devonian platform-to-basin carbonate sequences, Lennard Shelf, Canning Basin, Western Australia: Advances in carbonate margin-to-slope sequence stratigraphy and stacking patterns. In Playton T.E., Kerans C., Weissenberger J.A.W. (eds). SEPM Special Publication 107: New Advances in Devonian Carbonates: Outcrop Analogs, Reservoirs, and Chronostratigraphy, 248-301.

Ruiz-Agudo E., Putnis C.V. Rodriguez-Navarro C. (2017). Mineral reaction kinetics: Microstructures, textures, chemical and isotopic signatures (Eds. W. Heinrich, R. Abart). EMU short course, vol. 16, Ch. 13: Reactions between minerals and aqueous solutions.

Sawant, A.D., Gupta, S., Clark, C., Misra, S. (2017) The Rauer–Rengali connection in the Indo-Antarctica amalgam: evidence from structure, metamorphism and geochronology. In: Pant, N. C. & Dasgupta, S. (eds) Crustal Evolution of India and Antarctica: The Supercontinent Connection. Geological Society, London, Special Publications, 457.

Saxey, D.W., Reddy, S. M., Fougerouse, D. and Rickard, W. D. A. 2017. The optimization of zircon analyses by laser-assisted atom probe microscopy: Insights from zircon standard 91500. In: Moser, D., Corfu, F. Reddy, S.M., Darling, J. & Tait. K. (eds.) "Microstructural Geochronology: Planetary Records Down to Atom Scale". American Geophysical Union. Geophysical Monograph 232. John Wiley & Sons, Inc. pp. 293-313.

Refereed Journal publications

Abbott, B. P. et al. with Bland, P. A. (2017) Multi-messenger observations of a binary neutron star merger. *The Astrophysical Journal* 848: L12

Aboueisha, H., Calo, V., Jopek, K., Moshkov, M., Paszyńka, A., Paszyński, M., Skotniczny, M. (2017). Element Partition Trees For H-Refined Meshes to Optimize Direct Solver Performance. Part I: Dynamic Programming. *International Journal of Applied Mathematics and Computer Science*, 27(2), 351-365.

Agutu N.O., Awange J.L., Zerihund A., Ndehedehe C.E., Kuhn M., Fukuda Y. (2017). Assessing Multi-satellite Remote Sensing, Reanalysis, and Land Surface Models' Products in Characterizing Agricultural Drought in East Africa. *Remote Sensing of Environment*, 194, 287-302.

Ai N., Li N., Rickard W.D.A., Cheng Y., Chen K. and Jiang S.P. (2017). Highly Stable Sr-Free Cobaltite–Based Perovskite Cathodes Directly Assembled on a Barrier-Layer-Free Y_2O_3-ZrO_2 Electrolyte of Solid Oxide Fuel Cells. *ChemSusChem*, 10, 993-1003.

Al-Khdheeawi E., Vialle S., Barifcani A., Sarmadivaleh M., and Iglauer S. (2017a), Impact of salinity on CO_2 storage efficiency in highly heterogeneous reservoirs, *Greenhouse Gases: Science and Technology*, 8(1), 95-105, doi: 10.1002/ghg.1723.

Al-Khdheeawi E., Vialle S., Barifcani A., Sarmadivaleh M., and Iglauer S. (2017b), Influence of Rock Wettability on CO_2 Migration and Storage Capacity in Deep Saline Aquifers, *Energia Procedia*, 114, 4357-4365, doi: 10.1016/j.egypro.2017.03.1587.

Al-Khdheeawi E., Vialle S., Barifcani A., Sarmadivaleh M., and Iglauer S. (2017d), Influence of injection well configuration and rock wettability on CO_2 plume behaviour and CO_2 trapping capacity in heterogeneous reservoirs, *Journal of Natural Gas Science and Engineering*, 43, doi:10.1016/j.jngse.2017.03.016.

Al-Khdheeawi E., Vialle S., Barifcani A., Sarmadivaleh M., and Iglauer S. (2017e), Impact of reservoir wettability and heterogeneity on CO_2 plume migration and trapping capacity, *International Journal of Greenhouse Gas Control*, 58, doi: 10.1016/j.ijggc.2017.01.012.

Al-Khdheeawi E., Vialle S., Barifcani A., Sarmadivaleh, M., and Iglauer S. (2017c) Effect of brine salinity on CO_2 plume migration and trapping capacity in deep saline aquifers, *The APPEA Journal*, 57, 100–109, doi: 10.1071/AJ16248.

Andreoni I. *et al*. with Bland P.A. (2017) Follow up of GW170817 and its electromagnetic counterpart by Australian-led observing programmes. *Pub. Astron. Soc. Australia* 34: e069.

Andronis C., Evans N.J., McDonald B. and Gagnon M.M. (2017). Otolith Microchemistry: Insights into Bioavailable Pollutants in a Contaminated Man-Made, Urban Inlet. *Baseline- Marine Pollution Bulletin*, February 2017. doi.org/10.1016/j.marpolbul.2017.02.037.

Awange JL, Anwar AHMF, Forootan E, Nikraz H, Khandu, Walker J (2017) Enhancing civil engineering surveying learning through workshops. *Journal of Surveying Engineering*, doi: 10.1061/(ASCE)SU.1943-5428.0000211#sthash.HFRzHTSX.dpuf.

Aylmore M.G., Merigot K., Quadir Z., Rickard W.D., Evans N.J., McDonald B.J., Catovic E. & Spitalny P. (2017). Applications of advanced analytical and mass spectrometry techniques to the characterisation of micaceous lithium-bearing ores. *Minerals Engineering*, 116, 182-195.

Ayupova N.R., Maslennikov V.V., Tessalina S.G., Shilovsky O.P., Sadykov S.A., Hollis S.P., Danyushevsky L.V., Safina N.P., Statsenko E.O. (2017). Tube fossils from gossanites of the Urals VHMS deposits, Russia: authigenic mineral assemblages and trace element distributions. *Ore Geology Reviews*, 85, 107-130.

Bállico M.B., Scherer C.M.S., Mountney N.P., Souza E.G., Chemale F., Pisarevsky S.A., Reis A.D. (2017). Wind-pattern circulation as a palaeogeographic indicator: Case study of the 1.5–1.6 Ga Mangabeira Formation, São Francisco Craton, Northeast Brazil. *Precambrian Research*, 298, 1-15.

Barham M., Blyth A.J., Wallwork M.D., Joachimski M.M., Martin L., Evans N.J., Mawson P. and McDonald B.J. (2017). Digesting the data – effects of predator ingestion on the oxygen isotopic signature of micro-mammal teeth. *Quaternary Science Reviews*, 176, 71-84.

Barrote V.R., Rosiere C.A., Rolim V.K., Santos J.O.S., McNaughton N.J. (2017). The Proterozoic Guanhães banded iron formations, southeastern border of the São Francisco Craton, Brazil: evidence of detrital contamination. *Geologia USP, Série Cientifica*, 17(2), 303-324.

Bartoň, M., Ait-Haddou, R., Calo, V. (2017). Gaussian quadrature rules for C1 quintic splines with uniform knot vectors. *Journal of Computational and Applied Mathematics*, 322, 57-70.

Bartoň, M., Calo, V. (2017). Gauss-Galerkin quadrature rules for quadratic and cubic spline spaces and their application to isogeometric analysis. *Computer-Aided Design*, 82, 57-67.

Bazaikin Y., Gurevich B,, Iglauer S., Khachkova T., Kolyukhin D., Lebedev M., Lisitsa V. and Reshetova G. (2017). Effect of CT image size and resolution on the accuracy of rock property estimates. *Journal Of Geophysical Research: Solid Earth* 122 (5): 3635-3647.

Beinlich A., Barker S.L.L., Dipple G.M., Gupta M., Baer D.S. (2017). Stable isotope ($\delta^{13}C$, $\delta^{18}O$) analysis of sulfide-bearing carbonate samples using laser spectrometry. *Economic Geology*, 112, 693-700.

Belica M.E., Tohver E., Pisarevsky S.A., Jourdan F., Denyszyn S., George A.D. (2017). Middle Permian paleomagnetism of the Sydney Basin, Eastern Gondwana: Testing Pangea models and the timing of the end of the Kiaman Reverse Superchron. *Tectonophysics*, 699, 178-198.

Belica M.E., Tohver E., Poyatos-Moré M., Flint S., Parra-Avila L.A., Lanci L., Denyszyn S., Pisarevsky S.A. (2017). Refining the chronostratigraphy of the Karoo Basin, South Africa: magnetostratigraphic constraints support an early Permian age for the Ecca Group. *Geophysical Journal International*, 211, 1354–1374.

Bellucci J.J., Whitehouse M.J. John T., Nemchin A.A., Snape J.F., Bland P.A. and Benedix G. K. (2017) Halogen and Cl isotope systematics in Martian phosphates: Implications for the Cl cycle and surface halogen reservoirs on Mars. *Earth and Planetary Science Letters* 458, 192-202.

Benedix G.K., Bland P.A., Friedrich J.M., Mittlefehldt D.W., Sanborn E., Yin Q.-Z., Greenwood R.C., Franchi I.A., Bevan A.W.R., Towner M.C., Perrotta G.C. and Mertzman S.A. (2017) Bunburra Rockhole: Exploring the geology of a new differentiated asteroid. *Geochimica et Cosmochimica Acta* 208, 145-159.

Bezuidenhout, G.A., Eksteen, J.J., Akdogan, G. Van Beek, B., Wendt, W. Persson, W., 2017. Implementation of flame optical emission spectroscopy system for converter Fe end-point control associated with Ni-Cu-S-PGM converter mattes. *Minerals Engineering*, 100,132-143

Bhowany K., Hand M., Clark C., Kelsey, D.E., Reddy, S.M., Pearce, M.A., Tucker, N.M. & Morrisey, L.J. 2017. Phase equilibria modelling constraints on P–T conditions during fluid catalysed conversion of granulite to eclogite in the Bergen Arcs, Norway. *Journal of Metamorphic Geology*; DOI: 10.1111/jmg.12294

Black, M., McCormack, K.D., Elders, C. & Robertson, D. (2017). Extensional fault evolution within the Exmouth Sub-basin, North West Shelf, Australia. *Marine and Petroleum Geology*, 85, 301-315

Bland P.A. and Travis B.J. (2017) Giant convecting mudballs of the early solar system. *Science Advances* 3: e1602514.

Blereau E., Clark C., Johnson T.E., Taylor R.J.M., Kinny P.D., Hand M. (2017). Reappraising the P–T evolution of the Rogaland–Vest Agder Sector, southwestern Norway. *Geoscience Frontiers*, 8, 1-16.

Blyth A.J., Hua Q., Smith A., Frisia S., Borsato A,. Hellstrom J. (2017). Exploring the dating of "dirty" speleothems and cave sinters using radiocarbon dating of preserved organic matter. *Quaternary Geochronology*, 39, 92-98.

Böhme, M., Spassov, N., Ebner, M., Geraads, D., Hristova, L., Kirscher, U., Kötter, S., Linnemann, U., Prieto, J., Roussiakis, S., Theodorou, G., Uhlig, G., Winklhofer, M. (2017). Messinian Age and savannah environment of the possible hominin Graecopithecus from SE Europe. *PlosOne*, 12(5), e0177347.

Burgos-Cara A. Putnis C.V., Rodriguez-Navarro, C., Ruiz-Agudo E. (2017). Hydration Effects on the Stability of Calcium Carbonate Pre-Nucleation Species. *Minerals*, 7, Article Number: 126, 10.3390/min7070126.

Burgos-Cara, A., Putnis, C. V., Ortega-Huertas, M., Ruiz-Agudo E. (2017). Influence of pH and citrate on the formation of oxalate layers on calcite revealed by in situ nanoscale imaging. *CrystEngComm*., 19, 3420-3429.

Byrne E., Raiteri P., Gale J.D. (2017). Computational insight into calcium-sulfate ion pair formation. *J. Phys. Chem*. C, 121, 25956-25966.

Cabri, L.J., Wilhelmij, H.R., Eksteen, J.J., (2017). Contrasting mineralogical and processing potential of two mineralization types in the platinum group element and Ni-bearing Kapalagulu Intrusion, western Tanzania. *Ore Geology Reviews*, 90, pp. 772-789.

Callegaro S., Marzoli A., Bertrand H., Blichert-Toft J., Reisberg L., Cavazzini G., Jourdan F., Davies J., Parisio L., Bouchet R., Paul A., Schaltegger U. and Chiaradia M. (2017) Origin of high-Ti tholeiitic magmas from the CAMP: geochemical constraints from the Freetown Layered Complex, Sierra Leone. *Journal of Petrology* 58 (9), 1811-1840

Calo, V., Deng, Q., Puzyrev, V. (2017). Quadrature blending for isogeometric analysis. *Procedia Computer Science*, 108, 798-807.

Cao M., Qin K., Li G., Evans N.J., Hollings P., Maisch M. and Kappler A. (2017). Mineralogical evidence for crystallization conditions and petrogenesis of ilmenite-series I-type granitoids at the Baogutu reduced porphyry Cu deposit (Western Junggar, NW China): Mössbauer spectroscopy, EPM and LA-(MC)-ICPMS analyses. *Ore Geology Reviews*, 86, 382-403.

Cao M., Qin K.Z., Li G.M., Evans N.J., McInnes B.I.A., Lu W.W. and Deng G. (2017). Petrogenesis of the Baishan granite stock, Eastern Tianshan, NW China: geodynamic setting and implications for potential mineralization. *Lithos*, 292-293, 278-293.

Cawood P.A., Pisarevsky S.A. (2017). Laurentia-Baltica-Amazonia relations during Rodinia assembly. *Precambrian Research*, 292, 386-397.

Cesar J., Grice K. (2017). The significance of benzo[b]naphtho[d]furans in fluids and source rocks: New indicators of facies type in fluvial-deltaic systems. *Organic Geochemistry*, 113, 175-183.

Cesar J., Grice K. (2017). $\delta^{13}C$ of polycyclic aromatic hydrocarbons to establish the facies variations in a fluvial deltaic Triassic record (Dampier sub-Basin, Western Australia). *Organic Geochemistry*, 107, 59-68.

Chang S-C., Gao K-Q., Zhou C-F and Jourdan F. (2017) New chronostratigraphic constraints on the Yixian Formation with implications for the Jehol Biota. *Palaeogeography, Palaeoclimatology, Palaeoecology* 487, 399-406.

Chen, B., Long, X., Wilde, S.A., Yuan, C., Wang, Q., Xia, X., Zhang, Z. (2017). Delamination of lithospheric mantle evidenced by Cenozoic potassic rocks in Yunnan, SW China: A contribution to uplift of the Eastern Tibetan Plateau. *Lithos*, 284-285, 709-729.

Corbett M.K., Eksteen J.J., Niu X-Z., Croue J-P. and Watkin E.L.J. (2017). Interactions of phosphate solubilising microorganisms with natural rare-earth phosphate minerals: a study utilizing Western Australian monazite. *Bioprocess and Biosystems Engineering*, 40, 929–942.

Corbett M.K., Eksteen J.J., Watkin E.L.J. (2017). Application of phosphate solubilizing microorganisms on Western Australian monazite ores. *Bioprocess and Biosystems Engineering*. 40(6), 929-942 doi 10.1007/s00449-017-1757-3

Corbett, M.K., Eksteen, J.J., Niu, X.-Z., Watkin, E.L.J., (2017). Incorporation of indigenous microorganisms increases leaching rates of rare earth elements from Western Australian monazite. *Solid State Phenomena*, 262 SSP, 294-298.

Correa, J., A. Egorov, K. Tertyshnikov, A. Bona, R. Pevzner, T. Dean, B. Freifeld, and S. Marshall. 2017. Analysis of signal to noise and directivity characteristics of das VSP at near and far offsets-A CO2CRC Otway Project data example. *Leading Edge* 36 (12): 994a1-994a7.

Cortes, A., Dalcin, L., Sarmiento, A., Collier, N., Calo, V. (2017). A scalable block-preconditioning strategy for divergence-conforming B-spline discretizations of the Stokes problem. *Computer Methods in Applied Mechanics and Engineering*, 316, 839-858.

Crossley, R.J., Evans, K.A., Reddy, S.M. & Lester, G.W. (2017). Redistribution of iron and titanium in high-pressure ultramafic rocks. *Geochemistry, Geophysics, Geosystems*, 18, 3869-3890.

Cucciniello C., Melluso L., le Roex A.P., Jourdan F., Morra V., de Gennaro R. and Grifa C.. (2017) From Nephelinite, basanite and basalt to peralkaline trachyphonolite and comendite in the Ankaratra volcanic complex, Madagascar: 40Ar/39Ar ages, phase compositions, and bulk rock geochemical and isotopic evolution. *Lithos* 274-275, 363-382.

Cui X., Zhu W., Fitzsimons I.C.W., Wang X., Lu Y., Wu X. (2017). A possible transition from island arc to continental arc magmatism in the eastern Jiangnan Orogen, South CVhina: Insights from a Neoproterozoic (870-860 Ma) gabrroic-dioritic complex near the Fuchuan ophiolite. *Gondwana Research*, 46, 1-16.

Daly, L., Bland, P.A., Dyl, K. A., Forman, L. V., Saxey, D. W., Reddy, S.M., Fougerouse, D., Rickard, W.D.A., Trimby, P. W., Moody, S.Yang, L., Liu, H., Ringer, S.P., Saunders, M., & Piazolo, S. 2017. Crystallography of refractory metal nuggets in carbonaceous chondrites: A transmission Kikuchi diffraction approach. *Geochimica et Cosmochimica Acta*, 216, 42-60.

Daly, L., Bland, P.A., Dyl, K.A., Forman, L.V., Evans K.A., Trimby P.W., Moody S., Yang L., Liu H., Ringer S., Ryan C.G. and Sauders M. (2017). In situ analysis of Refractory Metal Nuggets in carbonaceous chondrites. *Geochimica et Cosmochimica Acta*, 216: 61-81.

Daly, L., Bland, P.A., Saxey, D.W., Reddy, S.M., Fougerouse, D., Rickard, W.D. & Forman, L.V. (2017). Nebula sulfidation and evidence for migration of free-floating refractory metal nuggets revealed by atom probe microscopy. *Geology*, 49, 847-850.

Danisk M., McInnes B.I.A., Kirkland C., McDonald B.J., Evans N.J. and Becker T. (2017). Seeing is believing: Visualization of He distribution in zircon and implications for thermal history reconstruction on single crystals. *Science Advances*, 3, no2, DOI: 10.1126/sciadv.1601121.

Danišík, M., Schmitt, A.K., Stockli, D.F., Lovera, O.M., Dunkl, I., Evans, N.J. (2017). Application of combined U-Th-disequilibrium/U-Pb and (U-Th)/He zircon dating to tephrochronology. *Quaternary Geochronology*, 40, 23-32.

De La Pierre M., Raiteri P., Stack A.G., Gale J.D. (2017). Uncovering the atomistic mechanism for calcite step growth. *Angewandte Chem. Int. Ed.*, 56, 8464-8474.

Delle Piane C., Piazolo, S., Timms N.E., Luzin V., Saunders M., Bourdet J., Giwelli A., Clennell M.B., Kong C., Rickard W.D., Verrall M. (2017). Generation of amorphous carbon and crystallographic texture during low-temperature subseismic slip in calcite fault gouge. *Geology*. 46 (2), 163-166.

Deng, Q., Ginting, V. (2017). Locally Conservative Continuous Galerkin FEM for Pressure Equation in Two-Phase Flow Model in Subsurfaces. *Journal of Scientific Computing*, 1-22.

Deng, Q., Ginting, V., McCaskill, B., Torsu, P. (2017). A locally conservative stabilized continuous Galerkin finite element method for two-phase flow in poroelastic subsurfaces. *Journal of Computational Physics*, 347, 78-98.

Despaigne-Díaz, A.I., García Casco, A., Cáceres Govea, D., Wilde, S.A., Millán Trujillo, G. (2017). Structure and tectonic evolution of the southwestern Trinidad dome, Escambray complex, Central Cuba: Insights into deformation in an accretionary wedge. *Tectonophysics*, 717, 139-161.

Di Lorenzo, F., Burgos-Cara, A., Ruiz-Agudo, E., Putnis C.V., Prieto M. (2017). Effect of ferrous iron on the nucleation and growth of $CaCO_3$ in slightly basic aqueous solutions. *CrystEngComm.*, 19, 447-460.

Dopson M., Holmes D.S, Lazcano M., McCredden T.J., Bryan C.G, Mulroney K.T, Steuart R., Jackaman C. and Watkin E.L.J. (2017). Multiple osmotic stress responses in Acidihalobacter prosperus result in tolerance to chloride ions. *Frontiers in Microbiology* 05 January 2017 | https://doi.org/10.3389/fmicb.2016.02132

Egorov, A., Pevzner, R., Bona, A., Glubokovskikh, S., Puzyrev, V., Tertyshnikov, K., Gurevich, B. (2017). Time-lapse full waveform inversion of vertical seismic profile data: workflow and application to the CO2CRC Otway project. *Geophysical Research Letters*, 44, 7211-7218.

Eiler J., Cesar J., Chimiak L., Dallas B., Grice K., Griep-Raming J., Juckelka D., Kitchen N., Lloyd M., Makarov A., Robins R,. Schwieters J. (2017). Analysis of molecular isotopic structures at high precision and accuracy by Orbitrap mass spectrometry. International *Journal of Mass Spectrometry*, 422, 126-142.

Eksteen, J.J. Oraby, E.A. and Tanda, B.C., 2017. A conceptual process for copper extraction from chalcopyrite in alkaline glycinate solutions. *Minerals Engineering*, 108, pp. 53-66

El-Mowafy, A. (2017). Advanced Receiver Autonomous Integrity Monitoring Using Triple Frequency Data with a Focus on Treatment of Biases. *Advances in Space Research*, 59(8), 2148-2157.

El-Mowafy, A. (2017). Impact of Predicting Real-Time Clock Corrections during their Outages on Precise Point Positioning. *Survey Review*, DOI 10.1080/00396265.2017.1405155.

El-Mowafy, A., Deo, M. Kubo, N. (2017), Maintaining real-time precise point positioning during outages of orbit and clock corrections. *GPS Solutions*, 21(3), 937-947. ARC-DP170103341.

El-Mowafy, A., Kubo N. (2017). Integrity Monitoring of Vehicle Positioning in Urban Environment Using RTK-GNSS, IMU and Speedometer. *Measurement, Science and Technology*, 28(5), 055102, 1-12.

Erickson, T.M., Pearce, M.A., Reddy, S.M., Timms, N.E., Cavosie, A.J., Bourdet, J., Rickard, W.D.A. & Nemchin, A.A. (2017). Microstructural constraints on the mechanisms of the transformation to reidite in naturally shocked zircon. *Contributions to Mineralogy and Petrology*, 172, 6.

Erickson, T.M., Timms, N.E., Kirkland, C.L., Tohver, E., Cavosie, A.J., Pearce, M.A., Reddy, S.M. 2017. Shocked monazite chronometry: integrating microstructural and in situ age data for determining precise impact ages. *Contributions to Mineralogy and Petrology*, 172:11, 1-19.

Espath, L., Sarmiento, A., Dalcin, L., Calo, V. (2017). On the thermodynamics of the Swift-Hohenberg theory. *Continuum Mechanics and Thermodynamics*, 29(6), 1335-1345.

Evans, K.A., Reddy, S.M., Tomkins, A.G., Crossley, R.J. & Frost, B.R. (2017). Effects of geodynamic setting on the redox state of fluids released by subducted mantle lithosphere. *Lithos*, 278, 26-42.

Feng, C., Aldrich, C., Eksteen, J.J. and Arrigan, D.W.M. (2017). Removal of Arsenic from Alkaline Process Waters of Gold Cyanidation by Use of γ-Fe_2O_3-ZrO_2 Nanosorbents. *Hydrometallurgy*, 174, pp. 71-77.

Feng, C., Aldrich, C., Eksteen, J.J. and Arrigan, D.W.M. (2017). Removal of Arsenic from Alkaline Process Waters of Gold Cyanidation by Use of Fe_3O_4-SiO_2-TiO_2 Nanosorbents. *Minerals Engineering*, 110, pp. 40-46.

Fielding I.O.H., Johnson S.P., Zi J-W., Rasmussen B., Muhling J.R. Dunkley D.J., Sheppard S., Wingate M.T.D. and Rogers J.R. (2017) Using In Situ SHRIMP U-Pb Monazite and Xenotime Geochronology to Determine the Age of Orogenic Gold Mineralization: An Example from the Paulsens Mine, Southern Pilbara Craton. *Economic Geology* 112, 1205-1230.

Forman L.V., Bland P.A., Timms N.E., Daly L., Benedix G.K., Trimby P.W., Collins G.S., Davison T.M. (2017). Defining the mechanism for compaction of the CV chondrite parent body. *Geology*, 45 (6), 559-562.

Forootan E, Safari A, Mostafaie A, Schumacher M, Delavar M, Awange JL (2017). Large-Scale Total Water Storage and Water Flux Changes over the Arid and Semiarid Parts of the Middle East from GRACE and Reanalysis Products. *Surveys in Geophysics* 38(3): 591-618, doi: 10.1007/s10712-016-9403-1.

Fougerouse, D., Micklethwaite, S., Ulrich, S., Miller, J., Godel, B., Adams, D.T., and McCuaig, T.C. (2017) Evidence for Two Stages of Mineralization in West Africa's Largest Gold Deposit: Obuasi, Ghana. *Economic Geology*, 112(1), 3-22.

Garcia, D., Pardo, D., Dalcin, L., Paszyński, M., Collier, N., Calo, V. (2017). The value of continuity: Refined isogeometric analysis and fast direct solvers. *Computer Methods in Applied Mechanics and Engineering*, 316, 586-605.

Gardiner N.J., Hawkesworth C.J., Robb L.J., Whitehouse M.J., Roberts N.M.W., Kirkland C.L. and Evans N.J. (2017). Contrasting Granite Metallogeny through the zircon record: A case study from Myanmar. *Scientific Reports* 7: 748 DOI:10.1038/s41598-017-00832-2.

Gardiner, N.J., Hawkesworth, C.J., Robb, L.J., Whitehouse, M.J., Roberts, N.M.W., Kirkland, C.L., Evans, N.J., (2017). Contrasting Cu–Au and Sn–W granite metallogeny through the zircon record. Transactions of the Institutions of Mining and Metallurgy, Section B: Applied Earth Science, 1. In press

Gardiner, N.J., Hickman, A.H., Kirkland, C.K., Lu, Y., Johnson, T.E., Zhao, J.-X. (2017). Processes of Crust Formation in the Early Earth imaged through Hf isotopes from the East Pilbara Terrane. *Precambrian Research*, 297, 56-76.

Gardiner, N.J., Johnson, T.E., Kirkland, C.L., Smithies, R.H. (2017). Melting Controls on the Lutetium–Hafnium Evolution of Archaean Crust. *Precambrian Research*, 305, 479-488

Gardiner, N.J., Robb, L.J., Searle, M.P, Kyi Htun, Khin Zaw (2017). The Bawdwin Mine: A review of its Geologic Setting and Genesis. In: Barber, A., Khin Zaw, Crow, M.J. (eds). Myanmar: *Geology, Resources and Tectonics. The Geological Society Memoir*, 48, 669-686.

Ge Y.K., Dai J.G., Wang C.S., Li Y.L., Xu G.Q. and Danišík M. (2017). Cenozoic thermo-tectonic evolution of the Gangdese batholith constrained by low-temperature thermochronology. *Gondwana Research*, 41, 451-462.

Gillespie, J., Glorie, S., Jepson, G., Zhang, Z.Y., Xiao, W.J., Danišík, M., Collins, A.S. (2017). Differential Exhumation and Crustal Tilting in the Easternmost Tianshan (Xinjiang, China), Revealed by Low-Temperature Thermochronology. *Tectonics*, 36(10), 2142-2158.

Gladkochub D.P., Donskaya T.V., Sklyarov E.V., Kotov, A.B. Vladykin N.V., Pisarevsky S.A., Larin A.M., Salnikova E.B., Saveleva V.B., Sharygin V.V., Starikova A.E., Tolmacheva E.V., Velikoslavinsky S.D., Mazukabzov A.M., Bazarova E.P., Kovach V.P., Zagornaya N.Yu., Alymova N.V., Khromova E.A. (2017). The unique Katugin rare-metal deposit (southern Siberia): Constraints on age and genesis. *Ore Geology Reviews*, 91, 246-263.

Gladkochub D.P., Donskaya T.V., Zhang S., Pisarevsky S.A., Stanevich A.M., Mazukabzov A.M., Motova Z.L. (2017). Early stage of the Central Asian Orogenic Belt building: evidences from the southern Siberian craton. *Geodynamics and Tectonophysics*, 8, 461–463

Glen R.A., Fitzsimons I.C.W., Griffin W.L., Saeed A. (2017). East Antarctic sources of extensive Early-Middle Ordovician turbidites in the Lachlan Orogen, Tasmanides, SE Australia. *Australian Journal of Earth Sciences*, 64(2), 143-224.

Glorie S., Agostino K., Dutch R., Pawley M., Hall J., Danišík M., Evans N.J. and Collins A.S. (2017). Thermal history and differential exhumation across the Eastern Musgrave Province, South Australia: Insights from low-temperature thermochronology. *Tectonophysics* 703-704, 23-41.

Glubokovskikh, S., and B. Gurevich. (2017) Optimal bounds for attenuation of elastic waves in porous fluid-saturated media. *Journal of the Acoustical Society of America* 142 (5): 3321-3329.

Goddéris, Y., Hir, G.L., Macouin, M., Donnadieu, Y., Hubert-Théou, L., Dera, G., Aretz, M., Fluteau, F., Li, Z.X., Halverson, G.P. (2017). Paleogeographic forcing of the strontium isotopic cycle in the Neoproterozoic. *Gondwana Research*, 42, 151-162.

Goncalves R, Awange JL (2017) Evaluation of three mostly used GNSS-based shoreline monitoring methods to support Integrated Coastal Zone Management Policies. *Journal of Surveying Engineering*. Doi 10.1061/(ASCE)SU.1943-5428.0000219#sthash.avHUkvBk.dpuf.

Grotheer H., Greenwood P.F., McCulloch M.T., Böttcher M.E., Grice K. (2017). - 34S character of organosulfur compounds in kerogen and bitumen fractions of sedimentary rocks. *Organic Geochemistry*, 110, 60-64.

Grotheer H., Le Métayer P., Piggott M.J., Lindeboom E. J., Holman A. I., Twitchett R. J., Grice K. (2017). Occurrence and significance of phytanyl arenes across the Permian-Triassic boundary interval. *Organic Geochemistry*, 104, 42-52.

Guo, J., J. G. Rubino, S. Glubokovskikh, and B. Gurevich. (2017). Effects of fracture intersections on seismic dispersion: theoretical predictions versus numerical simulations. *Geophysical Prospecting* 65: 1264-1276.

Hagos M., Koeberl C. and Jourdan F.. Geochemistry and Geochronology of Phonolitic and Trachytic Source Rocks of the Axum Obelisks and Other Stone Artifacts. *Geoheritage* 9 (4), 479-494. 2016. DOI 10.1007/s12371-016-0199-7.

Han, J., Zhou, J.B., Wilde, S.A., Song, M.C. (2017). Provenance analysis of the Late Paleozoic sedimentary rocks in the Xilinhot Terrane, NE China, and their tectonic implications. *Journal of Asian Earth Sciences*, 144, 69-81.

Harrison A.L., Dipple G.M., Song W., Power I.M., Mayer K.U., Beinlich A., Sinton D. (2017). Pore scale visualization of mineral-fluid reactions in Earth's shallow subsurface. *Chemical Geology*, 463, 1-11.

Healy D., Rizzo R.E., Cornwell D.G., Farrell N.J., Watkins H., Timms N.E., Gomez-Rivas E., Smith M. (2017). FracPaQ: a MATLABTM toolbox for the quantification of fracture patterns. *Journal of Structural Geology*, 95, 1-16.

Herrington R.J., Plotinskaya O.Yu., Maslennikov V.V., Tessalina S.G. (2017). An overview of mineral deposits in the Urals: A special issue of Ore Geology Reviews. *Ore Geology Reviews*, 85, 1-3.

Hír, J., Venczel, M., Codrea, V., Rössner, G.E., Angelone, C., van den Hoek Ostende, L.W., Rosina, V.V., Kirscher, U., Prieto, J., 2017. Badenian and Sarmatian s.str. from the Carpathian area: Taxonomical notes concerning the Hungarian and Romanian small vertebrates and report on the ruminants from the Felsőtárkány Basin. *Comptes Rendus Palevol*, v.6(3), p. 312-332.

Hirt C., Kuhn M. (2017). Convergence and divergence in spherical harmonic series of the gravitational field generated by high-resolution planetary topography – a case study for the Moon. *Journal of Geophysical Research: Planets*, 122(8), 1727-1746.

Hirt C., Rexer M., Claessens S.J., Rummel R. (2017). The relation between degree-2160 spectral models of Earth's gravitational and topographic potential: a guide on global correlation measures and their dependency on approximation effects. *Journal of Geodesy*, 91, 1179-1205.

Hoffman P.F., Abbot D.S., Ashkenazy Y., Benn D.I., Brocks J.J., Cohen P.A., Cox G.M., Creveling J.R., Donnadieu Y., Erwin D.H., Fairchild I.J., Ferreira D., Goodman J.C., Halverson G.P., Jansen M.F., Le Hir G., Love G.D., Macdonald F.A., Maloof A.C., Partin C.A., Ramstein G., Rose B.E.J., Rose C.V., Sadler P.M., Tziperman E., Voigt A., Warren S.G., (2017). Snowball Earth climate dynamics and Cryogenian geology-geobiology. *Science Advances*, 3(11), e1600983. https://doi.org/10.1126/sciadv.1600983

Hollis S.P., Mole D., Gillespie P., Barnes S.J., Tessalina S., Cas R.A.F., Hildrew C., Pumphrey A., Goodz M.D., Caruso S., Yeats C.J., Verbeeten A., Belford S.M., Wyche S., Martin L.A.J. (2017). 2.7 Ga plume associated VHMS mineralization in the Eastern Goldfields Superterrane, Yilgarn Craton: insights from the low temperature and shallow water, Ag-Zn-(Au) Nimbus deposit. *Precambrian Research*, 291, 119-142.

Hopkinson, T.N., Harris, N.B.W., Warren, C.J., Spencer, C.J., Roberts, N.M.W., Horstwood, M.S.A., Parrish, R.R., EIMF, 2017. The identification and significance of pure sediment-derived granites. *Earth and Planetary Science Letters* 467, 57-63.

Hou Z., Zhou Y., Wang R., Richards J.P., Zheng Y., He W., Zhao M., Evans N.J. and Weinberg R.F. (2017). Recycling of metallogenically-fertilized lower continental crust: origin of non-arc Au-Rich porphyry deposits at cratonic edges. *Geology* 45(6), 563-566.

Howie R.M., Paxman J., Bland, P.A, Towner M.C., Cupak M., Sansom E.K. and Devillepoix, H.A.R. (2017) How to build a continent scale fireball camera network. *Experimental Astronomy* DOI 10.1007/s10686-017-9532-7.

Howie R.M., Paxman J., Bland P.A. , Towner M.C., Sansom E.K. and Devillepoix H.A.R. (2017) Submillisecond fireball timing using de Bruijn timecodes. *Meteoritics & Planetary Science* 52, 1669-1682.

Hu K, Awange JL, Khandu, Forootan E, Goncalves RM, Fleming K (2017) Hydrogeological characterisation of groundwater over Brazil using remotely sensed and model products. *Science of the Total Environment* 599–600: 372–386.

Hu S.Y., Evans K., Craw D., Rempel K., Grice K. (2017). Resolving the role of carbonaceous material in gold precipitation in metasediment-hosted orogenic gold deposits. *Geology*, 45, 167-170.

Hunt A.C., Benedix G.K., Hammond S.J., Bland P.A., Rehkamper, M., Kreissig K. and Strekopytov S. (2017) A geochemical study of the winonaites: Evidence for limited partial melting and constraints on the precursor composition. *Geochimica et Cosmochimica Acta* 199, 13-30.

Ironside, C., Saxey, D., Rickard, W., Gray, C., McGlynn, E., Reddy, S. & Marks, N. (2017). Atom probe microscopy of zinc isotopic enrichment in ZnO nanorods. *AIP Advances*, 7, 025004.

Ito, H., Spencer, C.J., Danišík, M., Hoiland, C.W. (2017). Magmatic tempo of Earth's youngest exposed plutons as revealed by detrital zircon U-Pb geochronology. *Scientific Reports*, 7, 1-6.

Jahn I., Strachan R.A., Fowler M., Bruand E., Kinny P.D., Clark C., Taylor R.J.M. (2017). Evidence from U-Pb zircon geochronology for early Neoproterozoic (Tonian) reworking of an Archaean inlier in northeastern Shetland, Scottish Caledonides. J*ournal of the Geological Society*, London, 174, 217–232.

Jansen N.H., Gemmell J.B., Chang Z., D. Cooke D., Jourdan F., and Creaser R.A. (2017). Geology and Genesis of the Cerro la Mina Porphyry-High Sulfidation Au (Cu-Mo) Prospect, Mexico. *Economic Geology* 112. 799-827. 2017.

Jiao S., Fitzsimons I.C.W., Guo, J. (2017). Paleoproterozoic UHT metamorphism in the Daqingshan Terrane, North China Craton: New constraints from phase equilibria modeling and SIMS U–Pb zircon dating. *Precambrian Research*, 303, 208-227.

Johnson T.E., Kirkland C.L., Viete D.R., Fischer S., Reddy S.M., Lister G.S., Evans N.J. and McDonald B.J. (2017). Zircon geochronology reveals polyphase magmatism and crustal anataxis in the Buchan Block, NE Scotland: Implications for the Grampian Orogeny. *Geoscience Frontiers* 8(6), 1469-1478.

Johnson, L.M., Rezaee, R., Kadkhodaiea, A., Smith, G., Yu, H. (2017). A new approach for estimating the amount of eroded sediments, a case study from the Canning Basin, Western Australia. *Journal of Petroleum Science and Engineering*, 156, 19-28.

Johnson, S.P., Korhonen, F.J., Kirkland, C.L., Cliff, J.B., Belousova, E.A., Sheppard, S., (2017). An isotopic perspective on growth and differentiation of Proterozoic orogenic crust: From subduction magmatism to cratonization. *Lithos* 268-271, 76-86.

Johnson, T.E., Brown, M., Gardiner, N.J., Kirkland, C.L. & Smithies, R.H. (2017). Earth's first stable continents did not form by subduction. *Nature*, 543, 239–242.

Jourdan F. and Eroglu E. 40Ar/39Ar and (U-Th)/He model age signatures of elusive mercurian and venusian meteorites. *Meteoritics & Planetary Science* 52, 884-905.

Jourdan F., Timms N.E., Eroglu E., Mayers C., Frew A., Bland P.A., Collins G.S., Davison T.M., Abe M., Yada T. (2017). Collisional history of asteroid Itokawa. *Geology*, 45 (9), 819-822.

Kelsey D.E., Morrissey L.J., Hand M., Clark C., Tamblyn R., Gaeh, A.A. and Marshall S. (2017) Significance of post-peak metamorphic reaction microstructures in the ultrahigh temperature Eastern Ghats Province, India. *Journal of Metamorphic Geology*. 35, 1081-1109

Khaki M., Ait-El-Fquih B., Hoteit I., Forootan E., Awange J.L., Kuhn M. (2017). A two-update ensemble Kalman filter for land hydrological data assimilation with an uncertain constraint. *Journal of Hydrology*, 555, 447-462.

Khaki M., Hoteit I., Kuhn M., Awange J.L., Forootan E., van Dijk A.I.J.M., Schumacher M., Pattiaratchi C. (2017). Assessing sequential data assimilation techniques for integrating GRACE data into a hydrological model. *Advances in Water Resources*, 107, 301-316.

Khaki M., Schumacher M., Forootan E., Kuhn M., Awange J.L., van Dijk A.I.J.M. (2017). Accounting for spatial correlation errors in the assimilation of GRACE into hydrological models through localization. *Advances in Water Resources*, 108, 99-112.

Khaleque H.N., Corbett M.K., Ramsay J.P., Kaksonen A., Boxall N.J., Watkin E.L.J.(2017). Complete genome sequence of Acidihalobacter prosperus strain F5, an extremely acidophilic, iron- and sulfur-oxidizing halophile with potential industrial applicability in saline water bioleaching of chalcopyrite. *Journal of Biotechnology* 262: 56–59.

Khaleque H.N., Ramsay J.P., Murphy R., Kaksonen A., Boxall N.J., Watkin E.L.J. (2017). Draft genome sequence of *Acidihalobacter ferrooxidans* DSM 14175 (strain V8), a new iron- and sulfur-oxidizing, halotolerant, acidophilic species. *Genome Announc*. May 2017; 5:Doi:10.1128/Genomea.00413-17

Khaleque H.N., Ramsay J.P., Murphy R., Kaksonen A., Boxall N.J., Watkin E.L.J. (2017). Draft genome sequence of the acidophilic, halotolerant, and iron/sulfur-oxidizing Acidihalobacter prosperus DSM 14174 (strain V6). *Genome Announc*. January 2017 5:DOI:10.1128/GENOMEA.01469-16

Khandu, Awange J.L., Anyah R., Kuhn M., Fukuda Y. (2017). Assessing regional climate simulations of the last 30 years (1982-2012) over Ganges-Brahmaputra-Meghna River Basin. *Climate Dynamics*, 49(7-8), 2329-2350.

Khandu, Awange J.L., Kuhn M., Anyah R., Forootan E. (2017). Changes and variability of precipitation and temperature in the Ganges–Brahmaputra–Meghna River Basin based on global high-resolution reanalyses. *International Journal of Climatology*, 37(4), 2141-2159.

Kheriji, W., Efendiev, Y., Calo, V., Gildin, E. (2017). Model reduction for near-well & reservoir models using multiple space-time discretizations. *Model Red of Param Systems,* 17, 471-490.

King H., Plümper O., Putnis C.V., O'Neill H. St C., Klemme S., Putnis A. (2017). Enhanced surface rearrangement at high temperatures: Implications for extra-terrestrial mineral grain reactivity. *ACS Earth and Space Chemistry*. 1, 113-121.

Kirilova M., Toy V.G., Timms N., Halfpenny A., Menzies C., Craw D., Beyssac O., Sutherland R., Townend J., Boulton C., Carpenter B.M. (2017). Textural changes of graphitic carbon by tectonic and hydrothermal processes in an active plate boundary fault zone, Alpine Fault, New Zealand. *Geological Society, London, Special Publications*, 453, SP453-13.

Kirkland C.L., Hollis J., Danišík M., Peterson J., Evans N.J. and McDonald B. (2017) Apatite and titanite from the Karrat Group, Greenland; Implications for charting the thermal evolution of the crust from the U-Pb geochronology of common Pb-bearing phases. *Precambrian Research*, 300, 107-120.

Kirkland, C.L., Abello, F., Danišík, M., Gardiner, N.J., Spencer, C.J. (2017). Mapping temporal and spatial patterns of zircon U-Pb disturbance: A Yilgarn Craton Case Study. *Gondwana Research*, 52, 39-47.

Kirkland, C.L., Smithies, R., Spaggiari, C., Wingate, M., De Gromard, R., Clark, C., Gardiner, N., Belousova, E. (2017) Uncovering the deep: Proterozoic crustal evolution of the Eucla basement and implications for destruction of modern-style oceanic crust during emergence of Nuna. *Lithos*. 278, 427-444.

Kirscher, U., Bachtadse, V., Mikolaichuk, A., Kröner, A., Alexeiev, D.V. (2017). Palaeozoic evolution of the North Tianshan based on palaeomagnetic data – transition from Gondwana towards Pangaea. *International Geology Review*, 59(16), 2003-2020.

Kirscher, U., Oms, O., Bruch, A.A., Shatilova, I., Chochishvili, G., and Bachtadse, V. (2017). The Calabrian in the Western Transcaucasian Basin (Georgia): paleomagnetic constraints from the Gurian regional stage. *Quaternary Science Reviews*, 160, 96-107.

Kohút, M., Danišík, M. (2017). Rapid cooling and geospeedometry of granitic rocks exhumation within a volcanic arc: A case study from the Central Slovakian Neovolcanic Field (Western Carpathians). *Island Arc*, 26(5), e12201.

Kong, L., B. Gurevich, Y. Zhang, and Y. Wang. (2017). Effect of fracture fill on frequency-dependent anisotropy of fractured porous rocks. *Geophysical Prospecting* 65 (6): 1649-1661.

Korhonen, F.J., Johnson, S.P., Wingate, M.T.D., Kirkland, C.L., Fletcher, I.R., Dunkley, D.J., Roberts, M.P., Sheppard, S., Muhling, J.R., Rasmussen, B., (2017). Radiogenic heating and craton-margin plate stresses as drivers for intraplate orogeny. *Journal of Metamorphic Geology* 35, 631-661.

Krapez B., Müller S.G., Fletcher I.R and Rasmussen B. (2017) A tale of two basins? Stratigraphy and detrital zircon provenance of the Palaeoproterozoic Turee Creek and Horseshoe basins of Western Australia. *Precambrian Research* 294, 67-90.

LaFlamme, C., McFarlane, C.R.M., Fisher, C.M., Kirkland, C.L., (2017). Multi-mineral geochronology: insights into crustal behaviour during exhumation of an orogenic root. *Contributions to Mineralogy and Petrology* 172.

Lebrun E., Thebaud N., Miller J., Roberts M. and Evans N.J. (2017) Mineralisation footprints and regional timing of the world-class Siguiri orogenic gold district (Guinea, West Africa). *Mineralium Deposita*, 52, 539-564.

Lengger S.K., Fromont J., Grice K. (2017). Tapping the archives: the sterol composition of marine sponge species, as determined non-invasively from museum-preserved specimens, reveals biogeographical features. *Geobiology*, 15, 184-194.

Lengger S.K., Melendez I.M., Summons R.E., Grice K. (2017). Mudstones and embedded concretions show differences in lithology-related, but not source-related biomarker distributions. *Organic Geochemistry*, 113, 67-74.

Lewandowski, M., Kusiak, M.A., Michalczyk, Ł., Szmigiel, D., Sledziewska-Gojska, E., Barzycka, B., Wawrzyniak, T., Luks, B., Thordarson, T., Wilde, S.A. and Hoskuldsson, A. (2017). Message in a Stainless Steel Bottle Thrown into Deep Geological Time. *Gondwana Research*, 52: 139-141.

Li G., Qin K., Li J., Zhao J., Cao M., Zhang X., and Evans N.J., (2017). Cretaceous magmatism and metallogeny in the Bangong–Nujiang metallogenic belt, central Tibet: Evidence from petrogeochemistry, zircon U–Pb ages, and Hf–O isotopic compositions. *Gondwana Research*, 41, 110-127.

Li H., Sun H.S., Wu J.H., Evans N.J., Xi X.S., Peng N.L., Cao J.Y. and Gaob-Ratio J.A.S. (2017). Re-Os and U-Pb geochronology of the Shazigou Mo polymetallic ore field, Inner Mongolia: implications for Permian-Triassic mineralization at the northern margin of the North China Craton. *Ore Geology Reviews*, 83, 287-299.

Li M., Wang L.J., Putnis C.V. (2017). Energetic basis for inhibition of calcium phosphate biomineralization by osteopontin. *J. Physical Chemistry Chemistry* B, 121, 5968-5976.

Li M., Wang L.J., Putnis C.V. (2017). Energetic basis for inhibition of calcium phosphate biomineralization by osteopontin. *J. Physical Chemistry Chemistry* B, 121, 5968-5976.

Li Z., Wang X.C., Liu K., Tessalina S., Yang X.M., Ma X.Z. Sun H.T. (2017). Rhenium-osmium geochronology in dating petroleum systems: Progress and challenges. *Acta Petrolei Sinica*, 38, 297-306.

Li, C.F, Feng, L.J., Wang, X.C., Wilde, S.A., Chu, Z.Y., Guo, J.H. (2017). A low-blank two-column chromatography separation strategy based on a $KMnO_4$ oxidizing reagent for Cr isotope determination in micro-silicate samples by thermal ionization mass spectrometry. *Journal of Analytical Atomic Spectrometry*, 32, 1938-1945.

Li, C.F., Feng, L.J., Wang, X.C., Chu, Z.Y., Guo, J.H., Wilde, S.A. (2017). Precise measurement of Cr isotope ratios using a highly sensitive Nb_2O_5 emitter by thermal ionization mass spectrometry and an improved procedure for separating Cr from geological materials. *Journal of Analytical Atomic Spectrometry*, 31, 2375-2383.

Li, C.F., Wang, X.C., Wilde, S.A., Li, X.H., Wang, Y.F., Li, Z. (2017). Differentiation of the early silicate Earth as recorded by 142Nd-143Nd in 3.8–3.0 Ga rocks from the Anshan Complex, North China Craton. Precambrian Research, 301, 86-101.

Li P., Sun M., Rosenbaum G., Jourdan F., Li S. and K. Cai K. (2017) Late Paleozoic closure of the Ob-Zaisan Ocean along the Irtysh shear zone (NW China): Implications for arc amalgamation and oroclinal bending in the Central Asian orogenic belt. *Geological Society of America Bulletin* 129 (5-6), 547-569. 2017.

Li, S., Chung, S.L., Wang, T., Wilde, S.A., Chu, M.F., Guo, Q.Q. (2017). Tectonic significance and geodynamic processes of large-scale early Cretaceous granitoid magmatic events in the southern great Xing'an range, north China. *Tectonics*, 36, 615-633.

Li, S., Chung, S.L., Wilde, S.A., Jahn, B.M., Xiao, W.J., Wang, T., Guo, Q.Q. (2017). Early-Middle Triassic high Sr/Y granitoids in the southern Central Asian Orogenic Belt: Implications for ocean closure in accretionary orogens. *Journal of Geophysical Research: Solid Earth*, 122, 2291-2309

Liu K., Zhang J., Wilde S.A., Liu S., Guo F., Kasatkin S.A., Golozoubov V.V Ge M.,Wang, M. and Wang, J. (2017). U-Pb dating and Lu-Hf isotopes of detrital zircons from the southern Sikhote-Alin Orogenic Belt, Russian Far East: Tectonic implications for the Early Cretaceous evolution of the Northwest Pacific Margin. *Tectonics*, 36, 2555-2598.

Liu L-P., Li Z-X., Danišík M., Li S., Evans N.J., Jourdan F. and Tao N. (2017). Thermochronology of the Sulu ultrahigh-pressure metamorphic terrane: Implications for continental collision and lithospheric thinning. *Tectonophysics*, 712-13. 10-29.

Liu X., Fan H., Evans N.J., Yang K., McInnes B.I.A., Danišík M., Qin K. and Yu X. (2017). Exhumation history of the Sanshandao Au deposit, Jiaodong District: constraints from structural analysis and (U-Th)/He thermochronology. *Scientific Reports* 7: 7787 DOI:10.1038/s41598-017-08103-w.

Liu, K., Zhang, J., Wilde, S,A,, Zhou, J., Wang, M., Ge, M., Wang, J., Ling, Y. (2017) Initial subduction of the Paleo-Pacific Oceanic plate in NE China: Constraints from whole-rock geochemistry and zircon U–Pb and Lu–Hf isotopes of the Khanka Lake granitoids. *Lithos*, 274-275, 254-270.

Liu, K., Zhang, J., Wilde, S.A., Liu, S., Guo, F., Kasatkin, S.A., Golozoubov, V.V., Ge, M., Wang, M., Wang, J. (2017). U-Pb dating and Lu-Hf isotopes of detrital zircons from the southern Sikhote-Alin Orogenic Belt, Russian Far East: Tectonic implications for the Early Cretaceous evolution of the Northwest Pacific Margin. *Tectonics*, 36, 2555-2598.

Liu, L.-P., Li, Z.-X., Danišík, M., Li, S., Evans, N., Jourdan, F., and Tao, N., 2017. Thermochronology of the Sulu ultrahigh-pressure metamorphic terrane: Implications for continental collision and lithospheric thinning. *Tectonophysics* 712–713, 10-29. https://doi.org/10.1016/j.tecto.2017.05.003

Liu, L., Li, Z., Li, S., Zhu, K., Cui, F.,2017. Early Cretaceous basin framework in northwest Jiaobei region: evidence from SHRIMP zircon U-Pb dating for "Penglai Group" at Qimudao. *Marine Geology and Quarternary Geology* 37, 126-136 (in Chinese with English abstract).

Lubnina N.V., Pisarevsky S.A., Stepanova A.V., Bogdanova S.V., Sokolov S.J. (2017). Fennoscandia before Nuna/Columbia: Paleomagnetism of 1.98–1.96 Ga mafic rocks of the Karelian craton and paleogeographic implications. *Precambrian Research*, 292, 1-12.

Ma L., Wang Q., Li Z.X., Wyman D.A., Yang J.H., Wu F.Y., Jiang Z.Q., Gou G.N., Guo H.F. (2017). Subduction of Indian continent beneath southern Tibet in the latest Eocene (~ 35 Ma): Insights from the Quguosha gabbros in southern Lhasa block. *Gondwana Research*, 41, 77-92.

Magee Jr, C.W., Danišík, M., Mernagh, T. (2017). Extreme isotopologue disequilibrium in molecular SIMS species during SHRIMP geochronology. *Geoscientific Instrumentation, Methods and Data Systems*, 6(2), 523.

Maravelis A.G., Catuneanu O., Nordsvan A., Landenberger B., Zelilidis A., (2017). Interplay of tectonism and eustasy during the Early Permian icehouse: Southern Sydney Basin, southeast Australia. *Geological Journal*, 1-32. https://dx.doi.org/10.1002/gj.2962

Maravelis A.G., Chamilaki E., Pasadakis N., Zelilidis A., Collins W.J. (2017). Hydrocarbon generation potential of a Lower Permian sedimentary succession (Mount Agony Formation): Southern Sydney Basin, New South Wales, Southeast Australia. *International Journal of Coal Geology*, 183, 52-64. https://doi.org/10.1016/j.coal.2017.09.017

Markwitz V., Kirkland C.L. and Evans N.J. (2017) Early Cambrian metamorphic zircon in the northern Pinjarra Orogen: Implications for the structure of the West Australian Craton margin. *Lithosphere*, 9(1), 3-13.10.

Martin, E.L., Collins, W.J., Kirkland, C.L., (2017). An Australian source for Pacific-Gondwanan zircons: Implications for the assembly of northeastern Gondwana. *Geology* 45, 699-702.

Maslennikov V.V., Maslennikova S.P., Large R.R., Danyushevsky L.V., Herrington R.J., Ayupova N.R. Zaykov V.V., Lein A.Yu., Tseluyko A.S., Melekestseva I.Yu., Tessalina S.G. (2017). Chimneys in Paleozoic massive sulfide mounds of the Urals VMS deposits: Mineral and trace element comparison with modern black, grey, white and clear smokers. *Ore Geology Reviews*, 85, 64-106.

Mayr, C., Brandlmeier, B., Diersche, V., Stojakowits, P., Kirscher, U., Eigler, M., Lempe, B., Haas, U., Bachtadse, V., Reimer, P.J., Spötl, C. (2017). Nesseltalgraben, a new reference section of the Last Glacial period in southern Germany. *Journal of Paleolimnology*, 58(2), 213-229.

McCubbine J.C., Featherstone W.E., Kirby J.F. (2017). Fast-Fourier-based error propagation for the gravimetric terrain correction. *Geophysics*, 82, G71-G76.

McCubbine J.C., Stagpoole V., Caratori Tontini F., Amos M.J., Smith E., Winefield R. (2017a). Gravity Anomaly Grids for the New Zealand region. *New Zealand Journal of Geology and Geophysics*, 60(4), 381-391.

Menneken, M., Geisler, T., Nemchin, A.A., Whitehouse, M.J., Wilde, S.A., Gasharova, B., Pidgeon, R.T. (2017), CO_2 fluid inclusions in Jack Hills zircons. *Contributions to Mineralogy and Petrology*, 172, 66.

Meredith A.S., Collins A.S., Williams S.E., Pisarevsky S., Foden J.D., Archibald D.B., Blades M.L., Alessio B.L., Armistead S., Plavsa D., Clark C., Műller R.D. (2017). A full-plate global reconstruction of the Neoproterozoic. *Gondwana Research*. 50, 84-134.

Merle R., Marzoli A., Aka F.T., Chiaradia J.M., Reisberg L., Castorina F., Jourdan F., Renne P.R., N'ni J. and Nyobe J.B. (2017) Mt. Bambouto volcano, Cameroon Line: mantle source and differentiation of within-plate alkaline rocks. *Journal of Petrology* 58 (5), 933-962

Merle R.E., Nemchin A.A., Whitehouse M.J., Pidgeon R.T., Grange M.L. Snape J.F and Thiessen F. (2017). Origin and transportation history of lunar breccia 14311. *Meteoritics and Planetary Science* 52, 842-858

Miljkovic, K., Lemelin, M., Lucey, P.G. (2017) Depth of Origin of the Peak (Inner) Ring in Lunar Impact Basins. *Geophys. Res. Lett*., 44, 10,140–10,146.

Millonig L.J., Beinlich A., Raudsepp M., Devine F., Archibald D.A., Linnen R., Groat L.A., (2017). The Engineer Mine, British Columbia: An Example of Epithermal Au-Ag Mineralization with Mixed Alkaline and Subalkaline Characteristics. *Ore Geology Reviews*, 83, 235-257.

Mirasol-Robert A., Grotheer H., Bourdet J., Suvorova A., Grice K., McCuaig T.C., Greenwood P.F. (2017). Evidence and origin of different types of sedimentary organic matter from a Paleoproterozoic orogenic Au deposit. *Precambrian Research*, 299, 319-338.

Montalvo, S.D., Cavosie, A.J., Erickson, T.M., and Talavera, C. (2017. Fluvial transport of impact evidence from cratonic interior to passive margin: Vredefort-derived shocked zircon on the Atlantic coast of South Africa. *American Mineralogist*, v. 102, 813-823.

Mora, J., Mantilla, J., Calo, V. (2017). A multiscale formulation for FEM and IGA. *Boletin de Matematicas*, 24(1), 101-115.

Morrissey, L.J., Payne, J.L., Hand, M., Clark, C., Taylor, R.J.M., Kylander-Clark, A.R.C. (2017) Linking the Windmill Islands, east Antarctica and the Albany–Fraser Orogen: insights from U–Pb zircon geochronology and Hf isotopes. *Precambrian Research*. 293, 131-149

Mothersole, F.E., Evans, K., Frost, B.R. (2017). Abyssal and hydrated mantle wedge serpentinised peridotites: a comparison of the 15 degrees 20 minutes N fracture zone and New Caledonia serpentinites. *Contributions to Mineralogy and Petrology*, 172(8).

Mpinga, C.N., Eksteen, J.J., Aldrich, C., Dyer, L., 2017. Identification of the significant factors determining extractability of Ni and Cu after sulfation roasting of a PGM-bearing chromitite ore. *Minerals Engineering*, 110, pp. 153-165.

Mucek, A.E., Danišík, M., de Silva, S.L., Schmitt, A.K., Pratomo, I., Coble, M.A. (2017). Post-supereruption recovery at Toba Caldera. *Nature Communications*, 8, 15248.

Munteanu M, Wilson A.H., Costin G., Yao Y., Lum J., Jiang S-Y., Jourdan F. and Cioacă M-E. (2017) The olivine-rich dikes in the Yanbian terrane (Sichuan, SW China): record of the primary magma differentiation in the Emeishan large igneous province. *Journal of Petrology* 58 (3), 513-538.

Muñoz Matute, J., Alberdi Celaya, E., Pardo, D., Calo, V. (2017). Time-domain goal-oriented adaptivity using pseudo-dual error representations, *Computer Methods in Applied Mechanics and Engineering*, 325, 395-415.

Nachtergaele, S., De Pelsmaeker, E., Glorie, S., Zhimulev, F., Jolivet, M., Danišík, M., Buslov, M.M., De Grave, J. (2017). Meso-Cenozoic tectonic evolution of the Talas-Fergana region of the Kyrgyz Tien Shan revealed by low-temperature basement and detrital thermochronology. *Geoscience Frontiers*, DOI: 10.1016/j.gsf.2017.11.007.

Nalback M., Raiteri P., Klassen S., Schäfer S., Gale J.D., Bechstein R., Kühnle A. (2017). Where is the most hydrophobic region? Benzopurpurine self-assembly at the calcite-water interface. *J. Phys. Chem*. C, 121, 24144-24151.

Ndehedehe C.E., Awange J.L., Kuhn M., Agutu N.O., Fukuda Y. (2017). Climate teleconnections influence on West Africa's terrestrial water storage. *Hydrological Processes*, 31(18), 3206-3224.

Ndehedehe C.E., Awange J.L., Kuhn M., Agutu N.O., Kukuda Y. (2017). Analysis of hydrological variability over the Volta river basin using in-situ data and satellite observations. *Journal of Hydrology: Regional Studies*, 12, 88-110.

Nemchin A.A., Jeon H., Bellucci J.J., Timms N.E., Snape J.F., Kilburn M.R., Whitehouse M.J. (2017). Pb-Pb ages of feldspathic clasts in two Apollo 14 breccia samples. *Geochimica et Cosmochimica Acta*, 217, 441-461

O'Leary M.J., Ward I., Key M., Rawson C. and Evans N.J. (2017). Challenging the 'offshore hypothesis' for fossiliferous chert artefacts in southwestern Australia and consideration of inland trade routes. *Quaternary Science Reviews*, 156, 36-46.

Olierook H., R. Merle R. and Jourdan F. (2017) Toward a Greater Kerguelen Large Igneous Province: Evolving mantle source contributions in and around the Indian Ocean. *Lithos* 282-283, 163-172.

Oostingh K., Jourdan F., Danišík M., Evans N.J. (2017). Advancements in cosmogenic 38Ar exposure dating of terrestrial rocks. *Geochimica et Cosmochimica Acta*, 217(C), 193-218.

Oostingh K., Jourdan F., Matchan E.L. and Phillips D. (2017) Ultra – precise 40Ar/39Ar geochronology reveals rapid change from plume-assisted to stress-dependent volcanism in the Newer Volcanic Province, SE Australia. *Gcubed* 18, doi:10.1002/2016GC006601, 1-25.

Oraby E.A., Eksteen J.J., and Tanda B.C. (2017). Gold and copper leaching from gold-copper ores and concentrates using a synergistic lixiviant mixture of glycine and cyanide. *Hydrometallurgy*, 169, 339-345

Orsi W.D., Coolen M.J.L., Wuchter C., He L., More K.D., Irigoien X., Chust G., Johnson C., Hemingway J.D., Lee M., Galy V., Giosan L. (2017). Climate oscillations reflected within the microbiome of Arabian Sea sediments. *Scientific Reports*, 7, 6040.

Otakwa RVM, Othieno H, Awange JL, Oduor AO (2017) Technology Options for the Built Environment in Kenya: Dye-Sensitized and Amorphous Silicon Photovoltaics for Application in NZE Buildings. *Current Alternative Energy* 1: 1-10, doi: 10.2174/2405463102666170306162043

Palancz B, Awange JL (2017) Nonlinear homotopy in geodesy. *Acta Geod Geophys*, 52: 1-4, doi:10.1007/s40328-016-0169-1

Paláncz B, Awange JL, Lovas T, Lewis R, Molnár B, Heck B, Fukuda Y. (2017). Algebraic method to speed up robust algorithms: Example of laser-scanned point clouds. *Survey Review* 49 (357): 408-418, doi: 10.1080/00396265.2016.1183939

Paláncz, B., Awange JL, Völgyesi L (2017): A novel RANSAC approach to robustly solve the 3D similarity transformation problem, *Australian Journal of Earth Sciences* 64(4): 565-576, doi: 10.1080/08120099.2017.1316313

Parker A.L., Featherstone W.E., Penna N.T., Filmer M.F., Garthwaite M.C. (2017) Practical considerations before installing ground-based geodetic infrastructure for integrated InSAR and cGNSS monitoring of vertical land motion. *Sensors*, 17(8), 1753, doi:10.3390/s17081753.

Parker A.L., Filmer M.F., Featherstone W.E. (2017) First results from Sentinel-1A InSAR over Australia: Application to the Perth Basin. *Remote Sensing*, 9(3), 299, doi:10.3390/rs9030299.

Pedrosa, E.T. Boeck, L., Putnis, C.V., Putnis A. (2017). The replacement of a carbonate rock by fluorite: Kinetics and microstructure. *American Mineralogist*, 102, 126-134.

Pertille J., Hartmann L.A., Santos J.O.S., McNaughton N.J., Armstrong R. (2017). Reconstructing the Cryogenian-Ediacaran evolution of the Porongos fold and thrust belt, southern Braziliano Orogen, based on U-Pb-Hf-O isotopes. *International Geology Review*, 59, 1532-1560.

Pevzner, R., M. Urosevic, D. Popik, V. Shulakova, K. Tertyshnikov, E. Caspari, J. Correa, T. Dance, A. Kepic, S. Glubokovskikh, S. Ziramov, B. Gurevich, R. Singh, M. Raab, M. Watson, T. Daley, M. Robertson, and B. Freifeld. (2017). 4D surface seismic tracks small supercritical CO_2 injection into the subsurface: CO2CRC Otway Project." *International Journal Of Greenhouse Gas Control* 63: 150-157.

Pidgeon R.T., Chapman, P., Danisik, M. and Nemchin A.A. (2017) Dry annealing of metamict zircon: a differential scanning calorimetry study. *American Mineralogist* 102, 1066-1072.

Pidgeon R.T., Nemchin A.A. and Whitehouse, M.J. (2017). The effect of weathering on U-.Th-Pb and oxygen isotope systems of ancient zircons from the Jack Hills, Western Australia. *Geochimica et Cosmochimica Acta*, 197, 142-166.

Piechocka A.M., Courtney J.G., Zi J-W., Sheppard S., Wingate M.T.D. and Rasmussen B. (2017) Monazite trumps zircon: applying SHRIMP U–Pb geochronology to systematically evaluate emplacement ages of leucocratic, low-temperature granites in a complex Precambrian orogen. *Contibutions to Mineralogy and Petrology* 172:63 https://doi.org/10.1007/s00410-017-1386-5

Pippèrr M., Reichenbacher B., Kirscher U., Sant K., Hanebeck H., (2017). The middle Burdigalian in the North Alpine Foreland Basin (Bavaria, SE Germany) – a lithostratigraphic, biostratigraphic and magnetostratigraphic re-evaluation. *Newsletters on Stratigraphy*. https://doi.org/10.1127/nos/2017/0403

Plet, C., Grice, K., Pagès, A., Verrall, M., Coolen, M.J.L., Ruebsam, W., Rickard, W.D.A. & Schwark, L. (2017). Palaeobiology of red and white blood cell-like structures, collagen and cholesterol in an ichthyosaur bone. *Scientific Reports*, 7, 13776.

Plotinskaya O.Y., Grabezhev A.I., Tessalina S., Seltmann R., Groznova E.O., Abramov S.S. (2017). Porphyry deposits of the Urals: geological framework and metallogeny. *Ore Geology Reviews*, 85, 153-173.

Poveda, L., Galvis, J., Calo, V. (2017). Localized harmonic characteristic basis functions for multiscale finite element methods. *Computational and Applied Mathematics*, 1-15.

Proborukmi M.S., Urban B., Mischke S., Mienis H.K., Melamed Y., Dupont-Nivete G., Jourdan F. and Goren-Inbarg N. (2017) Evidence for climatic changes around the Matuyama-Brunhes Boundary (MBB) inferred from a multi-proxy palaeoenvironmental study of the GBY#2 core, Jordan River Valley, Israel. *Palaeogeography, Palaeoclimatology, Palaeoecology* 489, 166-185.

Puetz S.J., Kent K.C., Pisarevsky S.A., Davaille A., Schwarz C.J., Ganade C.E. (2017). Quantifying the evolution of the continental and oceanic crust. *Earth-Science Reviews*, 164, 63-83.

Putnis A., Jamtveit B. and Austrheim H. Metamorphic processes and seismicity: The Bergen Arcs as a natural laboratory. *Journal of Petrology* 58, 1871-1898 (2017)

Puzyrev, V., Deng, Q., Calo, V. (2017). Dispersion-optimized quadrature rules for isogeometric analysis: modified inner products, their dispersion properties, and optimally blended schemes. *Computer Methods in Applied Mechanics and Engineering*, 320, 421-443.

Puzyrev, V., Vilamajo, E., Queralt, P., Ledo, J., Marcuello, A. (2017). Three-dimensional modeling of the casing effect in onshore controlled-source electromagnetic surveys. *Surveys in Geophysics*, 38(2), 527-545.

Qin L., Wang L., Putnis C.V., Putnis A. (2017). Halide-dependent Dissolution of dicalcium phosphate dihydrate and its modulation by an organic ligand. *Crystal Growth & Design*, 17, 3868-3876.

Rabett R., Ludgate N., Stimpson C., Hill E., Hunt C., Ceron J., Farr L., Morley M., Reynolds T., Zukswert H., Simpson D., Nyiri B., Verhoven M., Appleby J., Meneely J., Phan L., Dong N.N., Lloyd-Smith L., Hawkes J., Blyth A., Nguyễń Cao Tâń. (2017). Tropical limestone forest resilience and late Pleistocene foraging during MIS-2 in the Tràng An massif, Vietnam. *Quaternary International*, 448, 62-81.

Rabieh, A., Eksteen, J.J. and Albijanic, B., 2017. Galvanic interaction of grinding media with arsenopyrite and pyrite and its effect on gold cyanide leaching. *Minerals Engineering*, 116, pp. 46-55.

Rabieh, A., Eksteen, J.J. and Albijanic, B., 2017. Influence of grinding media and water quality on flotation performance of gold bearing pyrite. *Minerals Engineering*, 11, pp. 68-76.

Rabieh, A., Eksteen, J.J. and Albijanic, B., 2017. The effect of grinding chemistry on cyanide leaching of gold in the presence of pyrrhotite. *Hydrometallurgy*, 173, pp. 115-124.

Raimondo, T, Payne, J., Lanari, P., Clark, C., Hand, M. (2017) Trace element mapping by LA-ICPMS: assessing geochemical mobility in garnet. *Contributions to Mineralogy and Petrology*. 172, 17.

Rasmussen B. (2017) Fungus-like mycelial fossils in 2,4 billion year old vesicular basalt. *Nature Ecology and Evolution*, 141, 1-6.

Rasmussen B., Muhling J.R., Suvarova A. and Krapez B. Greenalite precipitation linked to the deposition of banded iron formations downslope from a late Archaen carbonate platform. *Precambrian Geology* 290, 49-62.

Reid A.J., Jourdan F. and Jagodzinsk E.A. (2017) Mesoproterozoic fluid events affecting Archean crust in the northern Olympic Cu–Au Province, Gawler Craton: insights from 40Ar/39Ar thermochronology. A*ustralian Journal of Earth Science* 64, 103-119.

Reid A.J., Jagodzinsk E.A., Wade C., Payne J. and Jourdan F. (2017) Recognition of c. 1780 Ma magmatism and metamorphism in the buried northeastern Gawler Craton: correlations with events of the Arunta Region. *Precambrian Research* 302, 198-220.

Renard, F., Putnis, C.V., Montes-Hernandez, G, King, H.E (2017). Siderite dissolution coupled to iron oxyhydroxide precipitation in the presence of arsenic revealed by nanoscale imaging. *Chemical Geology*, 44, 123-134.

Rezagholilou, A., Behnoudfar, P., Vialle S., Madadi M. (2017), Determination of Safe Mud Window Considering Time-Dependent Variations of Temperature and Pore Pressure; Analytical and Numerical Approaches, *Journal of Rock Mechanics and Geotechnical Engineering*, 9(5), doi: 10.1016/j.jrmge.2017.02.002.

Roche L.K., Korhonen F.J., Johnson S.P., Wingate M.T.D., Hancock E.A., Dunckley D., Zi J-W., Rasmussen B., Muhling J.R., Occhipiniti S.A., Dunbar M. and Goldsworth J. (2017) The evolution of Precambrian arc-related granulite facies gold deposit: Evidence from the Glenburgh deposit, Western Australia. *Precambrian Geology* 290, 63-85.

Roelofs, B., Barham, M., Cliff, J., Joachimski, M., Martin, L., Trinajstic, K. (2017). Assessing the fidelity of fossil marine microvertebrate δ18O signatures and their potential for palaeo-ecological and –climatic reconstructions. *Palaeogeography, Palaeoclimatology, Palaeoecology*, 465 (A), 79-92.

Roger L. M., George A. D., Shaw J., Hart R. D., Roberts M., Becker T., McDonald B. J., and Evans N. J. (2017). Geochemical and microstructural characterisation of two species of cool-water bivalves (Fulvia tenuicostata and Soletellina biradiata) from Western Australia, *Biogeosciences*, 14, 1721-1737.

Rutherford M.E., Chapman D.J., Derrick J.G., Patten J.R.W., Blan, P.A., Rack A., Collins G.S. and Eakins D.E. Probing the early stages of shock-induced chondritic meteorite formation at the mesoscale. *Nature Scientific Reports* 7: 45206.

Sansom E.K., Rutten M.G. and Bland P.A. (2017) Analyzing meteoroid flights using particle filters. *The Astronomical Journal* 158: 87.

Sant, K., Kirscher, U., Reichenbacher, B., Pippèrr, M., Jung, D., Doppler, G., and Krijgsman, W. (2017). Late Burdigalian sea retreat from the North Alpine Foreland Basin: new magnetostratigraphic age constraints. *Global and Planetary Change*, 152, 38-50.

Santos J.O.S. Chernicoff C.J., Zappettini E.O., McNaughton N.J., Greau Y. (2017). U-Pb geochronology of the Martin Garcia, Sola, and Dos Hermanas Islands (Argentina and Uruguay): Unveiling Rhyacian, Statherian, Ectasian and Stenian of a forgotten area of the Rio de la Plata Craton. *Journal of South American Earth Sciences*, 80, 207-228.

Sarmiento A., Cortes A., Garcia D., Dalcin L., Collier N., Calo V. (2017). PetIGA-MF: a multi-field high-performance toolbox for structure-preserving B-splines spaces. *Journal of Computational Science*, 18, 117-131.

Sarmiento A., Espath L., Vignal P., Dalcin L., Parsani M., Calo V. (2017). An energy-stable generalized-α method for the Swift-Hohenberg equation. *Journal of Computational and Applied Mathematics*, DOI: 10.1016/j.cam.2017.11.004.

Schoeman E., Bradshaw S.M., Akdogan G., Snyders C.A., Eksteen J.J. (2017). The elution of platinum and palladium cyanide from strong base anion exchange resins. *International Journal of Mineral Processing*, 162, pp. 19-26

Schoeman E., Bradshaw S.M., Akdogan G., Snyders C.A., Eksteen J.J. (2017). The extraction of platinum and palladium from a synthetic cyanide heap leach solution with strong base anion exchange resins. *International Journal of Mineral Processing*, 162, 27-35

Scholze, F., Wang, X., Kirscher, U., Kraft, J., Schneider, J.W., Götz, A.E., Joachimski, M.M. Bachtadse, V. (2017). A multistratigraphic approach to pinpoint the Permian-Triassic boundary in continental deposits: The Zechstein–Lower Buntsandstein transition in Germany. *Global and Planetary Change*, 152, 129-151.

Scott, S.R., Sims K.W.W., Frost B.R., Kelemen P.B., Evans K.A. and Swapp S.M. (2017). On the hydration of olivine in ultramafic rocks: Implications from Fe isotopes in serpentinites. *Geochimica et Cosmochimica Acta*, 215, 105-121.

Schmieder M, Kennedy T., Jourdan F., Buchner E. and Reimold W.E. (2017) A high-precision 40Ar/39Ar age for the Nördlinger Ries impact crater, Germany, and implications for the accurate dating of terrestrial impact events. *Geochimica et Cosmochimica Acta 220*, 146-157

Searle, M.P., Morley, C.K., Waters, D.J., Gardiner, N.J., Kyi Htun, Than Than Nu, Robb, L.J. (2017). Tectonic and metamorphic evolution of the Mogok Metamorphic and Jade Mines belts and ophiolitic terranes of Burma (Myanmar). In: Barber, A., Khin Zaw, Crow, M.J. (eds). Myanmar: Geology, Resources and Tectonics. *The Geological Society Memoir*, 48, 261-293.

Sergeev N., Burlow R., Tessalina S. (2017). The Paroo Station Mine supergene lead deposits, Western Australia: Geological and geochemical constraints. *Ore Geology Reviews*, 80, 564-593.

Sheppard S., Krapež B., Zi J-W, Rasmussen B. and Fletcher I.R. (2017) SHRIMP U-Pb zircon geochronology establishes that banded iron forkmations are not chronostratigraphic markers across Archaen greenstone belts of the Pilbara Craton. *Precambrian Geology* 292, 290-304.

Sheppard S., Krapež B., Zi J-W, Rasmussen B. and Fletcher I.R. (2017) Young ores in old rocks: Proterozoic iron mineralisation in Mesoarchean banded iron formation, northern Pilbara Craton, Australia. *Ore Geology Reviews* 89, 40-69.

Sheppard, S., Rasmussen, B., Zi, J.W., Soma Sekhar, V., Srinivasa Sarma, D., Ram Mohan, M., Krapež, B., Wilde, S.A., McNaughton, N.J. (2017). U-Pb dating of metamorphic monazite establishes a Pan-African age for tectonism in the Nallamalai Fold Belt, India. *Journal of the Geological Society of London*, 174, 1062-1069.

Sheppard, S., Rasmussen, B., Zi, J.W., Somasekhar, V., Srinivasa Sarma, D., Ram Mohan, M., Krapež, B., Wilde, S.A., McNaughton, N.J. (2017). Sedimentation and magmatism in the Paleoproterozoic Cuddapah Basin, India: Consequences of lithospheric extension. *Gondwana Research*, 48. 153-163.

Shi X., Kirby J., Yu C., Jiménez-Díaz A., Zhao J. (2017). Spatial variations in the effective elastic thickness of the lithosphere in Southeast Asia. *Gondwana Research*, 42, 49-62.

Silvestri A., Budi A., Ataman E., Olsson M.H.M., Andersson M.P., Stipp S.L.S., Gale J.D., Raiteri P. (2017). A quantum mechanically derived force field to predict CO2 adsorption on calcite {10.4} in an aqueous environment. *J. Phys. Chem. C*, 121, 24025-24035.

Slagstad, T., Kirkland, C.L., (2017). The use of detrital zircon data in terrane analysis: A nonunique answer to provenance and tectonostratigraphic position in the Scandinavian Caledonides. *Lithosphere* 9, 1002-1011.

Spaak G., Edwards D.S., Foster C.B., Pagès A., Summons R.E., Sherwood N., Grice K. (2017). Environmental conditions and microbial community structure during the Great Ordovician Biodiversification Event; a multi-disciplinary study from the Canning Basin, Western Australia. *Global and Planetary Change*, 159, 93-112.

Spencer C.J., Cavosie A.J., Raub T.D., Rollinson H., Searle M.P., Miller J.A., and Jeon H. (2017). Evidence for melting mud in Earth's mantle from extreme oxygen isotope signatures in zircon. *Geology*, v. 45(11), 975-978.

Spencer C.J., Gunderson K.L., Hoiland C.W., Schleiffarth W.K. (2017). Earth-Science Outreach Using an Integrated Social Media Platform. *GSA Today*, v. 27(8), p. 28-29.

Spencer C.J., Roberts N.M.W., Santosh M. (2017). Growth, destruction, and preservation of Earth's continental crust. *Earth-Science Reviews*, 172, 87-106.

Spencer C.J., Yakymchu, C., Ghaznavi M. (2017). Visualising data distributions with kernel density estimation and reduced chi-squared statistic. *Geoscience Frontiers*, 8(6),1247-1252.

Spruzeniece L., Piazolo S., Daczko N.R., Kilburn M.R. and Putnis A. (2017) Symplectite formation in the presence of a reactive fluid: insights from hydrothermal experiments. *Journal Metamorphic Geology* 35, 281-299.

Sun, H., Li, H., Danišík, M., Xia, Q., Jiang, C., Wu, P., Yang, H., Fan, Q., Zhu, D. (2017). U–Pb and Re–Os geochronology and geochemistry of the Donggebi Mo deposit, Eastern Tianshan, NW China: Insights into mineralization and tectonic setting. O*re Geology Reviews*, 86, 584-599.

Tanda, B.C., Eksteen, J.J. and Oraby, E.A., 2017. An investigation into the leaching behaviour of copper oxide minerals in aqueous alkaline glycine solutions. *Hydrometallurgy*, 167, pp. 153-162

Tanda, B.C., Oraby, E.A., & Eksteen, J.J. (2017b). Recovery of copper from alkaline glycine leach solution using solvent extraction. *Separation and Purification Technology* 187, 389–396.

Tang D., Qin K., Chen B., Mao Y., Guo H. and Evans N.J. (2017). Mineral chemistry and genesis of the Permian Cihai and Cinan magnetite deposits, Beishan, NW China. *Ore Geology Reviews*, 86, 79-99.

Tang D., Qin K., Xue S., Mao Y., Evans N.J., Niu Y. and Chen J. (2017). Genesis of the Permian Kemozibayi sulfide-bearing mafic-ultramafic intrusion in Altay, NW China: evidence from zircon geochronology, Hf and O isotopes and mineral chemistry. *Lithos* 292-293C, 49-68.

Tao N., Li Z-X., L., Danišík M., Batt G., Evans N.J., Li W-X., Pang C-J., Jourdan F., Xu Y-G., and Liu L-P. (2017). Thermochronological record of tectonic events in the SE South China: From Late Jurassic magmatic reheating to Eocene rift-related rapid cooling. *Gondwana Research*, 46, 191-203.

Taylor R.J.M., Clark C., Harley S.L., Kylander-Clark A.R.C., Hacker B.R., Kinny P.D. (2017). Interpreting granulite facies events through rare earth element partitioning arrays. *Journal of Metamorphic Petrology*, 35, 759–775.

Tessalina S. Belousova E. (2017). Highly Siderophile Element distribution, Os-S isotope systematics and U-Pb dating of mafic-ultramafic hosted massive sulphide deposits (Southern Urals) - implication for source of metals. *Ore Geology Reviews,* 86, 734-754.

Tessalina S.G., Jourdan F., Belogub E.V. (2017). Significance of Late Devonian - Lower Carboniferous ages of hydrothermal sulphides and sericites from the Urals Volcanic-Hosted Massive Sulphide deposits. *Ore Geology Reviews,* 85, 131-139.

Tessalina S.G., Plotinskaya O.Y. (2017). Silurian to Carboniferous Re-Os molybdenite ages of the Kalinovskoe, Mikheevskoe and Talitsa Cu- and Mo porphyry deposits in the Urals: implications for geodynamic setting. *Ore Geology Reviews*, 85, 174-180.

Thyse E.L., Akdogan G., Mainza A., Eksteen J. (2017). PGM converter matte mineral characteristics and effects on downstream processing. *International Journal of Mineral Processing*, 166(10), pp. 89-101

Tian, Y., Vermeesch, P., Danišík, M., Condon, D.J., Chen, W., Kohn, B., Schwanethal, J., Rittner, M. (2017). LGC-1: A zircon reference material for in-situ (U-Th)/He dating. *Chemical Geology*, 454, 80-92.

Timms N.E., Erickson T.M., Pearce M.A., Cavosie A.J., Schmieder M., Tohver E., Reddy S.M., Zanetti M., Nemchin A.A., Wittmann A. (2017). A pressure-temperature phase diagram for zircon at extreme conditions. *Earth Science Reviews*, 165, 185-202.

Timms N.E., Erickson T.M., Zanetti M.R., Pearce M.A., Cayron C., Cavosie A.J., Reddy S.M., Wittmann A., Carpenter P.K. (2017). Cubic zirconia in >2370 ºC impact melt records Earth's hottest crust. *Earth and Planetary Science Letters*, 477, 52-58.

Tominaga M., Beinlich A., Hampton B., Tivey M., Hart L., Lima E.A., Weiss B., Harigane Y. (2017). Multi-scale magnetic monitoring of peridotite carbonation processes. *Nature Communications*, 8, 1870.

Tucker N.M., Payne J.L., Clark C., Hand M., Taylor R.J.M., Kylander-Clark A.R.C. (2017) Proterozoic reworking of Archean (Yilgarn) basement in the Bunger Hills, east Antarctica. *Precambrian Research* 298, 16-38.

Tulipani S., Schwark L., Holman A.I., Bush R.T., Grice K. (2017). 1-Chloro-n-alkanes: Potential mangrove and saltmarsh vegetation biomarkers. *Organic Geochemistry*, 107, 54-58.

Ulven O.I., Beinlich A., Hövelmann J., Austrheim H., Jamtveit B. (2017). Subarctic physicochemical weathering of serpentinized peridotite. *Earth and Planetary Science Letters*, 468, 11-26.

van Riessen A., Rickard W.D.A., Williams R.P. & van Riessen G.A. (2017). Methods for Geopolymer Formulation Development and Microstructural Analysis. *Journal of Ceramic Science and Technology*, 8, 421-432.

Venkataramani D., Musgrave R.J., Boutelier D.A., Hack A.C., Collins W.J., (2017). Revised potential field model of the Gilmore Fault Zone. *Journal of the Australian Society of Exploration Geophysics*. https://doi.org/10.1071/EG16148

Vignal P., Collier N., Dalcin L., Brown D., Calo, V. (2017). An energy-stable time-integrator for phase-field models. *Computer Methods in Applied Mechanics and Engineering*, 316, 1179-1214.

Wang R., Tafi R., Hou Z., Mortensen J.K., Shen Z., Guo N., Evans N.J. and Jeon H. (2017). Across-arc geochemical variation in the Jurassic magmatic zone, Southern Tibet: Implications for the genesis of the Xietongmen (Xiongcun) porphyry Cu-Au deposit. *Chemical Geology*, 451, 116-134.

Wang, L.J., Putnis, C.V., King, H.E. Hoevelmann J., Ruiz-Agudo E., Putnis A. (2017). Imaging organophosphate and pyrophosphate sequestration on brucite by in situ atomic force microscopy. *Environmental Science & Technology*, 51, 328-336.

Wang, S., Wang, L., Brown, M., Piccoli, P., Johnson, T.E., Feng, P., Deng, H., Kitajima, K. & Huang, Y. (2017). Fluid generation and evolution during exhumation of deeply subducted UHP continental crust: petrogenesis of composite granite–quartz veins in the Sulu belt, China. *Journal of Metamorphic Geology*, 35, 601–629.

Watolla, M.-B., Gluth, G., Sturm, P., Rickard, W.D.A., Krüger, S. & Schartel, B. (2017). Intumescent geopolymer-bound coatings for fire protection of steel. *Journal of Ceramic Science and Technology*, 8, 351-364.

Whitehouse, M.J., Nemchin, A.A. and Pidgeon, R.T. (2017) What can Hadean detrital zircon really tell us? A critical evaluation of their geochronology with implications for the interpretation of oxygen and hafnium isotopes. *Gondwana Research* 51, 78-91

Wu S., Yu M., Li M., Wang L., Putnis C.V., Putnis A. (2017). In situ atomic force microscopy imaging of octacalcium phosphate crystallization and its modulation by amelogenin's C-terminus. *Crystal Growth & Design*, 17, 2194-2202.

Wu, T., Xiao, L., Wilde, S.A., Ma, C.Q., Zhou, J.X. (2017). A mixed source for the Late Triassic Garzê-Daocheng granitic belt and its implications for the tectonic evolution of the Yidun arc belt, eastern Tibetan Plateau. *Lithos*, 288-289, 214-230.

Yakymchuk, C., Clark, C., White, R.W. (2017) Phase relations and petrochronology. *Reviews in Mineralogy and Geochemistry*. 83, 13-53.

Yao, W., Li, Z.X., (2017). Tectonostratigraphy and provenance analysis to define the edge and evolution of the eastern Wuyi-Yunkai orogen, South China. *Geological Magazine*, 1-16. https://doi.org/10.1017/S0016756817000784

Yao, W.H., Li, Z.X., Li, W.-X., Li, X.-H., 2017. Proterozoic tectonics of Hainan Island in supercontinent cycles: new insights from geochronological and isotopic results. *Precambrian Research*, 290, 86-100.

Zhao X.M., Cao H.H., Mi X., Evans N.J., Zi Y.H., Huang F. and Zhang H.F. (2017). Combined iron and magnesium isotope geochemistry of pyroxenite xenoliths from Hannuoba, North China Craton: Implications for mantle metasomatism. *Contributions to Mineralogy and Petrology*, 172:40 doi:10.1007/s00410-017-1356-y.

Zhu, K.Y., Li, Z.X., Xia, Q.K., Xu, S.X., Wilde, S.A., Chen, H.L. (2017). Revisiting Mesozoic granitoids and syenites in eastern South China: some spatial and temporal variations. *Lithos* 294-293, 147-163.

Zi J-W., Courtney J.G., Rasmussen B., Sheppard S. and Muhling J.R. Using monazite geochronology to test the plume model for carbonatites: The example of Gifford Creek Carbonatite Complex, Australia. *Chemical Geology* 463, 50-60 (2017)

Zou, Q., Guo, L., Deng, Q. (2017). High Order Continuous Local-Conserving Fluxes and Finite-Volume-Like Finite Element Solutions for Elliptic Equations. *SIAM Journal on Numerical Analysis*, 55(6), 2666-2686.

Research reports

TIGeR MEMBERSHIP

TIGeR membership

Director

Andrew Putnis

TIGeR Business Manager

Yacoob Padia

The TIGeR Executive Committee

Andrew Putnis
Chris Clark
Will Featherstone
Kliti Grice
Boris Gurevich
Brent McInnes

Academic and Research Staff

Joseph Awange
Milo Barham
Andreas Beinlich
Phil Bland
Gretchen Benedix
Alison Blyth
Andrej Bona
Victor Calo
Aaron Cavosie
Sten Claessens
Chris Clark
Bill Collins
Marco Coolen
Jane Cuneen
Martin Danisik
Marco De La Pierre
Raffaella Demichelis
Jacques Eksteen
Ahmed El-Mowafy
Chris Elders
Katy Evans
Noreen Evans
Will Featherstone
Mick Filmer
Ian Fitzsimons
Lucy Forman
Denis Fougerouse
Julian Gale
Nicholas Gardiner
Rongfeng Ge
Paul Greenwood
Kliti Grice
Boris Gurevich
Brett Harris
Alex Holman
Davide Imparato
Tim Johnson
Fred Jourdan
Pete Kinny
Jon Kirby
Chris Kirkland
Uwe Kirscher
Kasia Koziara
Michael Kuhn
Zhen Li
Zheng-Xiang Li
Brent McInnes
Neal McNaughton
Katarina Miljkovic
Ross Mitchell
Janet Muhling
Alexander Nemchin
Amy Parker
Bob Pidgeon
Sergei Pisarevskiy
Amaury Porteau
Christine Putnis
Vladimir Puzyrev
Paolo Raiteri
Steven Reddy
William Rickard
Elloe Sansom
David Saxey
Alan Scarlett
Gregory Smith
Christopher Spencer
Svetlana Tessalina
Nick Timms
Martin Towner
Kate Trinajstic
Svenja Tulipani
Stephanie Vialle
Xuan-Ce Wang
Elizabeth Watkin
Simon Wilde
Domenik Wolff-Boenisch
Weihua Yao
Nan Zhang
Jianwei Zi

TIGeR Research students

Sonia Armandola
Samuel John Bain
Vitor Barrote
Eleanore Blereau
Emily Hannah Byrne
Giada Buferale
Matthew Campbell
Jaime Cesarcolmenares
Julian Chard
Darren Shawn Tek-Suen Cheah
Hamed Gamal El Dien
Peng Chen
Melissa Corbett
Franziska Crede
Lars-Steffen Crede
Rosalind Crossley
Hadrien Devillepoix
Homayoun Fathallahzadeh
Imogen Fielding
Natalya Garcia
Michael Hartnady
Sarah Hayes
Nannan He
Tania Hidalgo
Trent Jansen-Sturgeon
Yalimay Jimenez de Duarte
Calum Fox
Hendrik Grotheer
Inalee Jahn
Qiang Jiang
Liu Kai
Mehdi Khaki
Himel Nahreen Khaleque
Sureyya Kose
Megan Ladbrook
Marco Loche
Jiangyu Li
Shaojie Li
Yebo Liu
Marco Loche
Laura Lizeth Machuca Suarez
Charlotte Mack
Erin Martin
Sam McHarg
Holly Meadows
Ruairidh Mitchell
Stephanie Montalvo Delgado
Josephine Moore
Kuldeep More
Kikis Muchlis
Nicole Nevill
Adam Nordsvan
Korien Oostingh
Santiago Peña Clavijo
Agnieszka Piechocka
Chloe Plet
Jennifer Karin Porter
Alexander Prent
Brett Roelofs
Hayley Rohead-O'Brien
Mattia Sacco
Bettina Schaefer
Alicia Schuitemaker
Patrick Shober
Camilla Stark
Rick Verberne
Silvia Volante
Alexander Walker
Danlei Wang
Qian Wang
Bryant Ware
Tobias Wengorsch
Wen Zhao

Curtin University

Curtin University

THE INSTITUTE FOR
GEOSCIENCE RESEARCH (TIGeR)

CONTACT:

Andrew Putnis
Director
The Institute for Geoscience Research (TIGeR)

Curtin University
Kent Street Bentley WA 6102
GPO Box U1987 Perth WA 6845

Tel: +61 8 9266 7978
Email: andrew.putnis@curtin.edu.au

scieng.curtin.edu.au